Design of peptidomimetics towards new foldamers and 26S proteasome inhibitors

Dissertation

Zur Erlangung des Doktorgrades der Naturwissenschaften

Dr. rer. nat.

der Universität Paris 11 (Frankreich)

und

der Fakultät für Chemie und Pharmazie der Universität Regensburg

vorgelegt von

Lucia Formicola

aus

San Giorgio a Cremano (Italy)

Paris 2008

This work was supervised by Prof. Dr. Sames Sicsic and Prof. Dr. Oliver Reiser

Thesis defence on December 15th, 2008

Examination committee: Dr. Bruno Figadere
Prof. Dr. Chiara Cabrele
Dr. Régis Vanderesse
Prof. Dr. Gérard Chassaing
Dr. Sandrine Ongeri
Prof. Dr. Sames Sicsic
Prof. Dr. Oliver Reiser

The following research was performed from October 2005 to September 2007 at the Department of Medicinal Chemistry at the University of Paris-Sud 11 under the supervision of Prof. Dr. Sames Sicsic and from October 2007 to September 2008 at the Institute of Organic Chemistry at the University of Regensburg under the supervision of Prof. Dr. Oliver Reiser.

To my family

“One answer is the stretch of road that you have left behind.
Only one question can focus beyond.” *J.Gaarder*

Acknowledgements

I would like to thank *Professor Sames Sicsic* and *Dr. Sandrine Ongeri*, who gave me the opportunity to perform my PhD in France and *Professor Oliver Reiser* for this opportunity in Germany. They offered me the chance to work in their group, giving me an interesting research project in the world of foldamers. I thank them for their support and precious advices.

I am grateful to *Professor Chiara Cabrele* and *Dr. Régis Vanderesse* for evaluating this work. I thank also *Professor Gérard Chassaing* and *Dr. Bruno Figadere* that accepted to take part in the jury of my thesis.

I thank *Professor Danièle Bonnet-Delpon* and *Dr. Thierry Milcent* for their advices in fluorine chemistry.
I sincerely thank *Professor Michèle Reboud-Ravaux* and her group for the biological evaluation.
I am thankful to *Michèle, Sophie, Jean-Christophe, Jacqueline, Claire* for their assistance during 2D-NMR analysis and elementary analysis. I thank *Michèle* and *Audrey* for their disponibility in the mass service. A thanks to *Dr. Burgermeister, Mr. Kastner, Ms. Schramm* and *Ms. Stülher* for their patience in recording 2D-NMR spectra; *Dr. Mayer, Mr. Kiermeier* and *Mr. Söllner* for their assistance during MALDI-ToF-MS measurements and for the LC-ESI analysis. Additionally, I thank the group of *Prof. Dr. O. Wolfbeis* for the use of the circular dichroism spectrometer and *Dr. Vasold* and *Mr. Lautenschlager* for their assistance during preparative HPLC analysis. I thank *Dr. Kreitmeier* for his technical support.

For the financial support, I am grateful to «Marie Curie Early Stage training Fellowship of the European Community's sixth Framework Programme».

A special thanks to *Mireille, Jean-Louis* and my colleagues *Anamaria, Bertrand, Olivier, Kaouther, Mickaël, Maria Vittoria, Giuseppe, Sinda, Sebastian,* the little *Florian, Dominik, Clement, Valerio, Christopher, Ina* for the nice time we spent together in the lab and *Karine, Ana Sofia, Regis, Andrea* which take part in the same foldamers project.
I thank *Dr. Kirsten Zeitler* for their friendship and their disponibility.

Moreover, I would like to thank all the people who gave, inside and outside the lab, an important contribution to my experience:
my “family” in Paris: *Francesca*, *Fabiana*, *Michele*, *Barbara*, *Igor*, *Regina*, *Jessie*, *Elisa*, *Michele*, *Timo*, *Roberto* for their constant presence, their kindly patience and helpfulness, and, moreover, for all the nice weekends.
my “family” in Regensburg: *Silvia*, *Cristian*, *Carolina*, *Elena*, *Jack*, *Elena*, *Georg* for their sympathy and the nice Bavarian evenings in Apoteke and, of course, my flat met *Karine* and *Florian* for his support in the lab and for the special Italian-German communication.

A thanks to all my “old” Italian friends.

At the end I would like wholeheartedly thank my parents and my brother for their unconditioned understanding of my choices, their encouragement, and for their presence at any time.

SUMMARY

The 26S proteasome is a multicatalytic protease complex ATP-dependent which is responsible for intracellular protein turnover in prokaryotes and eukaryotes. It consists of a proteolytic core particle, the 20S proteasome, sandwiched between two 19S “cap” regulatory complexes. Since the proteasome hydrolyses various cell cycle regulators, transcription factors and antigenic proteins, it is a promising target for the development of drugs for the treatment of many different diseases, and in particular for cancer therapy. Various classes of proteasome inhibitors have been found.

In the first part of the presented work, we designed (by the help of molecular modelling) and synthesized a new original series of proteasome inhibitors introducing fluorinated peptidomimetics. Fluorine atom is able to favour hydrogen bonds and to increase hydrophobicity and metabolic stability of the molecules. The biological evaluation of these compounds showed that four molecules have a micromolar $IC_{50.}$

The second topic of the project is the synthesis of new δ-amino acids towards new foldamers. The function of peptides and proteins in living systems is strictly related to their three-dimensional architecture. Therefore, the development of synthetic tools mimicking the structure and activity of biologically interesting peptide and protein targets has become of crucial importance in pharmaceutical and medicinal chemistry research. In the last decade, many efforts have been made to design oligomers, so-called foldamers, which are able to adopt predictable and well-defined conformations. We designed two new enantiomeric δ-amino acids. On one hand, these cyclic scaffolds can be described as δ-amino acids bearing a lactone ring at β and γ positions. On the other hand, they mimic a glycyl-glycyl dipeptide unit, in which the amide bond is replaced by a lactone ring. We have investigated the properties of these building blocks as homo-δ-oligomers as well as dipeptide surrogates in α-amino acid sequences to define the secondary structural features

Keywords

Peptidomimetics, pseudopeptides, foldamers, proteasome, fluorinated scaffold, non covalent inhibitors, δ-amino acid, solid-phase chemistry, conformational studies.

ABBREVIATIONS

Ac	acetyl
CAN	acetonitrile
Bn	benzyl
Boc	*tert*-Butyloxycarbonyl
CAN	cerium ammonium nitrate
Cbz	benzyloxycarbonyl
CD	circular dicroism
COSY	correlation spectroscopy
DCM	dichloromethane
DIPEA	diisopropylethylamine
DMF	dimethylformamide
DMSO	dimethylsulfoxyde
EDC	*N*-(3-dimethylaminopropyl)-*N′*-ethylcarbodiimide
ESI	electrospray ionization
Fmoc	fluorenyl-9-methoxycarbonyl
HBTU	*O*-(1-benzotriazolyl)-*N*,*N*,*N′*,*N′*-tetramethyluronium hexafluorophosphate
HOBt	hydroxybenzotriazole
HPLC	high pressure liquid chromatography
IR	infra red spectroscopy
MALDI-	matrix-assisted-laser-desorption-
Tof	ionization time of flight
MBHA	methylbenzhydrylamine
Mp	melting point
NMR	nuclear magnetic resonance
NOESY	nuclear Overhauser effect
Pbf	2,2,4,6,7-pentamethyldihydro-benzofuran-5-sulfonyl
TFA	trifluoroacetic acid
TFE	2,2,2-trifluorethanol
THF	tetrahydrofurane
TIS	triisopropylsilane
TOCSY	total correlation spectroscopy
t_R	retention time
UV	ultraviolet

Amino Acid Codes

One-Letter Code	Three-Letter Code	Amino Acid
A	Ala	Alanine
C	Cys	Cysteine
D	Asp	Aspartic acid
E	Glu	Glutamic acid
F	Phe	Phenylalanine
G	Gly	Glycine
H	His	Histidine
I	Ile	Isoleucine
K	Lys	Lysine
L	Leu	Leucine
M	Met	Methionine
N	Asn	Asparagine
P	Pro	Proline
Q	Gln	Glutamine
R	Arg	Arginine
S	Ser	Serine
T	Thr	Threonine
V	Val	Valine
W	Trp	Tryptophan
Y	Tyr	Tyrosine
Unspecified amino acid	X	Xaa

DESIGN OF PEPTIDOMIMETICS TOWARDS NEW FOLDAMERS AND 26S PROTEASOME INHIBITORS

GENERAL INTRODUCTION

Over the last years peptidomimetics have attracted interest from both organic and medicinal chemists. In the biological, chemical, and pharmaceutical areas, they offer advantages over physiologically active peptides, which as active substances are crucial for the organism and may lead to severe side effects. There is much current interest in the preparation of peptides and peptidomimetics with a well-defined conformation. These conformationally constrained peptides are useful to probe protein folding and to mimic peptide structures.

In the first chapter, we report a brief description of the proteins organization and the bases to develop mimics of peptide and protein structures.

The second part of this PhD work has been focused on the synthesis of peptidomimetics as potential non covalent inhibitors of the 26S proteasome. The 26S proteasome is a multicatalytic protein complex implicated in the degradation of the majority of cellular proteins. Thus, proteasome inhibitors are new potential therapeutic agents for treating many disorders such as cancer, inflammation, immune diseases. As further “peptidomimetic tool”, we introduced in our molecules a fluorinated scaffold. In fact, fluorine atom is able to favour hydrogen bonds, to increase hydrophobicity and metabolic stability of the molecules. We described here the synthesis and the biological evaluation of these analogues.

In the last chapter of the work we described the synthesis of peptidomimetics containing a new unnatural amino acid, a δ-amino acid, which is a glycylglycine mimic where the central amide group is replaced by a lactone ring. Using solid-phase synthesis we obtained several peptides containing our pentalactone scaffold. The following step was a conformational analysis using CD, NMR, FT-IR measurements and the molecular modelling in order to establish the secondary structure adopted by these molecules.

I PEPTIDES AND PEPTIDOMIMETICS

I.1 Structure of Proteins

In nature, proteins constitute a class of biomacromolecules which virtually affect every feature that characterizes a living organism. Structural proteins such as collagen or elastin provide support in organisms. The rate of the chemical reactions in all organisms is increased, of many orders of magnitude, by the presence of enzymes, which are proteins. Defensive proteins such as antibodies provide protection. Proteins store and transport a variety of particles ranging from macromolecules to electrons and are the crucial components of muscles and other systems for converting chemical energy into mechanical energy. In spite of these diverse biological functions, proteins are all the linear polymers built on various combinations of 20 amino acids. They differ only for the sequence in which the amino acids are assembled into polymeric chains. The secret of their functional diversity lies in the diversity of the three-dimensional structures that these building blocks can form, simply by being linked in different sequences. In fact, the amino acid sequence itself contains all the instructions needed for proper folding (Figure 1).

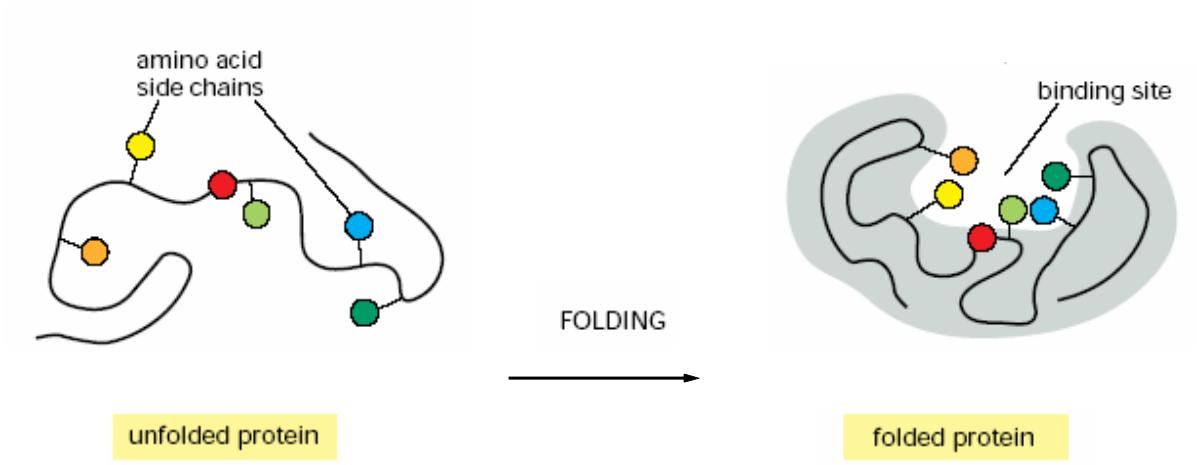

Figure 1. The folding of the polypeptide chain.[1]

The complex structure of proteins can be characterized in four general levels of structural organization: primary, secondary, tertiary and quaternary structure (Figure 2).

- The primary structure represents the linear arrangement of the individual amino acids in the protein sequence.
- The secondary structure describes the local architecture of linear segments of the polypeptide chain (i.e. α-helix, β-sheet), without regarding the conformation of the side chains. Another level of structural organization, which was introduced not before very recently, is the so-called *supersecondary structure*. It describes the association of secondary structural elements through side chain interactions.
- The tertiary structure portrays the overall topology of the folded polypeptide chain.
- The quaternary structure describes the arrangement of separate subunits or monomers into the functional protein.

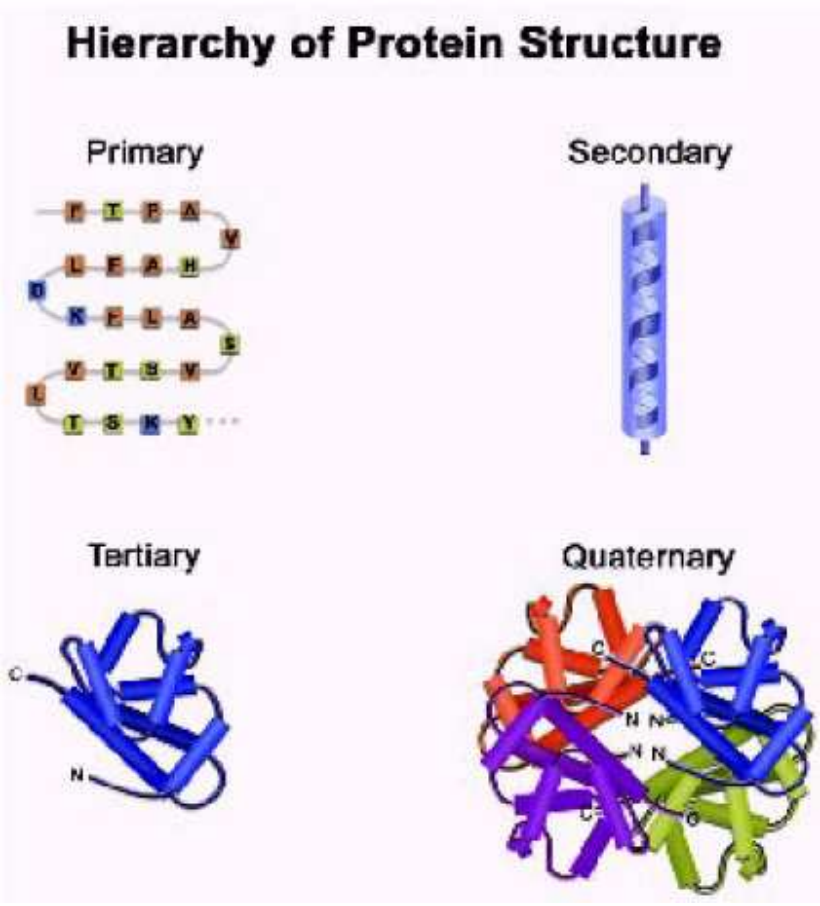

Figure 2. Hierarchy of protein structure.

A portion of the backbone of a polypeptide chain is shown in Figure 3. The main chain torsion angles in proteins are named φ, ψ, ω. Rotation about the N-C^{α} bond is described by the torsion angle φ, rotation about C^{α}-C bond by ψ, and rotation about the peptide bond C-N by ω.

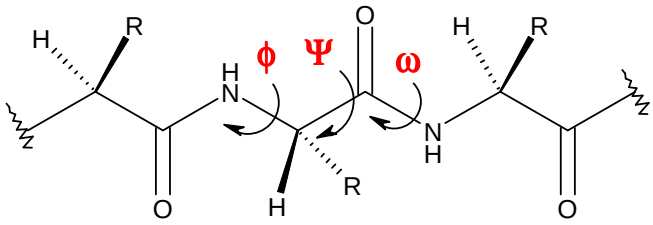

Figure 3. Torsion angles in a protein.

The peptide bond is usually planar because of its partial double bond character and nearly always has the *trans* configuration (ω = 180°). The permitted values of φ and ψ were first analyzed and determined by Ramachandran and co-workers.[2] Since φ and ψ constitute a virtually complete description of the backbone conformation, the 2D Ramachandran plot is an important and easy-to-analyze test for the validity of 3D protein structure (Figure 4).

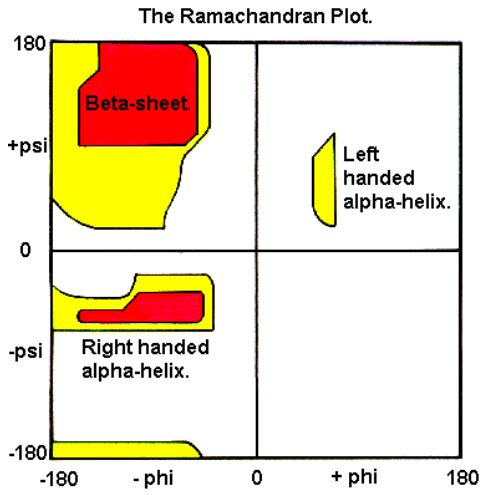

Figure 4. The Ramachandran plot.

Types of Secondary Structural Elements

The α-Helix

The right-handed α-helix is the best known and most easily recognized secondary structural element in protein.[3,4] Polymers of α-amino acids are characterized by precise hydrogen bond patterns and torsional angles along their backbone. A repeated hydrogen bond between the carbonyl function of residue *i* and the NH of residue *i*+4 leads to the α-helix.

Variations of the classical α-helix in which the protein backbone is either more tightly or more loosely coiled (with hydrogen bonds to residues *i*+3 and *i*+5), are named 3_{10}-helix and π-helix, respectively (Figure 5).

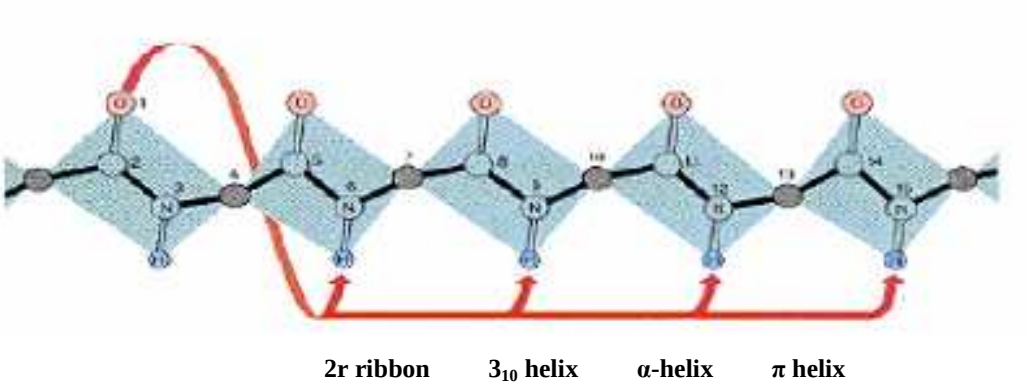

Figure 5. Some possible hydrogen bonds patterns in α-peptides helices.[5]

The β-Sheet

The second most regular and recognizable secondary structural motif is the β-sheet,[6,7] a periodic element like the α-helix. The β-sheets are formed from β-strands which develop when a linear extended conformation of a polypeptide backbone appears.[7] The amide bonds are almost coplanar and side chains are alternate above and below the plane of the peptide backbone (Figure 6a).

Since interactions between residues of the same strand are not possible, isolated β-strands are not common and are usually found hydrogen bonded in at least pairs, forming β-sheets structures. Adjacent β-strands can be arranged in either parallel or antiparallel fashion. In parallel sheets the strands all run in the same direction forming 12-membered hydrogen-bonded rings (Figure 6b), whereas in antiparallel sheets they run in opposite directions forming alternate 10 and 14-membered hydrogen-bonded rings (Figure 6c).

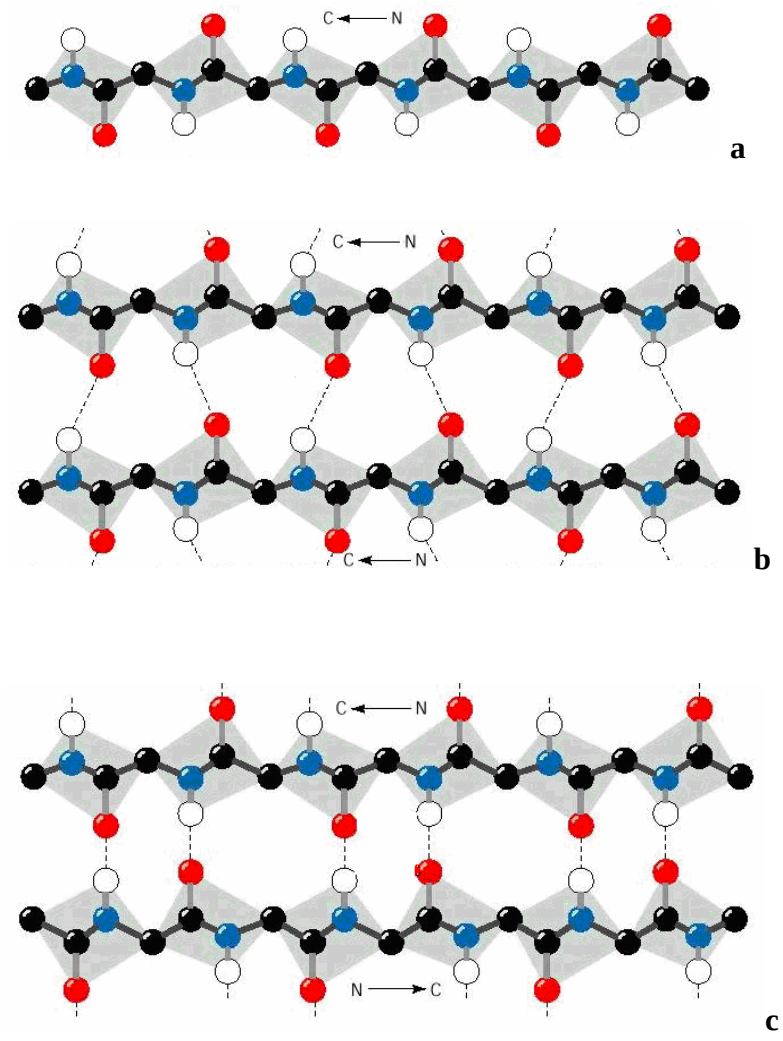

Figure 6. Architecture of a) β-strand b) parallel and c) antiparallel β-sheets.

Turns

The general function of turns is to reverse the direction of the polypeptide chain. Various different types of reverse turns have been observed in proteins and the most common are shown in Figure 7. A β-turns involve 4 amino acids with a $i \rightarrow i+3$ hydrogen bond. The repeating of the β-turn type III along the peptide chain leads to a 3_{10}-helix. A γ-turn involves 3 residues with a $i \rightarrow i+2$ hydrogen bond.

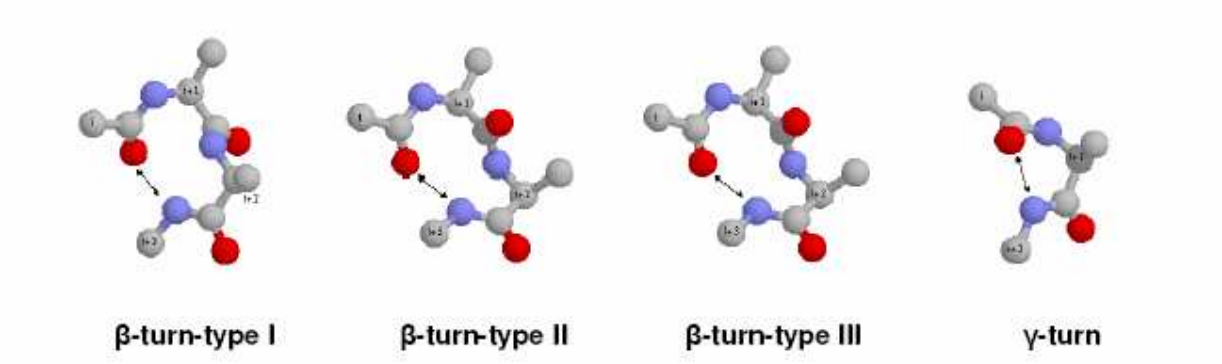

Turn type	Φ_2	Ψ_2	Φ_3	Ψ_3
β-turn-type I (I')	-60 (+60)	-30 (+30)	-90 (+90)	0
β-turn-type II (II')	-60 (+60)	+120 (-120)	+80 (-80)	0
β-turn-type III (III')	-60 (+60)	-30 (+30)	-60 (+60)	-30 (+30)
γ-turn	70	-70		
inverse γ-turn	-70	70		

Figure 7. Torsional angles of β-turns and γ-turns.

Peptides like drugs

Several endogenous peptides are biologically active, for example Somatostatin, Met- and Leu-enkephalin, Angiotensin II. However, the development of peptides as clinically useful drugs has to overcome their poor metabolic stability and to increase their low bioavailability, due in part to

their inability to cross biological membrane barriers. More, the peptide receptors can be widely distributed in organisms and their stimulation results in a variety of desired and undesired effects, especially, when the peptide is conformationally flexible and hence able to interact with alternative receptors.[8] The aim of peptide medicinal chemistry is, therefore, to develop strategies to overcome these problems.

I.2. Peptidomimetics

In biological, chemical, and pharmaceutical areas modified peptides and mimetics offer interesting advantages over physiologically active peptides. Beside increasing efficiency and selectivity of natural peptides, this class of compounds known as peptidomimetics may decrease side effects, improving oral bioavailability and prolonging the pharmacological activity by hindering enzymatic degradation within the organism.[9] The peptidomimetic research continues to inspire medicinal chemists for seeking either potential drugs or pharmacological tools to investigate how the secondary structure can affect activity.[10] This knowledge can be useful to modulate the activity of the studied target proteins and peptides.

Peptidomimetics can be prepared by approaches ranging from the slight modification of the initial structure of a peptide to the generation of a pure non-peptide. The very first steps in peptidomimetic design were based on simple N- or C- terminus modifications, methylation of amide nitrogen and C^{α}, replacement of L- with D-amino acids.[11,12,13] The introduction of amide bond isosters completely prevents protease degradation of the amide bond and it may also significantly modify the biochemical properties of a peptide, particularly its conformation and its hydrophobicity. The isosteres are used to investigate the role and function of backbone peptide bonds and to modify the properties of the parent peptides (Figure 8).[14]

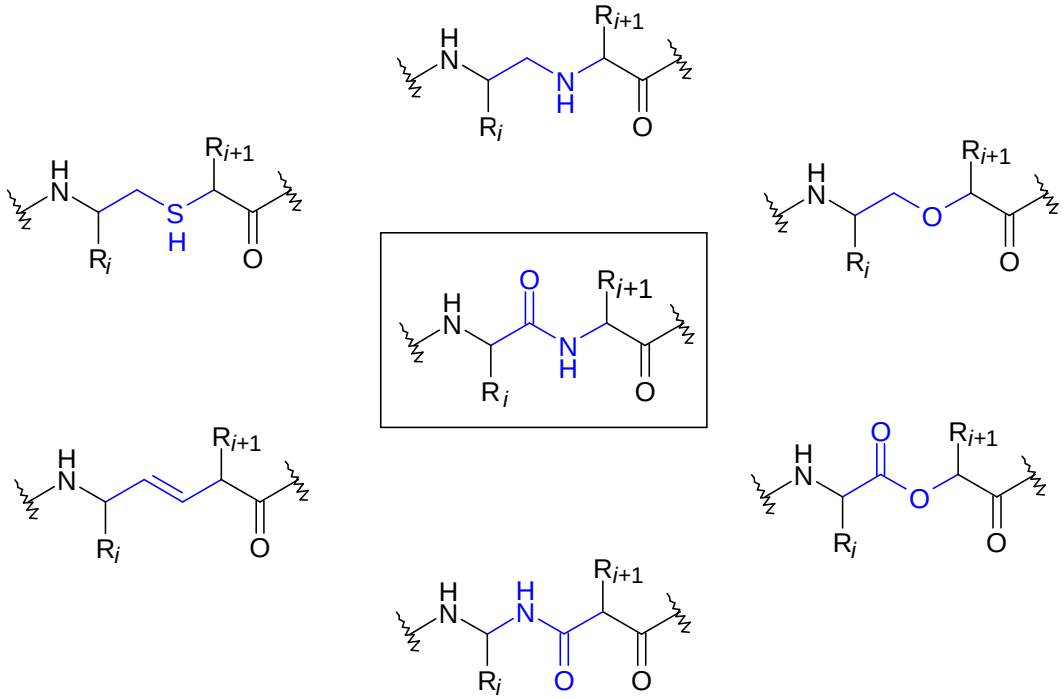

Figure 8. Examples of peptide bond isosters.

The replacement of CONH with a CH_2NH or CH_2SH can help to investigate the possible functional role of the carbonyl group. The replacement with a CH=CH is the best replacement to maintain the planarity and rigidity of the amide bond. Enkephalin analogues with the CH=CH N-terminus amide bond isoster were found to have similar activity to the original peptide, simultaneously providing protection from degradation.[15] There are also some examples of replacement of CONH with the retro amide NHCO.[16]

Chorev, Goodman, and co-workers synthesized the first highly bioactive, partially modified retro-inverso peptides, i.e. some enkephalin analogues that display higher activity than Metenkephalin and prolonged duration of action *in vitro* and *in vivo*.[17]

Another strategy for producing modified peptides is to use dehydroamino acids, cyclic amino acids and other structurally rigid mimetics because of their ability to give turns or helices.[10]

Cyclization reactions are very useful in the synthesis of peptidomimetic. The conformation of a peptide can be stabilized or blocked by the introduction of bridges of various lengths between different parts of the molecule. The bridging can either occur within a single amino acid residue, or involve several amino acid residues. Bridges can be introduced at various sites and involve various backbone regions. The bridge can be a link between two side chains, between two

backbone units, or between a side chain and backbone unit. In addition, the peptide bond can be completely or exclusively incorporated into a ring.

There are also interesting examples of cyclic peptides and peptidomimetics having a sugar moiety. Sugar amino acids offer many possibilities in the preparation of peptidomimetics with predictable conformational characteristics.

Few examples of the huge amount of available peptidomimetic compounds with structural motifs ranging from peptide chains to completely non-peptidic components are shown in Figure 9.

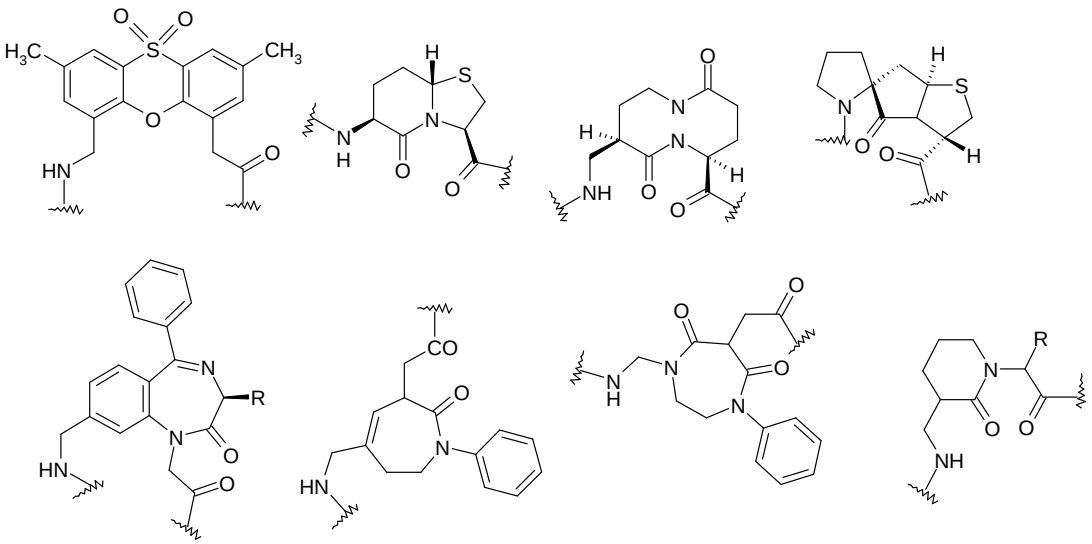

Figure 9. Structural motifs of some peptidomimetics.[18]

A peptidomimetic approach, which has emerged in recent years with significant potential, is the use of non-proteinogenic amino acids, such as β-,[19] γ-[19] and δ-amino acids,[20] in the construction of "foldamers",[21] conformationally ordered synthetic oligomers. The use of non-proteinogenic amino acids has became important because non-natural amino acid containing peptides form unique secondary structures,[19] show novel biological activities,[22] and can be used as rulers for the design of molecular devices and catalysts.[23] Non-proteinogenic amino acids can have pronounced effects on the conformation of the peptide backbone. For example, α,α-Disubstituted amino acids, such as Aib (α-aminoisobutyric acid or $C^{\alpha,\alpha}$-dimethylglycine) and α-ethylalanine,[24] rigidify the peptide backbone through the formation of helixes and β-turns.[25]

N-Substituted peptides may also exhibit enhanced hydrophobicity and improved stability to proteolytic enzymes, which can increase bioavailability and therapeutic potential.[26]

Facile synthesis is one of the most important attributes of a foldamer in the long run, as this will allow access to a wider variety of derivatized and ideally functional foldamers, but it is often underestimated that the coupling of these unusual residues is sometimes difficult, due to the amino acid structures that can complicate the amide bond formation by conventional synthetic methods.

β-strand peptidomimetics

As mentioned before, β-strands are usually found hydrogen bonded at least in pairs, forming β-sheet structures in proteins. Isolated β-strands are not common.

Many biological processes are connected with the creation of a β-sheet structure in peptide and proteins. Lack of control is often fatal. In fact, aggregation of some proteins to form insoluble β-sheet structures is responsible for a number of neurological disorders. For example, β-amyloid deposition leads to Alzheimer's disease,[27, 28] and the conversion of α-helices to larger β-sheet aggregates causes Creutzfeld-Jakob disease, BSE, and other prion diseases.[29-31]

Currently, despite their dramatic progression there is virtually no therapy for protein misfolding diseases. Therefore a better understanding of the mechanism of aggregation and the development of possible β-sheet ligands, which can slow down or prevent the pathological process, is of great interest from both a mechanistic and a therapeutic point of view. Historically mimicry of the β-strand conformation in a compound has been pursued for fundamental purposes, and subsequently it has been stimulated by the pursuit of inhibitors of enzymes such as HIV-protease and caspases. In fact, the proteases, that are involved in the synthesis and turnover of all proteins, bind their inhibitors/substrates using the same extended β-strand peptide backbone conformation or equivalent non-peptide structure.[32] The proteolytic enzymes are associated with most diseased states and their selective inhibition is a viable therapeutic strategy.

In consequence, β-strand peptidomimetics are of great interest to study biological systems such as aggregation of β-sheet structure or enzyme-substrates interaction. β-strands peptidomimetics are also of great interest to obtain inhibitors of these biological systems. We report herein few examples of β-strands mimics with a potential biological interest.

Martin and co-workers reported 1,2,3-trisubstituted cyclopropanes as peptide isosteres that mimic *β*-strand conformation to synthesize novel renin inhibitors.[33]

Strand mimetics have been developed by Hirschmann and co-workers using pyrrolinones[34] within novel scaffolds that replace the hydrolysable backbone of bioactive peptides. These mimetics are stable to protease,[35, 36] and have an extended conformation both in solution and solid states[34] (Figure 10).

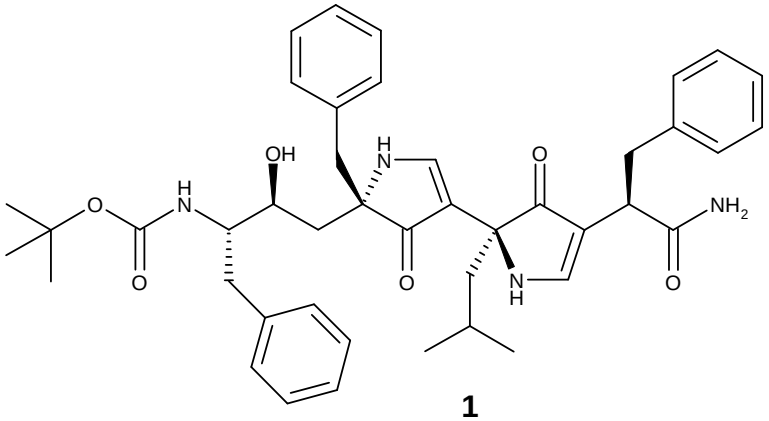

1

Figure 10. Mimetics pyrrolinone based inhibitor of HIV-1 protease.

Schrader and co-workers introduced acylated 3-aminopyrazoles as effective β-sheet ligands, which are able to stabilize an extended conformation in N/C-protected small peptides through three simultaneous hydrogen bonds on one face of a peptide strand.[37] Strands of larger size **2** (Figure 11), have been obtained by oligomerization of aminopyrazole ligands.[38] After, they developed a new class of peptide aminopyrazole hybrid compounds combining natural and unnatural amino acids, the latter derived from 3-aminopyrazole-5-carboxylic acid.[39]

Recently, Schrader and co-workers described 3-aminopyrazole derivatives and their oligomers as rationally designed non peptidic β-sheet templates that block the amyloid β-peptide aggregation. Thus, these β-sheet ligands are very interesting in the prevention of Alzheimer's disease associated with the amyloid deposition of the Aβ peptide.[40]

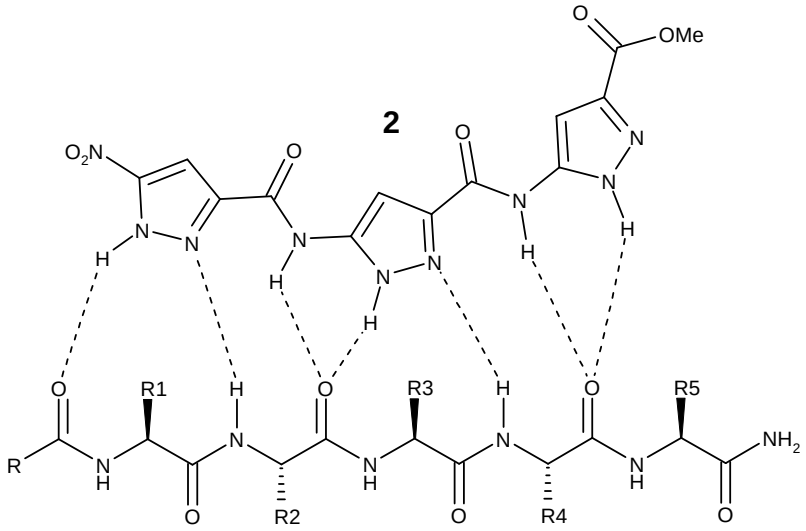

Figure 11. Schematic representation of hydrogen bonding between **2**, an aminopyrazole oligomer, and a peptide chain. Hydrogen bonds are indicated by dashed lines.

Since 1992, Nowick and co-workers reported on the development of peptidomimetic templates, which were termed "molecular scaffolds".[41] These templates have an oligourea structure. In 1996, they introduced 5-amino-2-methoxybenzamide as a β-strand mimic **3** (Figure 12).[42]

This aromatic system contains an intramolecular hydrogen bond between the oxygen atom of the methoxy group and the lone pair of the nitrogen atom of the amide bond making the receptor more rigid. To evaluate the ability of this derivative to be useful as β-strand mimic, Nowick synthesized an artificial antiparallel β-sheet **4** (Figure 12) in which the 5-amino-2-methoxybenzamide unit **3** and a diurea molecular scaffold stabilize β-sheet structure in an attached peptide strand.[42] With the goal of preparing larger artificial β-sheets, they required an extended β-strand mimic as in the case of **5** (Figure 12) a 5-hydrazino-2-methoxybenzoic acid β-strand mimic, obtained by linking two or more of these units **3** end-to-end, by the nitrogen atoms.[43] Thus, this extended β-strand mimic was applied to the creation of an artificial β-sheet.[43]

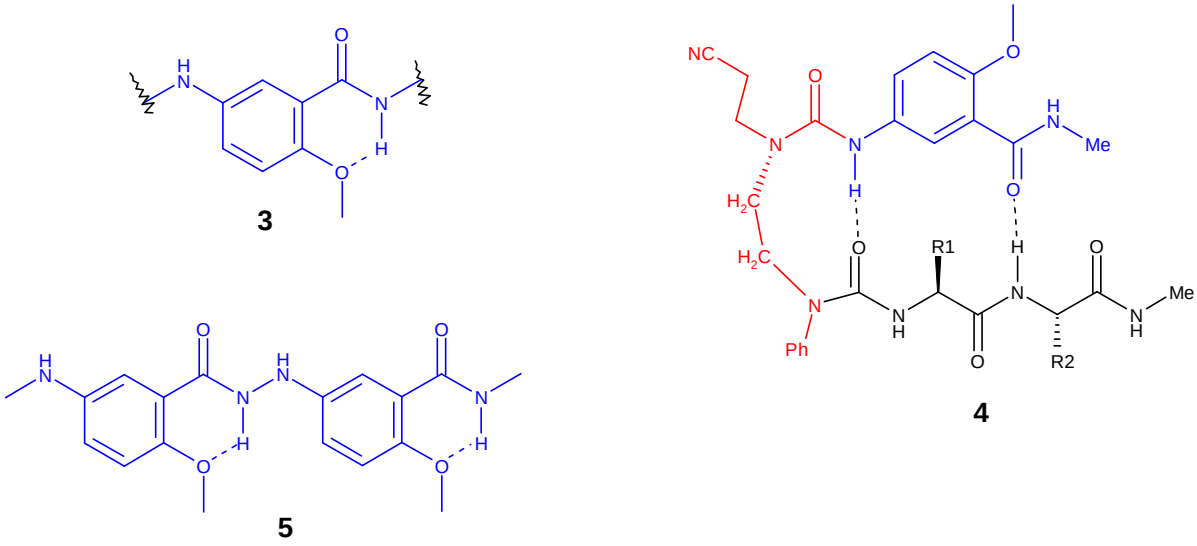

Figure 12. Schematic representation of β-strand mimics **3** and **5**, and an artificial β-sheet **4**. Hydrogen bonds are indicated by dashed lines.

Several artificial β-sheets with β-strand mimics positioned in the upper or the lower edge of the two and three-stranded β-sheets was described from Nowick and co-workers in the last years.[44-47] Currently, only a relatively scarce number of β-strand mimics have been developed and there are only few examples of biological and therapeutic applications.[48] It remains a lot of work in order to create new β-strand mimics with appropriate bioavailability characteristics and biological activities, and also to identify the importance of the β-strand structure in other examples of protein recognition.

α-Helix peptidomimetics containing δ-amino acids

As mentioned before, in the past years, the interest in a rational design of amino acid and peptide mimetics has extensively grown due to the pharmacological limitation of bioactive peptides. Numerous example of unnatural oligomeric sequences have been found that fold into well defined conformations in solution.[49, 50] Although the oligomers of β- and γ-amino acids are more extensively studied, experimental hints were also obtained for the formation of ordered structures in oligomers of δ-amino acids. However detailed structure information is still missing.

Members of the δ-peptide family are isosteric replacements of dipeptide units. As such, this is the first member of the peptidomimetics lineage in which a single unit represents two or more α-peptide repeats. Thus, δ-amino acid monomers are able to adopt the secondary structures of α-peptide sequences, particularly helices and β-turns.

In 2004, Hofmann and co-workers described on the basis of theoretical studies all possible helix types in oligomers of δ-amino acids (δ-peptides) and their stabilities.[51]

Thus far, the chemical literature has mostly involved carbopeptoid backbones. In fact, carbohydrate research produced interesting examples of new δ-amino acids as building blocks for peptidomimetic design. Sugar amino acids can adopt robust secondary turn or helical structures and they can be used as substitutes for single amino acids or dipeptide isosters **6** (Figure 13).

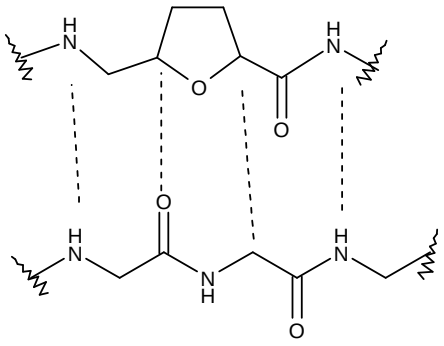

6

Figure 13. Comparison between the α-peptide subunit and the furanose-based subunit as a dipeptide isoster

Carbopeptoids,[52] homooligomers of sugar amino acids, have been prepared from both furanose[53] and pyranose[54] residues.

Motivated by the fact that *O*-glycoside oligomers of sialic acid were helical in solution,[55] Gervay and co-workers reported in 1998 that (1→5) amide-linked sialooligomers **7** longer than the trimer formed ordered secondary structures in water[56] (Figure 14). The conformational features apparently varied with chain length. After circular dichroism (CD) studies[57] and in combination with molecular medelling, the hypothesis was that for the shorter oligomers, 16-membered hydrogen-bonded rings stabilized a helix involving three residues per turn while for the octamer 22-membered hydrogen-bonding stabilized a helix involving four residues per turn. More recently, Gervay synthesized also new neuraminic acid analogues.[58]

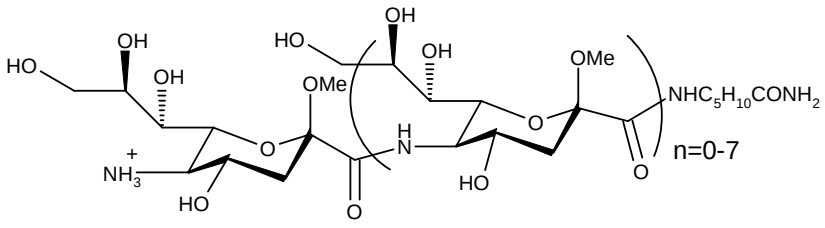

Figure 14. Amide-linked β-*O*-methoxy neuraminic acid oligomer.

In 2005, on the basis of their conformational investigations, Fleet and co-workers described an octameric chain of carbohydrate amino acids **8** that adopt in solution a left-handed helical secondary structure stabilized by 16-membered (i, i–3) interresidue hydrogen bonds (Figure 15).[20]

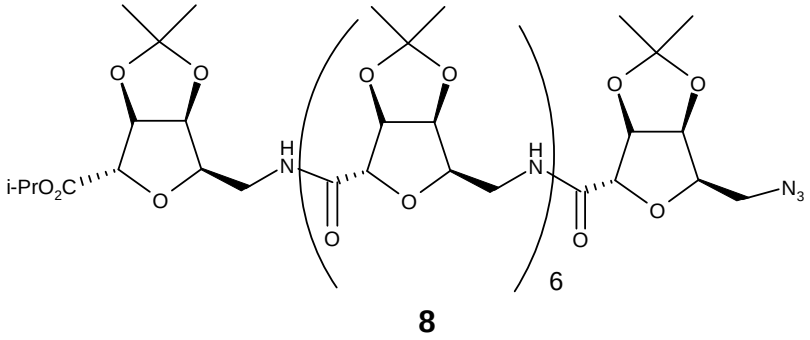

Figure 15. Octameric chain of *C*-glycosyl *α*-D-furanose configured tetrahydrofuran amino acids **8**.

Huc and co-workers reported on the stable helical conformation adopted by oligomers of a new quinoline-derived δ-amino acid **9** (Figure 16).[59, 60] This class of aromatics foldamers present the advantage that the quinoline amino acid monomers are easily accessible, functionalizable, and assembled into oligoamides. These oligomers adopt unusually stable helical conformations even in polar solvents at high temperature.

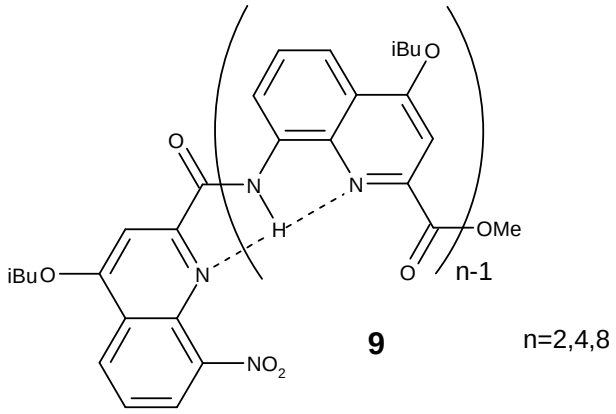

Figure 16. Structure of quinoline-derived oligoamide foldamers.

Turn peptidomimetics containing δ-amino acids

The β-turn is a common structural feature of proteins associated with the dipeptide fragment. Thus, much activity in the δ-peptide family has been aimed at creating β-turn mimics.

As in the case of helices, Hofmann and co-workers envisaged also β-turns as folding possibility, using δ-amino acid constituents.[51] In fact, since the first and the fourth amino acids of a β-turn are involved in periodic structures, the induction of the β-turn is controlled predominantly by the second and the third amino acid. So that, the replacement of this dipeptide unit by a δ-amino acid could be suitable for the induction of β-folded structures.

A long approach has involved δ-amino acid in which the "missing" amide bond is replaced by a (E)-alkene isosteres.[61-64]

Wipf and co-workers, reported in 1998, the synthesis and the evaluation of L-Ala-D-Ala dipeptide alkene isostere sequences that, for the first time, included the preparation of a (trifluoromethyl)alkene isostere.[64] It was established by X-ray studies that methyl and trifluoromethyl-substituted alkenes provided highly preorganized peptide mimetics.

The D–L methyl-(E)-alkene isostere sequence **10** preferred an intramolecularly hydrogen bonded type-II′ β-turn in the solid state, while the corresponding trifluoromethyl analogue **11** representing a L–D sequence showed a preference for a type-II β-turn (Figure 17).

10 **11**

Figure 17. Structures of alkene peptide isosteres **10**, **11**.

In 2000, Chakraborky and coworkers reported on the design and synthesis of peptidic turn mimics using the new furanoid sugar amino acids Gaa (6-amino-2,5-anhydro-6-deoxy-D-gluconic acid) **12** and Iaa (6-amino-2,5-anhydro-6-deoxy-D-idonic acid) **13** (Figure 18).[65] These amino acids were incorporated into Leu-enkephalin **14** replacing its glycine-glycine portion to give two analogues **15**. Structural analysis of these molecules showed that they have folded conformations composed of an unusual nine-membered pseudo β-turn-like structure with a strong intramolecular H-bond between LeuNH→ sugarC3-OH.

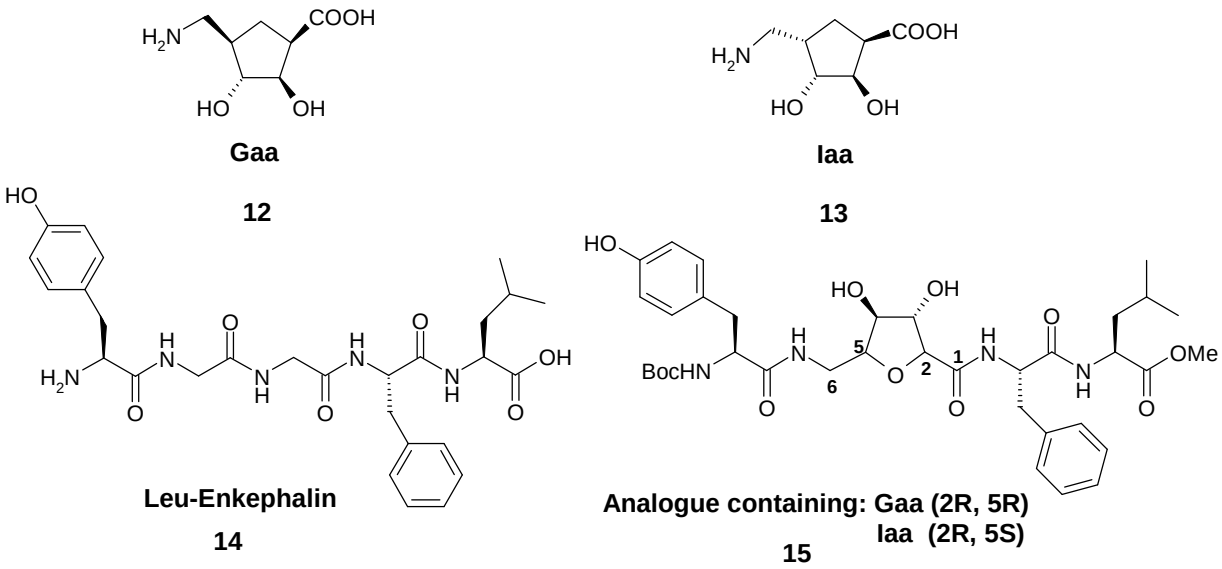

Figure 18. Furanoid sugar amino acids and their analogues.

In the course of this year, Fleet and co-worker described oxetane amino acids and oligomers **16** obtained from it (Figure 19).[66] These δ-2,4-*cis*-oxetane amino acid oligomers adopt well-defined

secondary structure in solution in which the major conformation is dictated by internal 10-membered H-bonded rings.[67] This β-turn motif is repeated along both the tetramer and hexamer.

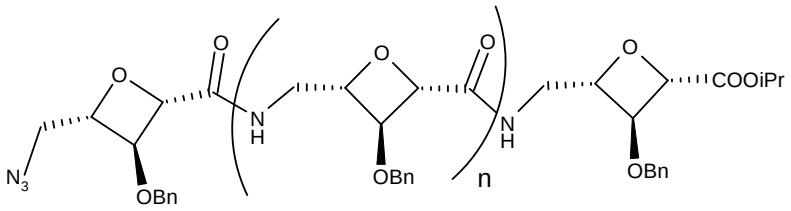

16 n=0, 2, 4

Figure 19. Structures of homo-oligomers of δ-2,4-*cis*-oxetane amino acid.

In the field of peptidomimetics, we will present in the next two chapters our work concerning the design and the synthesis of peptidomimetics as 26S proteasome inhibitors and as cyclic δ-amino acid to obtain new foldamers.

References of Chapter I

1. http://www.accessexcellence.org/RC/VL/GG/garland_PDFs/Fig_5.24.pdf.
2. Ramachandran, G. N.; Sasisekharan, V., Conformation of polypeptides and proteins. *Advan. Protein Chem.* **1968,** 23, 283-437.
3. Pauling, L.; Corey, R. B.; Branson, H. R., The structure of proteins: two hydrogen-bonded helical configurations of the polypeptide chain. *Proc. Natl. Acad. Sci. U. S. A.* **1951,** 37, 205-11.
4. Barlow, D. J.; Thornton, J. M., Helix geometry in proteins. *J. Mol. Biol.* **1988,** 201, (3), 601-19.
5. Mathews, C. K.; van Holde, K. E., *Biochemistry*. Second Edition. The Benjamin/Cummings Publishing Company, Inc.
6. Pauling, L.; Corey, R. B., Configurations of polypeptide chains with favored orientations around single bonds: two new pleated sheets. *Proc. Natl. Acad. Sci. U. S. A.* **1951,** 37, 729-40.
7. Chou, K. C.; Pottle, M.; Nemethy, G.; Ueda, Y.; Scheraga, H. A., Structure of beta-sheets. Origin of the right-handed twist and of the increased stability of antiparallel over parallel sheets. *J. Mol. Biol.* **1982,** 162, (1), 89-112.
8. Giannis, A.; Kolter, T., Peptide mimetics for receptor ligands: discovery, development, and medicinal perspectives *Angew. Chem. Int. Ed. Engl.* **1993,** 32, (9), 1244-1267.
9. Adessi, C.; Soto, C., Converting a peptide into a drug: Strategies to improve stability and bioavailability. *Curr. Med. Chem.* **2002,** 9, (9), 963-978.
10. Ramanathan, S. K.; Keeler, J.; Lee, H.-L.; Reddy, D. S.; Lushington, G.; Aube, J., Modular Synthesis of Cyclic Peptidomimetics Inspired by gamma -Turns. *Org. Lett.* **2005,** 7, (6), 1059-1062.
11. Alsina, J.; Albericio, F., Solid-phase synthesis of C-terminal modified peptides *Biopolymers* **2003,** 71, (4), 454-477.
12. Sagan, S.; Karoyan, P.; Lequin, O.; Chassaing, G.; Lavielle, S., N- and Calpha -methylation in biologically active peptides: Synthesis, structural and functional aspects. *Curr. Med. Chem.* **2004,** 11, (21), 2799-2822.
13. Luthman, K.; Hacksell, U., Peptides and peptidomimetics. *Textb. Drug Des. Discovery (3rd Ed.)* **2002**, 459-485.
14. Spatola, A. F., *Chemistry and Biochemistry of Peptides and Proteins*. Marcel Dekker: New York, **1983**, 17-37.
15. Handa, B. K.; Land, A. C.; Lord, J. A.; Morgan, B. A.; Rance, M. J.; Smith, C. F., Analogues of beta-LPH61-64 possessing selective agonist activity at mu-opiate receptors. *Eur. J. Pharmacol.* **1981,** 70, (4), 531-40.
16. Fletcher, M. D.; Campbell, M. M., Partially Modified Retro-Inverso Peptides: Development, Synthesis and Conformational Behavior. *Chem. Rev.* **1998,** 98, (2), 763-795.
17. Chorev, M.; Shavitz, R.; Goodman, M.; Minick, S.; Guillemin, R., Partially modified retro-inverso-enkephalinamides: topochemical long-acting analogs in vitro and in vivo. *Science* **1979,** 204, (4398), 1210-2.
18. Gante, J., Peptide mimetics - tailor-made enzyme inhibitors. *Angew. Chem. Int. Ed. Engl.* **1994,** 33, (17), 1699-1720
19. Seebach, D.; Beck, A. K.; Bierbaum, D. J., The world of beta - and gamma -peptides comprised of homologated proteinogenic amino acids and other components. *Chem. Biodiversity* **2004,** 1, (8), 1111-1239.

20. Claridge, T. D. W.; Long, D. D.; Baker, C. M.; Odell, B.; Grant, G. H.; Edwards, A. A.; Tranter, G. E.; Fleet, G. W. J.; Smith, M. D., Helix-Forming Carbohydrate Amino Acids. *J. Org. Chem.* **2005,** 70, (6), 2082-2090, and references therein.
21. Gellman, S. H., Foldamers: A Manifesto. *Acc. Chem. Res.* **1998,** 31, (4), 173-180.
22. Porter, E. A.; Wang, X.; Lee, H. S.; Weisblum, B.; Gellman, S. H., Non-haemolytic beta-amino-acid oligomers. *Nature* **2000,** 404, (6778), 565.
23. Sissi, C.; Rossi, P.; Felluga, F.; Formaggio, F.; Palumbo, M.; Tecilla, P.; Toniolo, C.; Scrimin, P., Dinuclear Zn(2+) complexes of synthetic heptapeptides as artificial nucleases. *J. Am. Chem. Soc.* **2001,** 123, (13), 3169-70.
24. Nagaraj, R.; Balaram, P., Solution phase synthesis of alamethicin I. *Tetrahedron* **1981,** 37, (6), 1263-70.
25. Valle, G.; Crisma, M.; Toniolo, C.; Beisswenger, R.; Rieker, A.; Jung, G., First observation of a helical peptide containing a chiral residue without a preferred screw sense. *J. Am. Chem. Soc.* **1989,** 111, (17), 6828-33.
26. Fusetani, N.; Matsunaga, S., Bioactive sponge peptides. *Chem. Rev.* **1993,** 93, (5), 1793-806.
27. Mager, P. P.; Penke, B.; Walter, R.; Harkany, T.; Hartig, W., Pathological peptide folding in Alzheimer's disease and other conformational disorders. *Curr. Med. Chem.* **2002,** 9, (19), 1763-1780, and references therein.
28. Murphy, R. M., Peptide aggregation in neurodegenerative disease. *Annu. Rev. Biomed. Eng.* **2002,** 4, 155–174.
29. Baldwin, M. A.; Cohen, F. E.; Prusiner, S. B., Prion protein isoforms, a convergence of biological and structural investigations. *J. Biol. Chem.* **1995,** 270, (33), 19197-200.
30. Harrison, P. M.; Bamborough, P.; Daggett, V.; Prusiner, S. B.; Cohen, F. E., The prion folding problem. *Curr. Opin. Struct. Biol.* **1997,** 7, (1), 53-59.
31. Prusiner, S. B., Prions. *Proc. Natl. Acad. Sci. U. S. A.* **1998,** 95, (23), 13363-13383.
32. Fairlie, D. P.; Tyndall, J. D.; Reid, R. C.; Wong, A. K.; Abbenante, G.; Scanlon, M. J.; March, D. R.; Bergman, D. A.; Chai, C. L.; Burkett, B. A., Conformational selection of inhibitors and substrates by proteolytic enzymes: implications for drug design and polypeptide processing. *J Med Chem* **2000,** 43, (7), 1271-81.
33. Martin, S. F.; Austin, R. E.; Oalmann, C. J.; Baker, W. R.; Condon, S. L.; DeLara, E.; Rosenberg, S. H.; Spina, K. P.; Stein, H. H.; Cohen, J.; Kleinert, H. D., 1,2,3-Trisubstituted cyclopropanes as conformationally restricted peptide isosteres: application to the design and synthesis of novel renin inhibitors. *J. Med. Chem.* **1992,** 35, (10), 1710-1721.
34. Smith, A. B.; Keenan, T. P.; Holcomb, R. C.; Sprengeler, P. A.; Guzman, M. C.; Wood, J. L.; Carroll, P. J.; R, H., Design, synthesis, and crystal structure of a pyrrolinone-based peptidomimetic possessing the conformation of a .beta.-strand: potential application to the design of novel inhibitors of proteolytic enzymes. *J. Am. Chem. Soc.* **1992,** 114, (26), 10672–10674.
35. Smith, A. B., III; Hirschmann, R.; Pasternak, A.; Akaishi, R.; Guzman, M. C.; Jones, D. R.; Keenan, T. P.; Sprengeler, P. A.; Darke, P. L.; Emini, E. A.; Holloway, M. K.; Schleif, W. A., Design and synthesis of peptidomimetic inhibitors of HIV-1 protease and renin. Evidence for improved transport. *J. Med. Chem.* **1994,** 37, (2), 215–218.
36. Smith, A. B.; Hirschmann, R.; Pasternak, A.; Guzman, M. C.; Yokoyama, A.; Sprengeler, P. A.; Darke, P. L.; Emini, E. A.; Schleif, W. A., Pyrrolinone-Based HIV Protease Inhibitors. Design, Synthesis, and Antiviral Activity: Evidence for Improved Transport. *J. Am. Chem. Soc.* **1995,** 117, (45), 11113–11123.
37. Kirsten, C. N.; Schrader, T. H., Intermolecular -Sheet Stabilization with Aminopyrazoles. *J. Am. Chem. Soc.* **1997,** 119, (50), 12061-12068.

38. Rzepecki, P.; Wehner, M.; Molt, O.; Zadmard, R.; Harms, K.; Schrader, T., Aminopyrazole oligomers for beta -sheet stabilization of peptides. *Synthesis* **2003**, (12), 1815-1826.
39. Rzepecki, P.; Gallmeier, H.; Geib, N.; Cernovska, K.; König, B.; and Schrader, T., New Heterocyclic -Sheet Ligands with Peptidic Recognition Elements. *J. Org. Chem.* **2004,** 69, (16), 5168-5178, and references therein.
40. Rzepecki, P.; Nagel-Steger, L.; Feuerstein, S.; Linne, U.; Molt, O.; Zadmard, R.; Aschermann, K.; Wehner, M.; Schrader, T.; Riesner, D., Prevention of Alzheimer's Disease-associated Abeta Aggregation by Rationally Designed Nonpeptidic beta -Sheet Ligands. *J. Biol. Chem.* **2004,** 279, (46), 47497-47505.
41. Nowick, J. S.; Powell, N. A.; Martinez, E. J.; Smith, E. M.; G., N., Molecular Scaffolds I: Intramolecular Hydrogen Bonding in a Family of Di- and Triureas. *J. Org. Chem.* **1992,** 57, (14), 3763–3765.
42. Nowick, J. S.; Holmes, D. L.; Mackin, G.; Noronha, G.; Shaka, A. J.; Smith, E. M., An Artificial β-Sheet Comprising a Molecular Scaffold, a β-Strand Mimic, and a Peptide Strand. *J. Am. Chem. Soc.* **1996,** 118, (11), 2764-2765.
43. Nowick, J. S.; Pairish, M.; Lee, I. Q.; Holmes, D. L.; Ziller, J. W., An Extended β-Strand Mimic for a Larger Artificial β-Sheet. *J. Am. Chem. Soc.* **1997,** 119, (23), 5413-5424.
44. Nowick, J. S.; Cary, J. M.; Tsai, J. H., A Triply Templated Artificial beta -Sheet. *J. Am. Chem. Soc.* **2001,** 123, (22), 5176-5180.
45. Nowick, J. S.; Lam, K. S.; Khasanova, T. V.; Kemnitzer, W. E.; Maitra, S.; Mee, H. T.; Liu, R., An Unnatural Amino Acid that Induces beta -Sheet Folding and Interaction in Peptides. *J. Am. Chem. Soc.* **2002,** 124, (18), 4972-4973.
46. Tsai, J. H.; Waldman, A. S.; Nowick, J. S., Two New β-Strand Mimics. *Bioorganic & Medicinal Chemistry* **1999,** 7, (1), 29-38.
47. Nowick, J. S.; Chung, D. M.; Maitra, K.; Maitra, S.; Stigers, K. D.; Sun, Y., An unnatural amino acid that mimics a tripeptide beta -strand and forms beta -sheet-like hydrogen-bonded dimers. *J. Am. Chem. Soc.* **2000,** 122, (32), 7654-7661.
48. Leung, D.; Abbenante, G.; Fairlie, D. P., Protease inhibitors: Current status and future prospects. *J. Med. Chem.* **2000,** 43, (3), 305-341, and references therein.
49. Hill, D. J.; Mio, M. J.; Prince, R. B.; Hughes, T. S.; Moore, J. S., A Field Guide to Foldamers. *Chem. Rev.* **2001,** 101, (12), 3893-4011.
50. Sanford, A. R.; Gong, B., Evolution of helical foldamers. *Curr. Org. Chem.* **2003,** 7, (16), 1649-1659.
51. Baldauf, C.; Guenther, R.; Hofmann, H.-J., delta -Peptides and delta -Amino Acids as Tools for Peptide Structure Design-A Theoretical Study. *J. Org. Chem.* **2004,** 69, (19), 6214-6220.
52. Nicolaou, K. C.; Florke, H.; Egan, M. G.; Barth, T.; Estevez, V. A., Carbonucleotoids and carbopeptoids: new carbohydrate oligomers. *Tetrahedron Lett.* **1995,** 36, (11), 1775-8.
53. Smith, M. D.; Long, D. D.; Marquess, D. G.; Claridge, T. D. W.; Fleet, G. W. J., Synthesis of oligomers of tetrahydrofuran amino acids: furanose carbopeptoids. *Chem. Commun.* **1998**, (18), 2039-2040.
54. Gervay, J.; Flaherty, T. M.; Nguyen, C., Solution phase synthesis of (1->5)-amide linked sugar amino acid dimers derived from sialic acids. *Tetrahedron Lett.* **1997,** 38, (9), 1493-1496.
55. Michon, F.; Brisson, J. R.; Jennings, H. J., Conformational differences between linear alpha (2----8)-linked homosialooligosaccharides and the epitope of the group B meningococcal polysaccharide. *Biochemistry* **1987,** 26, (25), 8399-405.

56. Szabo, L.; Smith, B. L.; McReynolds, K. D.; Parrill, A. L.; Morris, E. R.; Gervay, J., Solid Phase Synthesis and Secondary Structural Studies of (1->5) Amide-Linked Sialooligomers. *J. Org. Chem.* **1998,** 63, (4), 1074-1078.
57. McReynolds, K. D.; Gervay-Hague, J., Examining the secondary structures of unnatural peptides and carbohydrate-based compounds utilizing circular dichroism. *Tetrahedron: Asymmetry* **2000,** 11, (2), 337-362.
58. Gregar, T. Q.; Gervay-Hague, J., Synthesis of Oligomers Derived from Amide-Linked Neuraminic Acid Analogues. *J. Org. Chem.* **2004,** 69, (4), 1001-1009.
59. Jiang, H.; Leger, J.-M.; Dolain, C.; Guionneau, P.; Huc, I., Aromatic delta -peptides: design, synthesis and structural studies of helical, quinoline-derived oligoamide foldamers. *Tetrahedron* **2003,** 59, (42), 8365-8374.
60. Jiang, H.; Leger, J.-M.; Huc, I., Aromatic delta -Peptides. *J. Am. Chem. Soc.* **2003,** 125, (12), 3448-3449.
61. Gardner, R. R.; Liang, G. B.; Gellman, S. H., β-Turn and b-Hairpin Mimicry with Tetrasubstituted Alkenes. *J. Am. Chem. Soc.* **1999,** 121, (9), 1806 - 1816.
62. Gardner, R. R.; Liang, G.-B.; Gellman, S. H., An achiral dipeptide mimetic that promotes b-haipin formation. *J. Am. Chem. Soc.* **1995,** 117, (11), 3280-3281.
63. Hann, M. M.; Sammes, P. G.; Kennewell, P. D.; Taylor, J. B., On double bond isosters of the peptide bond: an enkephalin analogue. *J. Chem. Soc., Chem. Commun.* **1980,** 24, 234-235.
64. Wipf, P.; Henninger, T. C.; Geib, S. J., Methyl- and (Trifluoromethyl)alkene Peptide Isosteres: Synthesis and Evaluation of Their Potential as beta-Turn Promoters and Peptide Mimetics. *J. Org. Chem.* **1998,** 63, (18), 6088-6089 and references therein.
65. Chakraborty, T. K.; Ghosh, S.; Jayaprakash, S.; Sarma, J. A.; Ravikanth, V.; Diwan, P. V.; Nagaraj, R.; Kunwar, A. C., "Synthesis and conformational studies of peptidomimetics containing furanoid sugar amino acids and a sugar diacid". *J. Org. Chem.* **2000,** 65, (20), 6441-6457.
66. Lopez-Ortega, B.; Jenkinson, S. F.; Claridge, T. D. W.; Fleet, G. W. J., Oxetane amino acids: synthesis of tetrameric and hexameric carbopeptoids derived from L-ribo 4-(aminomethyl)-oxetan-2-carboxylic acid. *Tetrahedron Asymmetry* **2008,** 19, 976-983.
67. Claridge, T. D. W.; Lopez-Ortega, B.; Jenkinson, S. F.; Fleet, G. W. J., Secondary structural investigations into homo-oligomers of δ-2,4-*cis* oxetane amino acids. *Tetrahedron Asymmetry* **2008,** 19, 984-988.

II INHIBITORS OF THE 26S PROTEASOME

II.1. INTRODUCTION

II.1.1. Structure and Functions of the 26S Proteasome

The amount of proteins in a living cell is a balance between the rate of synthesis and the rate of degradation. The cell has different strategies to eliminate abnormal proteins or to decrease the intracellular concentration of one kind of protein. Eukaryotic cells are degraded primarily by two distinct proteolytic mechanisms. Proteins that enter the cells from extracellular compartment are degraded by lysosomes. Lysosomal-mediated breakdown is mainly involved in the degradation of intracellular proteins under stressed conditions, membrane-associated proteins or extracellular proteins taken up by endocytosis. Another more selective proteolytic mechanism, the ubiquitin-proteasome pathway (UPP), which is present in the cytosol and the nucleus, is responsible for the majority of non lysosomal proteolysis of intracellular proteins in stressed and non-stressed cellular environments. This pathway (Figure 20) which involves ATP and contains the 26S proteasome at its core, plays a primary role not only in the degradation of short-lived and long-lived proteins, which comprise the bulk of proteins in mammalian cells,[1,2] but also in the selective removal of abnormal, misfolded or incorrectly assembled proteins. In this way, UPP produces most of the antigenic peptides presented to the immune system by MHC (Major Histocompatibility Complex) class I molecules. Another important function of the UPP is in the regulation of various cellular processes such as cell cycle progression, cell differentiation, signal transduction, inflammatory and stress responses and apoptosis.[3]

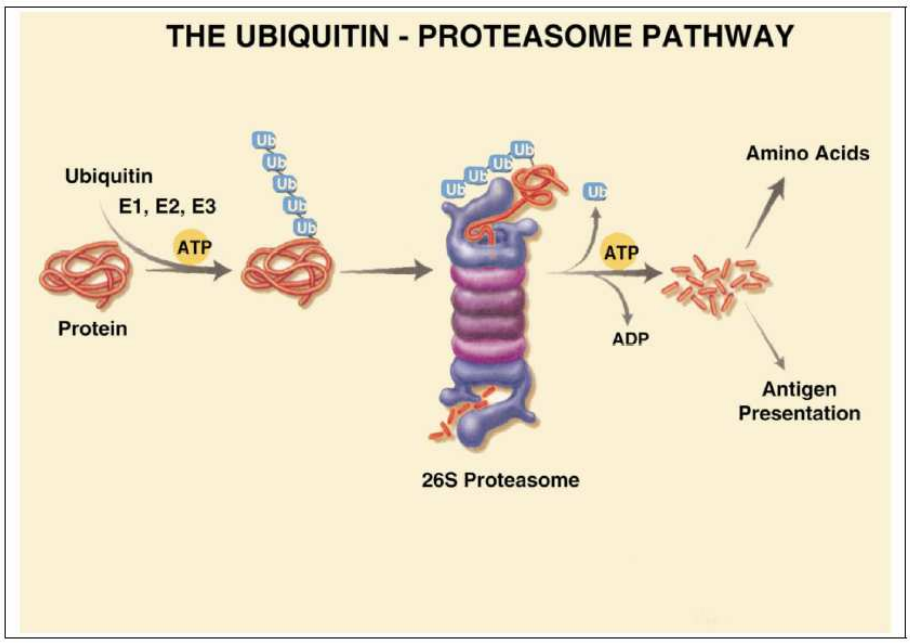

Figure 20. The simplified scheme of the ubiquitin-proteasome pathway. From Kisselev *et al.*[3] (Reproduction by courtesy of Prof. Goldberg).

The ubiquitin system

The majority of substrates of this pathway are marked for degradation by covalent attachment of multiple molecules of ubiquitin (Ub). A minimum of four Ub molecules are required for efficient targeting and destruction of proteins, whereas attachment of mono-Ub has other regulatory effects, e.g., the internalization of cell-surface proteins.[4] Ubiquitin is a small 76 amino acid protein (8,5 kDa) found throughout eukaryotic cells and is highly conserved, with only three amino acid differences between yeast and human homologues. This remarkable conservation reflects the importance of Ub's biological functions in eukaryotic cells. The conjugation of Ub to substrates is accomplished by three different enzymes:[5,6] ubiquitin-activating enzyme (E1), ubiquitin-carrier enzyme (E2), ubiquitin- ligase enzyme (E3), (Figure 21). First, a thioester bond between the C-terminal glycine of Ub and the active cysteine of E1 is formed in a ATP-dependent manner. Ub is then transferred to a cysteine of E2, again forming a thioester linkage. Finally, an E3 catalyzes the formation of an isopeptide bond between the C-terminal glycine of Ub and ε-amino group of lysine residue of a specific target protein. The E3 enzyme can recognize the protein target which is to be destroyed. In fact, it is the specificity of this enzyme that determines which proteins in the cell are to be marked for destruction in proteasome.

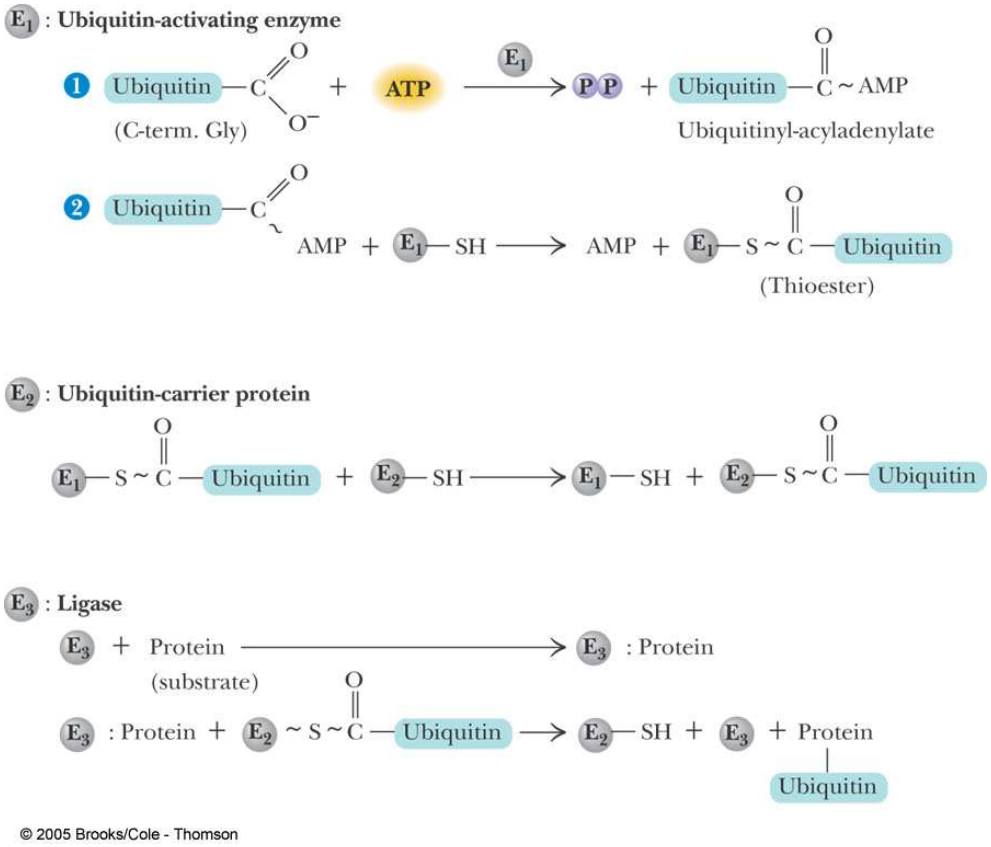

Figure 21. Enzymatic reactions in the ligation of ubiquitin to proteins.

The resulting ubiquitinylated proteins are then recognized and degraded by a 2.4 MDa proteolytic complex, the 26S proteasome.

The 26S proteasome: a multifunctional proteolytic machine

The structure and function of the proteasome are highly conserved from archaebacteria to eukaryotes. This large ATP-dependent complex consists of a proteolytic core particle, the 20S proteasome, sandwiched between two 19S "cap" regulatory complexes, also termed PA700 (Figure 22). These complexes associate together in an ATP-dependent manner.

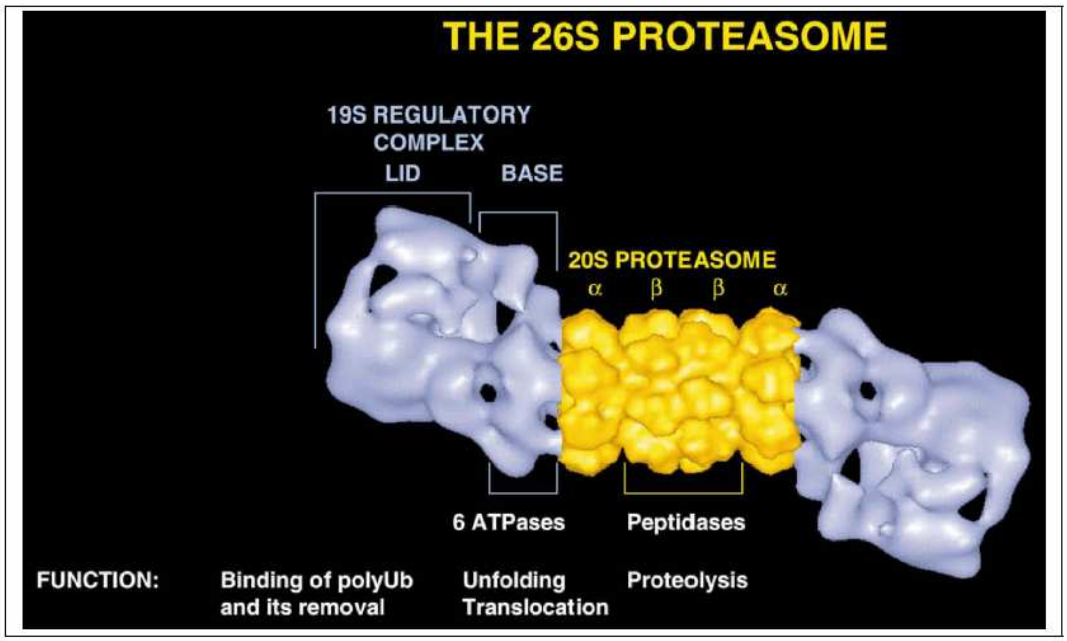

Figure22. The 26S proteasomes and its components. From Kisselev *et al*.[3] (Reproduction by courtesy of Prof. Goldberg).

The 20S proteasome

The 20 S proteasome, a 700 kDa particle, is a hollow cylindrical particle formed by four stacked rings. Each outer ring is composed of seven different α subunits, while each inner ring is composed of seven different β subunits.[7] Each β-ring contains three proteolytic active sites which differ in their specificities: the β1 subunit contains a post-acidic (PA) active site, which cleaves peptide bonds preferentially after acidic residues; the β2 is associated with a trypsin-like (T-L) activity and splits peptide bonds after basic amino acids; the β5 subunit has a chymotrypsin-like (CT-L) active site and cut after hydrophobic residues (Figure 23).[8] All the proteolytic sites utilize a N-terminal threonine residue of β-subunits as nucleophile in the hydrolysis reaction and classify the proteasome as member of the Ntn (N-terminal nucleophilic) hydrolases group.[9] The β-subunits are genetically encoded as precursors and are processed during particle maturation by autolysis. In the eukaryotic proteasome, only β1, β2, and β5 of the seven different β-subunits can be activated by this autolytic process, with the release of the amino-terminal Thr1 functioning as the nucleophile.[10] In mammalian proteasomes, γ-interferon provokes the substitution of these three active β-subunits (β1, β2,and β5) for three new β-type subunits termed "induced β-type subunits, βi": β1i, β2i, and β5i. The incorporation of the γ-interferon inducible subunits into the proteasome requires its *de novo* assembly and depends on the cell development state and the tissue type.[11,12] In this alternative

proteasome form, known as the immunoproteasome, 19S particles are replaced by the protein complexes termed PA28 or 11S. The immunoproteasome is involved in processing of antigens for presentation by MHC class I molecules.[13] In contrast to the majority of other proteases which have easily accessible active sites, proteasomes have active sites which are confined to the inner cavity of the 20S core, thereby preventing uncontrolled destruction of the bulk of cellular proteins. The X-ray crystal structure of the yeast proteasome complexed with TMC-95A[14] **43** (Figure 36, page 42) showed that in β1, β2, and β5 active sites two hydrophobic pockets, known as S1 and S3, are of fundamental importance to accommodate the substrate/inhibitor. The formation of crucial hydrogen bonds to have a non covalent interaction is generally permitted by some common amino acidic residues in the three active sites, such as Ser 20, Thr 21, Gly 47 and Ala 49 (*vide infra* chapter II.2.2 Molecular Modelling: tool for the conception, page 47, for details).

Generally, the major responsible for the formation of the S1-specificity pocket is locate in the position 45. Additionally, adjacent subunits in the β-rings to the S1 pockets contribute to their selectivity. The β1 subunit presents in position 45 a charged arginine, for this reason electrostatic interactions have a fundamental role in the activity of this subunit.

In the subunit β2, a glycine residue is situated in position 45, consequently S1 pocket in this subunit is very spacious and suitable for very large residues.

Finally, in the case of the β5 subunit we can see in the key position 45 a methionine residue, that minimize the space of the S1 pocket.

The 19S regulatory complexes control the access of substrates into the proteolytic core.

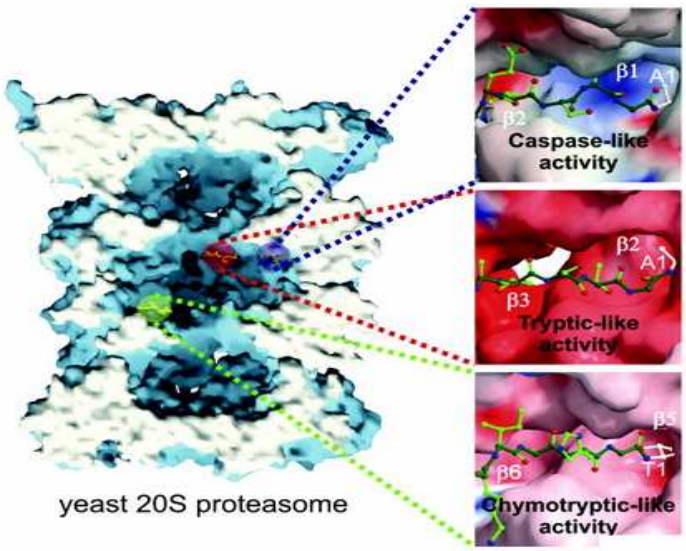

Figure23. Active sites of the 26S proteasomes. From Borissenko *et al.*[15]
(Reproduction by courtesy of Prof. Groll).

The PA700 or 19S Regulatory Complex

The PA700 or 19S Regulatory Complex provides components necessary for selective degradation of ubiquitinated proteins**.** Each 19S cap consists of a base, which associates with the 20S particle, and a lid[16] and plays a role in the recognition of substrates that have been targeted for degradation by the addition of multiple molecules of the ubiquitin. The lid binds to the polyubiquitin chain with high affinity and cleaves it away from the substrate. The base consists of eight polypeptides including six homologous ATPases of the AAA family, a superfamily of proteins with one or two nucleotide-binding domains ('AAA modules'), which often form ring-like oligomers and function as chaperones in diverse cellular processes.

The six ATPases were suggested to assemble into a ring that forms the interface of the 19S complex with the 20S core particle.[17] Several functions have been proposed for the ATPases. First, the hydrolysis of ATP by the 19S ATPases is supposed to promote the assembly of 26S proteasomes from 19S complexes and 20S proteasomes.[18-21] Second, these ATPases, interacting directly with α-rings of the 20S core particle, have a role in the ATP-depended opening of the channel in the α-rings, allowing polypeptide access into the proteolytic chamber of the 20S particle.[22] Third, substrate proteins are likely bound[23] and unfolded by the ATPases,[24] which also catalyze their translocation into 20S proteasomes.[25] In fact, the only way for substrates to reach this chamber is through the gated channels in the α-ring, which is too narrow to be traversed by tightly folded globular proteins. Deubiquitinating enzymes (DUBs or isopeptidades) in the 19S cap disassemble ubiquitin chains. Ubiquitin molecules can then be reused in degradation of other substrates. The process of deubiquitination plays an essential role in cellular ubiquitin homeostasis because the ubiquitin recycled by this process is required to maintain cellular ubiquitin at normal levels.[26,27] The mechanistic details of this recycling process, including the identity and relative roles of specific DUBs that catalyze substrate deubiquitination, have remain poorly defined.

Products Generated by the Proteasome

Target proteins are degraded in a processive manner by the 20S proteasome and the size distribution of released peptides is broad, ranging from 3 to 25 residues, with an average length of 8 to 9 amino acids.[28] Until recently, the mechanism of peptide product length control was unclear. Some of these oligopeptides are presented by MHC class I molecules on the cell surface for generation of immune response. In fact, the immunoproteasome generates oligopeptides which have higher affinity to bind

to MHC class I receptors,[29,30] but the majority of these oligopeptides are being further degraded to free amino acids by different cytosolic peptidases.

Biological role and Potential therapeutic applications

Given the fact that all mammalian cells have ubiquitin ligases and proteasomes, dysregulation of the ubiquitin-proteasome pathway (UPP) causes onset of many inherited and acquired diseases. In fact, the majority of cellular proteins are degraded by this ubiquitin- and proteasome-dependent proteolytic pathway. Among those proteins are various regulators of crucial processes, like the cell-cycle progression, apoptosis, inflammatory responses, NF-kB activation, antigen presentation, and others.[31-34] Therefore, the proteasome constitutes an interesting target for drug discovery.

Particularly, the UPP pathway has been extensively studied in human cancers, which is known to play an important role in regulating cell proliferation and cell death.[35,5] It has been well-established that through a tight regulation of cell growth inducers and growth inhibitors, an optimum balance of cell proliferation and cell death can be achieved. In cancer cells, however, an altered balance between cell growth inducers and inhibitors leads to disruption of the cell cycle, causing deregulated growth and inhibition of intrinsic apoptotic cell death pathways. Thus, proteasome inhibition is a desirable target for controlling the aberrant growth of tumor cells. Proteasome inhibitors are known to induce cell death rapidly and selectively in oncogene-transformed but not normal or untransformed cells. They are also able to trigger apoptosis in human cancer cells that are resistant to chemotherapy.[36,37]

Various inhibitors of this multicatalytic enzyme complex are already available.[3] Experiments on animal models of various diseases have shown, that they can be useful anticancer, anti-inflammatory, anticachectic and antiparasital drugs. The inhibitors are usually short peptides linked to a reactive function, generally located at their C-terminus (epoxyketone, aldehyde, boronic acid, α-ketoaldehyde, and vinyl sulfone). The reactive function interacts with the Thr1 of the proteasome with the formation of reversible or irreversible covalent adduct, while the peptide portion specifically associates with the enzyme's substrate binding pocket in the active site. Moreover, recently some non covalent inhibitors have been described. So, in this manuscript the 20S proteasome modulators covered are categorized in two broad groups: covalent and non covalent inhibitors.

II.1.2 Covalent inhibitors of the 20S proteasome

An advantage of such covalent inhibitors is that they can be used both as tools to investigate regulation of the ubiquitin-proteasomal system in different tissues and cells and as lead structures for design of fine-tuned proteasome inhibitors with perspectives for possible drug development. On the other hand, the ultimate effect of proteasome inhibitors depends on several parameters, such as cell type and the proliferation status, nature and dose of the inhibitor, and the time of the exposure.[38] In fact, long-term exposure to these compounds is toxic to nearly all cells and causes death by apoptosis. The estimation of the overall biological effect of the inhibitor treatment should be made cautiously, since many of the inhibitors affect not only the proteasome but also other cytosolic proteases. For example, peptide aldehydes and vinyl sulfones are also able to inhibit the activity of proteases such as cathepsins and calpains. The treatment with Bortezomib (Velcade®) **26** (Figure 28) the first 20S proteasome inhibitor approved for the clinical treatment of multiple myeloma and currently in use, results in severe side effects, such as peripheral neuropathy, cardiac and pulmonary disorders, gastrointestinal adverse events.

Peptide aldehydes

Peptide aldehydes were the first proteasome inhibitors to be developed.[1] In earlier studies was used calpain inhibitor I, also termed ALLN (Ac-Leu-Leu-NLeu-al) **17** (Figure 24).[39] The aldehyde forms a reversible covalent hemiacetal intermediate **21** with the hydroxyl group of the amino terminal threonine of all proteasomal β-subunits (Figure 25). Upon binding, the inhibitor adopts a β-conformation and fills the gap between two strands by forming hydrogen bonds with residues 20, 21, 47 and generating an antiparallel β-sheet structure. In eukaryotic proteasomes, ALLN **17** inhibits the chymotrypsin-like peptidase with an IC_{50} of 2.1 μM, and only with IC_{50} values > 100 μM the post-acidic and tryptic-like peptidase. This compound as inhibitor is 25-fold more potent against cathepsin B and calpain than the proteasome.[1] Generally, aldehyde inhibitors enter in cells rapidly and their effect is reversible. In fact, they have fast dissociation rates, they are rapidly oxidized in inactive carbonic acids, and they are transported out of cell by the multi-drug resistance (MDR) system carrier.[40] Many peptide aldehydes have been designed and synthesized, and some of them are now used for proteasome inhibition experiments. For example, MG132 (Z-Leu-Leu-Leu-al) **18** (Figure 24) has a leucine (instead of Nle in ALLN) that is more favourable for ligand stabilisation. This inhibitor is not only significantly more potent than ALLN to inhibit the

proteasome, but is also much more selective. A dipeptide aldehyde CEP1612, compound **19** (Figure 24), appears at least as good as **18** in potency and selectivity[41] and induces apoptosis in a panel of human tumor cell lines.

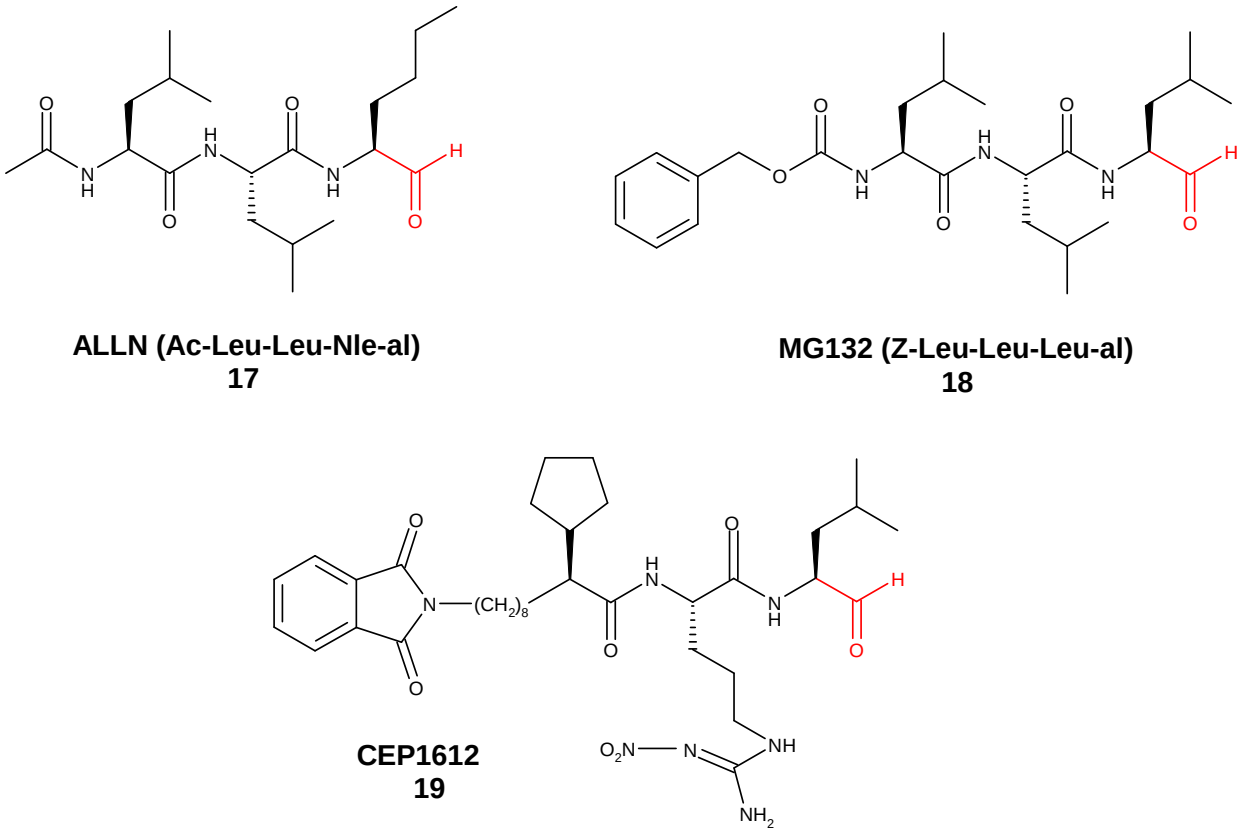

Figure 24. Example of peptide aldehydes.

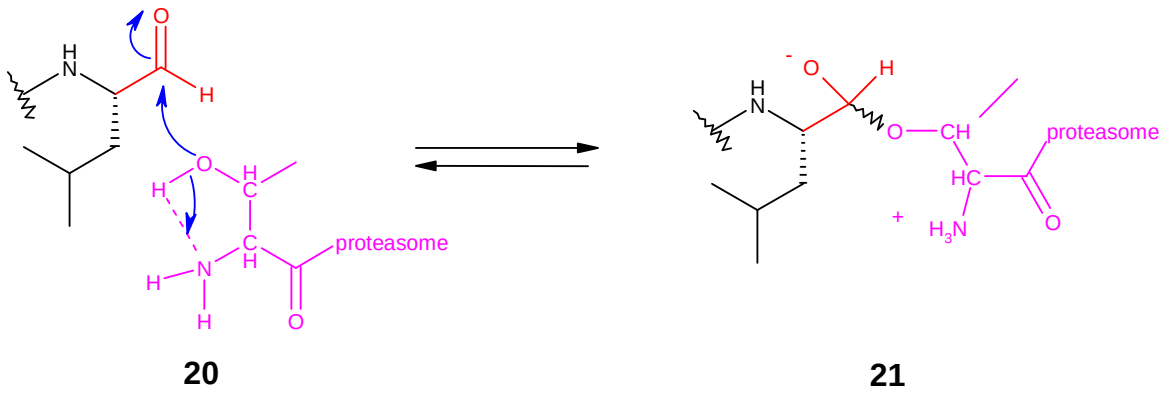

Figure 25. Mechanism of proteasome inhibition by peptide aldehydes.

Design of new bi- or multivalent proteasome inhibitors is a strategy to increase inhibitor potency. These inhibitors contain polyethylene glycol (PEG) as a spacer that is appropriate for simultaneous binding at two active sites. The spacer links two monovalent binding head groups to each other, with the formation of homo- or heterobivalent compounds.[42] Homobivalent compounds can neutralize the active subunits of the same type (β1-β1, β2-β2, β5-β5). In the case in which two different head groups are connected with PEG spacer, it is possible to obtain[31-34] a simultaneous inactivation of two distinct proteolytically active subunits (Figure 26). This hypothesis was confirmed experimentally by designing a heterobivalent inhibitor containing as head groups the tripeptide aldehydes calpain inhibitor I and Arg-Val-Arg-al.

These kinds of inhibitors are promising compounds for further investigations and applications in biomedical field.

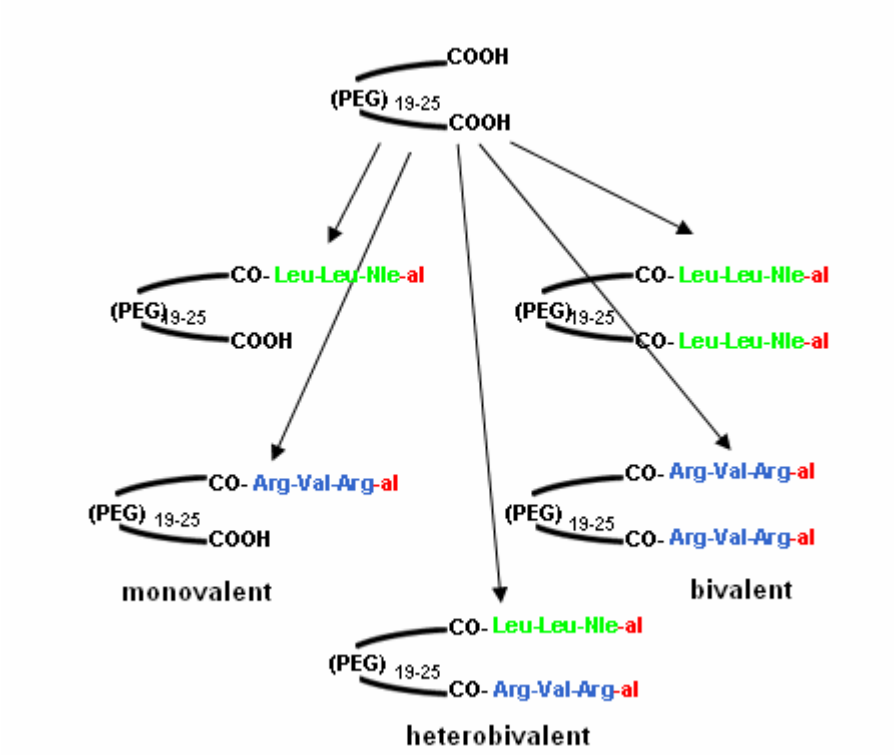

Figure 26. Strategy of creation of monovalent, bivalent, and heterobivalent PEG-peptide aldehyde conjugates.

Peptide boronates

Peptide boronates are much more potent inhibitors of proteasome than aldehydes.[43] The mechanism of inhibition for both compounds is the same, also boronates form a tetrahedral adduct **23** with the active site N-terminal threonine (Figure 27) but the boronate-proteasome adducts have much slower

dissociation rates than proteasome-aldehyde adducts. Boronates are also more selective inhibitors than aldehydes. In fact, because of the weak interactions between sulphur and boron atoms, boronates are poor inhibitors of cysteine proteases. Finally, boronates, unlike aldehydes, are not inactivated by oxidation and are not rapidly secreted from cells by MDR (J. Adams, personal communication).

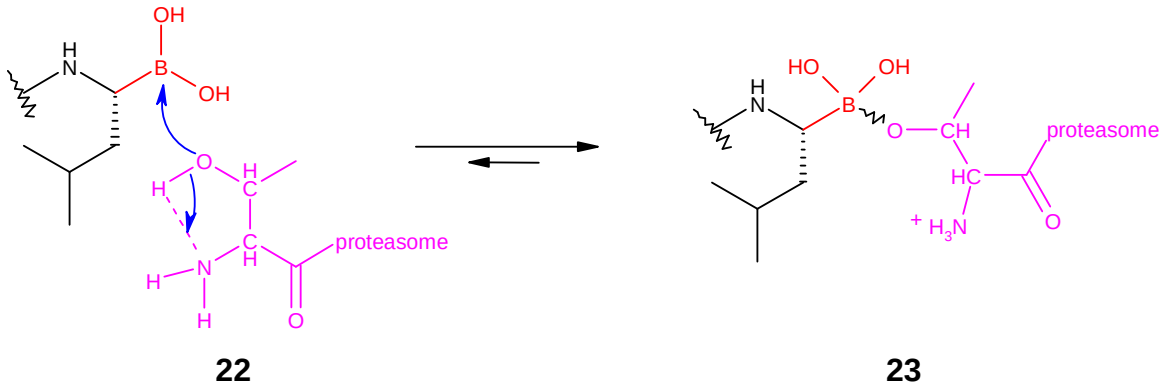

Figure 27. Mechanism of proteasome inhibition by peptide boronates.

Two peptide boronates, dansyl-Phe-Leu-boronate (DFLB) **24** and morpholino-naphthylalanine-Leu-boronate (PS-273, also termed MNLB or MG273)[3] **25** (Figure 28) were used as useful fluorescent probes to analyze proteasomal active sites in living cells.[44] Another boronic acid dipeptide derivative, PS-341 (Bortezomib, Velcade®) **26** (Figure 28) has been the first 20S proteasome inhibitor approved by the US FDA for the clinical treatment of multiple myeloma in patients who have received at least two prior therapies and have demonstrated disease progression on the last therapy.[45] Bortezomib is a covalent inhibitor of the proteasomal chymotrypsin-like activity (Ki = 0.6 nM) binding to the proteasome with very high affinity and dissociates slowly, conferring stable but reversible proteasome inhibition.[46] In the multiple myeloma the compound abrogated TNF-α induced NF-κB activation and IL-6 secretion, and decreased the binding of multiple myeloma cells to bone marrow stromal cells. The most clinically significant toxicity was cumulative dose-related peripheral sensory neuropathy. At this moment, ongoing clinical trials are evaluating bortezomib in a variety of cancers to provide critical data to confirm the activity and to clarify its potential adverse effect profile further.

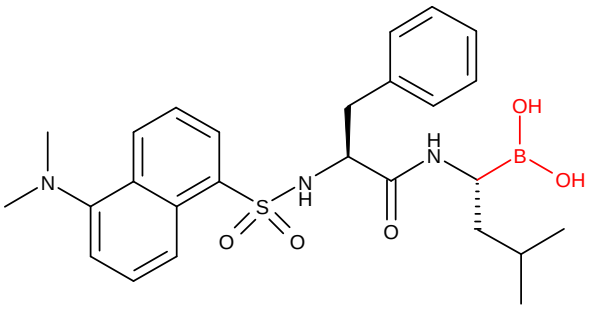

DFLB (Dansyl-Phe-Leu-boronate)
24

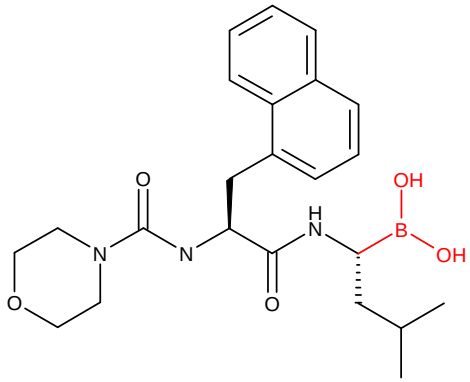

PS273 (Morpholino-Napthylalanyl-Leu-boronate)
25

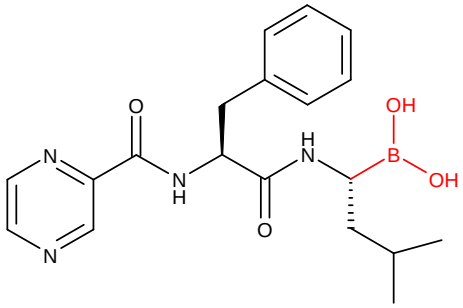

PS-341 (Pyrazylcarbonyl-Phe-Leu-boronate), Bortezomib, Velcade®
26

Figure 28. Example of peptide boronates.

Non-peptide inhibitors: Lactacystin, Salinosporamide A

Lactacystin **27** (Figure 29) is a *Streptomyces* metabolite, which was discovered by Omura and coworkers as a result of its ability to induce differentiation of cultured neuronal cells.[47] Radioactive lactacystin was shown to bind mainly to the proteasomal subunit β5,[48] effectively and irreversibly inhibiting the chymotrypsin-like activity. The trypsin-like and the post-acidic activities are also blocked, but to a lower extent.[2] Subsequent studies, however, demonstrated that lactacystin itself is not active against proteasomes *in vitro* but undergoes in aqueous solutions at pH 8 a spontaneous conversion - lactonization - to the active proteasome inhibitor, *clasto*-lactacystin β-lactone,[49] also termed 'omuralide'[50] **28** (Figure 29). It is this β-lactone which reacts with the active site Thr1 O^{γ} of the enzyme,[49] resulting in the opening of the β-lactone ring and acylation of the N-terminal threonine β5 subunit of the 20S proteasome **30** (Figure 29). This acylation has been confirmed by

X-ray crystallography studies.[7] Although the β-lactone is considered an irreversible inhibitor, the acyl ester intermediate is slowly ($t_{½} \approx 20$ h) hydrolyzed by the nucleophilic water molecule, releasing the peptide and restoring the proteolytic activity of the enzyme. The main reason for increased selectivity of omuralide for the chymotrypsin-like peptidase is the apolar nature of this site's S1 specificity pocket.

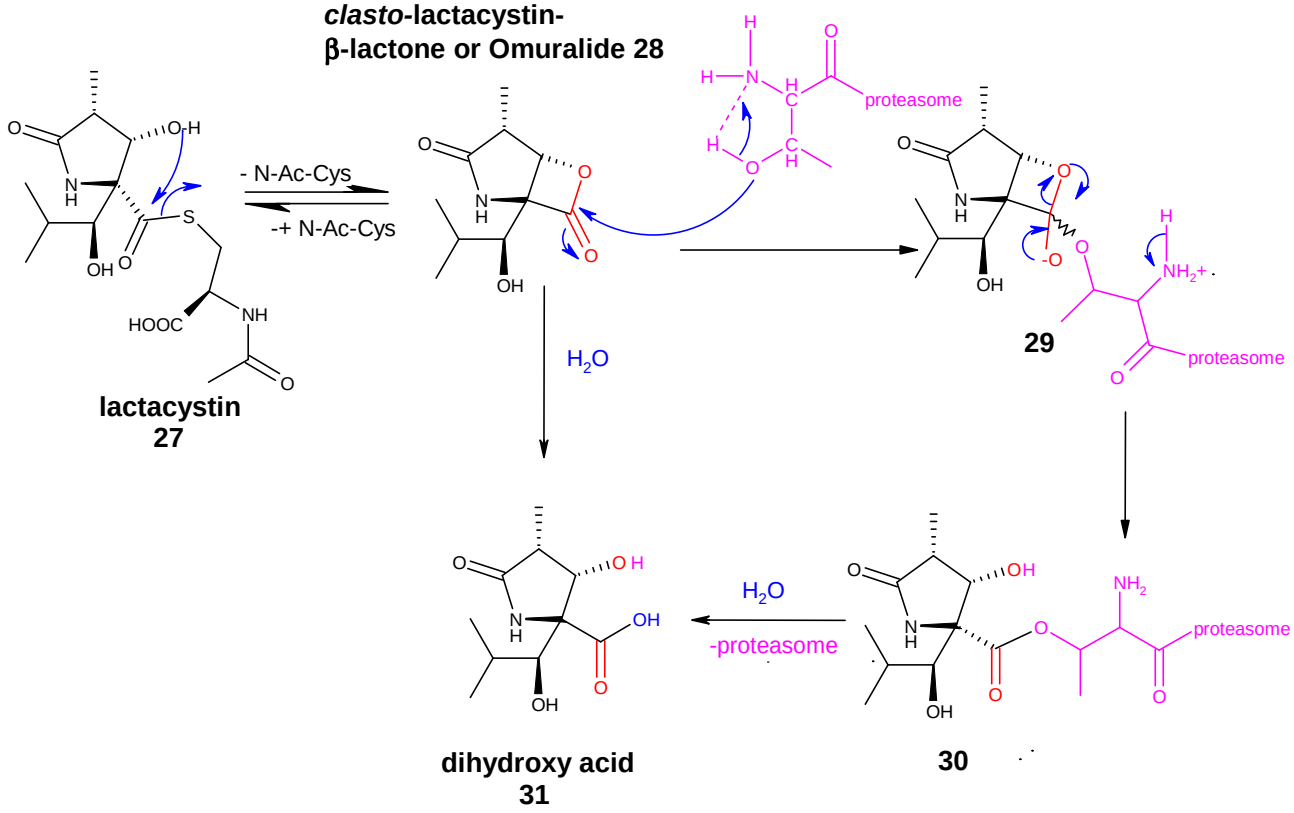

Figure 29. Mechanism of proteasome inhibition by lactacystin and its β-lactone.

A structurally related analogue of clasto-lactacystin β-lactone is Salinosporamide A (compound **32**, Figure 30) a small secondary metabolite of the marine actinomycete *Salinospora tropica*.[51] This natural product is a potent and selective inhibitor of the proteasome that exhibits low nM IC_{50} values against a broad panel of tumor cell lines and, for this reason, currently undergoing clinical studies as potential drug for cancer treatment.[52] The presence in this compound of a cyclohexene ring and a chloroethyl group in place, respectively, of the isopropyl and methyl groups of the omuralide, collectively enhances its potency both *in vitro* and *in vivo*.[53]

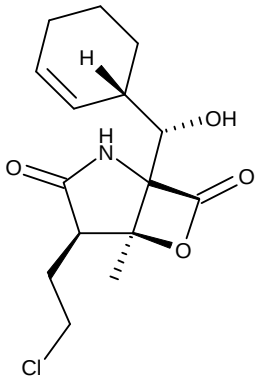

Salinosporamide A
32

Figure 30. Structure of Salinosporamide A.

Peptide vinyl sulfones

Another class of proteasome inhibitors exemplified by NLVS (NIP-Leu$_3$-vinyl sulfone) **33** (Figure 31) possesses a vinyl sulfone moiety at the C-terminus.[54]

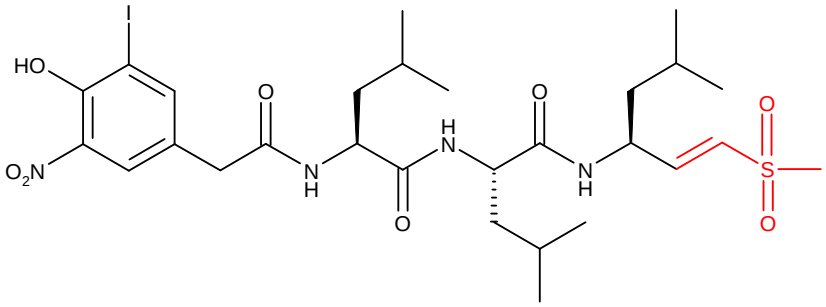

NLVS (NIP-Leu$_3$-vinyl sulfone)
33

Figure 31. Example of peptide vinyl sulfone.

This group forms an irreversible covalent adduct with the hydroxyl group of the catalytic threonine residue, acting as Michael acceptor (Figure 32). The structure of the resulting covalent adduct **36** has been determined by X-ray diffraction.[55] Peptide vinyl sulfones do not inhibit serine proteases, but they were first described as inhibitors of cysteine proteases,[56] which implies certain restrictions to their application *in vivo*. Therefore the selectivity of inhibition depends on the peptide portion of these inhibitors. Vinyl sulfones are easier to synthesize than other irreversible inhibitors of the

proteasome, and they can be used as sensitive probes to study substrate binding and specificity of the proteasome in different tissues and cells.[57]

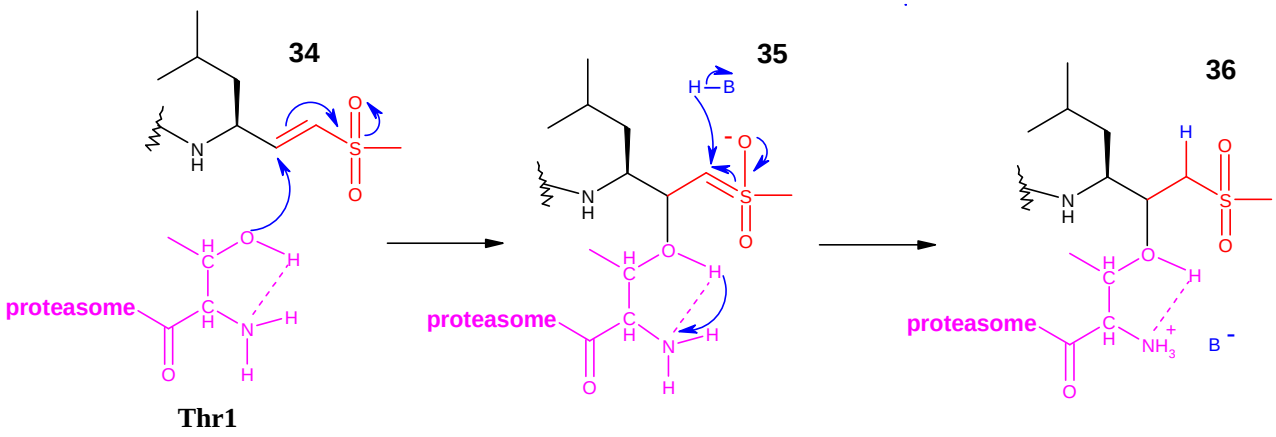

Figure 32. Mechanism of proteasome inhibition by peptide vinyl sulfone. Candidate residue for H-B are Thr1 amino terminus, a bound water molecule, and invariant Ser129 O^{γ}.

Epoxyketones

Representative examples of natural products that exert their biological effects by proteasome inhibition[58,59] are α',β'-ketoepoxides: epoxomicin **37** and eponemycin **38** (Figure 33). Epoxomicin, isolated from the actinomycete strain Q996-17,[60] was cocrystallized with the yeast *S. cerevisiae* 20S proteasome to show the specificity of this compound for the proteasome.[61] The epoxomicin **37** binds to the catalytic subunits completing an antiparallel β-sheet.[7] This natural product reacts potently and irreversibly with the chymotrypsin-like site at low concentrations,[58] while inhibits post-acidic and trypsin-like activity only at the higher concentration used to obtain the cocrystal. The less potent epoxyketone eponemycin **38** and its synthetic analogue dihydroeponemycin **39** (Figure 33) react with the post-acidic-like and chymotrypsin-like sites at similar rates.

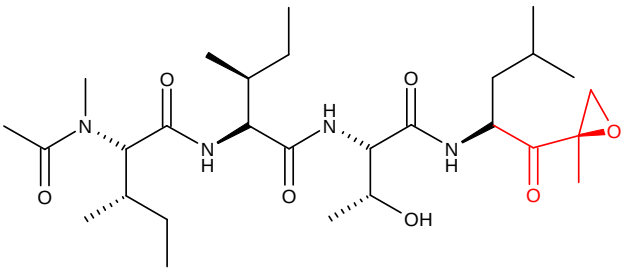

Epoxomicin (Ac(Me)-Ile-Ile-Thr-Leu-EX)
37

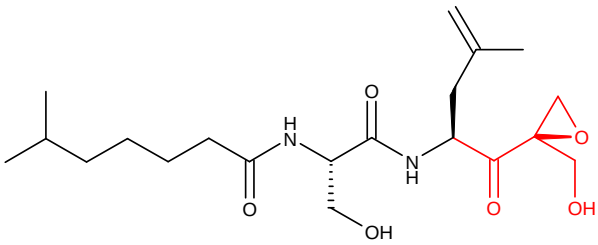

Eponemycin
38

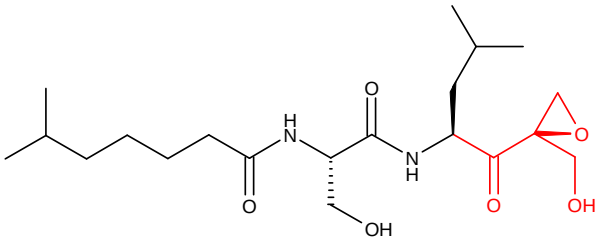

Dihydroeponemycin
39

Figure 33. Natural and synthetic α', β'-epoxyketone containing compounds.

All these compounds act by an interesting and unique mechanism, in which they react with both the hydroxyl and amino groups of the catalytic N-terminal threonine of the proteasome with formation of a morpholino ring **41** (Figure 34).[61] Epoxyketones, because of their unique mechanism, are the most selective inhibitors of the proteasome known. Epoxomicin causes cell morphology change and growth arrest, leading to apoptosis, and also exhibits anti-inflammatory activity in mice, presumably by inhibition of NF-kB activation.[58] Biotinylated derivatives of epoxomicin[62] **38** and dihydroeponemycin[63] **39** (dihydroeponemycin retains the biological activity of eponemycin) are inhibitors which can be used as active site probes.

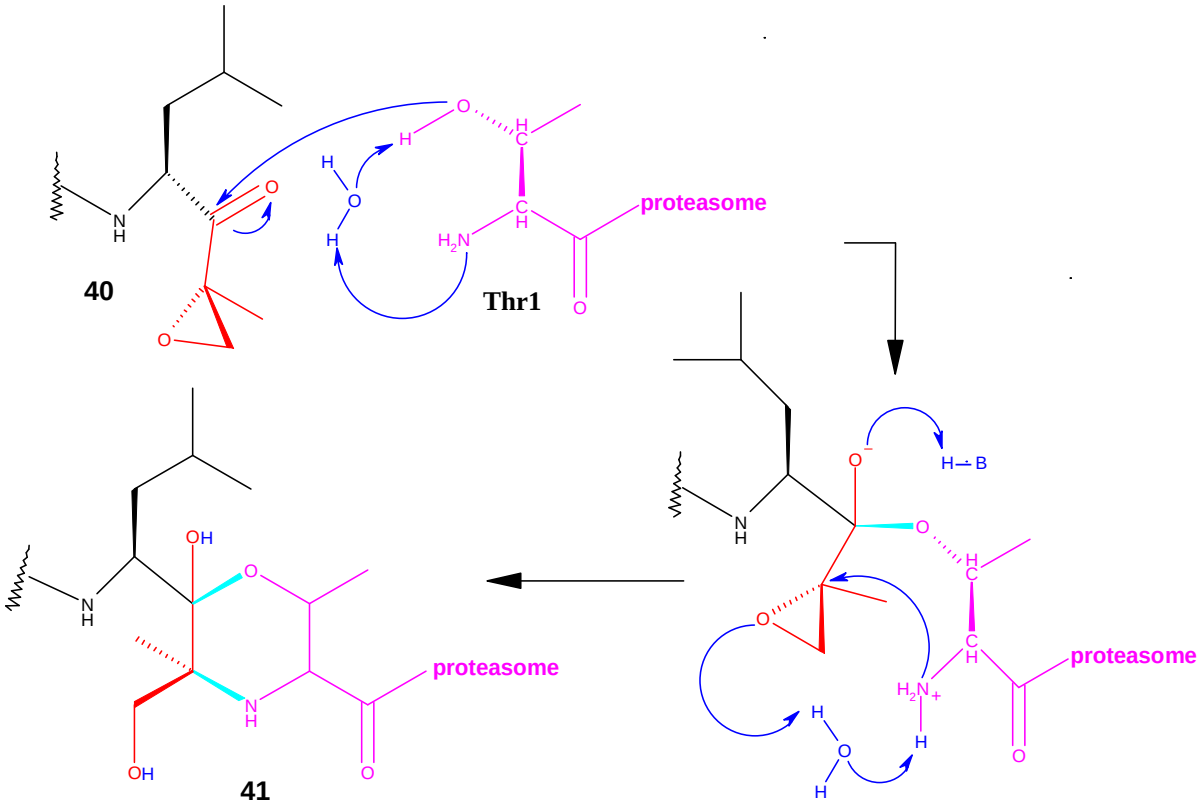

Figure 34. Schematic representation of the proposed morpholino derivative adduct formation mechanism.

II.1.3 Non Covalent inhibitors of the 20S proteasome

Application of covalent inhibitors *in vivo* often induces apoptosis and causes cell death. Thus, the covalent inhibitors of 20S proteasome by their mechanism of action if in one hand are operative, on the other hand they also can be toxic and show severe side effects.[64-66] That is why their potential in possible disease treatment is strongly limited. Identification and development of inhibitors that do not covalently modify the protein should avoid the inherent drawbacks often associated with the reactive groups used for the establishment of the covalent interaction: lack of specificity, excessive reactivity and instability. So far, non covalent inhibitors have been investigated less extensively judging from the paucity of reports on this type of compounds.

TMC-95 and Its Derivatives

The natural products from *Apiospora Montagnei*, TMC-95s (TMC-95A, B, C, D) selectively and competitively inhibit the proteolytic activity of the proteasome in the low nanomolar range.[67,68] Particularly TMC-95A has a higher effect on chymotrypsin-like activity (IC_{50} = 5.4 nM) than on trypsin-like (IC_{50} = 200 nM) and post-acidic activity (IC_{50} = 60 nM). TMC-95B inhibits these activities to the same extent as TMC-95A, while the inhibitory activities of TMC-95C and D are 20 to 150 times weaker than TMC-95A and B. All these compounds consist of a heterocyclic ring system made of modified amino acids **42** (Figure 35).

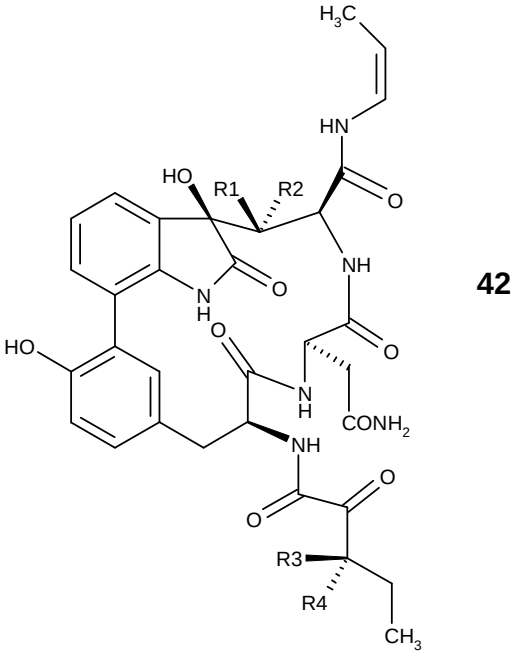

42

TMC-95	R1	R2	R3	R4
A	H	OH	CH_3	H
B	H	OH	H	CH_3
C	OH	H	CH_3	H
D	OH	H	H	CH_3

Figure 35. Chemical structure of TMC-95s including diastereomers A to D.

TMC-95A **43**, crystallized in a complex with the yeast 20S proteasome,[14] is linked non-covalently to all proteolytically active β-subunits, not modifying their N-terminal threonine residues, in contrast to all previously structurally analysed proteasome inhibitor-complexes. A tight array of hydrogen bonds connects this inhibitor with protein, stabilizing the compound in its bound status (Figure 36). The backbone of TMC-95A adopts a β-conformation and forms an antiparallel β-sheet structure in the active site. The n-propylene group of this inhibitor protrudes into the S1 pocket, making weak hydrophobic contacts with Lys33, while the side-chain of the asparagine residue is inserted deeply into the S3 pocket and has been ascribed a major role in the differing IC_{50} values

amongst the post- acidic, chymotrypsin- and trypsin-like activity. TMC-95s have been the first non-covalent and reversible inhibitors of the proteasome to be discovered.

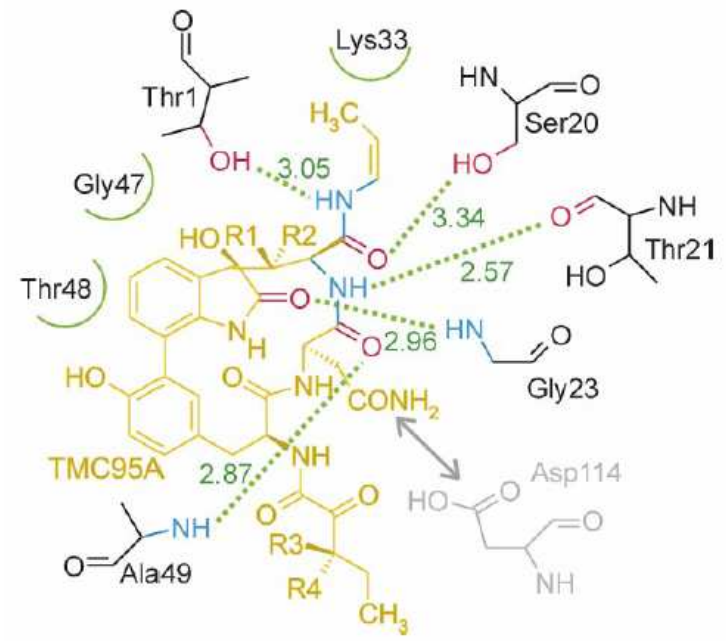

43

Figure 36. Schematic overview of TMC-95A **43** (yellow) bound to the active site of subunit β2. Hydrogen bonds with their correlated distances in Å are shown as green dashed lines. Non-polar hydrogen interactions are drawn as green cycle segments. The amino acid which is in particular responsible for the character of the S3 pocket (aspartic acid in the case of the yeast subunit β2) is shown in grey. From Groll *et al.*[14]
(Reproduction by courtesy of Prof. Groll).

Linear TMC-95 derivatives

As already mentioned, the natural constrained cyclopeptide TMC-95A **43** was the first product discovered that inhibits the proteasome noncovalently.[68] 45 linear analogues of this compound[69] were designed and evaluated. The basic idea was that the structural elements of the natural product that are required for proteasome inhibition could be identified and used to design linear TMC-95A mimics that are less difficult to prepare than TMC-95A itself or its cyclic mimics. The objective was to determine how the catalytic activities of the 20S proteasome were influenced by elements derived from TMC-95A. Therefore, the tripeptide compounds **44** and **45** (Figure 37), were synthesized and depending on the structures of the R1, R2, R3, and R4 groups, gave inhibition on all three active sites, two active sites**,** or only one active site with *K*i values of 0.32-84 μM. These

linear TMC-95 derivatives are significant inhibitors *in vitro* and in cell tumor lines and are metabolically stable.

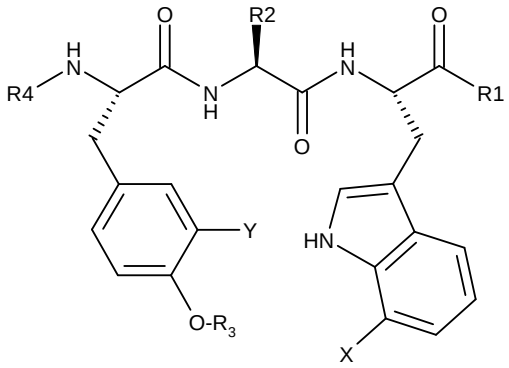

44: X = Br, Y = I
45: X = Y = H

Figure 37. Structures of linear TMC-95A-Based Proteasome Inhibitors.

2-Aminobenzylstatine Derivatives and Synthetic Analogues

A series of 2-aminobenzylstatine derivatives (Figure 38) which were originally designed to target the HIV-1 protease, have shown to inhibit non-covalently the chymotrypsin-like activity of the human 20S proteasome.[70] The SAR data generated during the optimization of this compound class has allowed to design an alternative inhibitor scaffold with reduced size and attenuated peptidic character[71] **48** (Figure 38). In this scaffold, the non-productive structural features have been removed and the critical interactions of the 2-aminobenzylstatine inhibitors have been incorporated or mimicked. The two crucial amide bonds flanking the valine residue and the C-terminal phenol group filling the S1 pocket are preserved whereas the statine moiety is replaced by a 3,4,5-trimethoxy-*L*-phenylalanine residue. This nonproteinogenic amino acid is able to form exactly the same interactions with the S3 pocket as the entire 2-aminobenzylstatine moiety. The two other critical pharmacophore features, i.e., the *tert*-leucine side chain and the hydrophobic N-terminal group, are mimicked in the prototype compound by a single phenoxy substituted benzylic N-terminal group. Molecular studies suggested that the two phenyl rings of this bulky N-terminal group present a spatial arrangement adequate to simultaneously fill the AS1 and AS2 accessory hydrophobic pockets.

This compound, potent and selective, blocks the chymotrypsin-like activity with IC_{50} = 15 nM. That is why, it is an interesting tool for investigations of proteasome function in many aspects of cellular regulation. In addition, the high antiproliferative activity obtained is encouraging to develop an anticancer drug based on the concept of proteasome inhibition.

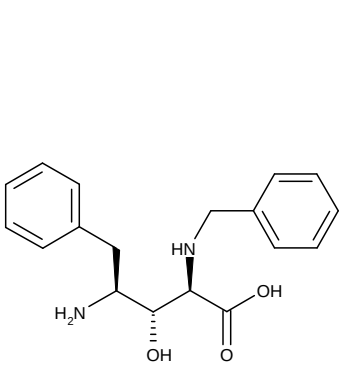

2-Aminobenzyl-substituted statine building block
46

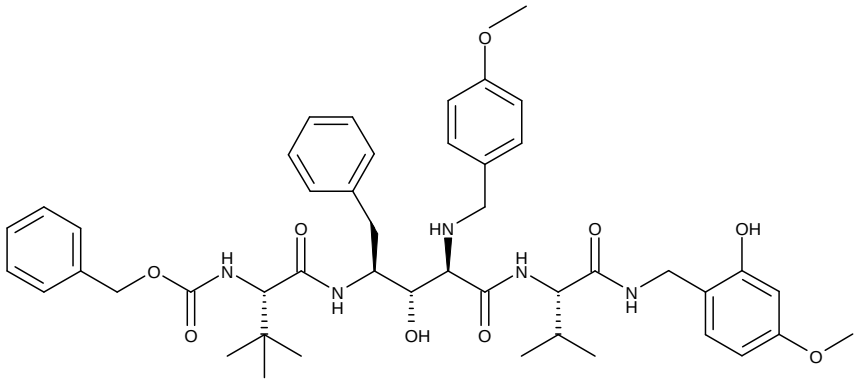

2-Aminobenzyl-substituted statine derivative
47

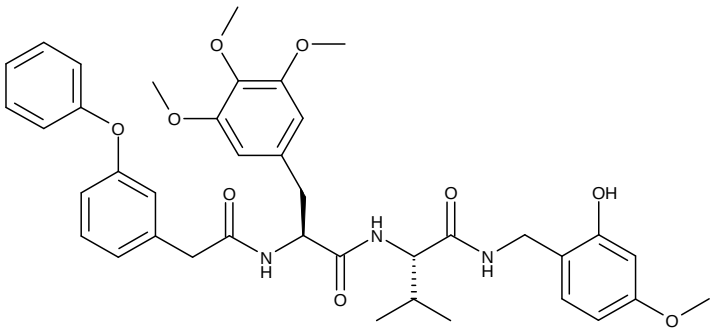

Analogue of 2-Aminobenzylstatine
48

Figure 38. 2-Aminobenzylstatine derivatives and their synthetic analogue **48**.

Lipopeptides

The lipopeptides[72] are a new class of non-covalent inhibitors. If was postulated that adding a large aliphatic blocking group to the N-terminus of a short peptide that is known to inhibit proteasome activities would make it a better inhibitor. The ability of these compounds to inhibit at micromolar concentrations chymotrypsin-like and post-acid activities depends on peptide length (3 or 6 amino acids), sequence (presence of a positively or negatively charged amino acid), and alkyl chain length (C6–C18). These structural features could be varied to selectively inhibit one or more of the three proteasome activities. The best result was obtained with compound **49** (Figure 39) that inhibited

rabbit 20S proteasome with an inhibitory effect increased (CT-L and PA with Ki = 18 and 15 nM, respectively) or decreased (T-L, Ki = 80 nM) by a factor of 2 compared to yeast 20S proteasome.

$CH_3–(CH_2)_{14}–CO–YEL$

49

Figure 39. Lipotripeptide proteasome inhibitor.

New potential drugs

Clinical studies with Bortezomib **26** (Figure 28) have validated the proteasome as a therapeutic target for the treatment of multiple myeloma and non-Hodgkin's lymphoma. However, significant toxicities have restricted the intensity of bortezomib dosing. Therefore, clinical evaluation of additional proteasome inhibitor classes is warranted. Currently, three irreversible proteasome inhibitors are under development: (*a*) salinosporamide A (NPI-0052)[52, 53] **32** (Figure 30) a natural product related to lactacytsin, as mentioned before (*b*) PR-171 (Carfilzomib)[73] **50** (Figure 40) a modified peptide related to the natural product epoxomicin and (*c*) CEP-18770[74] **51** (Figure 40).

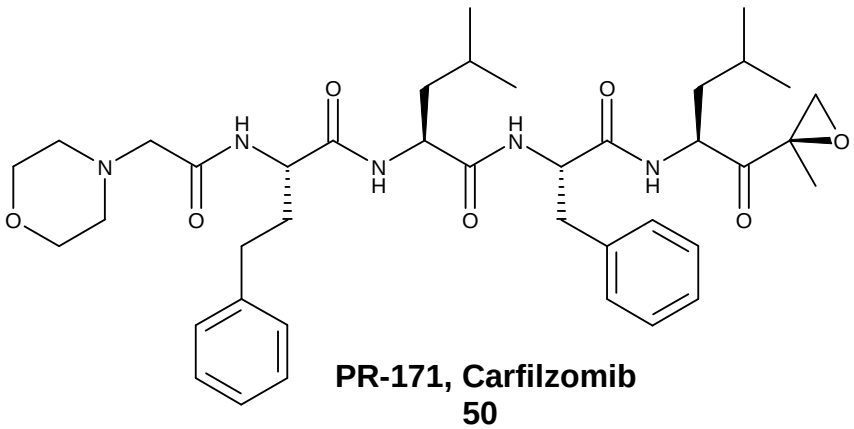

PR-171, Carfilzomib
50

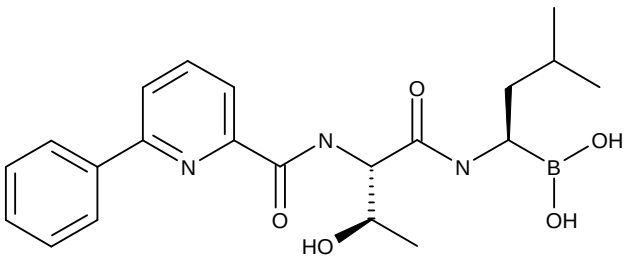

CEP-18770
51

Figure 40. New inhibitors of the proteasome.

II.2. Objectives and Design

II.2.1. Objectives

Noncovalent inhibitors of the 20S proteasome have been investigated less extensively, although they should have weaker side effects in therapeutic applications, as already mentioned in chap II.1.3. The inherent drawbacks of the classical protease inhibitors (e.g., non-target specific, too reactive or unstable) prompted us to focus our efforts in developing new molecules that have no reactive group ("warhead") that could react with the catalytic O^{γ}-Thr1 of the proteasome. Thus, the goal of our work was the design and the synthesis of new peptidomimetics able to bind the proteasome non-covalently and to modulate its function, in particular to inhibit its activity.

A peptidomimetic, as discussed above, is a compound containing non-peptidic structural elements that is capable of mimicking or blocking the biological action of a natural parent peptide.[75] The advantages of these molecules in comparison with native peptides are a possible improvement of pharmacological properties and the increase of metabolic stability, oral availability and cell-permeability. The requirements for the peptidomimetics are a few or no peptide bonds, a low molecular weight and a similar pharmacophore to have an analogous binding mode of the natural peptide.

Regarding the non covalent inhibition of the active sites of the proteasome core particle, we could note, for example in the case of TMC-95A **43** that the inhibitor interacts with two peptidic chains of the proteasome active site by adopting a β-conformation and forming an antiparallel three strands β-sheet (by filling a gap between strands including residues 20, 21 and 47, 49 in particular). We could also note that parts of the inhibitor fill two pockets S1 and S3 of the active site of the proteasome. These concepts will form the basis for the development of new synthetic non covalent proteasome inhibitors as promising drugs.

II.2.2. Molecular Modelling: tool for the conception

We have carried out computer simulations in the hope of understanding the properties of assemblies of molecules in terms of their structure and the microscopic interactions between them. This serves as a complement to conventional experiments, enabling us to learn something new. The use of theoretic methods to obtain models that allow predicting structures, properties and molecular interactions is known as "Molecular Modelling".

Molecular structures generated *in silico* have to be geometry optimized to find the individual energy minimum state by applying a molecular mechanics method. This is a method employed to calculate molecular geometries and energies. In the framework of the molecular mechanics method the atoms in molecules are treated as rubber balls of different sizes (atom types) joined together by springs of varying length (bonds). For calculating the potential energy of the atomic ensemble Hooke's law is used. In the course of a calculation the total energy is minimized with respect to atomic coordinates where:

$$E_{tot} = E_{str} + E_{bend} + E_{tors} + E_{vdw} + E_{elec}$$

where E_{tot} is the total energy of the molecule, E_{str} is the bond-stretching energy term, E_{bend} is the angle-bending energy term, E_{tors} is the torsional energy term, E_{vdw} is the van der Waals energy term, and E_{elec} is the electrostatic energy term. Molecular mechanics enables the calculation of the total steric energy of a molecule. The set of parameters consisting of equilibrium bond lengths, bond angles, partial charge values, force constants and van der Waals parameters is known as the *force field*. In our work was used the MMFF94 Force Field[76] that was developed as a combined "organic/protein" force field, one which was equally applicable to small molecules as well as proteins and other systems of biological importance.

The technique known as energy minimization is used by molecular mechanics only to find the local energy minimum but not implicitly the global energy minimum. Lower energy states are more stable and are commonly investigated because of their role in chemical and biological processes. Molecules can be modeled either in vacuum or in the presence of a solvent. Simulations of systems in vacuum are referred to as *gas-phase* simulations, while those that include the presence of solvent molecules are referred to as *explicit solvent* simulations. In another type of simulation, the effect of solvent is estimated using an empirical mathematical expression; these are known as *implicit solvation* simulations. In our work the molecular modelling was performed in vacuum.

In order to design new proteasome inhibitors, we first studied the known inhibitors and tried to establish which parts of these inhibitors were essential for the proteasome inhibitor activity, meaning that we had to point out some structure-activity-relationships. For this purpose we extracted from the PDB (Protein Data Bank) the known inhibitors crystallised in the active sites of the 20S proteasome from yeast. Three inhibitors were described in the PDB: TMC-95A[14] (PDB code: 1JD2) **43** (Figure 36) morpholino adduct of epoxomicin [61] (PDB code: 1G65) **41** (Figure 34) and ALLN[7] (PDB code: 1RYP) **17** (Figure 24). In the three cases the active site used to obtain the complex with the inhibitor was not always the same, but all the three inhibitors were able to bind and block all active subunits, also if with different activities. For this reason, we decided not to choose a specific active site in our study.

Then, by using the Sybyl program (version 7.0) we studied the structure and the interactions of the two covalent inhibitors (morpholino adduct of epoxomicin **41** and ALLN **17**) and the non covalent inhibitor (TMC-95A **43**) into the proteasome.

For all three inhibitors we found some constant interactions: hydrogen bonds between the CO and the NH of Thr21; the CO of Gly47 and the NH of Ala49 (Figure 41). In the case of TMC-95A **43** hydrogen bonds with the NH of Gly23 and with the COOH of the lateral chain of Asp114 are also observed. In the case of morpholino adduct of epoxomicin **41**, hydrogen bond with Asp114 is also observed. We could note that for these three inhibitors there is an interaction with the proteasome mediated by hydrogen bonds implicating in particular residues 21, 47 and 49 with the formation of an antiparallel β-sheet between the inhibitor and the amino acid residues of the binding pockets.[15] We could also note that hydrophobic parts of the three inhibitors occupied the two pockets S1 and S3 of the active sites of the proteasome (Figure 41).

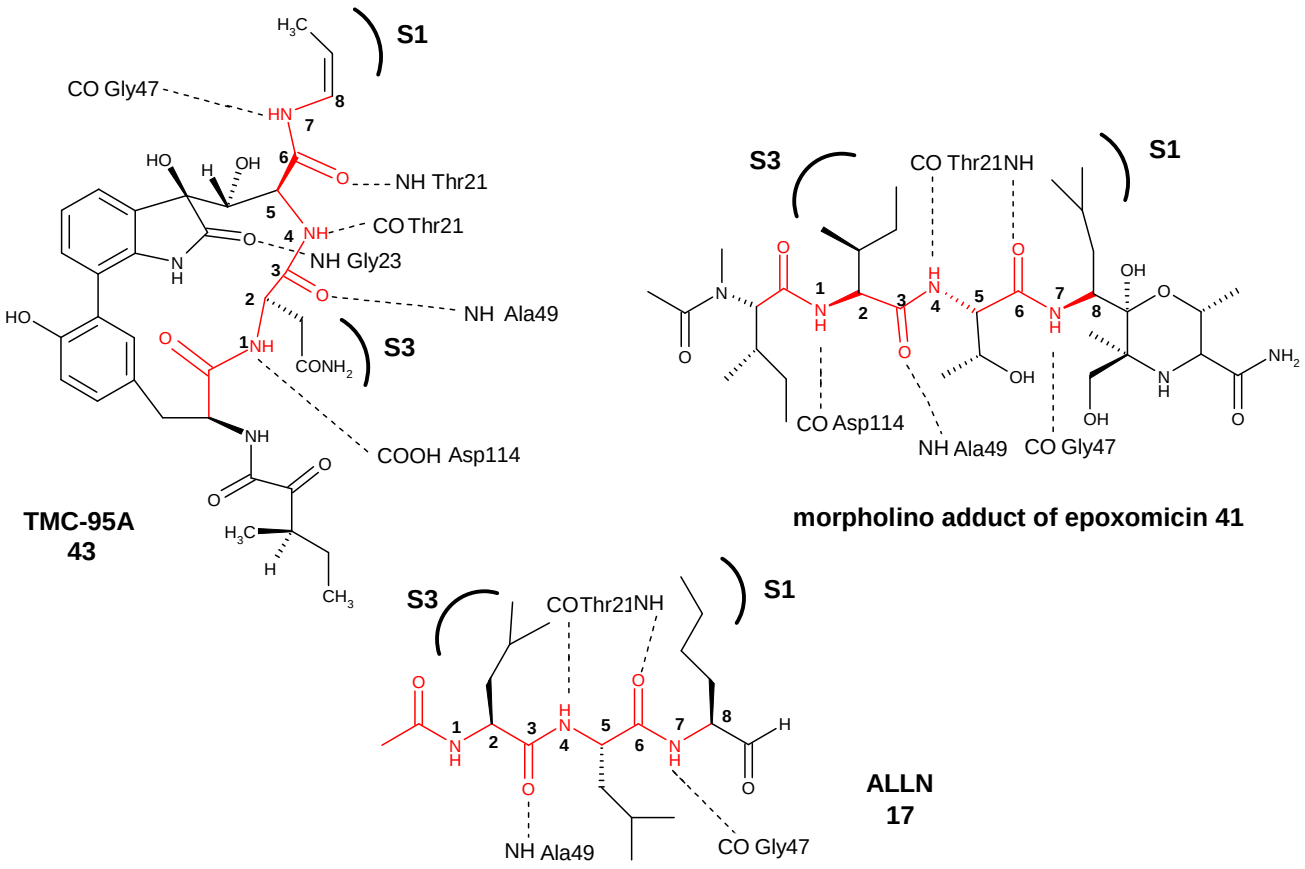

Figure 41. Overview of TMC-95A, morpholino adduct of epoxomicin and ALLN bound to the active site of the proteasome.

In the second time we checked the ability of superposition of these inhibitors. Therefore, we tried to compare TMC95-A **43** and morpholino adduct of epoxomicin **41**, by superposing points from 1 to 8 (Figure 41). Both molecules were kept fixed in the conformation adopted in the proteasome binding site.

It resulted in a good superposition of the eight atoms, in particular the ones that contract the hydrogen bonds with residue 21, 47 and 49. More, the superposition indicates that the S1 and S3 pockets are occupied in a unique way by the corresponding residues of the inhibitors (Figure 42). The superposition has also been achieved between morpholino adduct of epoxomicin **41** and ALLN **17** and resulted in a good superposition as well.

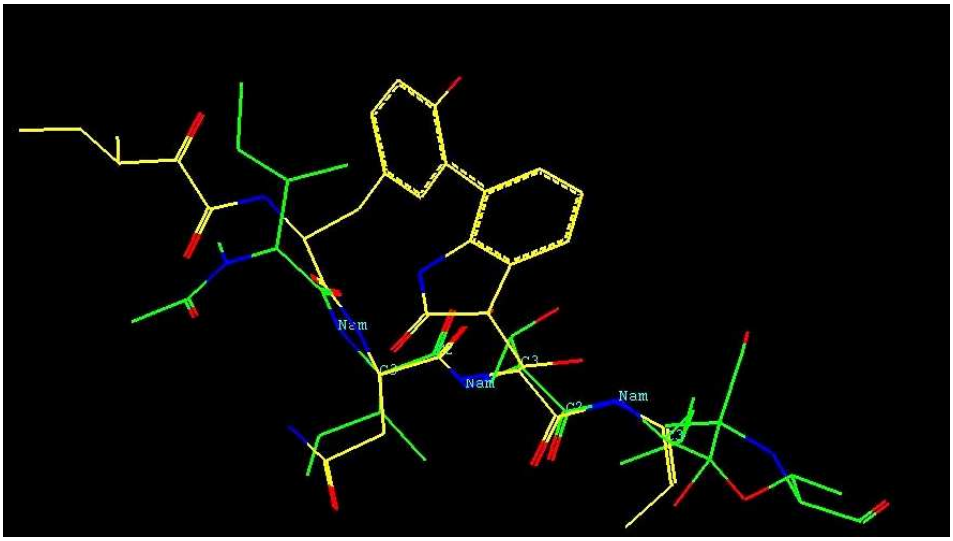

Figure 42. Result of the superposition in eight points between TMC-95A **43** (yellow) and morpholino adduct of epoxomicin **41** (green). Hydrogen atoms are omitted for clarity.

The pharmaceutical company Novartis described the molecule **48**[71] (Figure 38) that inhibits the 20S proteasome in a non covalent mode and that is highly specific for the chymotrypsin-like activity.

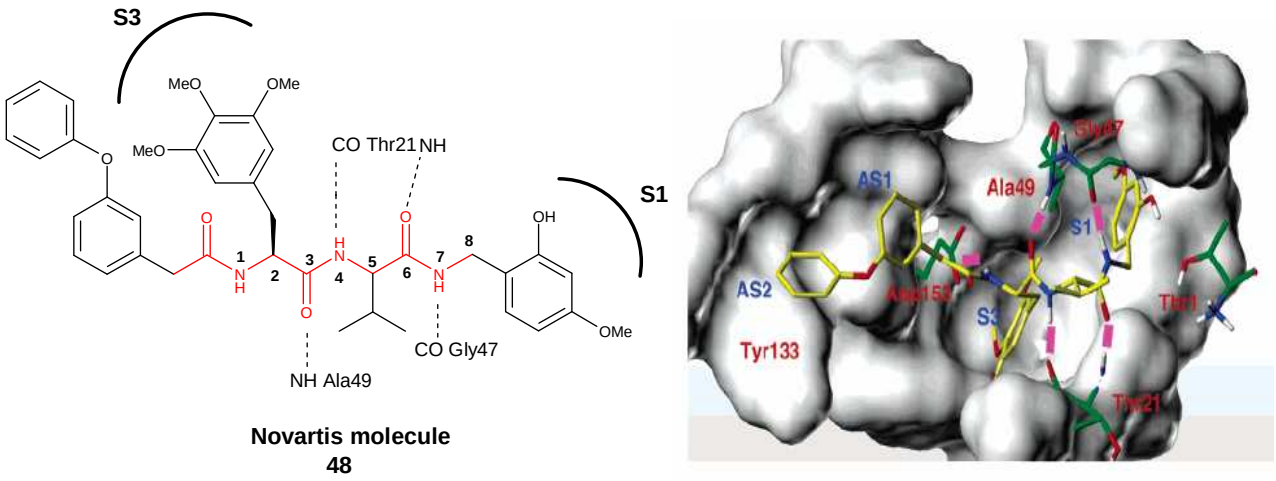

Figure 43. Left: chemical structure of Novartis molecule **48** showing the correspondence between their respective chemical moieties in terms of interaction with the proteasome binding site. Right: model of designed Novartis molecule bound to the CT-L active site into the proteasome. Hydrogen bonds are shown in magenta. From Furet *et al.*[71] (Reproduction by courtesy of Dr. Garcia-Echeverria).

This molecule was not crystallized into the proteasome but it was studied by molecular modelling.[77] It was shown that it contracts similar hydrogen bonds with residues of the active site of proteasome than the three previous inhibitors. In fact, four β-sheet like hydrogen bonds are formed between the amide bonds flanking the valine residue of the inhibitor and the residues Thr 21, Gly 47, and Ala 49.

These hydrogen bonds place the inhibitor in the active site in such a way that its C-terminal phenol and 3,4,5-trimethoxy-L-phenylalanine moieties fill the S1 and S3 pockets, respectively. The N-terminal group with its two phenyl rings also form favourable interactions with the active site by occupying small accessory hydrophobic pockets AS1 and AS2. By the help of molecular modelling we obtained **48** in our study by using the following steps:

- Construction of the molecule **48**.
- Choice of the conformation that gives the best superposition with adduct of epoxomicin **41** (points 1-8).
- Minimisation.
- Superposition between **48** and morpholino adduct of epoxomicin **41** (points 1-8).
- Further minimisation.
- Insertion of the resulting molecule **48** in the active site of the crystallised yeast 20S proteasome,[61] after that morpholino adduct of epoxomicin **41** was removed, in order to check the presence of the all fundamental interactions (hydrogen bonds, filling of the pockets…).

The superposition between **48** and morpholino adduct of epoxomicin **41** was satisfactory (Figure 44).

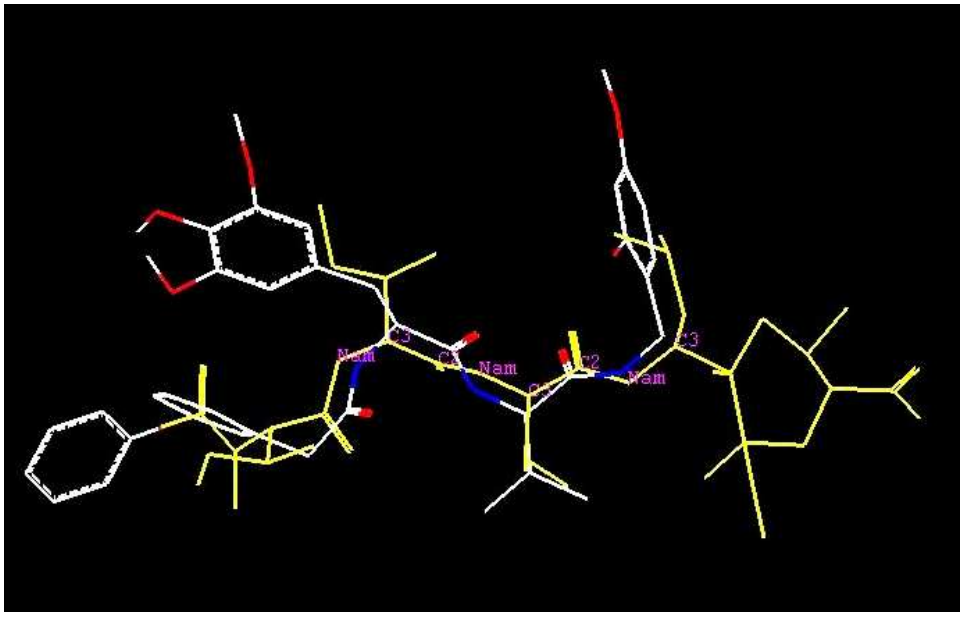

Figure 44. Result of the superposition in eight points between Novartis molecule **48** (white) and morpholino adduct of epoxomicin **41** (yellow). Hydrogen atoms are omitted for clarity.

We decided to use this molecule as our starting point for the design of new proteasome inhibitors.For the design of new inhibitors we will follow the same procedure described above, considering this time the molecule **48** as the molecule of reference for the superposition.

II.2.3. Design

As already mentioned, after the discovery of the natural compound TMC-95s **42** (Figure 35) as the first non covalent inhibitors, the pharmaceutical company Novartis developed the peptidomimetic compound **48** (Figure 38) a non covalent chymotrypsin-like activity inhibitor. Modulation of this enzymatic activity by β-subunit-specific inhibitors may convey an anti tumor effect by induction of cell cycle arrest and apoptosis in tumor cells.[78,79]

As described before, the peptidomimetic **48** inhibits the proteasome in a non covalent manner by hydrogen bonds formation with residues 21, 47 and 49, and by hydrophobic interactions with S1 and S3 pockets.

Our goal was to obtain by a simple and reproducible synthesis molecules of small size which met the following criteria:

- To be peptidomimetic compounds.
- To be able to contract essential hydrogen bonds in particular with Thr 21, Gly 47, and Ala 49 in the active sites of the proteasome.
- To be able to fill the S1 and S3 pockets and potentially the small accessory hydrophobic pockets AS1 and AS2.
- To be able to interact in a β-sheet like manner by forming an antiparallel β-sheet in particular with residue 21 on a side and residues 47-49 on the other side.
- To inhibit the proteasome without forming an adduct with the catalytic threonine residue.

We used Novartis molecule **48** as our point of start and we tried to strengthen its ability to form a β arm. In particular, we decided to replace the valine residue and the C-terminal phenol group of **48** by peptidomimetic fragment structure.

The subject of this presented PhD work was completely new in our laboratory but we had experience in the design and the synthesis of molecular tongs containing amino acid mimetic fragments, inhibitors of HIV-1 protease dimerization.[80] To be more precise, we incorporated in our molecular tongs a 5-amino-2-methoxybenzhydrazide group described by Nowick[81] as a rigid peptidomimetic able to stabilise a β-sheet.[80]

So we decided to incorporate this rigid peptidomimetic group in our molecules potentially proteasome inhibitors. To that purpose we replaced the valine residue and the C-terminal residue of Novartis molecule by a 5-amino-2-methoxybenzhydrazide derivative in molecule **52** (Figure 45).

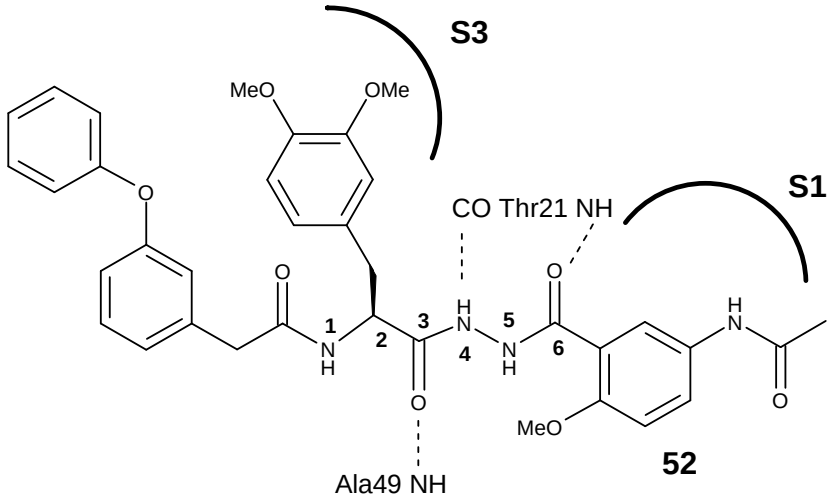

Figure 45. Structure and potential interactions of compound **52**.

We reasoned that this peptidomimetic group could stabilise the β-sheet like structure and that the aromatic ring could fill the S1 pocket, while the 3,4-dimethoxyphenylalanine should fill the S3 pocket. 3,4-dimethoxyphenylalanine was proposed in a first time because it is commercially available and a proteasome inhibitor was also described with it.[71] While 3,4,5-trimethoxyphenylalanine gave better results[71] but has to be synthesized. Essential hydrogen bonds with Thr 21 and Ala 49 should be contracted while no NH is available in molecule **52** to make a hydrogen bond with the CO of Gly47 (Figure 45). Superposition between Novartis molecule **48** and **52** is shown in Figure 46.

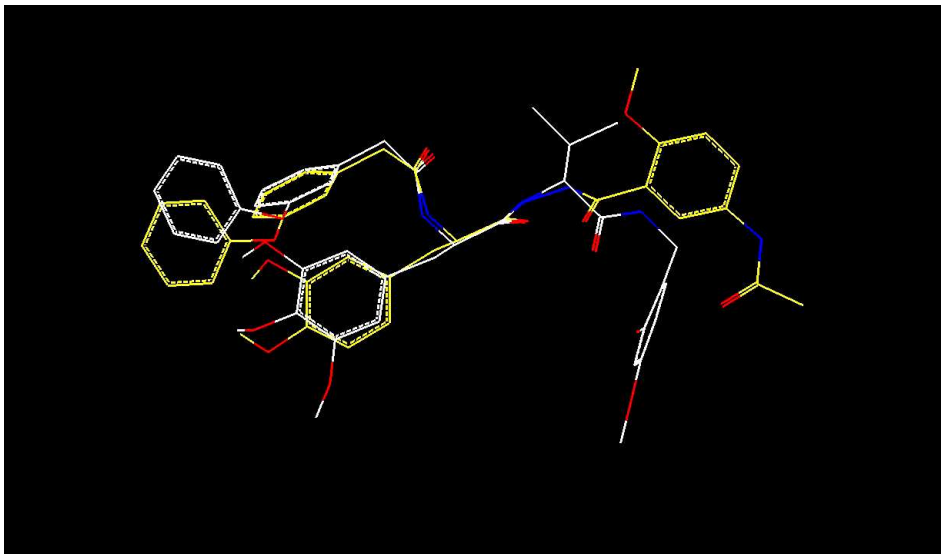

Figure 46. Result of the superposition in six points between Novartis molecule **48** (white) and molecule **52** (yellow). Hydrogen atoms are omitted for clarity.

Unfortunately at 100 μM, no inhibition could be observed on the post-acidic, trypsin- and chymotrypsin-like activities of the 20S proteasome of rabbit. It is known that the active site of the

proteasome is narrow and not easily reachable. Maybe compound **52** was too rigid and too bulky to enter in the core particle (CP) of the proteasome.

In parallel of this first objective and as part of ongoing investigations into the design of proteasome inhibitors and the development of new trifluoromethyl peptidomimetics,[82-87] we have decided to design less rigid molecule and to incorporate fluorinated peptidomimetics.

Fluorine has become a fundamental tool in the development of drugs.[88,89] Trifluoromethylated compounds are particularly important, as shown by the number of CF_3-containing drugs and drug-candidates in clinical use or in development. The introduction of one or more fluorines into a molecule modifies its physicochemical and/or biological properties:

- The C—F bond has a relatively important ionic character and a strong energy that increases metabolic stability of the fluorinated compound.
- Replacing some of the hydrogen by fluorine atoms can enhance the hydrophobicity and then strengthen the interaction with a hydrophobic pocket of the enzyme.
- Fluoroalkyl groups are strong electron-withdrawing substituents, and consequently, the acidity of neighbouring hydrogen atoms is greatly increased. The presence of fluorine atoms enhances the ability of its neighbouring function to donate a hydrogen bond ($\alpha_2{}^H$) (acidity) and lowers its ability to accept hydrogen bond ($_{\beta 2}{}^H$) (basicity).
- The trifluoromethyl group can mimic several naturally occurring functional groups such as methyl, isopropyl and phenyl, and consequently can have an effect on the conformational equilibrium of a molecule. For this reason, a non negligible impact is possible on the affinity.
- Fluorine is a poor acceptor of hydrogen bond. Most of the examples of H---F bonds reported in the literature concern intramolecular hydrogen bonds (fluoroalcohols, fluorophenols, and fluoroanilines).[90,91] Hydrogen bonds between fluorinated substrates and biological macromolecules have been postulated in some enzyme-substrate complexes. However, it is rather difficult to determine if these hydrogen bonds really exist: other factors may stabilize the conformation corresponding to the short H---F interatomic distance (distance between 2.0 and 2.3Å) considered as criterion to determine the existence of hydrogen bond with F.

The possibility to modify or modulate the pharmacological profile of a molecule by inserting fluorine atoms clearly explains why the bioorganic and medicinal chemistry of fluorine has become so important. The incorporation of a trifluoromethyl group into peptidomimetics to produce potent inhibitors of various enzymes has been extensively studied.

One example are the trifluoromethyl (Tfm)-malic peptidomimetics that are micromolar inhibitor of some metalloproteinases, proteolytic enzymes involved in the degradation of the extracellular matrix.[92] Another example of the use of fluorine to improve drug properties is represented by the fluoroartemisinins, metabolically more stable antimalarial artemisinin derivatives.[93]

We have developed new trifluoromethyl inhibitors based on the trifluoromethyl-β-hydrazino acid scaffold **53** (Figure 47).

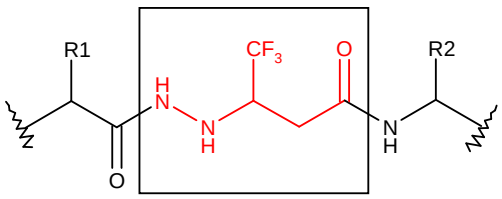

53

Figure 47. New trifluoromethyl-β-hydrazino acid scaffold **53**.

To overcome some of the pharmaceutical limitations inherent in peptides, hydrazino-azapeptoids[94] and more recently retro hydrazino-azapeptoids[95] were described as covalent proteasome inhibitors of the CT-L activity with IC_{50} ranging from 50 to 500 μM.

β-hydrazino acids are peptidomimetic building blocks that have two nitrogen atoms. They can be considered to be analogues of β-amino acids in which the amine group has been replaced by a hydrazine. But while the β-amino acids are well documented,[96-98] almost nothing is known about these peptidomimetics. Obviously, these structures can mimic the typical secondary structure of native α-peptides, making them useful tools with which to design new protease inhibitors. To our knowledge, the synthesis of CF_3-β-hydrazino acid has not been reported. This scaffold was also chosen because it has a trifluoromethyl group, which can greatly improve the acidity of the neighbouring hydrazine functional group and thus increase its hydrogen bond donor ability.[88] Finally, the elongation of the backbone may introduce flexibility, thus facilitating the putative interaction of substituants R_1 and R_2 with the enzyme S1 and S3 pockets.

Five compounds **54**-**58** (Figure 48) were designed and synthesized.

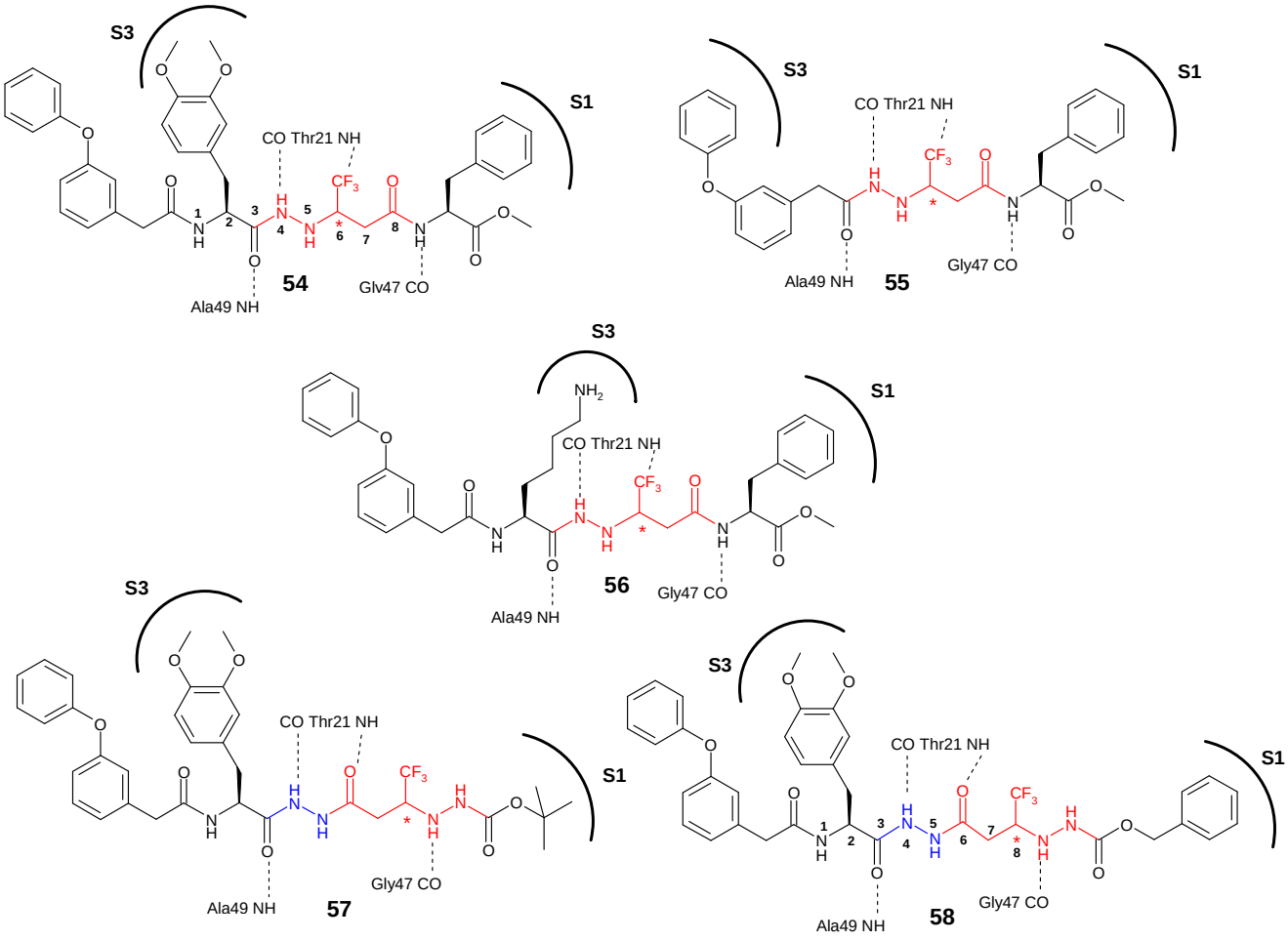

Figure 48. Designed trifluoromethyl-β-hydrazino compounds **54-58**.

The N-terminus of our starting molecule **54** was inspired by aminobenzylstatine derivatives,[71] which interact with the S3 pocket and, by the phenoxysubstituted benzylic *N*-terminal group, with the AS1 and AS2 accessory hydrophobic pockets. The smaller analogous **55** have been also designed. Replacing the 3,4-dimethoxyphenylalanine amino acid by the more hydrophilic lysine amino acid in molecule **56** could facilitate the interaction of the aspartic residues in the S3 pocket of the T-L active site with εNH$_2$ group.[99,69] It should also increase the solubility of the compound.

The phenyl group of the C-terminal phenylalanine of molecules **54-56** was assumed to occupy the S1 pocket. In the case of molecules **57** and **58** we decided to combine the similar Novartis motif with our scaffold that this time is inverted (Figure 49) to study the eventual change on the inhibition effect.

Figure 49. New trifluoromethyl-β-hydrazino acid scaffold regular **53** and inverse **59**.

For synthetic reasons we added in these two molecules another hydrazine group as a link between the scaffold and the N-terminal part of the molecule. In this way it was also possible to form the hydrogen bonds with the residue Thr 21 in the active site of the proteasome. The hydrazino group of the scaffold was protected with Boc or Cbz groups, in molecule **57** and **58** respectively, to test the different filling of the S1 pocket.

In both cases, either for molecules that contain regular scaffold or for those that contain inverse scaffold, it should be possible to make hydrogen bonds with all three residues 21, 47, 49.

The main difference was that in the first case (regular scaffold) the hydrogen bond between the molecules and NH of Thr 21 could potentially involve a fluorine atom, having in mind as described above about the examples of H---F bonds.

As explained in the previous chapter II.2.2., molecules **54** and **58** (Figure 48) were superposed with our Novartis molecule model **48**. The two superposition were rather satisfactory. The results are shown for molecule **54** and **58** in Figure 50 and Figure 51, respectively.

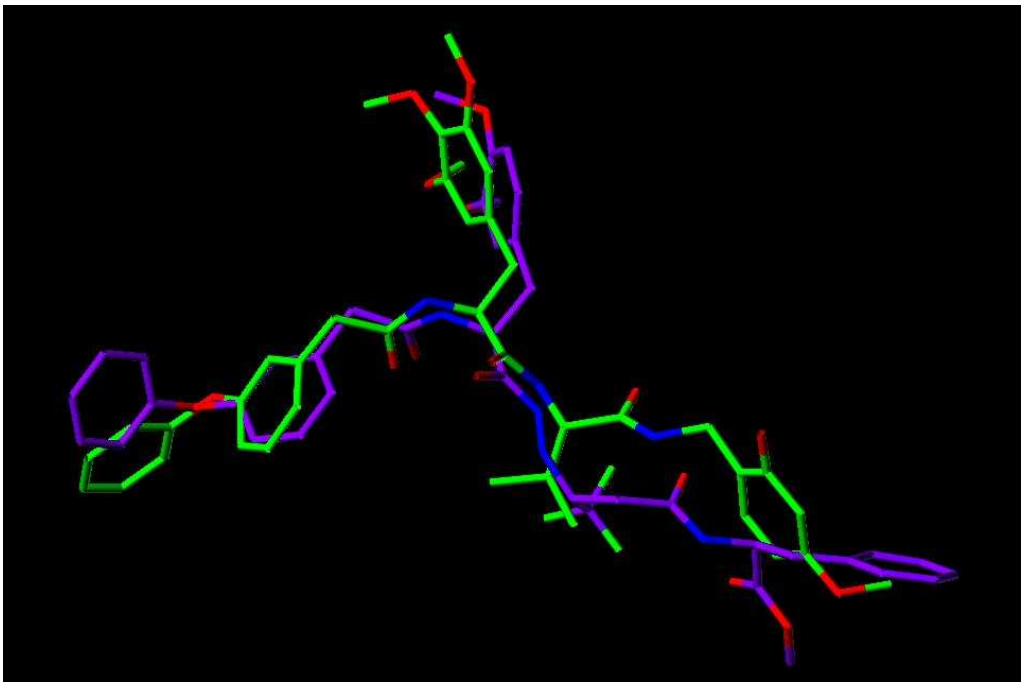

Figure 50. Result of the superposition in eight points between Novartis molecule **48** (green) and molecule **54** (purple). Hydrogen atoms are omitted for clarity.

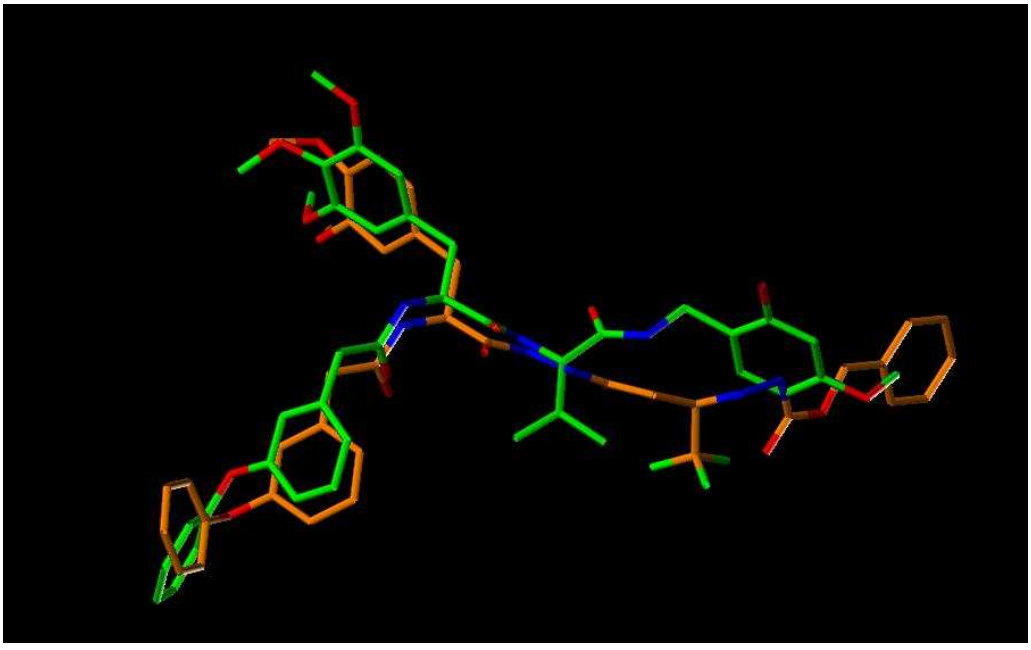

Figure 51. Result of the superposition in eight points between Novartis molecule **48** (green) and molecule **58** (orange). Hydrogen atoms are omitted for clarity.

We show in Figure 52 that hydrogen-bonds with essential amino acids Thr 21, Gly 47 and Ala 49 could be present.

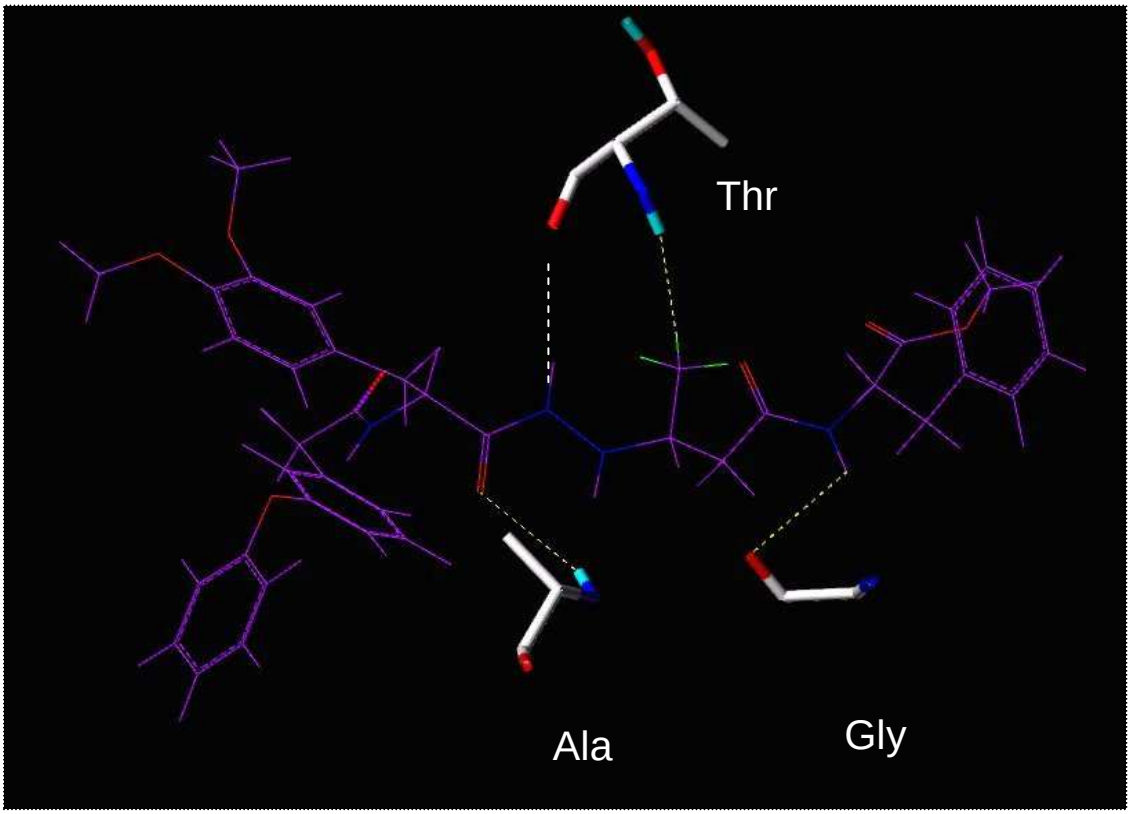

Figure 52. Overview of molecule **54** bound to the active site of the proteasome. Hydrogen atoms are omitted for clarity.

II.3. Synthesis of non fluorinated molecule 52

The synthesis of the molecule **52** is described in Scheme 1. This compound was synthesized in eight steps from commercially available 2-methoxy-benzoic acid **60**, which was converted to intermediate **61** by nitration with NH_4NO_3, H_2SO_4 in good yield (80%), following the Nowick's procedure.[100] The coupling with *tert*-butyl-carbazate with a good yield (86%), following a procedure described in the laboratory, and successive reduction of the nitro group of **63** gave the Boc-protected 5-amino-2-methoxybenzhydrazide **64**, described in literature by Nowick.[101] After classical acylation of compound **64** with Ac_2O in THF in quantitative yield, the resulting compound **65** was Boc deprotected by treating it with TFA in dry CH_2Cl_2 to give **66**. The compound **66**, obtained in quantitative yield, was coupled to the non natural amino acid Fmoc-*L*-3,4-dimethoxyphenylalanine, in presence of HBTU and HOBt as coupling agents, to afford the Fmoc-protected compound **68** in 50% yield. The purification of **68** was not easy to do because this

product had the tendency to form a gel in aqueous phase and was not soluble in several organic solvents. After Fmoc deprotection with 10% of piperidine in DMF, the coupling of **69** with 3-phenoxyphenylacetic acid **70** gave the desired product **52**. This product **52** had the same tendency as **68** to form a gel in aqueous and organic solutions. However it was possible to purify it by chromatography on silica gel to obtain **52** with a good yield (75%).

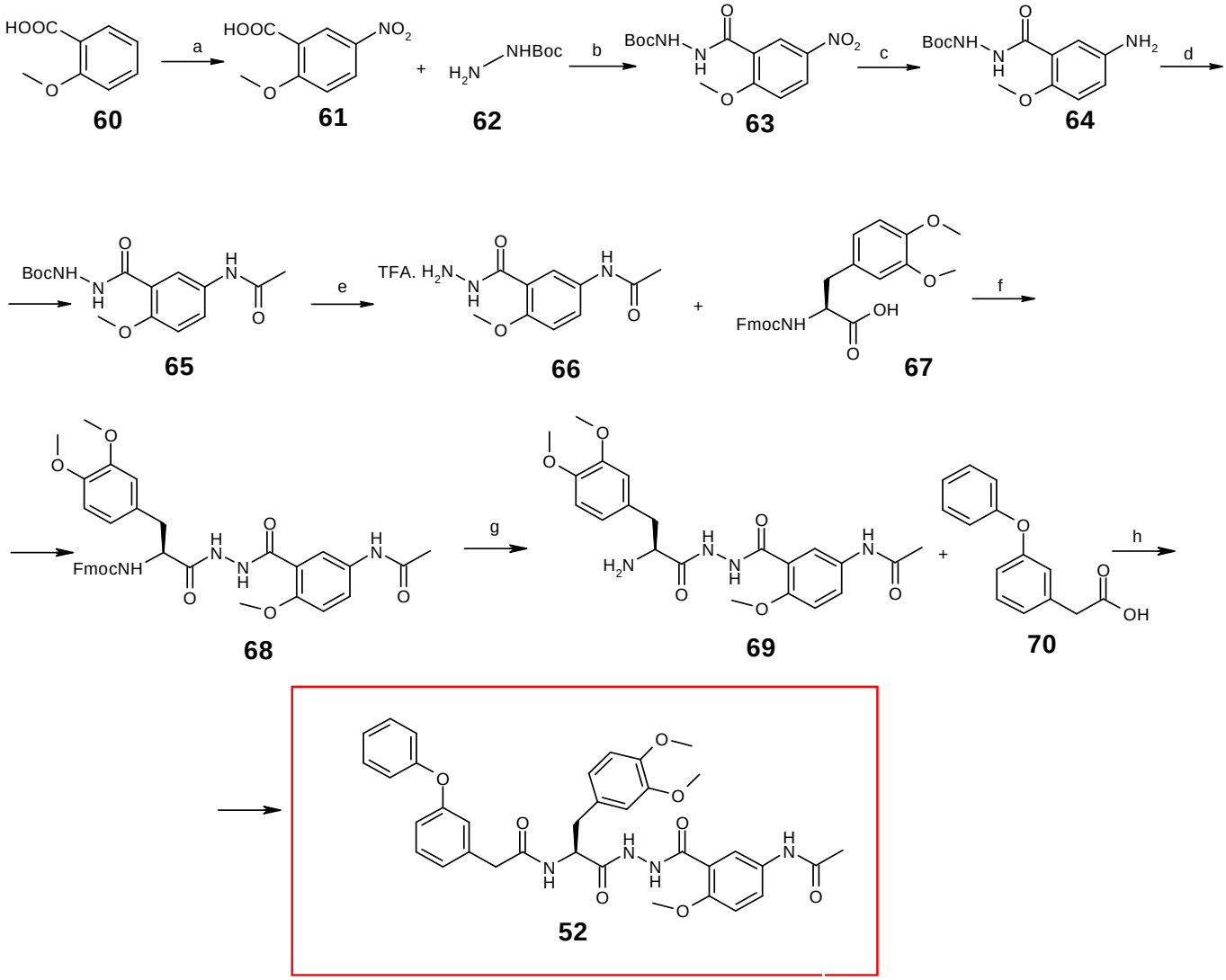

Scheme 1. Synthesis of compound **52**. Reagents:

a) NH_4NO_3, H_2SO_4, 80%; b) EDC.HCl, HOBt, CH_2Cl_2, DIPEA, 86%; c) H_2, Pd/C 10%, MeOH, 96%;
d) Ac_2O, THF, 100%; e) TFA, CH_2Cl_2, 100%; f) HBTU, HOBt, DMF, 2,4,6 collidine, 50%; g) 10% piperidine/DMF, 100%;
h) HBTU, HOBt, DMF, 2,4,6 collidine, 75%.

Note: The gel obtained with compound **52** in EtOAc was observed under Microscope Eclipse E600 Nikon (examination in white light) to check the presence or not of an organized structure.

The result was that we did not find any organization of this gel under form of the crystals or fibrils. The experience was done in collaboration with the Department of "Physico Chemistry of the Polyphase systems", UMR 8612 of the CNRS, University Paris-Sud 11.

II.4. Synthesis of fluorinated molecules 54-58

The first target compound **54** was synthesized starting from the ethyl 4,4,4- trifluorocrotonate[102] **71** as outlined in Scheme 2. Michael addition of *tert*-butyl-carbazate **62** on **71** in refluxing MeOH gave the N-protected trifluoromethyl-β-hydrazino ester **72** with a very good yield (95%). This product **72** after saponification with sodium hydroxide was coupled to the *L*-phenylalanine methyl ester to afford **75** in 91% yield using HBTU and HOBt as coupling agents in presence of DIPEA in DMF/CH_2Cl_2. The cleavage of the Boc group of the hydrazine moiety with trifluoroacetic acid (TFA) in dry CH_2Cl_2 gave compound **76** which was coupled with Fmoc-*L*-3,4-dimethoxyphenylalanine **67** using HBTU and HOBt in presence of 2,4,6-collidine in DMF. The resulting molecule **77** was really hard to purify and the yield dramatically fell (22%). In fact, during the washing with acidic and basic aqueous solutions we observed the formation of a gel very hard to disrupt. Addition of a solvent mixture H_2O/EtOAc, and subsequent extraction allowed the isolation of a residue which could be purified by chromatography on silica gel. The cleavage of the Fmoc group of **77** with 10% of piperidine in DMF afforded the amine **78** (in 86% yield) which was coupled with 3-phenoxyphenylacetic acid to give the final compound **54** in moderate yield (47%). It is important to note that the coupling of the racemic acid **73** with *L*-phenylalanine methyl ester **74** afforded **75** in a 1:1 diastereoisomeric mixture that could not be separated by flash chromatography or by crystallisation. Compounds **76**-**78** progressed then as 1:1 diastereoisomers mixtures. However compound **54** was obtained with a 2/3 ratio of diastereoisomers probably because of the loss of one diastereoisomer during the purification.

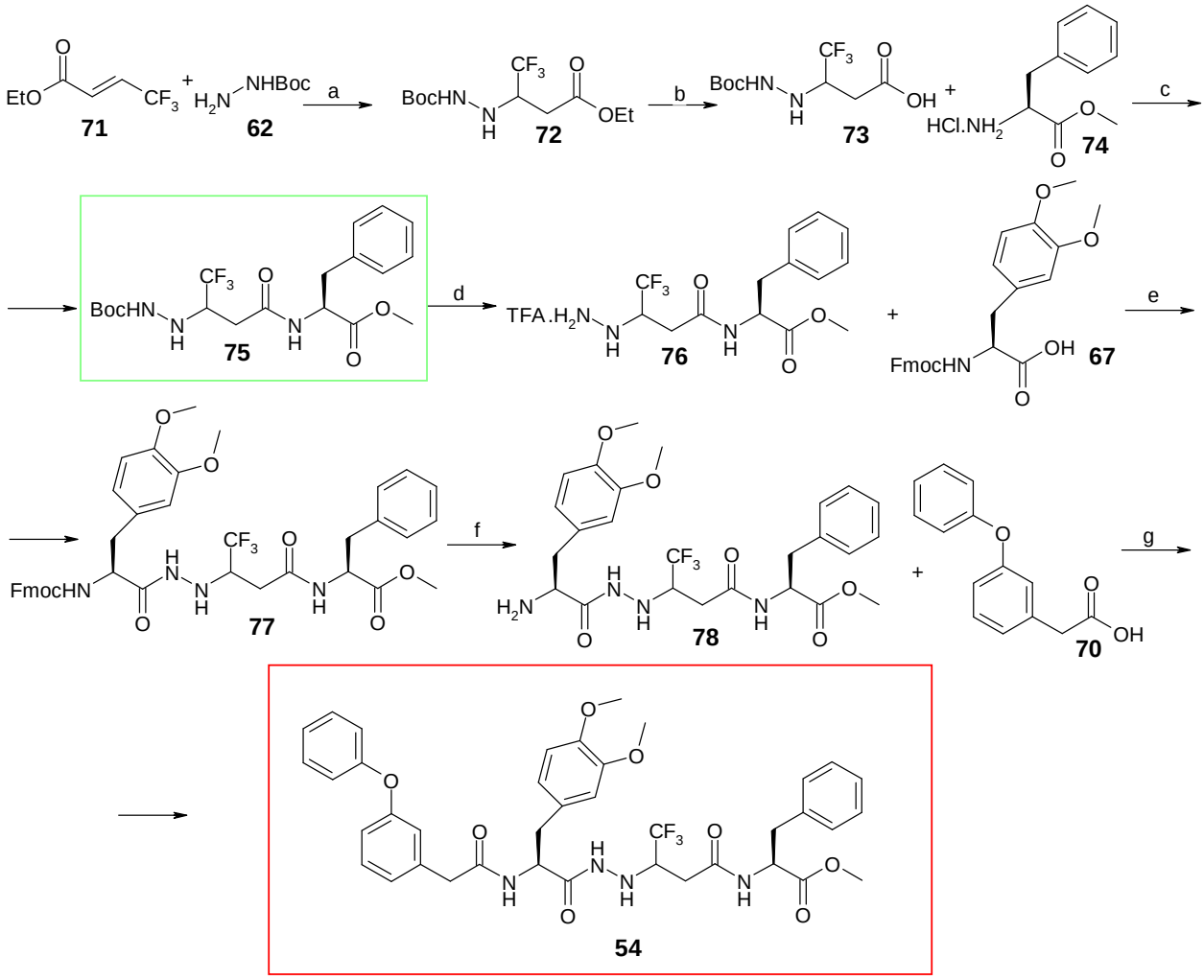

Scheme 2. Synthesis of compound **54**. Reagents:

a) MeOH, reflux, 94%; b) 2N aq. NaOH, THF/MeOH, 98%; c) HBTU, HOBt, DIPEA, CH_2Cl_2, DMF, 91%; d) TFA, CH_2Cl_2, 100%; e) HBTU, HOBt, 2,4,6-collidine, DMF, 22%; f) 10% piperidine/DMF, 86%; g) HBTU, HOBt,DIPEA, DMF, 41%.

As depicted in Scheme 3, the intermediate **76** was used to obtain the second target molecule **55** by a simple coupling with 3-phenoxyphenylacetic acid **70** with HBTU and HOBt as coupling agents. After purification by chromatography on silica gel a 1:1 mixture of diastereoisomers of **55** was obtained in 42% yield.

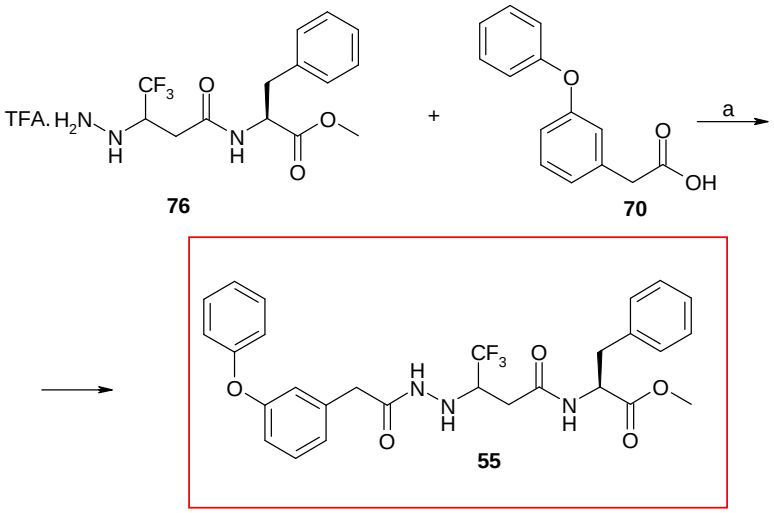

Scheme 3. Synthesis of compound **55**. Reagents:
a) HBTU, HOBt, 2,4,6-collidine, DMF, 42%.

The synthetic pathway to obtain the third target compound **56** is presented in Scheme 4.

The TFA salt **76** was converted to **80** by coupling with *N*α-Boc-*N*ε-Z-*L*-Lysine, using HBTU and HOBt as coupling reagents, in 57% yield. The *N*α-Boc protecting group was removed by treatment with TFA in dry CH_2Cl_2 and compound **81** was isolated in quantitative yield. The coupling reaction between **81** and 3-phenoxyphenylacetic acid **70** gave compound **82** with a good yield (71%). **82** was finally N-deprotected by hydrogenation over 20% Pd/C, and TFA was added to provide compound **56** in quantitative yield and in a 1:1 mixture of diastereoisomers.

In parallel, a part of product **80** was N-deprotected by hydrogenation over 20% Pd/C, and citric acid monohydrate was added to give **83** with a modest yield (51%) (Scheme 4). We decided to synthesize also compound **83**, analogous to molecule **56**, to test if was possible to have same inhibitor effect due to the different N-terminal groups.

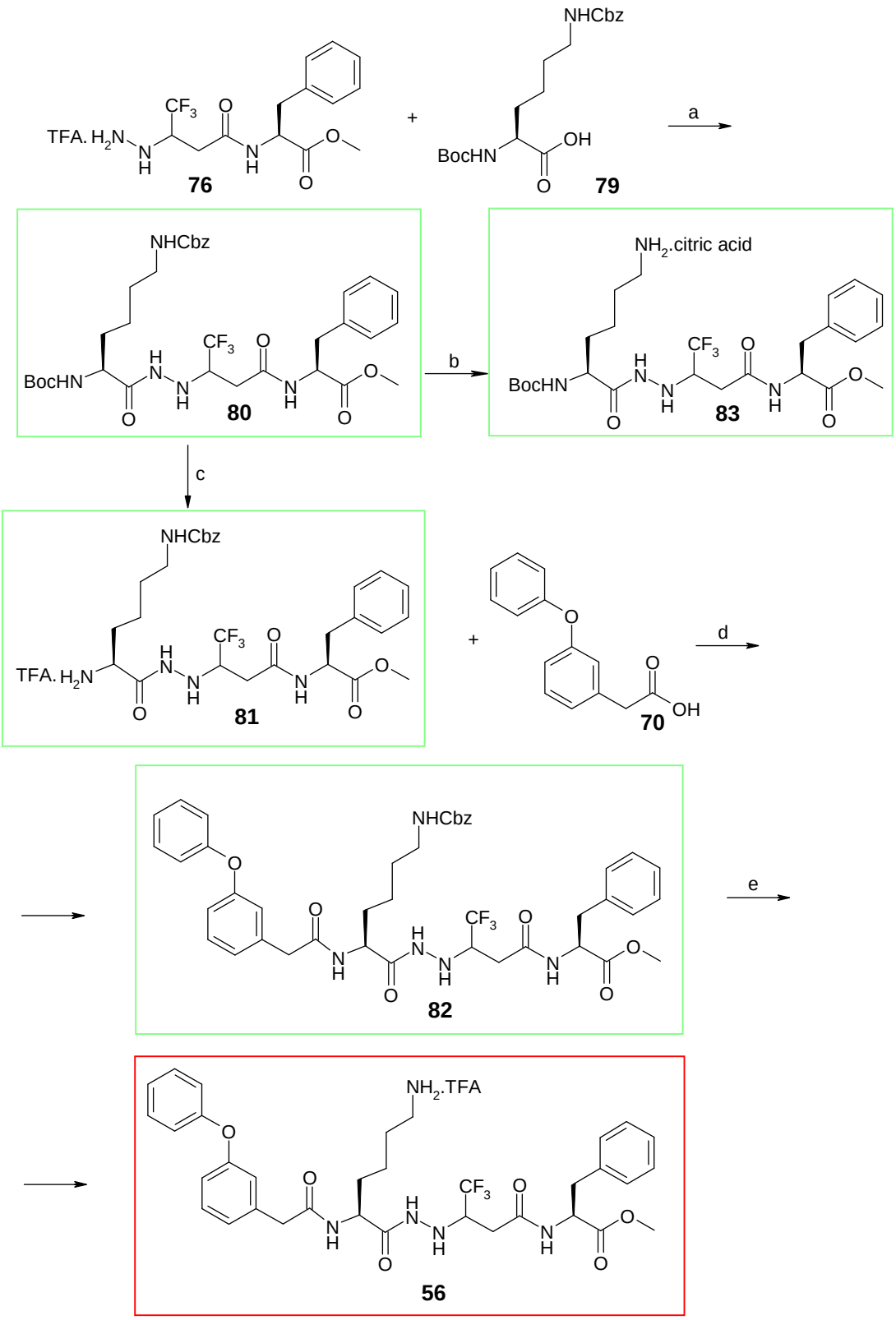

Scheme 4. Synthesis of compounds **56** and **83**. Reagents:

a) HBTU, HOBt, DIPEA, DMF, 57%; b) H_2, Pd/C 20%, MeOH, citric acid monohydrate, 51%; c) TFA, CH_2Cl_2, 100%; d) HBTU, HOBt, DIPEA, DMF, 71%; e) H_2, Pd/C 20%, MeOH,TFA,100%.

The only difference between the last two targets **57** and **58** was the protecting group, Boc or Cbz respectively. The synthesis of compound **57** is outlined in Scheme 5. Reaction of **72** with hydrazine monohydrate afforded the hydrazide compound **85** in quantitative yield. Coupling of **85** with Fmoc-*L*-3,4-dimethoxyphenylalanine, using HBTU, HOBt as coupling agents in presence of 2,4,6-collidine in DMF, gave **86** in 68% yield. The following deprotection of the Fmoc group and the final coupling of the resulting compound **87** with 3-phenoxyphenylacetic acid **70** provided compound **57** in satisfactory yield and in a 1:1 mixture of diastereoisomers.

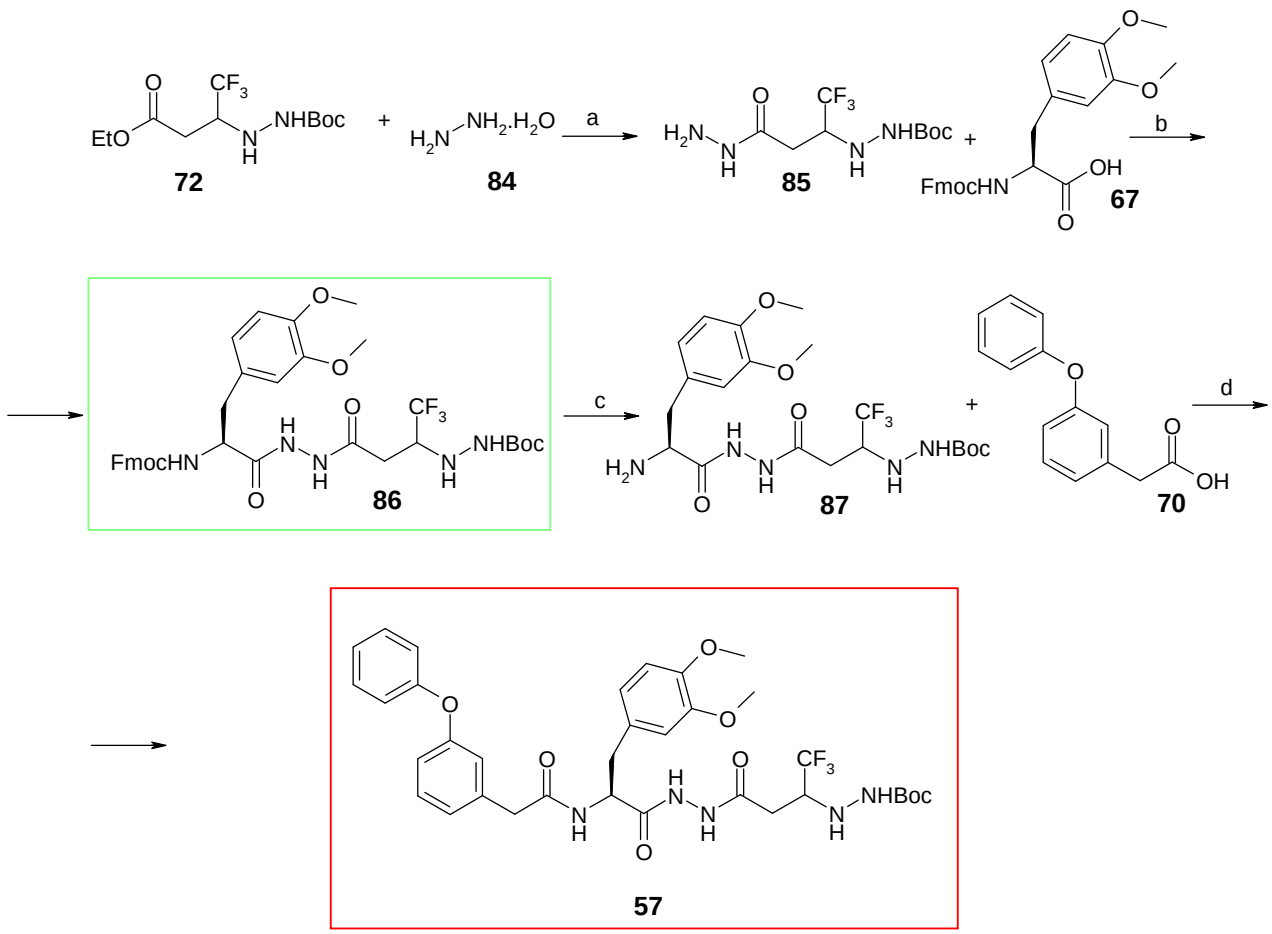

Scheme 5. Synthesis of compounds **57**. Reagents:

a) EtOH, 100%; b) HBTU, HOBt, DMF,2,4,6-collidine, 68%; c) 10% piperidine/DMF, 88%; d) HBTU, HOBt, DMF,2,4,6-collidine, 84%.

In a first approach we envisaged to synthesize the molecule **58** from the molecule **57**, by a simple removing of the Boc group and a reprotection of the amino group at the C-terminal side of the expected compound **88** with Cl-Cbz. Unfortunately, we could not obtain the desired product **58** using this way. Effectively, the reaction of the N-Boc removing by a solution of HCl/MeOH did not afforded the expected compound **88** but gave only compound **89** in a quantitative yield. We

supposed that the compound **89** is obtained by the nucleophilic attack of MeOH on the protonated carboxyl group of the hydrazide motif (Schema 6).

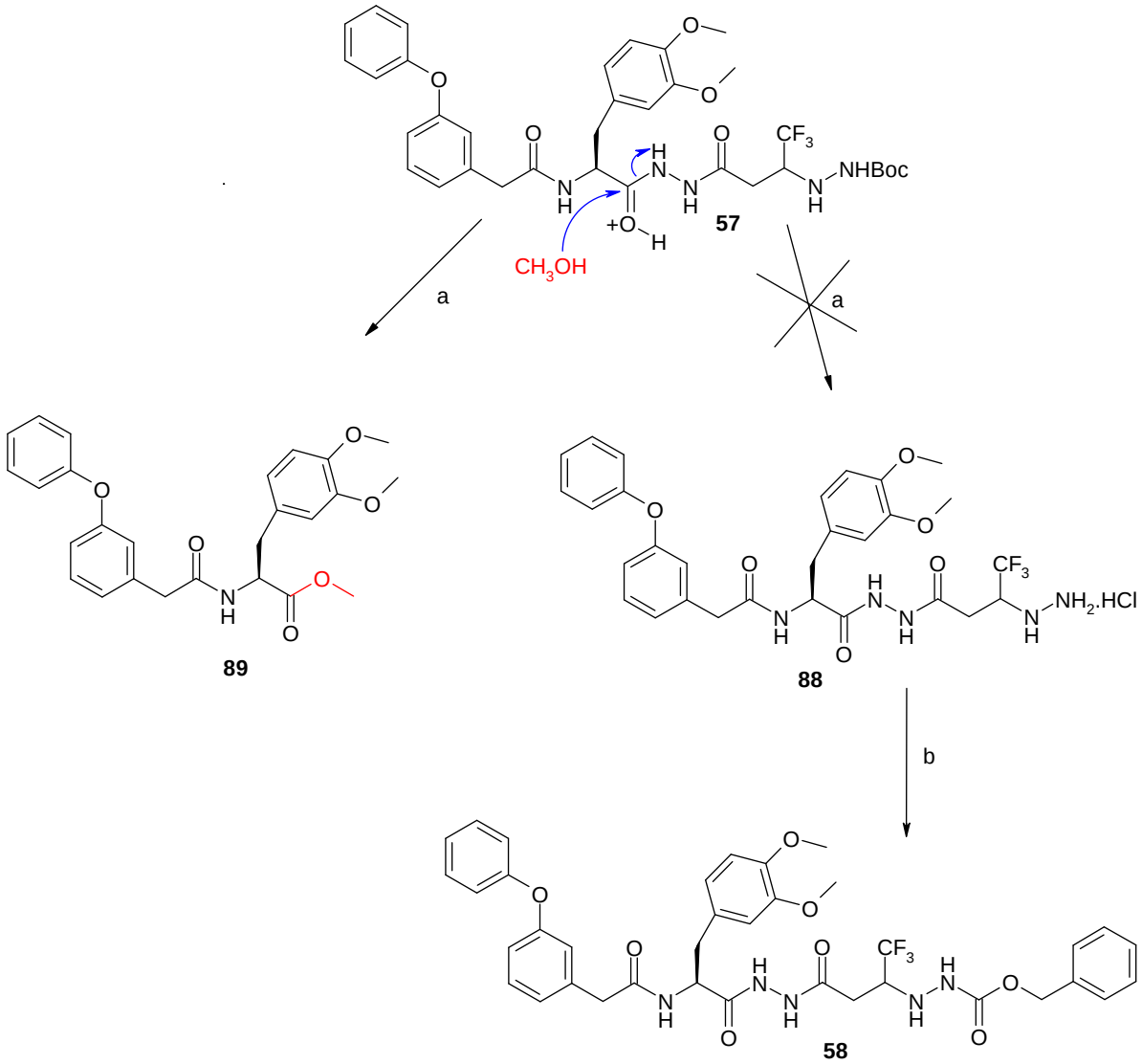

Scheme 6. Envisaged synthesis of compounds **58**. Reagents:

a) HCl/MeOH, MeOH b) Cbz-Cl, DIPEA, CH_2Cl_2.

Consequently, we decided to investigate a new route as illustrated in Scheme 7.

We started from the protected trifluoromethyl-β-hydrazino ester **72**. The first step was the N-Boc deprotection of **72** with TFA in dry CH_2Cl_2 in a quantitative yield followed by the N-protection of **90** with Cbz group. The resulting compound **91**, obtained in a good yield (81%), reacted with hydrazine monohydrate **84** to give compound **92** in quantitative yield. This compound was coupled with Fmoc-*L*-3,4-dimethoxyphenylalanine, using HBTU and HOBt as coupling agents in presence of 2,4,6-collidine in DMF to give **93**. As in the case of products **86** and **57** previously reported in Scheme 5, also **93** precipitated directly pure in EtOAc in 67% yield. After treatment with 10% of

piperidine in DMF to remove the Fmoc group, the last coupling between **94** and 3-phenoxyphenylacetic acid **70** using HBTU and HOBt in presence of DIPEA in DMF allowed to obtain the final product **58** in high yield (85%) and in 1:1 mixture of diadtereoisomers.

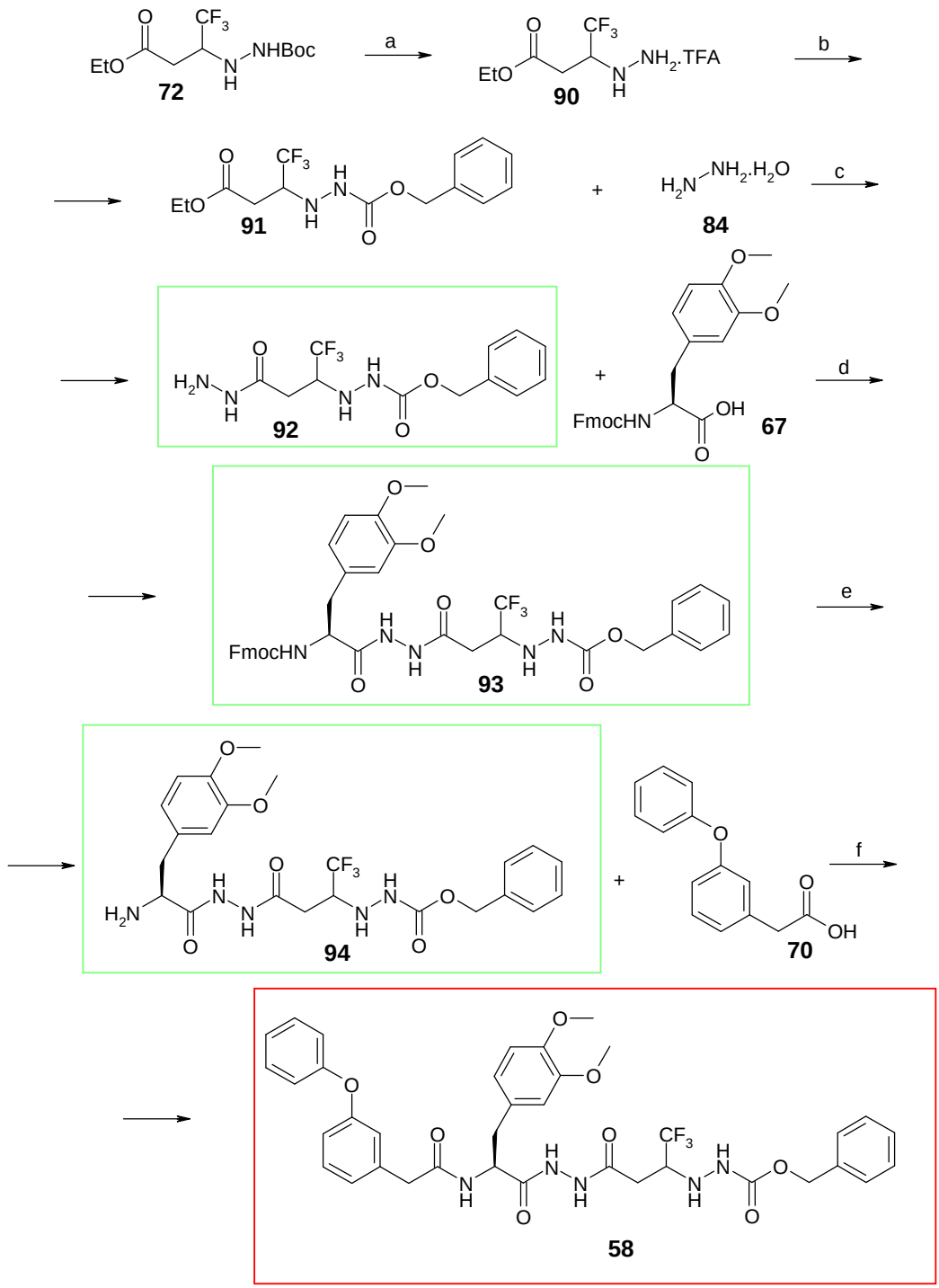

Scheme 7. Synthesis of compounds **58**. Reagents:

a) TFA, CH_2Cl_2, 100%; b) Cl-Cbz, CH_2Cl_2, DIPEA, 81%; c) EtOH, reflux, 100%;
d) HBTU, HOBt, DMF, 2,4,6 collidine, 67%; e) 10% piperidine/DMF, 78%; f) HBTU, HOBt, DIPEA, DMF, 85%.

II.5. Biological activity – Results and discussion

The abilities of non fluorinated peptidomimetic **52** and fluorinated compounds to inhibit the three catalytic activities of rabbit 20S proteasome were tested using appropriate fluorogenic substrates: Suc-LLVY-AMC (Suc, succinyl; AMC, aminomethylcoumaride) for the chymotrypsin-like activity (CT-L); Boc-LRR-AMC for the trypsin-like activity (T-L), and Z-LLE-β-NA (Z, benzyloxycarbonyl; β-NA, β-naphthylamine) for the post acidic activity (PA) (Figure 20).[69, 72] The aldehyde proteasome inhibitor MG132 (Z-LLL-H) was used as standard.[69]

The three peptidases activities were determined by monitoring the hydrolysis of these three fluorescent substrates for 45 min (30 min in the case of **52**) at 37 °C using a BMG Fluostar microplate reader, in the presence of untreated proteasome (control), or proteasome that had been incubated with the test compound (0.1-200 μM). The buffers (pH 7.5) were: 20 mM Tris, 1 mM DTT, 10% glycerol, 0.02% (w/v) SDS for CT-L and PA activities; 20 mM Tris, 1 mM DTT, 10% glycerol for T-L activity. In the case of **52** the buffers for all three activities contained also 3% (v/v) DMSO, thus the control experiments were run with the same amount of DMSO solvent.

The IC_{50} values (inhibitor concentrations giving 50 % inhibition) were obtained by plotting the percent inhibition against inhibitor concentration to equation: % inhibition = $100[I]/(IC_{50}{}^{nH} + [I]^{nH})$, or equation: % inhibition = $100[I]^{nH}/(IC_{50}{}^{nH} + [I]^{nH})$ where n_H is the Hill number. The K_m values of the fluorogenic substrates in our experimental conditions were: 30 ± 5 μM (Suc-LLVY-AMC), 77 ± 4 μM (Z-LLE-β-NA) and 26 ± 6 μM (Boc-LRR-AMC).

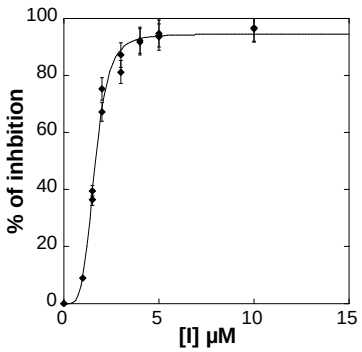

Figure 53. Inhibition of CT-L activity of rabbit 20S proteasome by compound **56** at pH 7.5 and 37 °C. The experimental data were fitted to equation % inhibition = $100[\mathbf{56}]^{nH}/(IC_{50}{}^{nH} + [\mathbf{56}]^{nH})$ with $n_H = 4.5$.

The results show that the non fluorinated compound **52** (Figure 45, see chapter II.2.3 Design, page 53) has no inhibitor effect on the three activities of the proteasome at the different doses tested, even changing the preincubation time in the first step of the experiment, while several fluorinated compounds gave inhibition of these three activities. IC_{50} values against proteasome subsite activities obtained after 45 min of incubation, as mentioned before, are reported in Table 1.

Compound	CT-L	PA	T-L
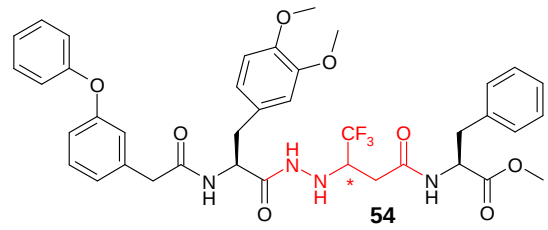 **54**	85 ± 15	72 ± 0.7	*x*4
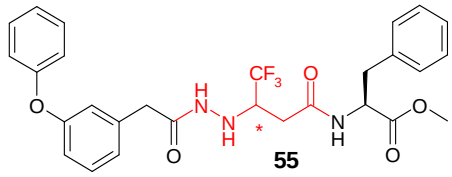 **55**	*x*2	ni	ni
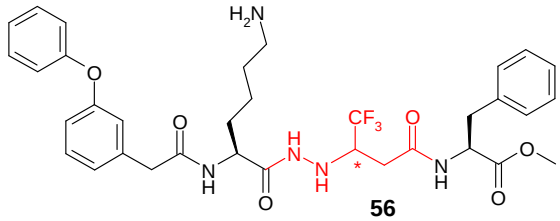 **56**	1.6 ± 0.1	2.7 ± 0.1	8.4 ±1.3
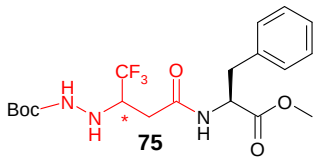 **75**	ni	16%	ni
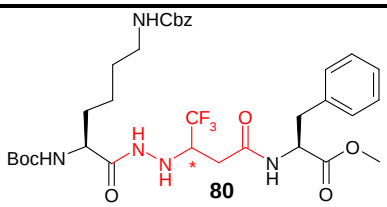 **80**	ni	ni	*x*3

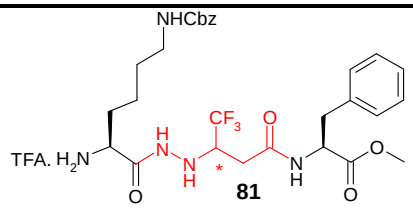 **81**	5.9±0.5	ni	4.4±1.2
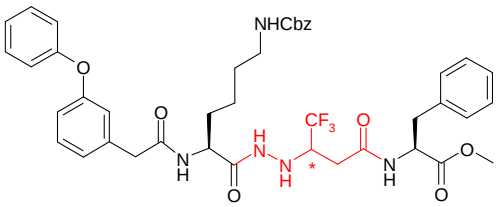 **82**	ni	200	ni
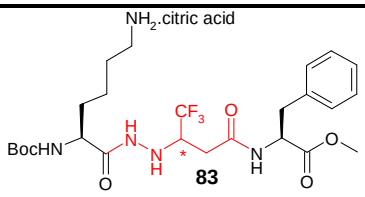 **83**	32±2	6±0.5	30%
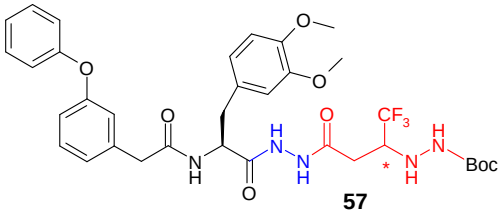 **57**	ni	ni	*x*1.3
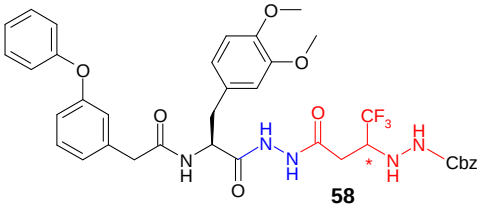 **58**	*x*6.7	30%	ni
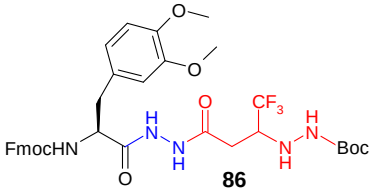 **86**	ni	ni	*x*2
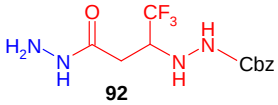 **92**	ni	ni	ni

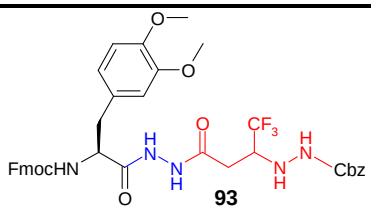 **93**	*x*3.6	53%	*x*2
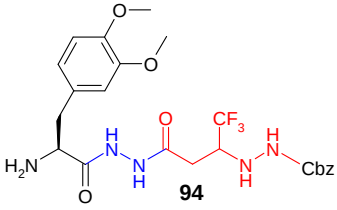 **94**	ni	ni	60%

Table 1. IC_{50} (µM) or % inhibition at 100 µM of compounds **54-58**, **75**, **80-83**, **86**, **92-94** against rabbit 20S proteasome at pH 7.5 and 37 °C. *x*: activation factor. Values are means of three experiments. CT-L: chymotrypsin-like activity; PA: post-acid activity; T-L: trypsin-like activity.

The data obtained from enzyme inhibition tests underlined that our fluorinated peptidomimetics are molecules able to interact with proteasome and could behave as inhibitors (**54**, **56**, **81**, **82**, **83**, **93**, and **94**) but also as activators (**54**, **80**, **86**, **57**, **93**, **55**, and **58**).

It is known that the protein degradation is predominantly catalyzed by the proteasome, then its activation should accelerate the intracellular proteolysis. This is an important effect for example in the case of accumulation of oxidized molecules. In fact, the activators of proteasome would present an interest in cosmetic against the cutaneous aging. Few natural compounds have been identified having proteasome activation properties and among them there are commipheroline and megassane, innovative active ingredients of the modern cosmetic industry.[103] There are in literature some examples of proteasome activators.[104-107]

We can observe a protein accumulation also in Alzheimer's and Parkinson's diseases. Therefore the application of activators for enhancement of the action of the 20S proteasome must be considered interesting.

Multiple non-catalytic sites exist in the 20S proteasome and the binding of hydrophobic peptides to these sites stimulates peptide hydrolysis by all three of its active sites. There is evidence that this stimulation occurs by peptide-induced opening of the channel in the α-rings of the 20 S proteasome.[105] Wilk and coworkers[107] synthesized four classes of peptide-based activators and described that the efficacy of these compounds is markedly dependent on both hydrophobicity and chain length.

In the presented work compounds **54**, **80**, **86**, and **57** showed to be activators of the T-L activity (with **54**> **80**> **86** >**57**) and compounds **58**, **93**, **55** activators of the CT-L activity (with **58**> **93**> **55**). However, for now we are unable to explain the origin of this activation effect.

The inhibitory effect was found with several molecules.

Two series of molecules were synthesized and tested for their activity on the three catalytic sites of 20S proteasome, the first series containing our new trifluoromethyl-β-hydrazino acid scaffold in a regular sense **53** and the second one containing the scaffold in an inverse sense **59** (Figure 49, see chapter II.2.3 Design, page 57). The results of the biological tests are shown in Table 1.

Only molecules of the first series (regular scaffold) showed interesting inhibitory properties against all three active sites (**56**, **83**), two active sites (**54**, **81**), or only one active site **(75**, **82)**.

Effectively, in the case of the inverse scaffold, molecules **58**, **93** and **94** showed a very moderate inhibition of one activity (PA for **58**, **93** and T-L for **94**). In other words, these results indicated clearly that only the non inverse scaffold induced molecules conformation and interactions allowing the molecules to interact with the catalytic sites of the proteasome.

Probably in the inverse scaffold the second hydrazine group (in blue) induces a too important elongation of the backbone thus moving away the groups that have to occupy simultaneously the S1 and S3 pockets.

Compound **54** inhibited the CT-L and PA activities of rabbit 20S proteasome with a IC_{50} = 85 and 72 µM respectively (Table 1). Shortening the pseudopeptide by connecting directly the phenoxy benzyl moiety on the trifluoromethyl-β-hydrazino acid scaffold and eliminating the 3,4-dimethoxyphenylalanine totally removed the capacity of molecule **55** to inhibit all three active sites (Table1). Also the very weak PA inhibitor effect of compound **75** showed the importance of the substitution of the hydrazido group in the activity of the first series of molecules.

Replacing the 3,4-dimethoxyphenylalanine amino acid by the more hydrophilic lysine amino acid could facilitate the interaction of the ε-NH_2 group with the aspartic acid residue in the S3 pocket of the T-L active site.[69,99] It should also increase the solubility of the compound. Indeed, molecule **56**, where the 3,4-dimethoxyphenylalanine amino acid was replaced by the free lysine amino acid, inhibited CT-L (IC_{50} = 1.6 µM) and PA (IC_{50} = 2.7 µM) activities and also T-L activity (IC_{50} = 8.4 µM), whereas protecting the lysine group eliminated inhibitory power (CT-L and T-L) or decreased it (PA, factor ≈ 100) (molecule **82**). The phenoxysubstituted benzylic *N*-terminal group was not essential for inhibition since molecule **83** was a moderate inhibitor (compare compound **56**). The free N-terminus was favorable (IC_{50} = 5.9 µM, CT-L) and (IC_{50} =

4.4 µM, T-L), although the εNH_2 group was protected (molecule **81** compared to molecule **83**). Again, a positive charge on the lysine lateral chain or N-terminus stimulated binding to the TL active site. Proteasome inhibition was selective. Effectively, neither lysosomal cathepsin B nor cytosolic calpain I was inhibited by compounds **56**, **81** and **83**.[108] Using purified enzymes to develop new inhibitors is of course the well-known strategy to obtain with security molecules acting on the targeted enzyme. It is also important then to test the capacity of the molecules to inhibit the enzyme in its cellular or acellular environment. We are performing in Professor M. Reboud-Ravaux laboratory such experiments and for now we have shown by using a cell-based chemiluminescent assay[109] that compound **56** behaved as an inhibitor of the CT-L activity in human HeLa cells (20% inhibition at 50 µM after 1h30 incubation).

II.6. Present work in the laboratory

Encouraged by these results and in agreement with our previous work, ongoing efforts in the laboratory have been made since Octobre 2007 (when I left the laboratory for going to Regensburg) more particularly by our colleague Bordessa A. The aim is a better knowledge of the Structure-Activity Relationship (SAR) around the fluorinated scaffold, and consequently the design and the synthesis of compounds that satisfy specific conformational requirements. In fact, the understanding of the mechanism of interaction between these molecules and the different active sites of the proteasome is of great importance for the rational design of new inhibitors. With the goal of developing a useful tool able to supply some important indications for the synthesis of new inhibitors, a docking approach, which allows to evaluate the interactions between a ligand and a receptor, has been chosen.

The work followed the steps below:

- Identification by means of the literature and crystallographic studies of the essential features (occupation of the hydrophobic pockets, hydrogen bonds, etc.) necessary for the inhibition of the proteasome from known inhibitors.
- Docking of known inhibitors to compare our results with the crystallised structures or with the reported molecular modelling studies. This allows to define the docking parameters and to validate the model.

- Docking of the lead compound **83** to formulate a first hypotesis of interaction.
- Systematic modification of **83** and subsequently docking of the results to address the synthetic work.
- Use of the biological evaluation results of the synthesized molecules to refine the docking parameters and to better understand the binding interaction between these molecules and the proteasome.

The first step was the docking of the known inhibitors.

Autodock4 program was chosen. The first docking experiments was done on the TMC-95 A[99] **43** and its biaryl analogues,[67, 68] because they are the only non covalent inhibitors co-crystallised with the 20S proteasome. The docking results fitted the experimental structure in an excellent way, with an RMSD less than 2.0 Å. Some aminostatine based inhibitors synthesised by Novartis[70, 71] were also docked and the resulting conformations in the CT-L site fitted quite good with the molecular modelling studies reported (filling of the S1 and S3 pockets by the same groups as described by the authors, and presence of the same principal hydrogen bonds, between the main chain of the molecules and the residues 21, 47 and 49 of the proteasome and between the methoxy groups of the central 3,4,5-trimethoxyphenylalanine and some serines (in particular the residues 118 present at the bottom of the S3 pocket).

The second step was the docking of the lead molecule 83 and virtual screening of new candidates.

At the begin of Andrea Bordessa's work, only our molecule **83** was tested and for this reason all the efforts to propose a first mechanism of binding were done only on the base of the molecule **83**. Moreover, the biological test was done only on the chymotrypsin-like site, and for this reason the first studies were done in the CT-L site. Because the pseudo amino acid **72** was obtained as racemic, it was necessary to perform two different calculations, respectively with the S and R configuration of the chiral centre bearing the CF_3. Unexpected to our preliminary design, the docking result for **83** suggested that the Boc group was inserted in the S1 pocket and the

phenylalanine in the S3, whereas the free amino group of the lateral chain of the lysine was involved in an hydrogen bond with the residue T21 (in Figure 54 is represented the result for the S configuration, in green dashed the intermolecular hydrogen bonds). Deeply analysing this result, it was possible to see as the Boc group is inserted in the S1 pocket, with a distance between the tert-butyl group and the T1 of 3.1 Å, which indicates a good filling of this pocket. The phenylalanine is inserted in the S3 pocket and the methoxy group could form an additional hydrogen bond with the serine 118, which is at the bottom of the S3 pocket. This hydrogen bond, also if is not on of fundamental for the interaction with the proteasome, is also reported by Novartis[71] as useful to stabilise the complex. In the region between the two hydrophobic pockets, the ligand formed hydrogen bonds with the residues G47 and A49 respectively with the oxygen and the nitrogen of the urethane moiety, and with T21 with the free amino group on the lateral chain of the lysine and with the hydrazine moiety. It was also present a strong interaction between the trifluoromethyl group and the residue D114. Moreover, the binding energy calculated by Autodock was excellent, with a value of -9.20 Kcal/mol. In addition, the other clusters generated by the program, presented an higher binding energy (more than -6.0 Kcal/mol) suggesting as this is the most probable conformation. Thus, we could conclude that in this active molecule it was possible to find all the features common to the other proteasome inhibitors. Less clear was the result obtained for the molecule with the R configuration of the carbonyl bearing the CF_3. In every case, when the cluster at minor binding energy did not present a good conformation, the second better cluster presented a result quite similar to that obtained for the S diastereomer, with the Boc group in the S1 pocket and the phenylalanine in the S3. The Boc group was less inserted in the S1 pocket (the distance with the T1 was of 4.8 Å), when the phenylalanine had a good filling of the S3 pocket (also in this case it was observed the hydrogen bond with the S118). Less intermolecular hydrogen bonds could be found (only with T21 and D114) and this fact was reflected in an higher binding energy (-6.30 Kcal/mol).

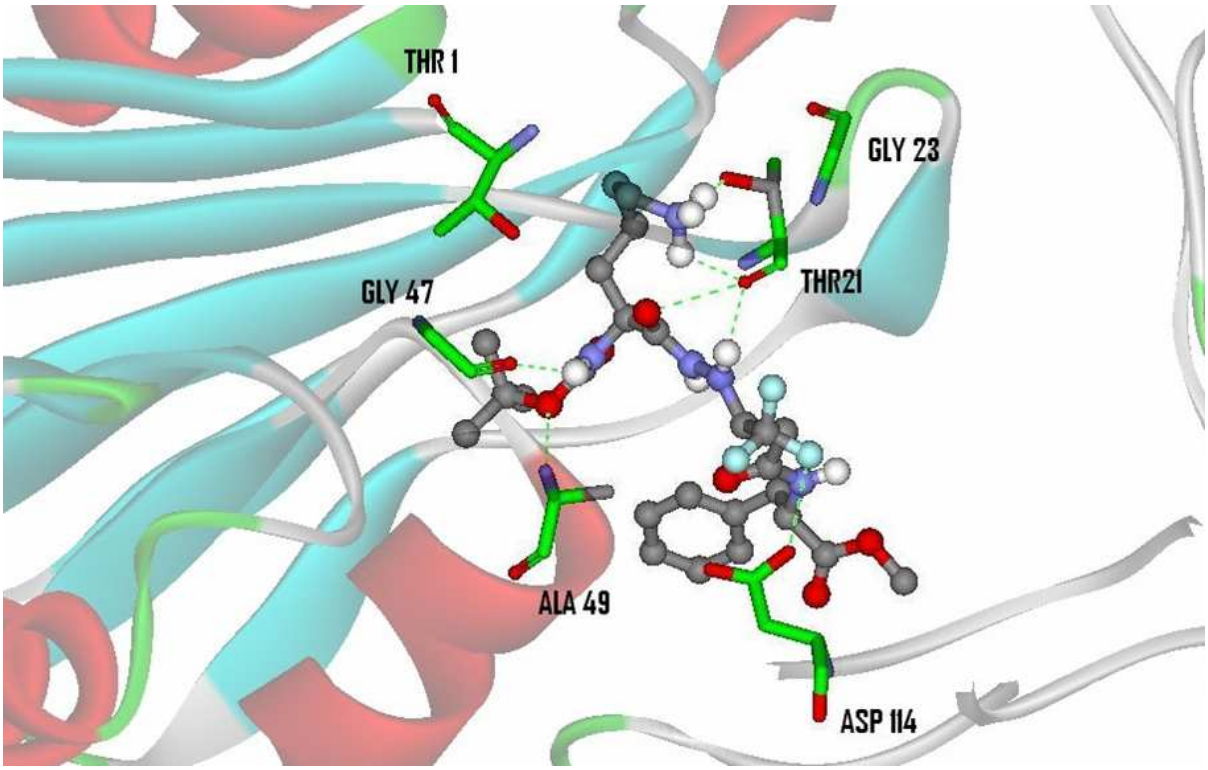

Figure 54. Molecule **83** in the CT-L site of the proteasome.

Based on this first model, it was decided to perform pharmacomodulation on the lead molecule **83** to evaluate the influence of each part of the molecule to try to establish structure-activity relationship and to try to obtain better proteasome inhibitors. It was decided to substitute the Boc group with other groups adapted to fill better the S1 pocket, the phenylalanine with groups able to fill the S3, the lysine with other amino acids and we also tried to see the influence of the substitution the central core of the molecules (in Figure 55 the groups tested and, with a red bar, the rejected).

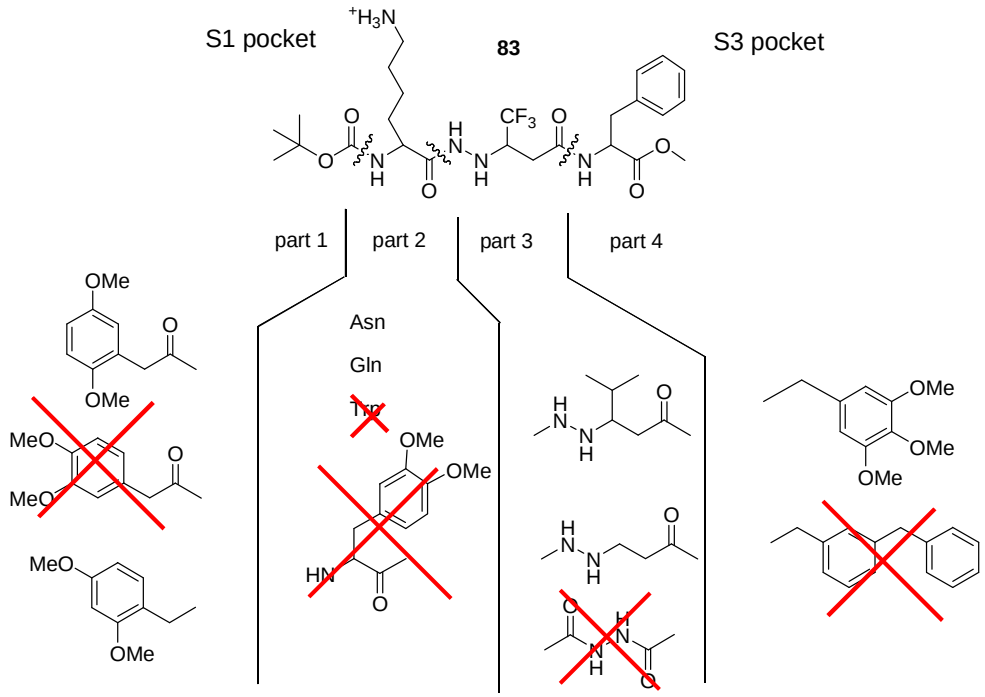

Figure 55. Several substitutions of the molecule **83** on the basis of the previous results.

It was envisaged to substitute the Boc group with a dimethoxy-phenylacetic acid group and the docking result showed that a methoxyl group in position 2 of the ring was the most favorable to have a good interaction with the T1. The lysine was substituted by different amino acids and the docking results showed that the most favorable amino acids were asparagine and glutamine, whereas tryptophan and the unnatural 3,4-dimethoxyphenylalanine have the tendency to fill the S3 pocket without leaving enough space for a good filling of the S1 pocket by the part 1. For the part 3 other peptidomimetics used as β-sheet mimetics and non fluorinated analogues of the same peptidomimetic have been evaluated. In particular, this is interesting to prove the role of the fluorine to reinforce the hydrogen bond of the adjacent groups. In the part 4 it was decided to substitute the phenylalanine with a 3,4,5-trimethoxybenzylamine, which is particularly able to form hydrogen bonds with the serines present at the bottom of the S3 pocket of the CT-L site, as proved by Novartis.[71]

From the already synthesised molecules, some have been already tested on 20S rabbit proteasome and the results are shown in Figure 56 and Table 2.

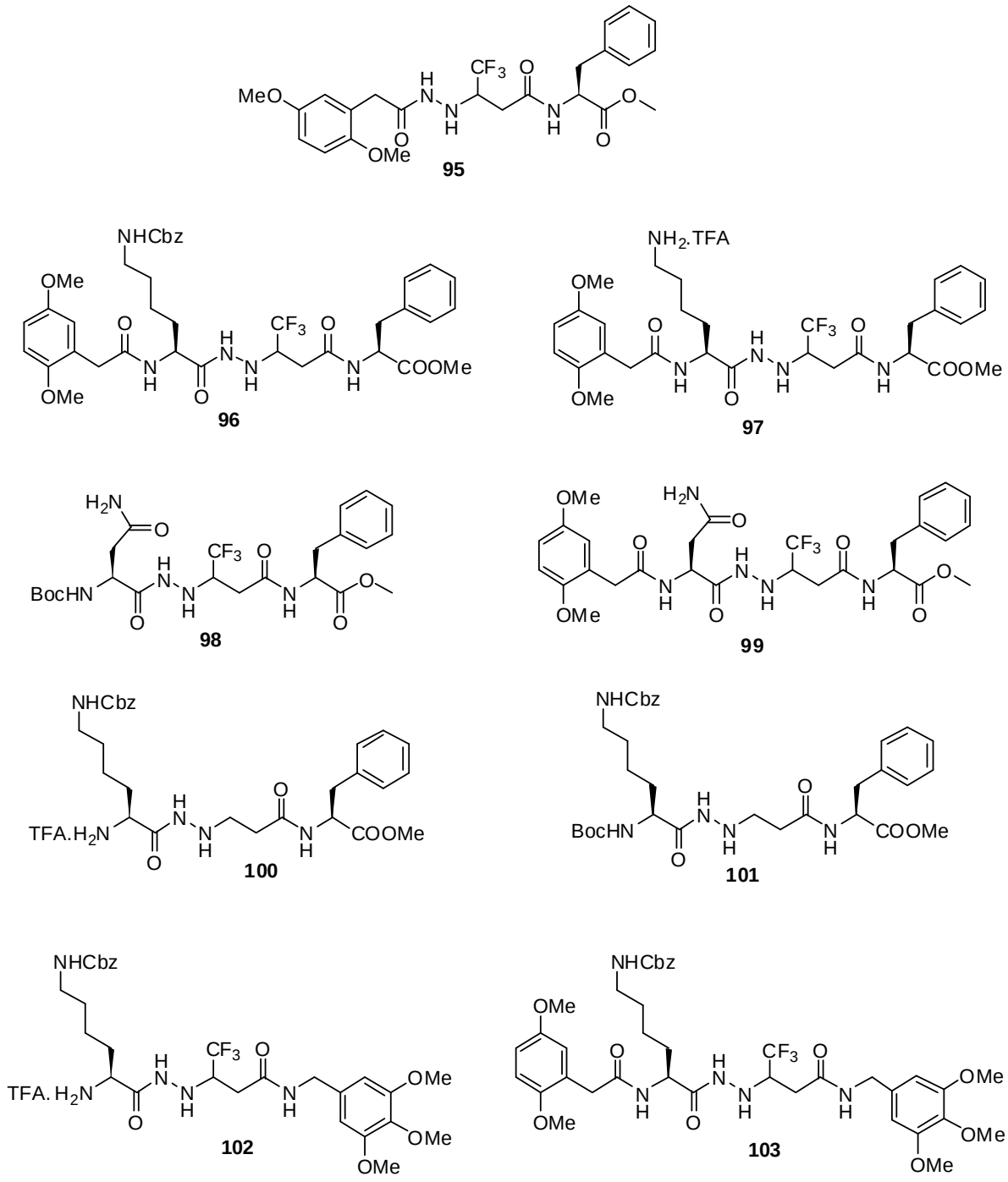

Figure 56. New molecules synthesised and tested on rabbit 20S proteasome.

Molecule	CT-L	PA	T-L
95	ni	ni	ni
96	30%	54	x1.6
97	8.6±0.3	i	i
98	30%	77	x2.7
99	ni	ni	ni
100	18.2±0.4	i	i
101	48.5±2.4	i	i
102	10.1±0.4	i	i
103	ni	ni	x1.8

Table 2. IC_{50} (µM) or % inhibition at 100 µM of compounds **95-103** against rabbit 20S proteasome at pH 7.5 and 37 °C. *x*: activation factor; i = inhibition at 50, 100 and 200 µM; ni = no inhibition.
Values are means of three experiments. CT-L: chymotrypsin-like activity; PA: post-acid activity; T-L: trypsin-like activity.

From these new biological results and from the biological results of my previous molecules (Table 1, page 51) we can establish some preliminary structure-activity relationship that will have to be confirmed in the future with the synthesis and the Docking of a large number of analogues :

- The presence of a free amino group is often decisive for the activity. In fact, all the compounds presenting a free amino group (**83, 81, 56, 102, 97** and **100**) are active, while the protected precursors are or inactive (**80, 82, 103**) or less active (**96, 101**).

- *Concerning the part 1 of the molecules* : the 2,5-dimethoxyphenyl acetic group is comparable (**97** versus **83** and **56**) or slightly superior (**96** versus **80** and **82**) to a Boc group or to the 3-phenoxyphenylacetic acid.

- *Concerning the part 2 of the molecules*, a Lysine residue is favorable, specially a free Lysine residue which is superior to the 3,4-dimethoxyphenylalanine residue (compare **56** and **54**) specially on the T-L activity. Moreover a protected or a free Lysine residue is slightly superior to the asparagine residue (compare **96** to **99**, **97** to **99** and **98** to **83**).

- *Concerning the part 3 of the molecules*, non fluorinated scaffold do not seem to decrease the activity. For now, only few non fluorinated analogues have been synthesised and tested, so it

is a little bit early to do some consideration. However, we could observe that the molecule **100**, which is the analogue of the fluorinated **81**, shows an inhibitory effect of all the active sites of the proteasome. The IC_{50} of molecule **100** was calculated only for the chymotrypsin-like active site, but also if this molecule resulted slightly less active of the molecule **81**, it was in the same order of magnitude (18.2 μM for **100** and 5.9 μM for **81**). We can also observe the apparition of a PA inhibition with the non-fluorinated molecule **100**. A greater difference was found between the behaviour of molecule **80**, which is not active, and its non fluorinated analogue **101**, which have an inhibitory activity in all the three active sites. Also if they are just preliminary results and a larger series of non fluorinated compounds is necessary to have a good comparison, it seems that the presence of the trifluoromethyl group does not greatly improve the activity of our inhibitors. In fact, we generally observed for the non fluorinated compounds an improvement of the solubility, which can also play an important role in the difference of reactivity observed between the molecules **81** and **100**. Moreover, as observed previously, the presence of a free amine is often very important for the activity. Thus, in the non fluorinated compounds the behaviour of the nitrogen of the hydrazine group is more similar to that of a free amine, due to the lack of the effect of the vicinal trifluoromethyl group. However, diastereoisomeric fluorinated compound must be separated and biologically evaluated individually as we really observe a big influence of the chiral center stereochemistry on the Docking analysis.

- *Concerning the part 4 of the molecules*, the phenylalanine residue is comparable to the 3,4,5-trimethoxybenzylamine (compare **102** and **81**). Even then an inhibitory activity on the PA site is observed with **102** while no inhibitory activity was shown on this site with **81**. This result would be very interesting if it is confirmed because in this case we suppressed the peptide character of the C-terminal part of our pseudo-peptides.

The docking of the active and non active molecules was done in the 3 active sites (CT-L, PA and T-L) in parallel to the synthesis and to the biological results, to establish if we could trust our model. In particular, the first thing was to recognize the conformations able to fill both the S1 and the S3 pockets of the proteasome. Whereas this research was quite simple for the active molecules, in the case of the inactive compounds it was often not possible to find conformations with these characteristics. The second step was the research of the intermolecular hydrogen bonds between the ligand and the receptor, in particular with the residues T21, G23, G47, A49 and D114 (this last residue not present in the caspase) and with D120 (in the T-L site), which are, as

illustrated above, the most important for the interaction with the active site of the proteasome. When possible, additionally hydrogen bonds were identified. The last element analyzed was the distance between the ligand and the T1, which can give us additional information about the filling of the S1 pocket. All these analysis have been repeated twice for all the molecules, one for the S configuration of the carbon bearing the trifluoromethyl, and one for the R configuration. Often, one diastereomer was fitting well in the active sites while the other was not. Almost all the docking results were in accordance with the biological results.

As an exemple of the mode of binding in the CT-L site, we show in Figure 57 the molecule **56** (S configuration of the carbon bearing the trifluoro methyl group). The biphenyl group is inserted in the S3 pocket (in red color) and the phenylalanine fills the S1 pocket (in blue color).

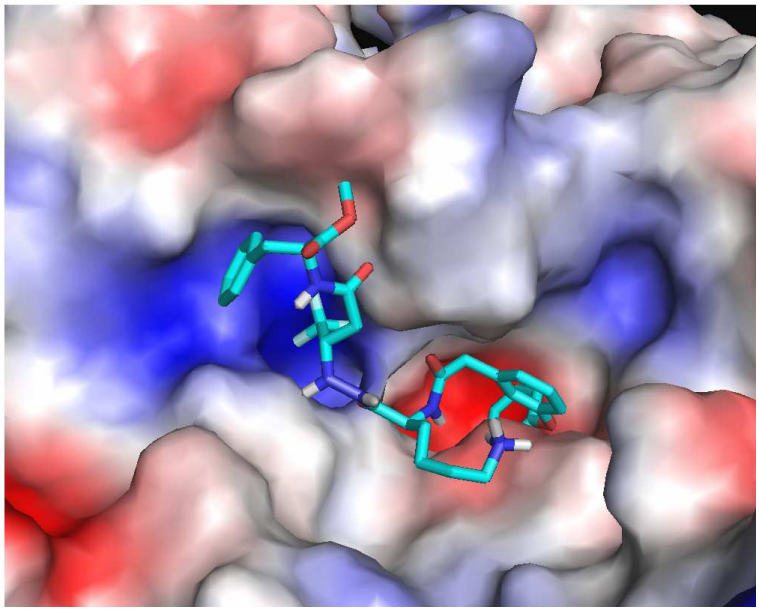

Figure 57. Molecule **56** (S configuration) bounds to the CT-L active site into the proteasome. The pockets S1 and S3 are showed in blue and red respectively.

From these recent results, we demonstrated that the docking can be a useful tool for a better understanding of the binding mechanism of small molecules and 20S proteasome and a useful tool to support and to drive the synthesis of new candidates for the inhibition of the 20S proteasome. In particular, it is possible to explain the differences in the activity between sets of similar molecules which bind the receptor in a similar manner. The limits in our methodology are particularly relied to the high number of torsions of the inhibitor candidates, which does not

allow to obtain a good clustering . Moreover, the structural diversity of the molecules synthesised joined with their high flexibility, makes plausible that it does not exist just one mechanism of binding interaction common to all the molecules, in particular we could not observe for all the active molecules the same way of fitting the two pockets S1 and S3. This fact makes more complicated the establishment of a structure-activity relationship.

II.7. Conclusion

Given that proteasome inhibition is currently being evaluated for a variety of therapeutic purposes, as mentioned before, the need for potent and selective small molecule proteasome inhibitors is well recognized. In the presented work, we have designed, synthesized, and defined the biological profile of a new series of fluorinated pseudopeptides that incorporate a trifluoromethyl-β-hydrazino acid scaffold, as a new class of non covalent proteasome inhibitors.
These new fluorinated pseudopeptides have also the advantage to be very easy to synthesize.
A limited SAR around the fluorinated scaffold resulted in the discovery of compounds having differential inhibitory capacities for CT-L, PA and T-L in micromolar range without effect on challenging proteolytic enzymes such as calpain I and cathepsin B. Part of this work have been recently accepted for publication in Bioorg. Med. Chem. Lett.[110]
These encouraging results have led us to further optimize the lead compounds **56**, **83** and **81** using molecular modelling and continuing biological evaluation.
In the series of compounds bearing our inverse scaffold **59** we did two changes: the inversion of the scaffold and the addition of another hydrazine group. In perspective we will check if the effect that molecules of this series presented no inhibitory effect or very modest effect is due only to the inversion or to the length of this scaffold. We envisaged for example to insert an amine group in the place of the hydrazine group.
The objective of my thesis project was to detect in a first step some biological activity in the new designed molecules. However, we worked with diastereoisomeric mixtures. In consequence, the priority for the next future will be to separate the diastereoisomeric fluorinated compounds to evaluate the influence of the chiral centre on the inhibitory activity. That way, we could maybe obtain with one isolated diastereoisomer some submicromolar inhibitory activity.

In the future other molecules will be designed with the help of molecular modelling (docking), synthesized and evaluated to try to obtain even more efficient proteasome inhibitors.

References of Chapter II

1. Rock, K. L.; Gramm, C.; Rothstein, L.; Clark, K.; Stein, R.; Dick, L.; Hwang, D.; Goldberg, A. L., Inhibitors of the proteasome block the degradation of most cell proteins and the generation of peptides presented on MHC class I molecules. *Cell* **1994,** 78, (5), 761-71.
2. Craiu, A.; Gaczynska, M.; Akopian, T.; Gramm, C. F.; Fenteany, G.; Goldberg, A. L.; Rock, K. L., Lactacystin and clasto-lactacystin beta-lactone modify multiple proteasome beta-subunits and inhibit intracellular protein degradation and major histocompatibility complex class I antigen presentation. *J Biol Chem* **1997,** 272, (20), 13437-45.
3. Kisselev, A. F.; Goldberg, A. L., Proteasome inhibitors: from research tools to drug candidates. *Chem. Biol.* **2001,** 8, (8), 739-758.
4. Shih, S. C.; Sloper-Mould, K. E.; Hicke, L., Monoubiquitin carries a novel internalization signal that is appended to activated receptors. *EMBO J.* **2000,** 19, (2), 187-198.
5. Ciechanover, A., The ubiquitin-proteasome proteolytic pathway. *Cell* **1994,** 79, (1), 13-21.
6. Hershko, A.; Ciechanover, A., The ubiquitin system for protein degradation. *Annu Rev Biochem* **1992,** 61, 761-807.
7. Groll, M.; Ditzel, L.; Lowe, J.; Stock, D.; Bochtler, M.; Bartunik, H. D.; Huber, R., Structure of 20S proteasome from yeast at 2.4 A resolution. *Nature* **1997,** 386, (6624), 463-71.
8. Groll, M.; Heinemeyer, W.; Jager, S.; Ullrich, T.; Bochtler, M.; Wolf, D. H.; Huber, R., The catalytic sites of 20S proteasomes and their role in subunit maturation: a mutational and crystallographic study. *Proc. Natl. Acad. Sci. U. S. A.* **1999,** 96, (20), 10976-10983.
9. Brannigan, J. A.; Dodson, G.; Duggleby, H. J.; Moody, P. C.; Smith, J. L.; Tomchick, D. R.; Murzin, A. G., A protein catalytic framework with an N-terminal nucleophile is capable of self-activation. *Nature* **1995,** 378, (6555), 416-9.
10. Borissenko, L.; Groll, M., 20S Proteasome and Its Inhibitors: Crystallographic Knowledge for Drug Development. *Chem. Rev.* **2007,** 107, (3), 687-717.
11. Schmidtke, g.; Kraft, R.; Kostka, S.; Henklein, P.; Froemmel, C.; Loewe, J.; Huber, R.; Kloetzel, P. M.; Schmidt, M., Analysis of mammalian 20S proteasome biogenesis: the maturation of beta -subunits is an ordered two-step mechanism involving autocatalysis. *EMBO J.* **1996,** 15, (24), 6887-6898.
12. Schmidtke, G.; Schmidt, M.; Kloetzel, P.-M., Maturation of mammalian 20 S proteasome: purification and characterization of 13 S and 16 S proteasome precursor complexes. *J. Mol. Biol.* **1997,** 268, (1), 95-106.
13. Pamer, E.; Cresswell, P., Mechanisms of MHC class I-restricted antigen processing. *Annu. Rev. Immunol.* **1998,** 16, 323-358.
14. Groll, M.; Koguchi, Y.; Huber, R.; Kohno, J., Crystal Structure of the 20 S Proteasome:TMC-95A Complex: A Non-covalent Proteasome Inhibitor. *J. Mol. Biol.* **2001,** 311, (3), 543-548.
15. Borissenko, L.; Groll, M., 20S Proteasome and Its Inhibitors: Crystallographic Knowledge for Drug Development. *Chem. Rev.* **2007,** 107, (3), 687-717.
16. Voges, D.; Zwickl, P.; Baumeister, W., The 26S proteasome: a molecular machine designed for controlled proteolysis. *Annu. Rev. Biochem.* **1999,** 68, 1015-1068.
17. Baumeister, W.; Walz, J.; Zuhl, F.; Seemuller, E., The proteasome: paradigm of a self-compartmentalizing protease. *Cell* **1998,** 92, (3), 367-80.
18. Armon, T.; Ganoth, D.; Hershko, A., Assembly of the 26 S complex that degrades proteins ligated to ubiquitin is accompanied by the formation of ATPase activity. *J Biol Chem* **1990,** 265, (34), 20723-6.
19. DeMartino, G. N.; Moomaw, C. R.; Zagnitko, O. P.; Proske, R. J.; Chu-Ping, M.; Afendis, S. J.; Swaffield, J. C.; Slaughter, C. A., PA700, an ATP-dependent activator of the 20 S

proteasome, is an ATPase containing multiple members of a nucleotide-binding protein family. *J Biol Chem* **1994,** 269, (33), 20878-84.
20. Hoffman, L.; Rechsteiner, M., Activation of the multicatalytic protease. The 11 S regulator and 20 S ATPase complexes contain distinct 30-kilodalton subunits. *J Biol Chem* **1994,** 269, (24), 16890-5.
21. Peters, J. M.; Franke, W. W.; Kleinschmidt, J. A., Distinct 19 S and 20 S subcomplexes of the 26 S proteasome and their distribution in the nucleus and the cytoplasm. *J Biol Chem* **1994,** 269, (10), 7709-18.
22. Kohler, A.; Cascio, P.; Leggett, D. S.; Woo, K. M.; Goldberg, A. L.; Finley, D., The axial channel of the proteasome core particle is gated by the Rpt2 ATPase and controls both substrate entry and product release. *Mol Cell* **2001,** 7, (6), 1143-52.
23. Rechsteiner, M.; Hoffman, L.; Dubiel, W., The multicatalytic and 26 S proteases. *J Biol Chem* **1993,** 268, (9), 6065-8.
24. Lupas, A.; Koster, A. J.; Baumeister, W., Structural features of 26S and 20S proteasomes. *Enzyme Protein* **1993,** 47, (4-6), 252-73.
25. Larsen, C. N.; Finley, D., Protein translocation channels in the proteasome and other proteases. *Cell* **1997,** 91, (4), 431-4.
26. Chernova, T. A.; Allen, K. D.; Wesoloski, L. M.; Shanks, J. R.; Chernoff, Y. O.; Wilkinson, K. D., Pleiotropic effects of Ubp6 loss on drug sensitivities and yeast prion are due to depletion of the free ubiquitin pool. *J. Biol. Chem.* **2003,** 278, (52), 52102-52115.
27. Hanna, J.; Meides, A.; Zhang, D. P.; Finley, D., A ubiquitin stress response induces altered proteasome composition. *Cell* **2007,** 129, (4), 747-59.
28. Beninga, J.; Rock, K. L.; Goldberg, A. L., Interferon-gamma can stimulate post-proteasomal trimming of the N terminus of an antigenic peptide by inducing leucine aminopeptidase. *J Biol Chem* **1998,** 273, (30), 18734-42.
29. Boes, B.; Hengel, H.; Ruppert, T.; Multhaup, G.; Koszinowski, U. H.; Kloetzel, P. M., Interferon gamma stimulation modulates the proteolytic activity and cleavage site preference of 20S mouse proteasomes. *J Exp Med* **1994,** 179, (3), 901-9.
30. York, I. A.; Rock, K. L., Antigen processing and presentation by the class I major histocompatibility complex. *Annu Rev Immunol* **1996,** 14, 369-96.
31. King, R. W.; Deshaies, R. J.; Peters, J. M.; Kirschner, M. W., How proteolysis drives the cell cycle. *Science* **1996,** 274, (5293), 1652-9.
32. Orlowski, R. Z., The role of the ubiquitin-proteasome pathway in apoptosis. *Cell Death Differ* **1999,** 6, (4), 303-13.
33. Palombella, V. J.; Rando, O. J.; Goldberg, A. L.; Maniatis, T., The ubiquitin-proteasome pathway is required for processing the NF-kappa B1 precursor protein and the activation of NF-kappa B. *Cell* **1994,** 78, (5), 773-85.
34. Rock, K. L.; Goldberg, A. L., Degradation of cell proteins and the generation of MHC class I-presented peptides. *Annu Rev Immunol* **1999,** 17, 739-79.
35. Hochstrasser, M., Ubiquitin, proteasomes, and the regulation of intracellular protein degradation. *Curr. Opin. Cell Biol.* **1995,** 7, (2), 215-23.
36. Dou, Q. P.; Li, B., Proteasome inhibitors as potential novel anticancer agents. *Drug Resist. Updates* **1999,** 2, 215-223.
37. Adams, J., Potential for proteasome inhibition in the treatment of cancer. *Drug Discovery Today* **2003,** 8, 307-315.
38. Lin, K. I.; Baraban, J. M.; Ratan, R. R., Inhibition versus induction of apoptosis by proteasome inhibitors depends on concentration. *Cell Death Differ* **1998,** 5, (7), 577-83.
39. Lowe, J.; Stock, D.; Jap, B.; Zwickl, P.; Baumeister, W.; Huber, R., Crystal structure of the 20S proteasome from the archaeon T. acidophilum at 3.4 A resolution. *Science* **1995,** 268, (5210), 533-9.

40. Shaw, E., Cysteinyl proteinases and their selective inactivation. *Adv Enzymol Relat Areas Mol Biol* **1990,** 63, 271-347.
41. Harding, C. V.; France, J.; Song, R.; Farah, J. M.; Chatterjee, S.; Iqbal, M.; Siman, R., Novel dipeptide aldehydes are proteasome inhibitors and block the MHC-I antigen-processing pathway. *J Immunol* **1995,** 155, (4), 1767-75.
42. Loidl, G.; Groll, M.; Musiol, H. J.; Huber, R.; Moroder, L., Bivalency as a principle for proteasome inhibition. *Proc Natl Acad Sci U S A* **1999,** 96, (10), 5418-22.
43. Adams, J.; Behnke, M.; Chen, S.; Cruickshank, A. A.; Dick, L. R.; Grenier, L.; Klunder, J. M.; Ma, Y. T.; Plamondon, L.; Stein, R. L., Potent and selective inhibitors of the proteasome: dipeptidyl boronic acids. *Bioorg Med Chem Lett* **1998,** 8, (4), 333-8.
44. Mc Cormack, T.; Baumeister, W.; Grenier, L.; Moomaw, C.; Plamondon, L.; Pramanik, B.; Slaughter, C.; Soucy, F.; Stein, R.; Zuhl, F.; Dick, L., Active site-directed inhibitors of Rhodococcus 20 S proteasome. Kinetics and mechanism. *J Biol Chem* **1997,** 272, (42), 26103-9.
45. Chauhan, D.; Hideshima, T.; Mitsiades, C.; Richardson, P.; Anderson, K. C., Proteasome inhibitor therapy in multiple myeloma. *Mol. Cancer Ther.* **2005,** 4, (4), 686-692, and references therein.
46. Adams, J., The proteasome: Structure, function, and role in the cell. *Cancer Treat Rev* **2003,** 29 suppl 1, 3-9.
47. Omura, S.; Fujimoto, T.; Otoguro, K.; Matsuzaki, K.; Moriguchi, R.; Tanaka, H.; Sasaki, Y., Lactacystin, a novel microbial metabolite, induces neuritogenesis of neuroblastoma cells. *J Antibiot (Tokyo)* **1991,** 44, (1), 113-6.
48. Fenteany, G.; Standaert, R. F.; Lane, W. S.; Choi, S.; Corey, E. J.; Schreiber, S. L., Inhibition of proteasome activities and subunit-specific amino-terminal threonine modification by lactacystin. *Science* **1995,** 268, (5211), 726-31.
49. Dick, L. R.; Cruikshank, A. A.; Grenier, L.; Melandri, F. D.; Nunes, S. L.; Stein, R. L., Mechanistic studies on the inactivation of the proteasome by lactacystin: a central role for clasto-lactacystin beta-lactone. *J Biol Chem* **1996,** 271, (13), 7273-6.
50. Corey, E. J.; Li, W.-D., Total synthesis and biological activity of lactacystin, omuralide and analogs. *Chem. Pharm. Bull. (Tokyo)* **1999,** 47, (1), 1-10.
51. Feling, R. H.; Buchanan, G. O.; Mincer, T. J.; Kauffman, C. A.; Jensen, P. R.; Fenical, W., Salinosporamide A: a highly cytotoxic proteasome inhibitor from a novel microbial source, a marine bacterium of the new genus Salinospora. *Angew. Chem., Int. Ed.* **2003,** 42, (3), 355-357.
52. Chauhan, D.; Catley, L.; Li, G.; Podar, K.; Hideshima, T.; Velankar, M.; Mitsiades, C.; Mitsiades, N.; Yasui, H.; Letai, A.; Ovaa, H.; Berkers, C.; Nicholson, B.; Chao, T.-H.; Neuteboom, S. T. C.; Richardson, P.; Palladino, M. A.; Anderson, K. C., A novel orally active proteasome inhibitor induces apoptosis in multiple myeloma cells with mechanisms distinct from bortezomib. *Cancer Cell* **2005,** 8, (5), 407-419.
53. Macherla, V. R.; Mitchell, S. S.; Manam, R. R.; Reed, K. A.; Chao, T.-H.; Nicholson, B.; Deyanat-Yazdi, G.; Mai, B.; Jensen, P. R.; Fenical, W. F.; Neuteboom, S. T. C.; Lam, K. S.; Palladino, M. A.; Potts, B. C. M., Structure-Activity Relationship Studies of Salinosporamide A (NPI-0052), a Novel Marine Derived Proteasome Inhibitor. *J. Med. Chem.* **2005,** 48, (11), 3684-3687.
54. Bogyo, M.; McMaster, J. S.; Gaczynska, M.; Tortorella, D.; Goldberg, A. L.; Ploegh, H., Covalent modification of the active site threonine of proteasomal beta subunits and the Escherichia coli homolog HslV by a new class of inhibitors. *Proc Natl Acad Sci U S A* **1997,** 94, (13), 6629-34.
55. Groll, M.; Nazif, T.; Huber, R.; Bogyo, M., Probing Structural Determinants Distal to the Site of Hydrolysis that Control Substrate Specificity of the 20S Proteasome. *Chem. Biol.* **2002,** 9, (5), 655-662.
56. Palmer, J. T.; Rasnick, D.; Klaus, J. L.; Bromme, D., Vinyl sulfones as mechanism-based cysteine protease inhibitors. *J Med Chem* **1995,** 38, (17), 3193-6.

57. Bogyo, M.; Shin, S.; McMaster, J. S.; Ploegh, H. L., Substrate binding and sequence preference of the proteasome revealed by active-site-directed affinity probes. *Chem Biol* **1998,** 5, (6), 307-20.
58. Meng, L.; Mohan, R.; Kwok, B. H.; Elofsson, M.; Sin, N.; Crews, C. M., Epoxomicin, a potent and selective proteasome inhibitor, exhibits in vivo antiinflammatory activity. *Proc Natl Acad Sci U S A* **1999,** 96, (18), 10403-8.
59. Meng, L.; Kwok, B. H.; Sin, N.; Crews, C. M., Eponemycin exerts its antitumor effect through the inhibition of proteasome function. *Cancer Res* **1999,** 59, (12), 2798-801.
60. Hanada, M.; Sugawara, K.; Kaneta, K.; Toda, S.; Nishiyama, Y.; Tomita, K.; Yamamoto, H.; Konishi, M.; Oki, T., Epoxomicin, a new antitumor agent of microbial origin. *J Antibiot (Tokyo)* **1992,** 45, (11), 1746-52.
61. Groll, M.; Kim, K. B.; Kairies, N.; Huber, R.; Crews, C. M., Crystal structure of epoxomicin:20S proteasome reveals a molecular basis for selectivity of alpha ',beta '-epoxyketone proteasome inhibitors. *J. Am. Chem. Soc.* **2000,** 122, (6), 1237-1238.
62. Sin, N.; Kim, K. B.; Elofsson, M.; Meng, L.; Auth, H.; Kwok, B. H.; Crews, C. M., Total synthesis of the potent proteasome inhibitor epoxomicin: a useful tool for understanding proteasome biology. *Bioorg Med Chem Lett* **1999,** 9, (15), 2283-8.
63. Sin, N.; Meng, L.; Auth, H.; Crews, C. M., Eponemycin analogues: syntheses and use as probes of angiogenesis. *Bioorg Med Chem* **1998,** 6, (8), 1209-17.
64. Hideshima, T.; Richardson, P.; Chauhan, D.; Palombella, V. J.; Elliott, P. J.; Adams, J.; Anderson, K. C., The proteasome inhibitor PS-341 inhibits growth, induces apoptosis, and overcomes drug resistance in human multiple myeloma cells. *Cancer Res* **2001,** 61, (7), 3071-6.
65. Imajoh-Ohmi, S.; Kawaguchi, T.; Sugiyama, S.; Tanaka, K.; Omura, S.; Kikuchi, H., Lactacystin, a specific inhibitor of the proteasome, induces apoptosis in human monoblast U937 cells. *Biochem Biophys Res Commun* **1995,** 217, (3), 1070-7.
66. Shinohara, K.; Tomioka, M.; Nakano, H.; Tone, S.; Ito, H.; Kawashima, S., Apoptosis induction resulting from proteasome inhibition. *Biochem J* **1996,** 317 (Pt 2), 385-8.
67. Koguchi, Y.; Kohno, J.; Nishio, M.; Takahashi, K.; Okuda, T.; Ohnuki, T.; Komatsubara, S., TMC-95A, B, C, and D, novel proteasome inhibitors produced by Apiospora montagnei Sacc. TC 1093. Taxonomy, production, isolation, and biological activities. *J. Antibiot.* **2000,** 53, (2), 105-109.
68. Kohno, J.; Koguchi, Y.; Nishio, M.; Nakao, K.; Kuroda, M.; Shimizu, R.; Ohnuki, T.; Komatsubara, S., Structures of TMC-95A-D: Novel proteasome inhibitors from Apiospora montagnei Sacc. TC 1093. *J. Org. Chem.* **2000,** 65, (4), 990-995.
69. Basse, N.; Piguel, S.; Papapostolou, D.; Ferrier-Berthelot, A.; Richy, N.; Pagano, M.; Sarthou, P.; Sobczak-Thepot, J.; Reboud-Ravaux, M.; Vidal, J., Linear TMC-95-Based Proteasome Inhibitors. *J. Med. Chem.* **2007,** 50, (12), 2842-2850.
70. Garcia-Echeverria, C.; Imbach, P.; France, D.; Furst, P.; Lang, M.; Noorani, M.; Scholz, D.; Zimmermann, J.; Furet, P., A New Structural Class of Selective and Non-covalent Inhibitors of the Chymotrypsin-like Activity of the 20S Proteasome. *Bioorg. Med. Chem. Lett.* **2001,** 11, (10), 1317-1319.
71. Furet, P.; Imbach, P.; Noorani, M.; Koeppler, J.; Laumen, K.; Lang, M.; Guagnano, V.; Fuerst, P.; Roesel, J.; Zimmermann, J.; Garcia Echeverria, C., Entry into a New Class of Potent Proteasome Inhibitors Having High Antiproliferative Activity by Structure-Based Design. *J. Med. Chem.* **2004,** 47, (20), 4810-4813.
72. Basse, N.; Papapostolou, D.; Pagano, M.; Reboud-Ravaux, M.; Bernard, E.; Felten, A.-S.; Vanderesse, R., Development of lipopeptides for inhibiting 20S proteasomes. *Bioorg. Med. Chem. Lett.* **2006,** 16, (12), 3277-3281.
73. Demo, S. D.; Kirk, C. J.; Aujay, M. A.; Buchholz, T. J.; Dajee, M.; Ho, M. N.; Jiang, J.; Laidig, G. J.; Lewis, E. R.; Parlati, F.; Shenk, K. D.; Smyth, M. S.; Sun, C. M.; Vallone, M. K.; Woo, T. M.; Molineaux, C. J.; Bennett, M. K., Antitumor Activity of PR-171, a Novel Irreversible Inhibitor of the Proteasome. *Cancer Res.* **2007,** 67, (13), 6383-6391.

74. Piva, R.; Ruggeri, B.; Williams, M.; Costa, G.; Tamagno, I.; Ferrero, D.; Giai, V.; Coscia, M.; Peola, S.; Massaia, M.; Pezzoni, G.; Allievi, C.; Pescalli, N.; Cassin, M.; di Giovine, S.; Nicoli, P.; de Feudis, P.; Strepponi, I.; Roato, I.; Ferracini, R.; Bussolati, B.; Camussi, G.; Jones-Bolin, S.; Hunter, K.; Zhao, H.; Neri, A.; Palumbo, A.; Berkers, C.; Ovaa, H.; Bernareggi, A.; Inghirami, G., CEP-18770: a novel, orally active proteasome inhibitor with a tumor-selective pharmacologic profile competitive with bortezomib. *Blood* **2008,** 111, (5), 2765-2775.
75. Giannis, A.; Kolter, T., Peptidomimetics for Receptor Ligands - Discovery, Development, and Medical Perspectives *Angewandte Chemie International Edition in English* **1993,** 32 (9), 1244-1267.
76. Halgren, T. A., Maximally diagonal force constants in dependent angle-bending coordinates. II. Implications for the design of empirical force fields. *J. Am. Chem. Soc.* **1990,** 112, (12), 4710-23.
77. Furet, P.; Imbach, P.; Furst, P.; Lang, M.; Noorani, M.; Zimmermann, J.; Garcı´a-Echeverrı´a, C., Modelling of the Binding Mode of a Non-covalent Inhibitor of the
20S Proteasome. Application to Structure-Based Analogue Design. *Bioorganic & Medicinal Chemistry Letters* **2001,** 11, (10), 1321–1324.
78. Adams, J., The proteasome: A suitable antineoplastic target. *Nat Rev Cancer* **2004,** 4, 349-360.
79. Adams, J., The development of proteasome inhibitors as anticancer drugs. *Cancer Cell* **2004,** 5, (5), 417-421.
80. Bannwarth, L.; Kessler, A.; Pèthe, S.; Collinet, B.; Merabet, N.; Boggetto, N.; Sicsic, S.; Reboud-Ravaux, M.; Ongeri, S., Molecular Tongs Containing Amino Acid Mimetic Fragments: New Inhibitors of Wild-Type and Mutated HIV-1 Protease Dimerization. *J Med Chem* **2006,** 49, (15), 4657-4664.
81. Nowick, J. S.; Holmes, D. L.; Mackin, G.; Noronha, G.; Shaka, A. J.; Smith, E. M., An Artificial β-Sheet Comprising a Molecular Scaffold, a β-Strand Mimic, and a Peptide Strand. *J Am Chem Soc* **1996,** 118, (11), 2764–2765.
82. Bonnamour, J.; Legros, J.; Crousse, B.; Bonnet-Delpon, D., Synthesis of new trifluoromethyl peptidomimetics with a triazole moiety. *Tetrahedron Lett.* **2007,** 48, (47), 8360-8362.
83. Magueur, G.; Crousse, B.; Bonnet-Delpon, D., Direct access to CF3-propargyl amines and conversion to difluoromethyl imines. *Tetrahedron Lett.* **2005,** 46, (13), 2219-2221.
84. Magueur, G.; Crousse, B.; Bonnet-Delpon, D., Stereoselective access to substituted [(E)- or (Z)-1-(trifluoromethyl)allyl]amines. *Eur. J. Org. Chem.* **2008**, (9), 1527-1534.
85. Martinelli, M.; Milcent, T.; Ongeri, S.; Crousse, B., Synthesis of new triazole-based trifluoromethyl scaffolds. *Beilstein J. Org. Chem.* **2008,** 4, (May), 19/1-19/9.
86. Rinaudo, G.; Narizuka, S.; Askari, N.; Crousse, B.; Bonnet-Delpon, D., Synthesis of fluorinated alpha ,beta -diamino esters by ring opening of activated 3-trifluoromethyl-aziridine-2-carboxylates. *Tetrahedron Lett.* **2006,** 47, (13), 2065-2068.
87. Tam, N. T. N.; Magueur, G.; Ourevitch, M.; Crousse, B.; Begue, J.-P.; Bonnet-Delpon, D., Analogues of Key Precursors of Aspartyl Protease Inhibitors: Synthesis of Trifluoromethyl Amino Epoxides. *J. Org. Chem.* **2005,** 70, (2), 699-702.
88. Bégué, J.-P.; Bonnet-Delpon, D., *Bioorganic and Medicinal Chemistry of Fluorine*. Wiley-VCH Ltd. 2008 and references therein.
89. Hagmann, W. K., The Many Roles for Fluorine in Medicinal Chemistry. *J. Med. Chem.* **2008,** 51, (15), 4359-4369.
90. Banks, R. E.; Smart, B. E., *Organofluorine Chemistry: Principles and Commercial applications* Plenum Press, New York, **1994**.
91. Smart, B. E., Fluorine substituent effects (on bioactivity). *J. Fluorine Chem.* **2001,** 109, (1), 3-11.
92. Zanda, M., Trifluoromethyl group: an effective xenobiotic function for peptide backbone modification. *New J. Chem.* **2004,** 28, (12), 1401-1411.

93. Begue, J.-P.; Bonnet-Delpon, D., Fluoroartemisinins: metabolically more stable antimalarial artemisinin derivatives. *ChemMedChem* **2007,** 2, (5), 608-624.
94. Bouget, K.; Aubin, S.; Delcros, J.-G.; Arlot-Bonnemainsc, Y.; Baudy-Floc'h, M., Hydrazino-Aza and N-Azapeptoids with Therapeutic Potential as
Anticancer Agents. *Bioorg. Med. Chem.* **2003,** 11, (23), 4881–4889.
95. Aubin, S.; Martin, B.; Delcros, J.-G.; Arlot-Bonnemains, Y.; Baudy-Floc'h, M., Retro Hydrazino-azapeptoids as Peptidomimetics of Proteasome Inhibitors. *J. Med. Chem.* **2005,** 48, (1), 330-334.
96. Cheng, R. P.; Gellman, S. H.; DeGrado, W. F., beta-Peptides: from structure to function. *Chem Rev* **2001,** 101, (10), 3219-32.
97. Juaristi, E.; Soloshonok, V. A., *Enantioselective Synthesis of beta-Amino Acids (SECOND EDITION)*. Wiley-VCH Ltd. **2005**.
98. Seebach, D.; Hook, D. F.; Glattli, A., Helices and other secondary structures of beta - and gamma -peptides. *Biopolymers* **2006,** 84, (1), 23-37.
99. Groll, M.; Goetz, M.; Kaiser, M.; Weyher, E.; Moroder, L., TMC-95-Based Inhibitor Design Provides Evidence for the Catalytic Versatility of the Proteasome. *Chem. Biol.* **2006,** 13, (6), 607-614.
100. Nowick, J. S.; Pairish, M.; Lee, I. Q.; Holmes, D. L.; Ziller, J. W., An Extended beta -Strand Mimic for a Larger Artificial beta -Sheet. *J. Am. Chem. Soc.* **1997,** 119, (23), 5413-5424.
101. Tsai, J. H.; Waldman, A. S.; Nowick, J. S., Two new beta-strand mimics. *Bioorg Med Chem* **1999,** 7, (1), 29-38.
102. Jagodzinska, M.; Huguenot, F.; Zanda, M., Studies on a three-step preparation of beta -fluoroalkyl acrylates from fluoroacetic esters. *Tetrahedron* **2007,** 63, (9), 2042-2046.
103. Rocquet, C.; Reynaud, R.; Sousselier, L.; Soliance; France, Innovative Global "Age-Defying" Strategy. *Cosmetic Science Technology* **2007**, 119-125.
104. Arribas, J.; Castano, J. G., Kinetic studies of the differential effect of detergents on the peptidase activities of the multicatalytic proteinase from rat liver. *J Biol Chem* **1990,** 265, (23), 13969-13973.
105. Kisselev, A. F.; Kaganovich, D.; Goldberg, A. L., Binding of hydrophobic peptides to several non-catalytic sites promotes peptide hydrolysis by all active sites of 20 S proteasomes: Evidence for peptide-induced channel opening in the alpha -rings. *J. Biol. Chem.* **2002,** 277, (25), 22260-22270.
106. Ruiz de Mena, I.; Mahillo, E.; Arribas, J.; Castano, J. G., Kinetic mechanism of activation by cardiolipin (diphosphatidylglycerol) of the rat liver multicatalytic proteinase. *Biochem J* **1993,** 296 (Pt 1), 93-7.
107. Wilk, S.; Chen, W.-E., Synthetic peptide-based activators of the proteasome. *Mol. Biol. Rep.* **1997,** 24, (1-2), 119-124.
108. Calpaïn I and cathepsin B obtained from Calbiochem, USA, were assayed at 37 °C using Suc-LLVY-AMC in 50 mM Tris-HCl (pH 7.2), 10 mM DTT, 2 mM CaCl2, and ZRR-AMC in 352 mM KH2PO4 (pH 6), 48 mM NaHPO4, 1mM EDTA, 1 mM DTT, respectively.
109. Proteasome Glo Cell-Based Assay (Promega) using MG-132 as a standard.
110. Formicola, L., Maréchal X., Basse N., Bouvier-Durand M., Bonnet-Delpon D., Milcent T., Reboud-Ravaux M., Ongeri S., Novel fluorinated pseudopeptides as proteasome inhibitors. *Bioorg. Med. Chem. Lett.* **2008**, in press.

III NEW δ-AMINO ACIDS TOWARDS NEW FOLDAMERS

This work has been realized in collaboration with Guitot Karine, PhD student.

III.1. INTRODUCTION

The folding of polypeptide chains into secondary and eventually into a bewildering array of tertiary structures results in protein molecules that are responsible for most of the biological interactions and functions found in nature. Therefore, peptides and proteins are attractive targets for drug design. Poor bioavailability and metabolic stability of peptidic drugs, however, have resulted in significant limitations. A logical next step is to mimic nature and create nonbiologically derived molecules that either fold into well-defined secondary structures, or assemble into larger architectures. The pioneering studies of Gellman and Seebach on β-peptides, a class of unnatural peptidomimetic folding oligomers, have demonstrated the feasibility of folding unnatural oligomers into well-defined conformations. Extending the concept of β-peptides has led to other peptidomimetic foldamers such γ-peptides[1,2] and δ-peptides.[3]

In the presented work we are interested in δ-amino acids towards new foldamers.

As mentioned in the chapter I, δ-amino acid residues **104** are isosteres of dipeptide elements in α-peptides **105** (Figure 58).

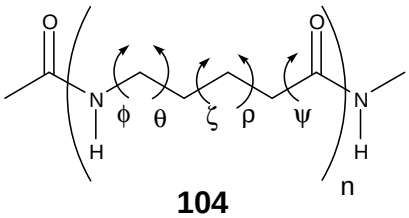

104

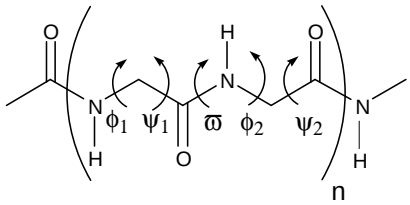

105

Figure 58. Comparison of δ-amino acid residues **104** with α-dipeptide elements **105**. φ, ψ, θ, ζ, ρ, ω are the backbone torsion angles.

Therefore, δ-amino acids are potential surrogates for α-dipetides and can be useful to improve the resistance of natural peptide chains toward degradation by proteases.

There are some examples of the incorporation of a single δ-amino acid into longer natural amino acid sequences,[4-6] but most of the cases deal with sequences based on repeating δ-amino acid units, particularly on sugar amino acids derived from furanose[7] and pyranose.[8] In fact, homo-oligomers of sugar amino acids have been extensively studied and provide many examples of foldamers.[8-11]

Oligomers of different types of amino acids are also important in conformational design and can be potentially useful to obtain new foldamers. Our approach presented in this chapter is based on the synthesis of peptides containing α- and δ-amino acids with different chain length and α-amino acid composition.

III.2. Model peptides containing δ-amino acid units

III.2.1. Previous work in the laboratory

The application of unnatural building blocks to induce a predictable conformation requires the investigation of their conformational preferences.

In our group we investigated the conformational preferences of peptide mimics containing the two enantiomers of a novel δ-sugar amino acid **106** and **107** (Figure 59). The synthesis of both enantiomers was previously developed by M. Haque in our group.[12]

106 (*S*,*S*) **107** (*R*,*R*)

Figure 59. (*S*,*S*)-**106** and (*R*,*R*)-**107** enantiomers of a novel δ-sugar amino acid.

The key intermediate **109** was obtained starting from inexpensive furan-2-carboxylic methyl ester **108** in four steps by using a procedure that has been previously developed in our group.[13] Treatment of γ-butyrolactonaldehyde **109** with 4-methoxybenzylamine to form the corresponding imine, followed by reduction with $NaBH_4$ provided the amine **110**[14] in 76% yield. *N*-Boc protection afforded the protected amine **111**,[15] in which the PMB group was removed with CAN to give the carbamate **112**[16] in 79% yield. Finally, ruthenium catalyzed oxidative cleavage of the allylic double bond with $NaIO_4$ gave the δ-amino acid enantiomers **106** and **107**[17] in 86% yield (Scheme 8).

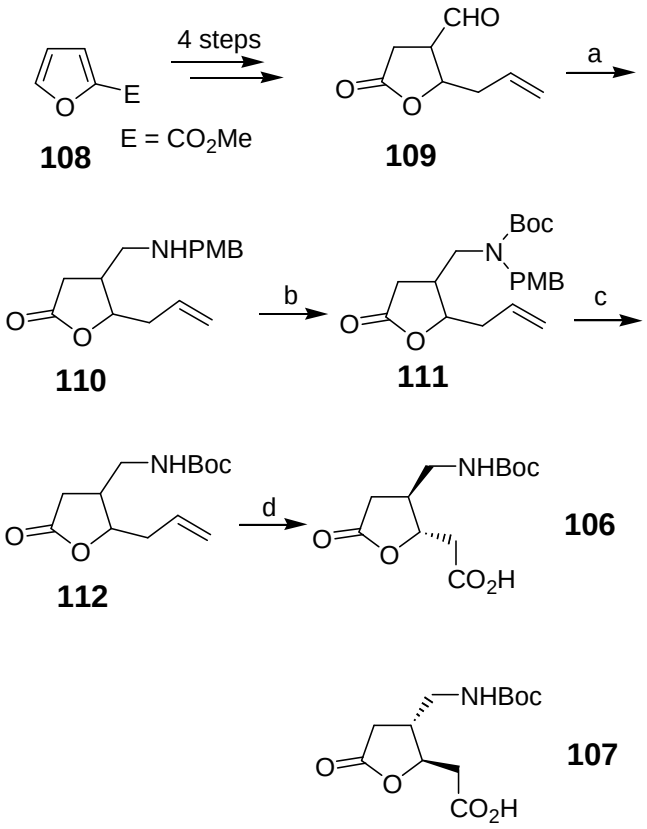

Scheme 8. Synthesis of compounds **106** and **107**. Reagents and conditions:

a) (i) Na_2SO_4, 4-methoxybenzylamine (1.1 equiv), CH_2Cl_2, 3 h; (ii) $NaBH_4$ (2equiv), MeOH, H_2O, 0 ℃, 30 min, 76%; b) $(Boc)_2O$, dioxane-1M K_2CO_3 (1:1.2), r.t., overnight, 74%; c) CAN (4 equiv), CH_3CN-H_2O (1:3), 0 ℃, 1 h and r.t., 2 h, 79%; d) $RuCl_3 \cdot 3H_20$ (6 mol%), $NaIO_4$ (4.0 equiv), CCl_4-CH_3CN-H_2O (1:1:2), 0 ℃, 1 h and r.t., 2 h, 86%.

Delatouche and Bordessa synthesized two α-δ pentapeptides **113** and **114** (Figure 60) using the scaffolds **106** and **107**, respectively, which were alternated with the natural amino acid

phenylalanine. In addition, Bordessa synthesized heptapeptide **115** using the R,R enantiomer and phenylalanine (Figure 60).

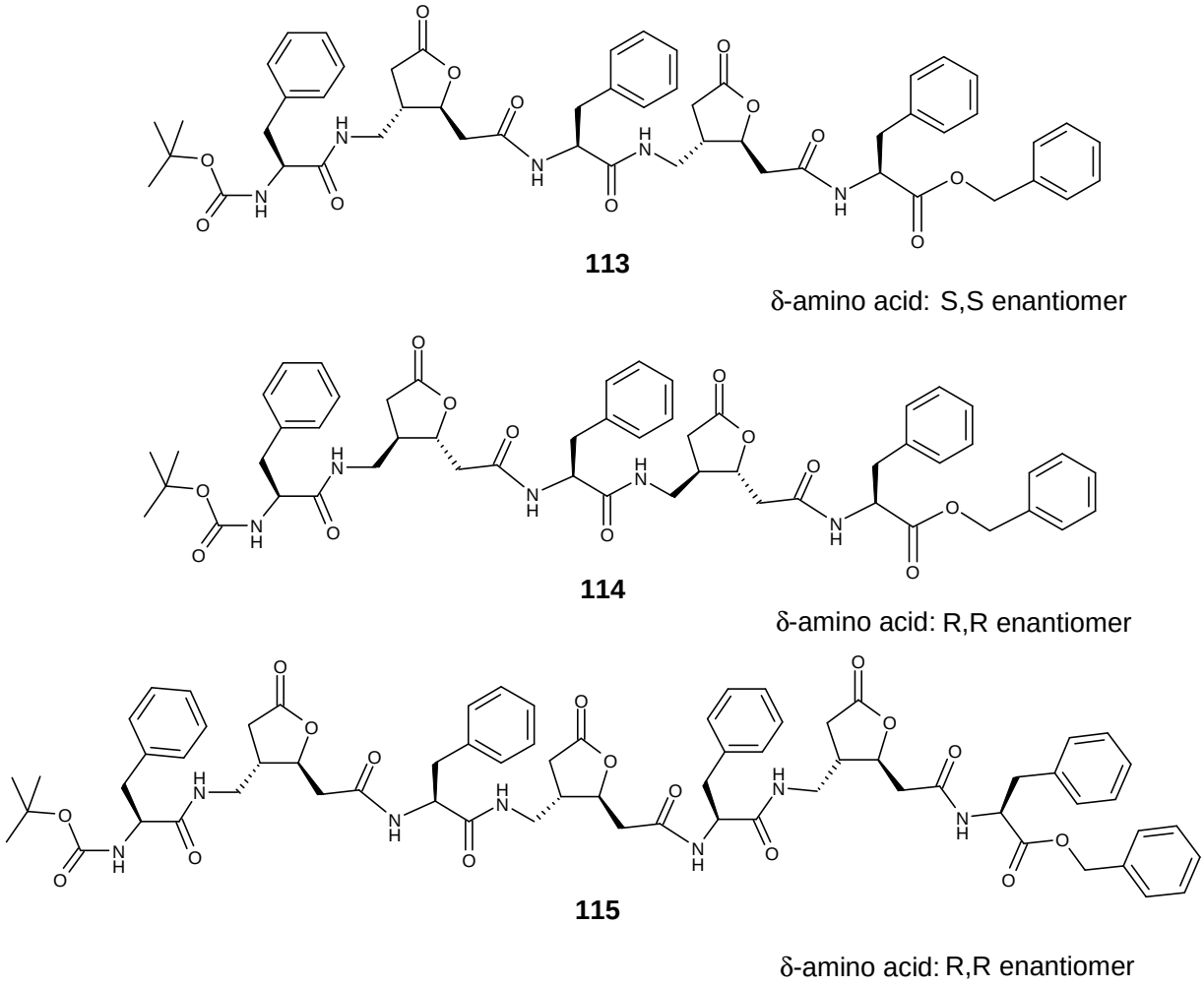

Figure 60. Pentapeptides containing α-δ amino acids **113** and **114** and heptapeptide **115**.

The aim of our work has been to investigate the conformational analyses of the two pentapeptides **113** and **114**, and of the heptapeptide **115**, in order to determine their secondary structure preferences.

III.2.2. Conformational investigations

The conformation of peptides depends principally on their amino acidic composition and on the sequence of these amino acids. As the physical and biological properties of peptides are determined by their structure, the knowledge of the latter is essential to understand these properties. There are many techniques to investigate the three dimensional structure of peptides. FT-IR and CD spectroscopy are important tools to indicate the presence or absence of secondary structure elements, while NMR spectroscopy and X-ray crystallography allow a detailed description of the localization and spatial arrangement of such elements within the amino acid sequence. However, for the X-ray crystallography single crystals are needed, and there always exists the possibility of a difference in the conformation between the solid state and the one seen in solution. In the present work we employed NMR, CD, FT-IR spectroscopy, and molecular modelling to characterize the peptides synthesized.

NMR investigation

The most common and useful tool to investigate the secondary and tertiary structure of peptides and proteins in solution is the Nuclear Magnetic Resonance (NMR) spectroscopy.[18]NMR spectroscopy allows an investigation of the structure of biopolymers on an atomic level in solution. Moreover, NMR investigations can highlight the presence of conformational equilibria and the dynamics of the folding. Important structural information can be obtained from both mono- and bidimensional NMR spectra.

Information from 1D-proton NMR spectra

Even though the NMR-spectra of biopolymers are derived from the nuclear spins of the monomers thea are build up from, there is no straightforward correlation between the NMR spectra of the low molecular weight components and the three-dimensional strucutre of the whole polymer.[18] A dispersion of nucleus's chemical shift values is the first indication of the presence of spatial folding in a peptide chain. When a peptide has a defined conformation in solution, a

proton in the sequence will have a different microenvironment compared to those in a random coil structure. It will also be different from the same proton contained in an identical residue type at a different point in the sequence. This fact leads to different specific chemical shift values compared to those for an unfolded structure and to a good dispersion of the signals.

The presence of a secondary structure in solution can lead to a slower exchange rate for labile protons, which can be measured by time dependent NMR-spectroscopy, while in small molecules proton exchange is too fast to be observed. Moreover the slower diffusional motions of the macromolecul in solution can substantially affect the spin relaxation and the Nuclear Overhauser Enhancement (NOE).[18] The presence of hydrogen bonds can be detected from onedimensional NMR spectra. These techniques are based on the assumption that the NHs involved in a H-bond are less sensitive to perturbations such as changing of temperature, concentration or solvent, than the NHs that are exposed to the solvent. The determination of the temperature coefficients ($\Delta\delta/\Delta T$) for the amide protons is based on the observation that, upon warming, NHs involved in hydrogen bonds display shifts at a smaller extent than the NHs that are exposed to the solvent. Generally, values of $-\Delta\delta/\Delta T > 3$ ppb/K indicate amide protons in an equilibrium between a hydrogen-bonded and a non-hydrogen-bonded state, while values of $-\Delta\delta/\Delta T < 2.6$ ppb/K are considered an indication of hydrogen-bonded NH protons or of NH protons locked in a hydrogen-bonded conformation.[19]

The secondary structures of peptides are characterized by distinct torsion angles along the backbone. Since the size of the spin-spin coupling constant $^3J_{HN\text{-}H\alpha}$ depends on the torsion angle NH-CHα, on the basis of Karplus relationship, the measurement of $^3J_{HN\text{-}H\alpha}$ is useful for secondary structure determination, as it can be directly related to the backbone dihedral angle φ.[18, 20] Generally, $^3J_{HN\text{-}H\alpha}$ values < 6 Hz indicate turn or helical conformations, whereas values higher than 6 Hz are referred to unordered structure or an extended conformation (Figure 61).

Secondary structure	φ	$^3J_{HN\alpha}$ (Hz)
α-helix	-57°	3.9
3_{10}-helix	-60°	4.2
antiparallel β-sheet	-139°	8.9
parallel β-sheet	-119°	9.7

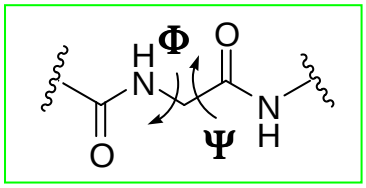

Figure 61: Table of the $^3J_{HN\text{-}H\alpha}$ values in regular secondary structures[18] (left side). Torsion angles φ and ψ present along the backbone of a α-peptide (right side).

Information from 2D-proton NMR spectra

The most useful data relating to a peptide conformation is gained from 2D-NMR investigation. Of particular interest are the correlation spectroscopy (COSY), total correlation spectroscopy (TOCSY) and NOE spectroscopy/rotational frame NOE (NOESY/ROESY) experiments.

The cross peaks observed in the COSY spectrum correspond to proton-proton correlations due to scalar (through-bond) couplings, though the respective protons may only be separated by a maximum of three covalent bonds. The TOCSY spectrum contains all correlations between protons of one spin system and in the case of peptides each amino acid has a particular spin-system pattern that allows the identification of every residue type in the sequence. With the help of these two experiments, it is possible to assign completely all the chemical shifts of the protons in a peptide. Further, NOESY experiment displays cross peaks due to dipolar coupling resulting from through space interactions. NOESY cross peaks depend on the distance between two protons and occur between two nuclei that are close in the space up to 5 Å. A NOE cross peak indicates that two non-covalently bonded nuclei are close enough to interact or to exchange. NOE cross peaks are usually defined as *sequential* distances when they are between backbone protons, or between a backbone proton and a β proton of residues that are nearest neighbours in the sequence. *Medium-range* distances are all non-sequential signals between residues within a segment of five consecutive residues. *Long-range* distances are between the backbone protons of the residues that are at least six positions away in the sequence.[18] Depending on the torsion angles that characterize the secondary structure of a peptide, sequential and medium-range proton-proton distances will have different values. For instance the sequential NH-NH and CHα-NH contacts for a regular α-helix are about 2.8 and 3.5 Å, respectively. The CHβ-NH contacts, since they depend also on the torsion angle on the side chain χi, vary between 2.5 and 4.1 Å for a α-helix.18 Medium-range contacts in helices are usually i,i+2, i,i+3, and i,i+4. In particular i,i+4 contacts are especially useful since they are present in a regular α-helix and not in a 3_{10}-helix. Tight turns have close *i,i*+2 values. In the case of β-structure short *medium-range* distances are not observed, since the polypeptide segments are almost fully extended.[18] Table 3 lists short *sequential* and *medium-range* distances that are found in known α-peptide conformations.

Distance	α-helix	3_{10}-helix	β-sheet
$d_{\alpha N}$	3.5	3.4	2.2
$d_{\alpha N}(i,i+2)$	4.4	3.8	
$d_{\alpha N}(i,i+3)$	3.4	3.3	
$d_{\alpha N}(i,i+4)$	4.2		
d_{NN}	2.8	2.6	4.2-4.3
$d_{NN}(i,i+2)$	4.2	4.1	
$d_{\beta N}$	2.5-4.1	2.9-4.4	3.2-4.7
$d_{\alpha\beta}(i,i+3)$	2.5-4.4	3.1-5.1	

Table 3. Short *sequential* and *medium-range* ^{1}H-^{1}H distances in some common secondary structures in α-peptides.[18]

Circular dichroism

Circular Dichroism (CD) spectroscopy is an important technique to investigate the secondary structure of proteins and peptides. It is based on the differential absorption of left and right circularly polarized light. To deliver a CD signal, a compound has to possess a chromophore, which is either inherent chiral or surrounded by a chiral environment and absorbs in the observed wavelength range. These prerequisites are met by the amide bond in peptides and proteins, rendering the CD spectroscopy a suitable methodology for the elucidation of their structural preferences. The observed bands in the CD spectra of peptides and proteins stem from the $n \rightarrow \pi^*$ and the $\pi \rightarrow \pi^*$ transitions of the amide bonds. Every secondary structure gives rise to a specific CD spectrum that represents a survey upon the averaged overall structure of a peptide or protein, while it is impossible to assign structural preferences to an individual residue (Figure 62). However, algorithms based on protein and peptide reference data sets enable the calculation of the secondary structure elements composition of a peptide/protein from its CD spectrum.

In addition to the far-UV region over the range 190-250 nm, also the near-UV region from 250 to 320 nm can deliver useful information, as it shows the contribution of aromatic residues like tyrosine or tryptophan.[21, 22]

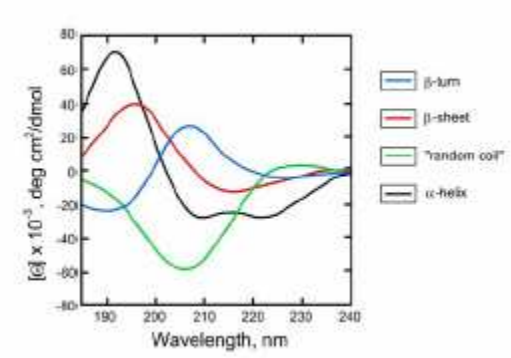

Figure 62: CD spectra characteristic for common secondary structure elements (adapted from Greenfield).[23]

The molar ellipticity $[\Theta]_\lambda$ at the wavelength λ is defined as follows (Equation 1):

$$\left[\Theta\right]\lambda = \frac{100 \cdot \Psi}{l \cdot c}\left[\frac{Deg \cdot cm^2}{dmol}\right] \qquad \textbf{Equation 1}$$

where Ψ is the deviance of left- and right-circularly polarized light in degree, *l* the cell length in cm and c the peptide concentration in M. To compare peptides with different chain lengths, the molar ellipticity per residue is used, which is obtained by dividing $[\Theta]_\lambda$ by the number of amino acids. The CD bands characteristic for helical peptides at 190, 208 and 222 nm stem from the $\pi \rightarrow \pi^*$ transition (190 nm and 208 nm are the components perpendicular and parallel to the helix axis, respectively) and $n \rightarrow \pi^*$ transition (222 nm), with the latter being sensitive to hydrogen bond formation.[24] The ratio R between the two minima at 222 and 208 nm can be used as an indicator for the presence of interacting helices, as the band at 208 nm, corresponding to the parallel component of the $\pi \rightarrow \pi^*$ transition, changes its energy upon an interhelical interaction. Ratios larger than 1 are commonly regarded as the result of interacting helices, as found in coiled coil structures, while ratios lower than 1 indicate the presence of non-interacting helices.[25]

Conformational analysis

As mentioned before (see chapter II.2.2. Molecular Modelling: tool for the conception, page 47), the use of theoretic methods to obtain models that allow predicting structures, properties and molecular interactions is known as "Molecular Modelling".

Molecular Modelling provides information that is not available directly from conventional experiments, thus it has a complementary role in the field of the experimental chemistry.

There are several simulation technique methods: quantum chemistry, molecular mechanics, molecular dynamics (MD).

It is known that the structures with lower energy states are more stable and take a part in chemical and biological processes. Molecular dynamics simulation offers an effective tool to detect the energetically most favored 3D structure of a system.

In our work simulations incorporating NOE derived distance constraints as well as "free" dynamics were investigated in vacuum (*gas-phase* simulations). MD calculations were performed using Sybyl program (version 7.0) with MMFF94 force field. The temperature was increased progressively from 300 to 700 K and the time period of each simulation was 222 ps, where a molecule was extracted every 500 steps. Among the resulting structures those energetically favored were then minimized and analyzed.

FT-IR spectroscopy

Infrared light is energetic enough to excite molecular vibrations to higher energy levels. The main characteristic bands of the peptide group are called amide A, amide I and amide II. Evidence exists that the position of these bands is related to the conformation of the peptide.[26] The amide A band is mainly due to the N–H stretching vibration. It is very sensitive to the strength of a hydrogen bond, thus providing an opportunity to gain information about any intra- or intermolecular hydrogen bond. Usually, in a non polar solvent, non hydrogen-bonded NHs adsorb above 3400 cm^{-1}, while NHs that are involved in hydrogen-bonds absorb below 3400 cm^{-1}.[27] The amide I and II bands are related to the backbone conformation. The amide I is associated with the C=O stretching vibration, while the amide II results from the N–H bending and from C–N stretching vibrations.

	α-helix	*3_{10}-helix*	*β-sheet*
Amide I	1652	1666-1662	1648-1645
Amide II	1548	1533-1531	1533-1536

Table 4. Frequencies (cm^{-1}) of the amide I and amide II bands found for different α-peptide conformations.

III.2.3. Results on alternated α/δ amino acids

The pentamer containing alternated (S,S)-δ-amino acid and phenylalanine was analyzed by NMR in both $CDCl_3$ and methanol-d_3 solvents. Comparing both analyses at different temperatures, the spectrum in $CDCl_3$ seemed to be less comprehensible than the spectrum in methanol-d_3, showing a lower dispersion of the NH signals, and higher temperature coefficients ($-\Delta\delta/\Delta T > 10$ppb/K). We therefore present here only the analyses performed in methanol-d_3. This choice was also supported by the CD experiment, where the CD curve appeared to be much more defined in methanol than in TFE. Thus, the synthesized α/δ-peptide **113** (Figure 60) was dissolved in methanol-d_3 and studied by NMR spectroscopy. 1D experiments were first acquired at five different temperatures (273, 278, 283, 293 and 303 K), and the one that gave the better resolved spectrum (283 K) was chosen to record the 2D experiments. The complete ^{1}H-NMR resonance and sequence assignments were done by using the COSY, TOCSY and ROESY spectra. Sequential and interresidue NOE cross-peak intensities were classified as strong (1.8-2.7 Å), medium (1.8-3.3 Å) and weak (1.8-5 Å) based on the number of contours in the contour plot of the ROESY spectrum. The NOE contacts observed for this peptide are shown in Figure 63.

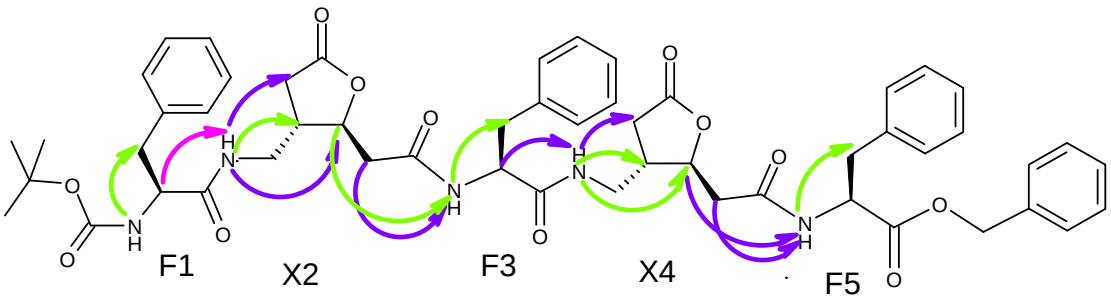

113 δ-amino acid: S,S enantiomer

Figure 63. Summary of the interresidue NOE contacts observed for the peptide **113** in methanol-d_3 at 283 K (pink arrows: strong NOEs; green arrows: medium NOEs; blue arrows: weak NOEs).

The values of the $^3J_{HN\text{-}H\alpha}$ coupling constants were estimated in the 1D ^{1}H-NMR spectrum and these vicinal coupling constants showed always values bigger than 6 Hz (Figure 64).

Amide protons showed high temperature coefficients (Figure 64), suggesting a non-hydrogen-bonded state. However, studies of deuterium exchange in methanol-d_4 showed a slow disappearance of one or both amide protons of the lactone residues. The presence of the hydrogen bond possibility in this molecule was confirmed by IR experiments in CH_2Cl_2, which showed two bands in the amide region: a broad and intense band at 3311 cm^{-1} in the H-bonded region, and a weaker one at 3420 cm^{-1}.

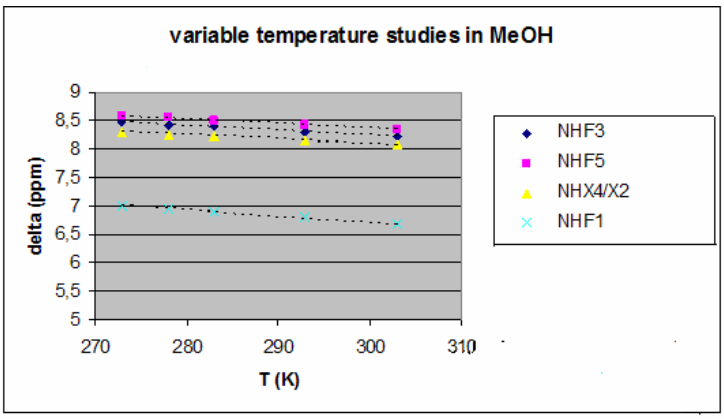

	-Δδ (ppb)/ ΔT(K)	$^3J_{HN\text{-}H\alpha}$ (Hz)
NHF1	10.3	7.2
NHX2	7.1	
NHF3	8.3	6.9
NHX4	7.1	
NHF5	8.1	8.2

Figure 64: Variable temperature studies in methanol-d_3 of peptide **113**.

Molecular modelling was performed using molecular dynamics experiments in vacuum. Introduction of four of the NOE contacts found in the ROESY spectrum as constraints in this experiment gave the structure shown in Figure 65 as the conformational energetic minimum, which is characterized by a large loop locked at the extremities by two hydrogen bonds.

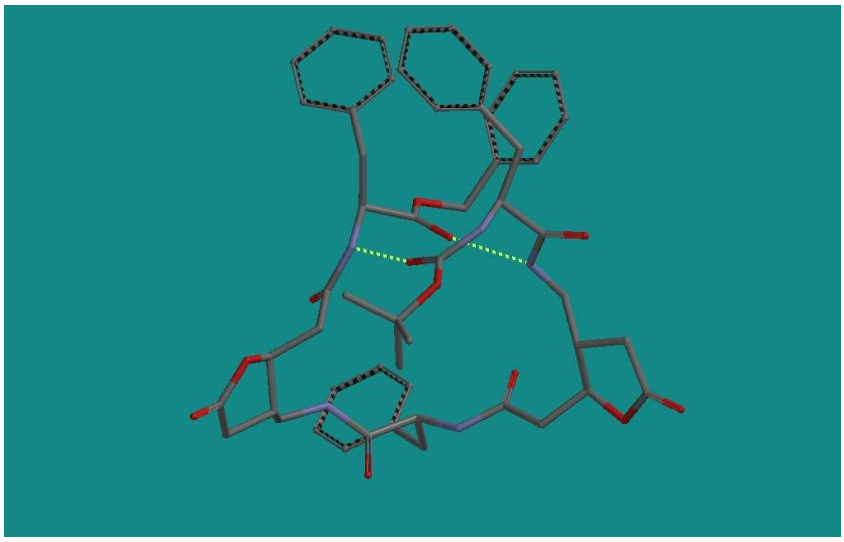

Figure 65: Structure of low-energy conformer calculated for peptide **113**. Hydrogen bonds are indicated with dashed lines and all hydrogen atoms have been omitted for clarity.

The CD spectrum in methanol at 0.1 mM showed two maxima at 200 and 219 nm that were not comparable with any data in the literature (Figure 66).

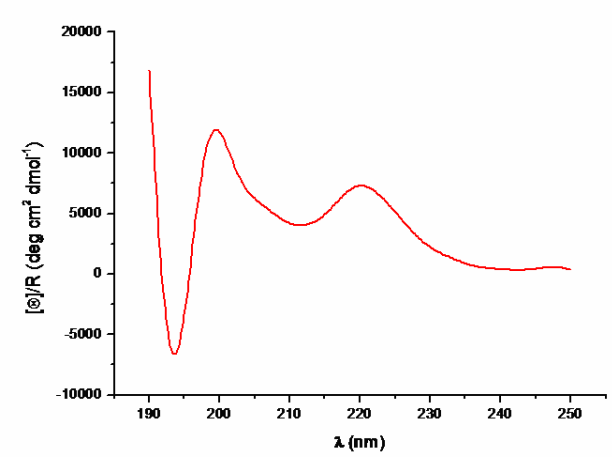

Figure 66: CD spectrum of the pentapeptide **113** in methanol.

The pentamer containing alternated (R,R)-δ-amino acid and phenylalanine **114** (Figure 60) was analyzed by NMR in both $CDCl_3$ and methanol-d_3 solvents. Due to low solubility and low dispersion of the signals in methanol, we used only the analyses in $CDCl_3$. The synthesized α/δ-peptide **114** was thus dissolved in $CDCl_3$ and studied by NMR spectroscopy. 1D experiments were first acquired at five different temperatures (278, 283, 288, 293, 298 and 303 K), and the one that gave the better resolved spectrum (288 K) was chosen to record the 2D experiments. The detected NOE contacts are shown in Figure 67.

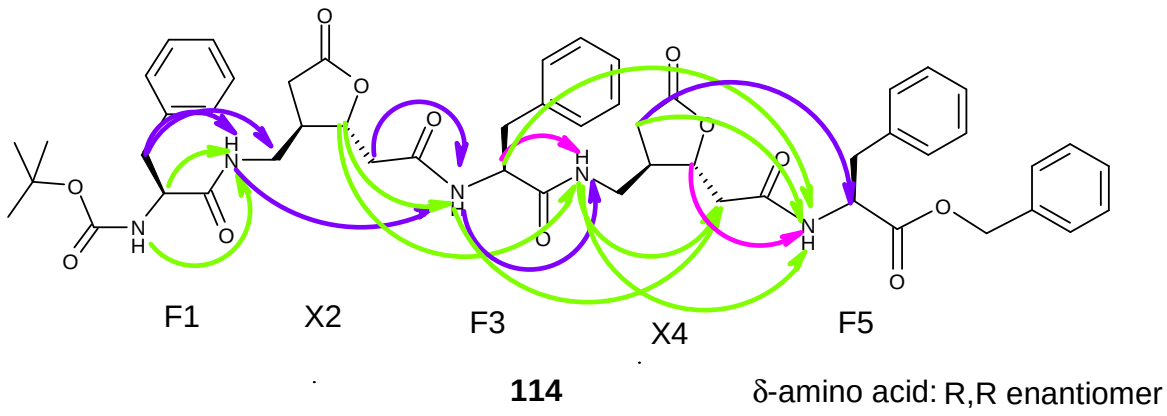

Figure 67: Summary of the interresidue NOE contacts observed for the peptide **114** in methanol-d_3 at 288 K (pink arrows: strong NOEs; green arrows: medium NOEs; blue arrows: weak NOEs).

In comparison with the pentamer containing the (S,S)-δ-amino acid, this oligomer had a better dispersion of the signals in the ^{1}H spectrum with no overlapping of the NH amides, and the ROESY spectrum allowed us to find numerous NOE contacts that are reported in Figure 67. In counterpart, we could see the presence of more than one conformer. We focused our study on the major conformer. NMR analyses showed amide protons at high ppm values (between 7.4 and 8.4 ppm), which is characteristic of protons involved in hydrogen bonding. However, $-\Delta\delta/\Delta T$ were quite high, ranging between 6 and 10.4 ppb/K, and also the ^3J coupling constants were higher than 6Hz (Figure 68).

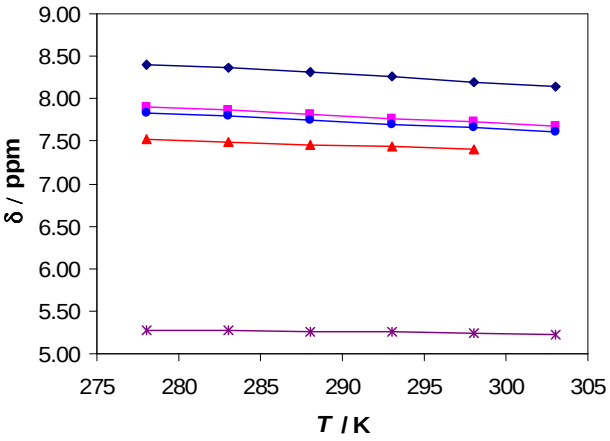

		-Δδ(ppb)/ ΔT(K)	$^{3}J_{HN-H\alpha}$ (Hz)
F3	NHF1	2.0	7.2
X2	NHX2	8.8	
X4	NHF3	10.4	6.9
F5	NHX4	6.0	
F1	NHF5	8.8	8.2

Figure 68: Variable temperature studies in methanol-d_3 of peptide **114**.

The CD spectrum was recorded in TFE (0.3 mM) and gave two maxima at 203 and 218 nm (Figure 69).

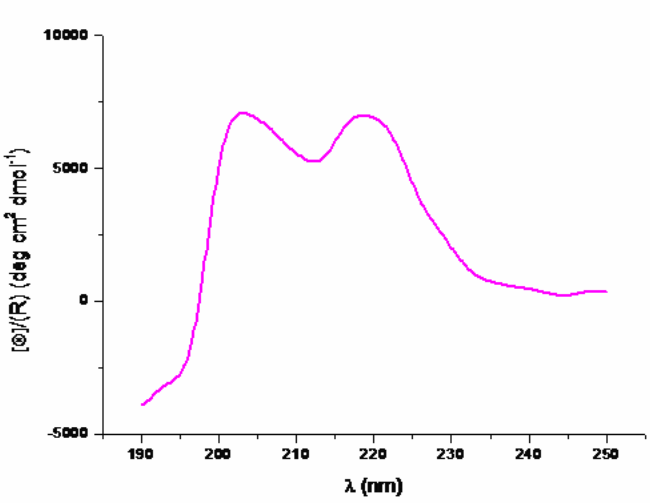

Figure 69: CD spectrum of the pentapeptide **114** in TFE.

Finally, molecular dynamics experiments, taking into account eleven NOE contacts, afforded the structure shown in Figure 70 corresponding to the energetic minimum.

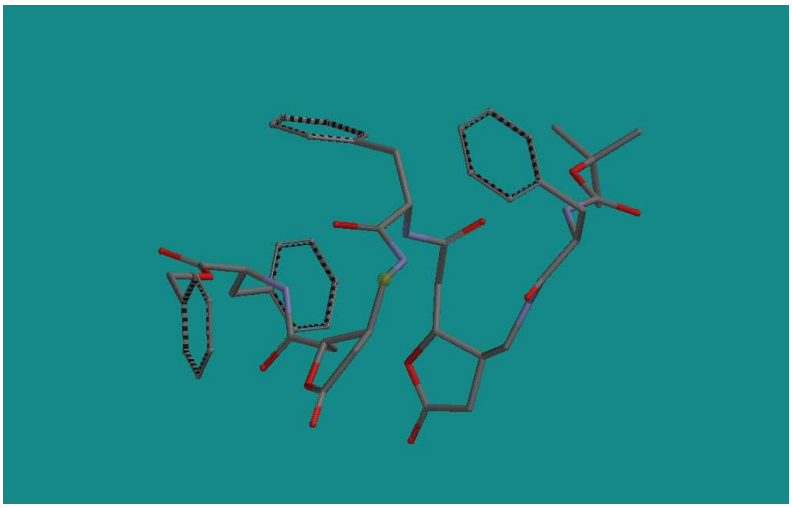

Figure 70: Structure of the low-energy conformer calculated for peptide **114**. For clarity hydrogen bonds are omitted.

The heptamer containing alternated (R,R)-δ-amino acid and phenylalanine was analyzed by 2D NMR only in $CDCl_3$, since it was insoluble in methanol. In this solvent it showed a high dispersion of the signals, as well as numerous NOE contacts, among them long range NOE contacts were also detected. We can remark that the major part of the contacts were found in the N-terminal part of the molecule (Figure 71): in particular, we detected contacts between two non neighbouring lactones, which gave indication about an eventual organisation of this part of the molecule. However, we could not see any repetitive contacts that would have been an evidence for the presence of a periodic structure.

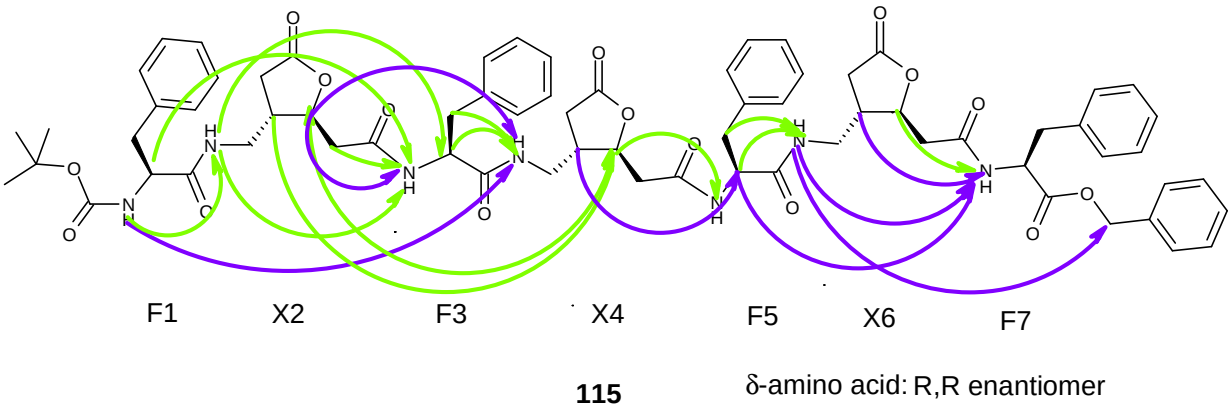

Figure 71: Summary of the interresidue NOE contacts observed for the peptide **115** in $CDCl_3$ at 292 K (green arrows: medium NOEs; blue arrows: weak NOEs).

Here again -Δδ/ΔT coefficients adopt quite high absolute values between 7 and 8 ppb/K, excepted for the third lactone and the Boc terminal phenylalanine, and ^{3}J coupling constants were also quite high, excepted for F5 that showed a ^{3}J of 4.8 Hz (Figure 72).

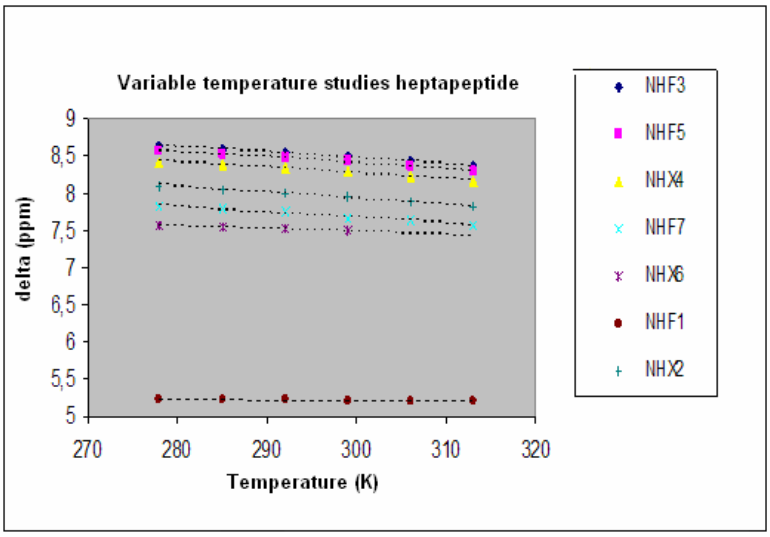

	-Δδ(ppm)/ΔT(K)	$^{3}J_{HN-H\alpha}$ (Hz)
NHF1	0.7	9.6
NHX2	7.8	
NHF3	7.7	8.4
NHX4	7.3	
NHF5	7.8	4.8
NHX6	3.9	
NHF7	7.2	7.2

Figure 72: Variable temperature studies in $CDCl_3$ of peptide **115.**

IR in solution was performed in CH_2Cl_2 at low concentration showing in this case again two bands, a weak one at 3420 cm^{-1} representing the non hydrogen-bonded amide, and an intense band at 3300 cm^{-1}, reflecting the presence of amide protons involved in hydrogen bonds. To gain further information about the amide protons involved in hydrogen bonding, we tried for the penta- and heptapeptides containing the (R,R)-δ-amino acid to perform solvent competition experiments, by progressive addition of DMSO in the NMR tube and controlling the changing in the chemical shifts. Unfortunately, this experiment failed due to the fact that by adding DMSO we were not able anymore to assign the amide protons. Deuterium exchange experiments revealed to be unrealisable, since our compounds were precipitating upon addition of minimum amounts of methanol-d_4. Molecular dynamics was performed including seventeen constraints taken from NOE contacts. Two pictures of the energetic minimum are represented below showing in the first segment, containing Boc-Phe-Lac-Phe-Lac-Phe, a folded part that describes a first loop of helix, while the folding in the C-terminal part seems to be disrupted from the last lactone. One reason for the loss of the folding properties in C-terminal part of the peptide could be the high spatial freedom of the benzyl ester group that directs the C-head of the peptide in

another direction. This is particularly evident in the second view of the structure, in which we can see the compact helical structure imposed by the two first lactones X2 and X4, followed by a reversal of the structure in the C-terminal part (Figure 73).

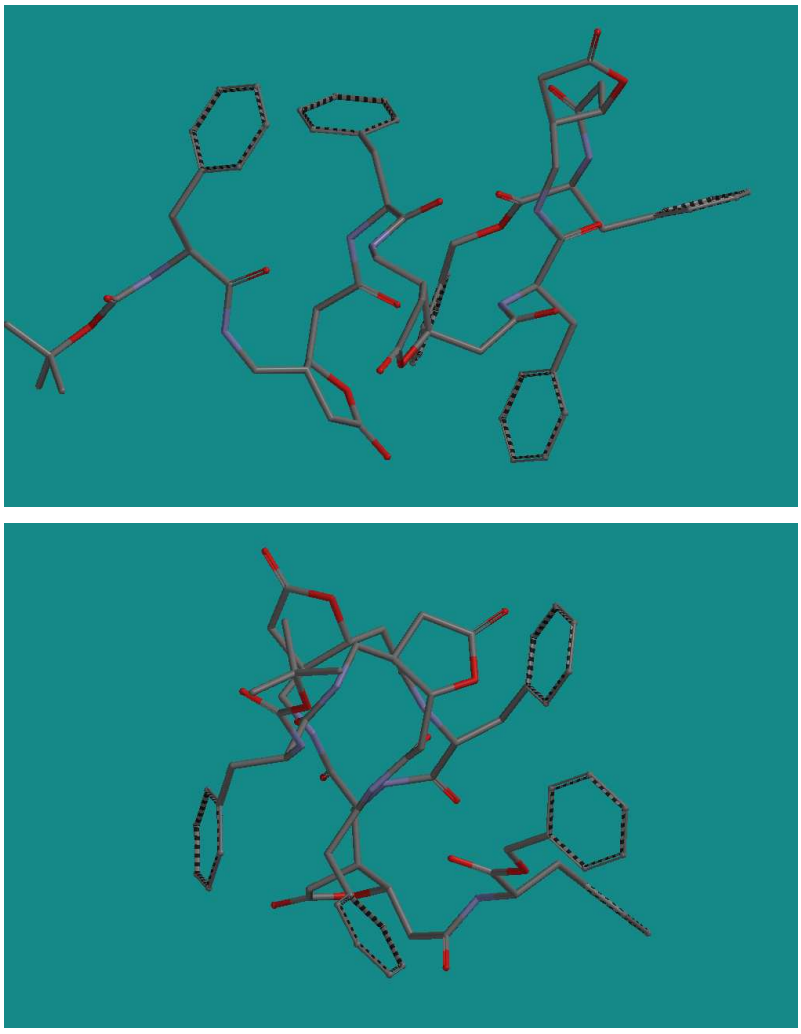

Figure 73: Two views of the structure of low-energy conformer calculated for peptide **115**. For clarity hydrogen bonds are omitted.

In contrast to the CD spectra of the pentamers, the CD spectrum of the heptamer in TFE at 0.5 mM showed only the maximum at 218 nm, whereas the second maximum near 200 nm found for

the pentamers disappeared (Figure 74). This might be indicative of the presence of an ordered structure stabilized by the longer peptide chain.

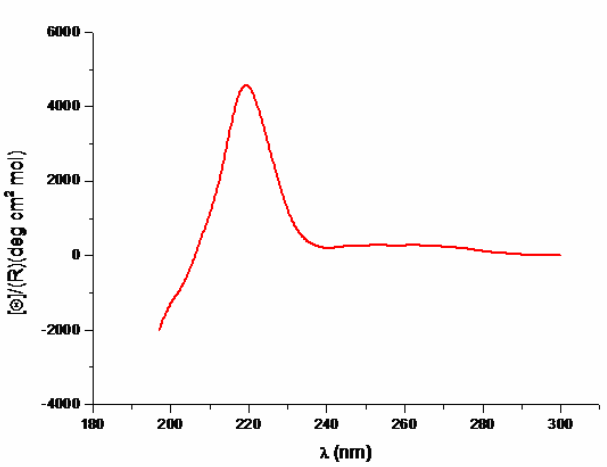

Figure74: CD spectrum of the heptapeptide **115** in TFE.

The results presented above on the conformational analysis of three peptidomimetics containing aromatic α-amino acids alternated with polar δ-amino acids suggest that these δ-amino acids have the potential to induce structural motifs, which, however, differ from those typically adopted by α-peptides. Interestingly, peptides containing the (S,S)-δ-amino acid showed major solubility in methanol, also showing better folding properties in polar solvents. In contrast, peptides containing the (R,R)-δ-amino acid showed better folding properties in non polar solvents. According to the numerous NOE contacts found in the analysis of pentamer and heptamer containing the (R,R)-δ-amino acid, this enantiomer is likely to have better folding properties than the S,S enantiomer. Finally, increase in the length of the peptide sequence led to a stabilization of the secondary structure.

III.3. New peptides containing δ-amino acids: Objectives and design

After the results obtained with peptides **113**, **114**, **115** (Figure 60), we decided to synthesize further α/δ-peptides containing a variety of -amino acids ranging from apolar to charged residues. This should avoid the overlapping of the signals in NMR spectra and lead to peptides with different properties. In the case of **116** (Figure 75), we modified the sequence by increasing the number of positively charged residues. Thus, two lysines and one glutamine were alternated with δ-units. To investigate the effect of our scaffold on the secondary structure of longer peptides, we carried out the synthesis of peptides **117** and **118** (Figure 75), which contain both apolar and polar α-amino acids. The synthesis and the results of the 2D-NMR, CD, FT-IR measurements and of the molecular modelling will be shown and discussed in the following paragraphs.

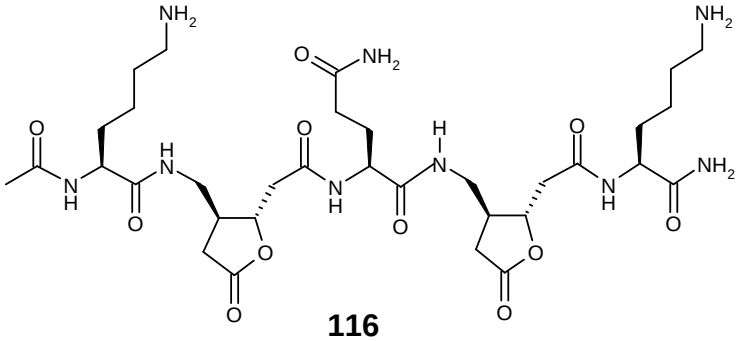

116

δ-amino acid: S,S enantiomer

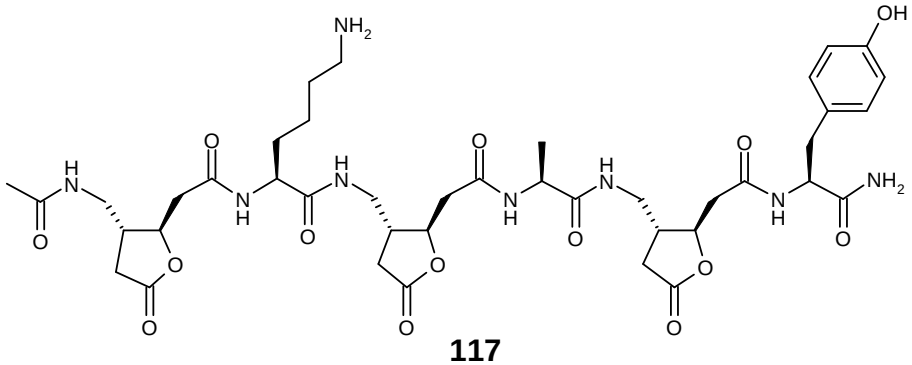

117

δ-amino acid: R,R enantiomer

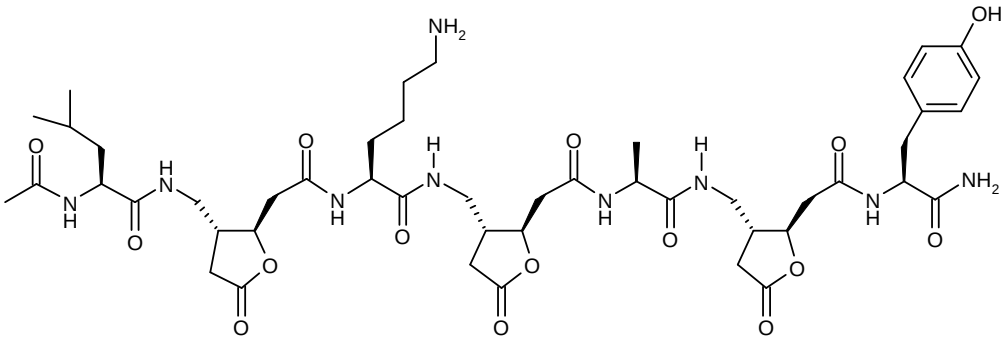

118

δ-amino acid: R,R enantiomer

Figure 75. Lactone containing peptides **116**, **117** and **118** that have been synthesized and investigated in this work.

III.4. Synthesis of peptides 116-118

The model peptides containing the enantiomers (S,S) or (R,R) of our lactone-scaffold that were synthesized and investigated in the course of this study are shown in Figure **75**.

The synthesis of the building block, being suitably functionalized to be introduced in peptides, has been carried out as developed in our group from γ-butyrolactonaldehyde **109** in enantiomerically pure form (S,S)[12]-**119** and (R,R)-**120** (Figure 76).

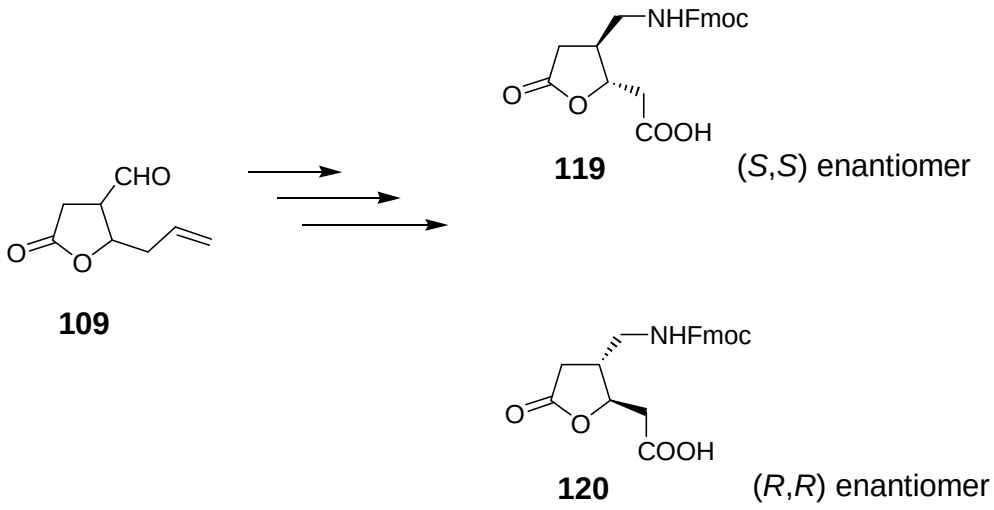

Figure 76. Pentalactone building blocks **119** and **120** for peptide synthesis.

Synthesis of Fmoc protected δ-amino acid (R,R) 120.

The synthesis of the Fmoc protected δ-amino acid (R,R)-**120** is described in Scheme 9. **120** was synthesized starting from (R,R) lactone **107** (Figure 59), by cleavage of the Boc protecting group with TFA in dry CH_2Cl_2. The resulted product **121** was treated with Fmoc-OSu in dioxane-1 M K_2CO_3 to afford the desired compound in moderate yield (60%).

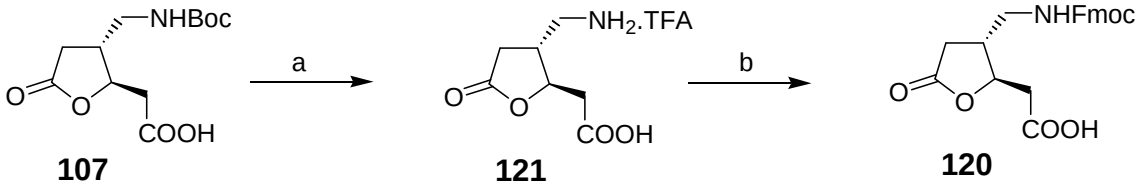

Scheme 9. Synthesis of the Fmoc protected δ-amino acid **120**. Reagents:
a) TFA, dry CH_2Cl_2, 100%; b) FmocOSu, dioxane-1M K_2CO_3 (1:2), 60%.

Synthesis of alternated α/δ-unit peptides

The peptides **116-118** were synthesized, as shown in Schemes 10 and 11, using a solid phase protocol. The solid phase synthesis can be commonly performed by using two alternative protecting groups, tert-butyloxycarbonyl (Boc)[28] and fluorenyl-9-methoxycarbonyl (Fmoc),[29, 30] to mask the α-amino group of the amino acid only temporarily to allow further chain elongation. Generally, the Fmoc strategy is more suitable for solid phase synthesis, as the Fmoc group is a base-labile protecting group which can be removed using secondary amines like piperidine and the cleavage of the peptide from the resin occurs under mild acidic conditions. Another very important advantage of the Fmoc group is its stability upon different conditions used to remove side-chain protecting groups, including strong acidic or reductive conditions.

The products presented in this work were synthesized by manual coupling using Fmoc chemistry on Rink amide MBHA resin **122** (loading 0.6 mmol g^{-1}) (Figure 77). The resin was in the Fmoc-protected form and, for this reason, to obtain N-free linker, the resin was treated with piperidine in DMF/NMP (80:20 v/v).

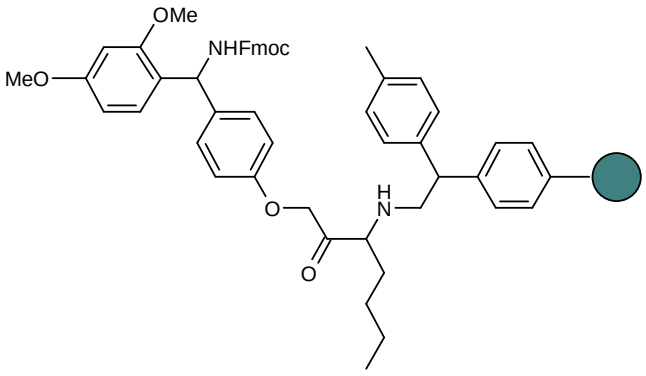

4-(2',4'-Dimethoxyphenyl-Fmoc-aminomethyl)-phenoxyacetamido-norleucyl-MBHA resin

122

Figure 77. Rink amide MBHA resin **122**.

In the case of peptide **116** the synthesis is outlined in Scheme 78, and was performed with (S,S)-δ-amino acid. The first amino acid (4 equiv.), lysine, was coupled activating *in situ* the carboxylic function with HBTU (3.9 equiv.), HOBt (4 equiv.) in DMF/NMP (80:20 v/v), in the presence of DIPEA (8 equiv.). Fmoc cleavage was accomplished by treating the peptidyl-resin with 20% piperidine in DMF/NMP (80:20 v/v). For the coupling of the second amino acid, Fmoc-δ-amino acid, 2.5 equiv. excess were used, together with HBTU (2.4 equiv.), HOBt (2.5 equiv.) in DMF/NMP (80:20 v/v), and DIPEA (5 equiv.). The following steps, the Fmoc deprotection and the coupling of glutamine, were done with the same conditions used for lysine. To monitor the progress of the synthesis, small scale cleavage was performed and the resulting sample was analyzed by MALDI-ToF-MS. To avoid a potential lactone ring opening, we decided to use milder conditions for the Fmoc deprotection (only 15% of piperidine in CH_2Cl_2 for 3 min. instead of 20% for 5 min. in DMF/NMP) and to change the coupling conditions for the second Fmoc-δ-amino acid: DIC (2.5 equiv.) and HOBt (2.5 equiv.) in CH_2Cl_2 without base. After the coupling of the second lysine and the Fmoc deprotection, the last step was the N-terminal acetylation using acetic anhydride (5 equiv.) and DIPEA (2.5 equiv.). Final cleavage of the peptide from the resin and simultaneous side-chain deprotection was achieved by treatment with a TFA/water/TIS mixture (90:5:5) for 2.5 hours. The peptide was then precipitated from ice-cold diethyl ether,

centrifuged and subjected to three ether-washing/centrifugation cycles to remove the scavengers. The characterization was performed by HPLC and MALDI-ToF-MS.

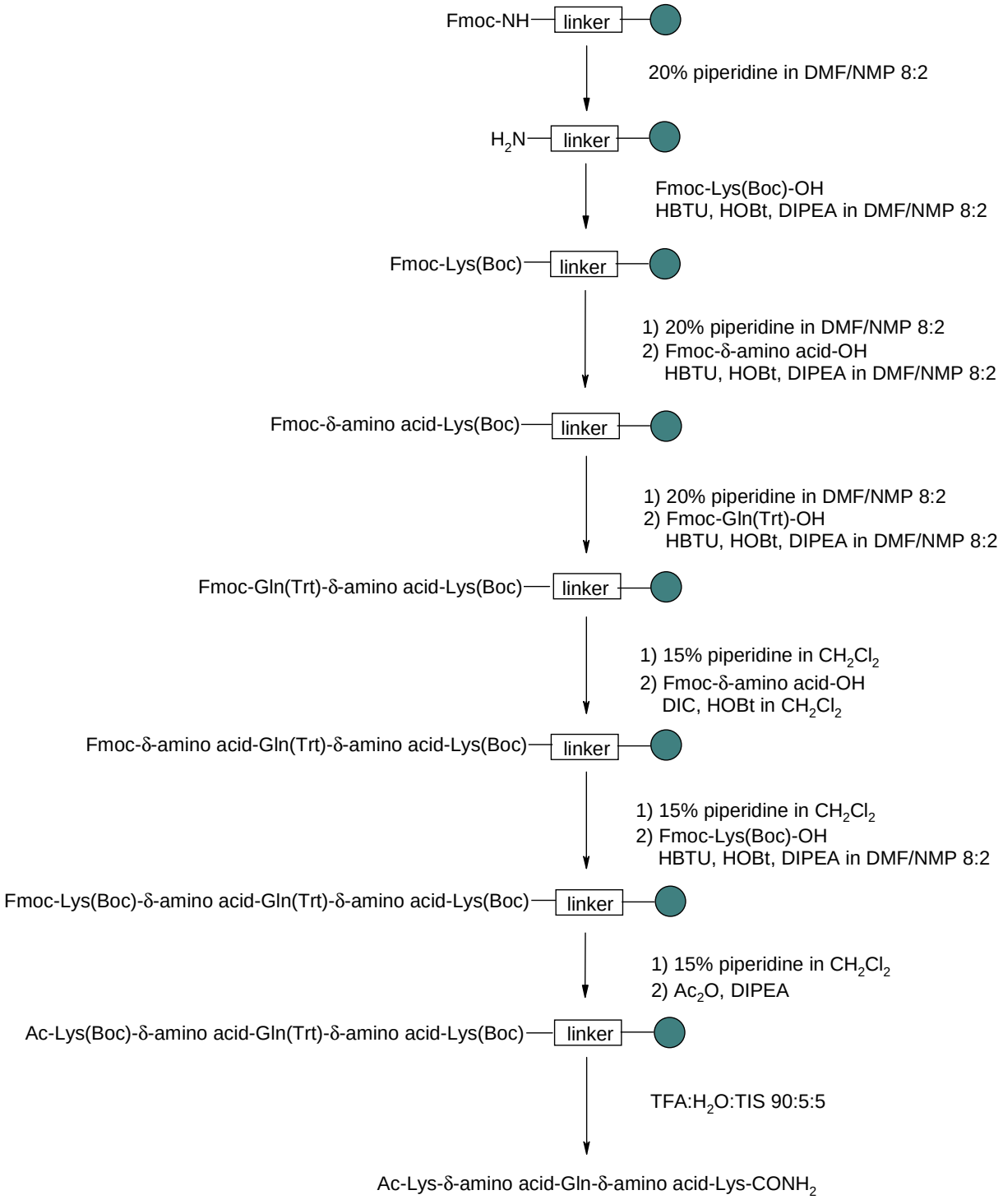

Scheme 10. Solid phase synthesis of **116** using the Fmoc chemistry.

In the case of peptides **117** and **118** containing (R,R)-δ-amino acid, the solid phase protocol used was the same as the one just described for **116**, but this time only DMF was used as the reaction solvent. A different number of equivalents of the amino acids (Xaa 5 equiv.), coupling reagents (HOBt 5 equiv./HBTU 4.8 equiv./DIPEA 10 equiv.) and acetic anhydride/DIPEA (8 equiv./ 7equiv.) were also used (Scheme 11).

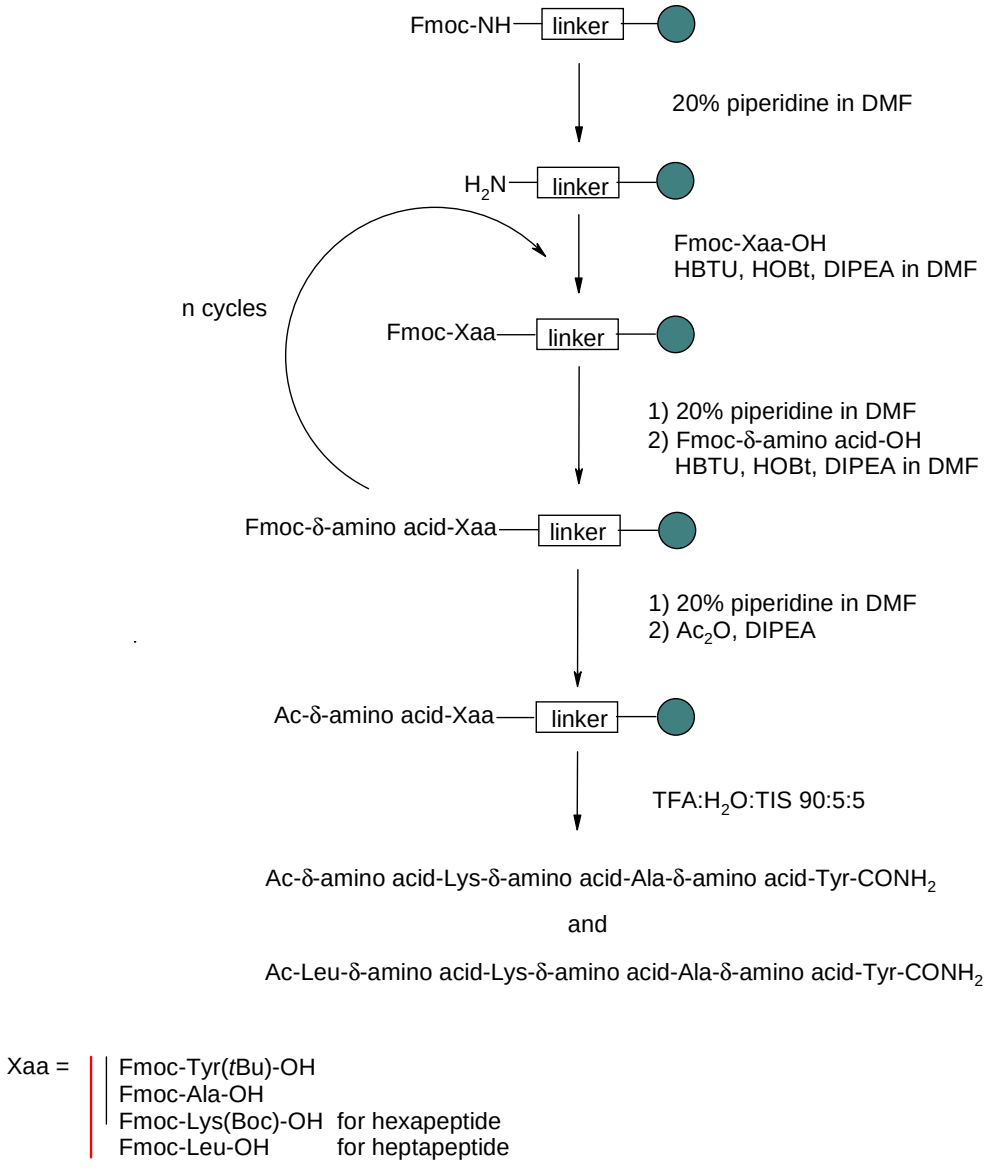

Scheme 11. Solid phase synthesis of **117** and **118** using the Fmoc chemistry.

III.5. Results and discussion

III.5.1. Alternated α/(S,S)-δ-unit peptide

The synthesized α/δ-pentapetide **116** was dissolved in methanol-d_3 and studied by NMR spectroscopy. 1D experiments were first acquired at five different temperatures (283, 288, 293, 298 and 303 K), and the one that gave the better resolved spectrum (303 K) was chosen to record the 2D experiments. The complete ^{1}H-NMR resonance and sequence assignments were done by using the COSY, TOCSY and ROESY spectra. Unfortunately only, medium and weak contacts were found and only between one residue and its neighbour, or intralactone in one case (Figure 78).

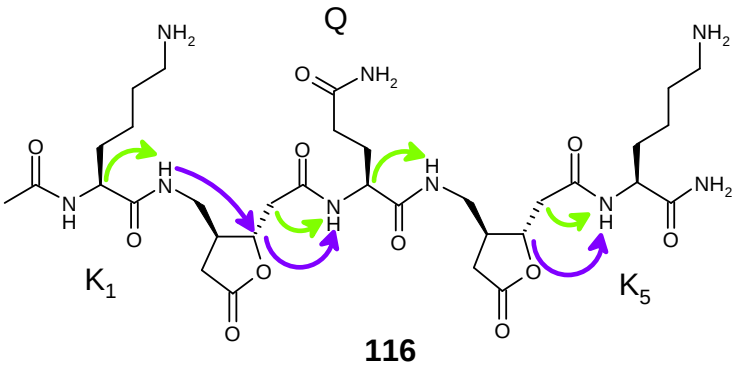

Figure 78. Summary of the interresidue ROE constraints observed for the peptide **116** in methanol-d_3 at 303 K (green arrows: medium ROEs; blue arrows: weak ROEs).

The values of the $^3J_{HN\text{-}H\alpha}$ coupling constants were estimated by using the amide region in the 1D-NMR spectrum and the vicinal coupling constant value is always bigger than 6 Hz. No estimation was possible in the case of the two lactones. These values are typical of an extended or unordered structure (Figure 79).

The temperature coefficients (Δδ/ΔT) for the pentapeptide **116** were also measured, which were in the range of -6.6/-8.0 ppb/K (Figure 79).

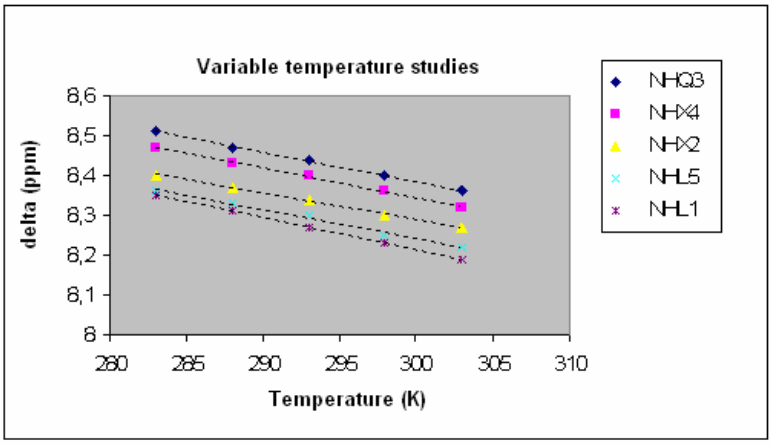

	$-\Delta\delta(ppm)/\Delta T(K)$	$^3J_{HN-H\alpha}$ (Hz)
NHQ_3	7.4	7.0
NHX_4	7.4	
NHX_2	7.2	
NHK_5	6.6	7.6
NHK_1	8.0	7.2

Figure 79. Temperature coefficients for the NHs and vicinal coupling constants for HN-Hα in methanol-d_3 for **116**.

We used molecular modelling to investigate the possible structures that the peptide could adopt. After the construction of the molecule *in silico* the observed NMR contacts were introduced as constraints before carrying out an energy minimization and Molecular Dynamics. In our analysis we excluded the molecules in which there were violations of the NMR-derived constraints and we considered only the structures energetically favored. The lowest energy conformer of this set of molecules is shown in Figure 80. Clearly, the peptide forms a large loop, in which the two lactones are located opposite to each other, with the central residue glutamine acting as a pivot.

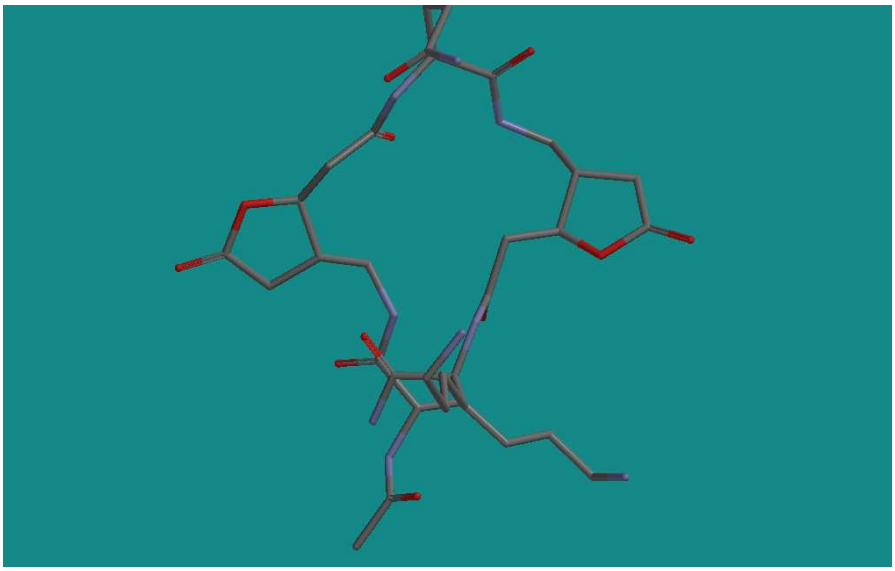

Figure 80. Structure of low-energy conformer calculated for compound **116**. Hydrogen atoms are omitted for clarity.

The CD investigation was performed in methanol (5 mM) and the peptide **116** displayed only one negative band at 230 nm (Figure 81). Unfortunately, no similar spectra have been reported either in the literature or in our previous work.

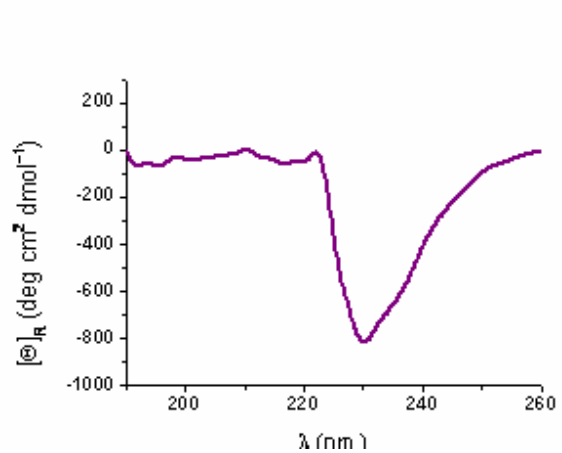

.

Figure 81. CD spectra of compound **116** (5 mM in methanol). The data are normalized for peptide concentration and number of residues.

III.5.2. Alternated α/(R,R)-δ-unit peptides

Two further peptides containing the (R,R)-δ-unit alternated with α-amino acids like lysine, alanine, tyrosine and leucine were prepared by solid phase methodology.The ^{1}H NMR spectra of hexapeptide **117** were recorded at five different temperatures (280, 287, 296, 303 and 310 K), and the one at which the dispersion of the signals was reasonable (280 K) was chosen to record the 2D experiments. Nevertheless, NMR characterization was complicated from the significant signal overlap in the spectrum. The ROESY spectrum in connection with COSY and TOCSY spectra revealed several contacts, including those between neighbour amino acids (Figure 82). The central part of the peptide seemed to be more structured and the temperature coefficient of lactone X_5 was relatively small (Figure 83).

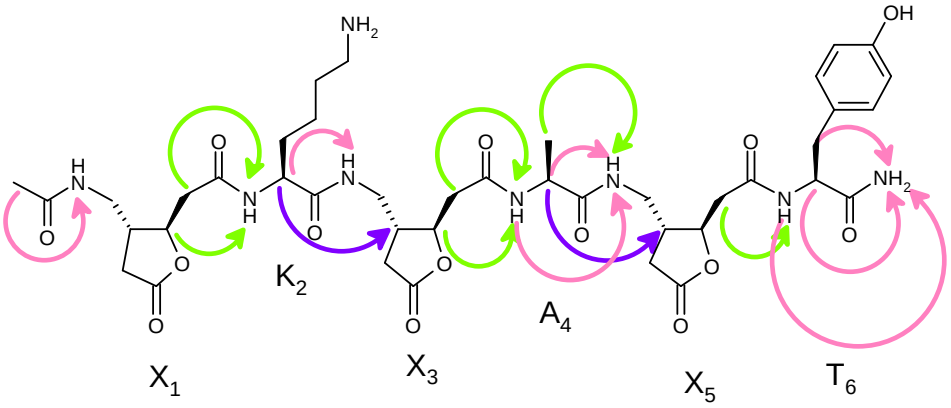

117

Figure 82. Summary of the interresidue NOE constraints observed for the peptide **117** in methanol-d_3 at 280 K (pink arrows: strong NOEs; green arrows: medium NOEs; blue arrows: weak NOEs).

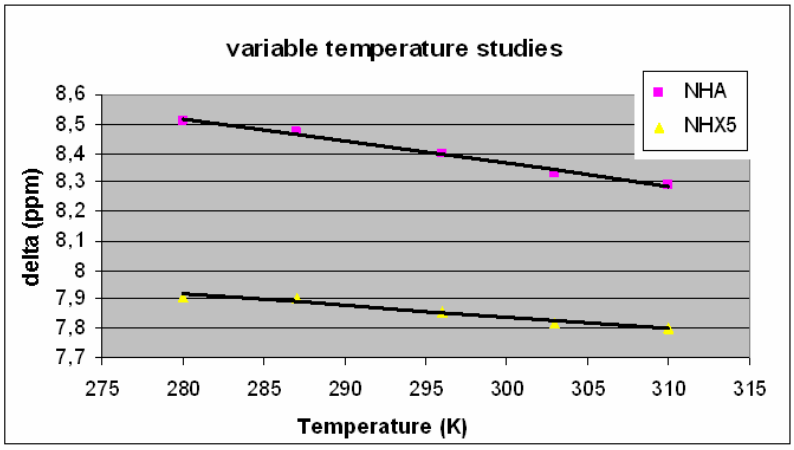

	-Δδ(ppm)/ ΔT(K)	$^3J_{HN\text{-}H\alpha}$ (Hz)
NHA_4	7.6	6.4
NHX_5	4.0	
NHK_2		7.9

Figure 83. Temperature coefficients for the NHs and vicinal coupling constants for HN-Hα in methanol-d_3 for **117**.

Using several NOE contacts as constraints, MD simulations were carried out, but we could not see a periodic structure (Figure 84).

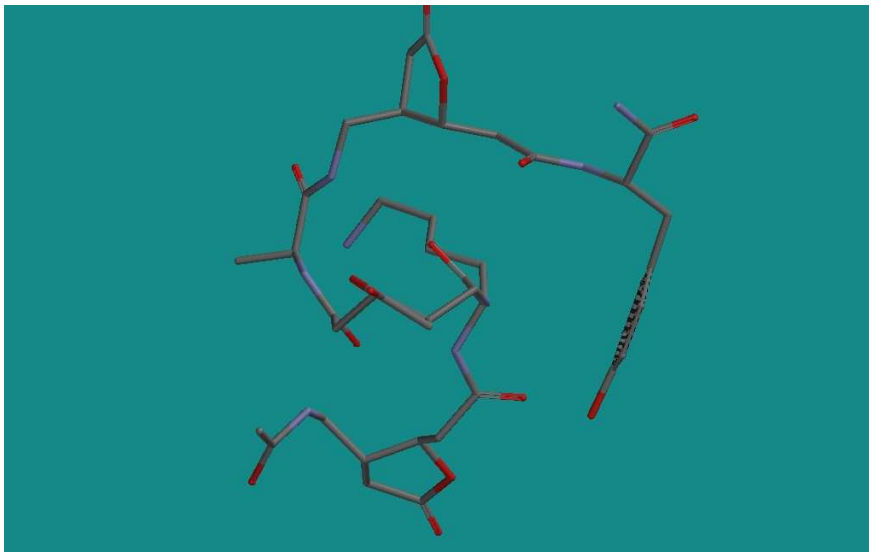

Figure 84. Structure of low-energy conformer calculated for compound **117**. Hydrogen atoms are omitted for clarity.

We recorded the circular dichroism spectrum in methanol at concentration of 2 mM (Figure 85), which exhibited a strong positive band at 238 nm.

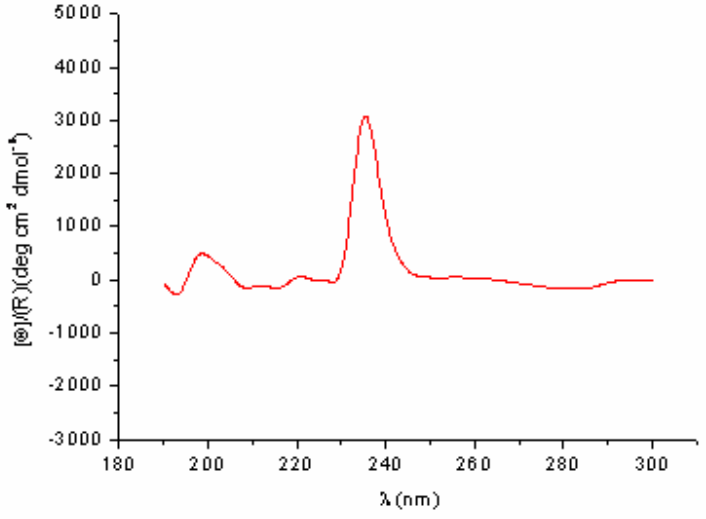

Figure 85. CD spectra of compound **117** (2 mM in methanol). The data are normalized for peptide concentration and number of residues.

The heptapeptide **118** was obtained from **117** after elongation with an additional α-amino acid, leucine. The 2D NMR analyses at 303 K revealed only few and non-relevant NOE contacts (Figure 86).

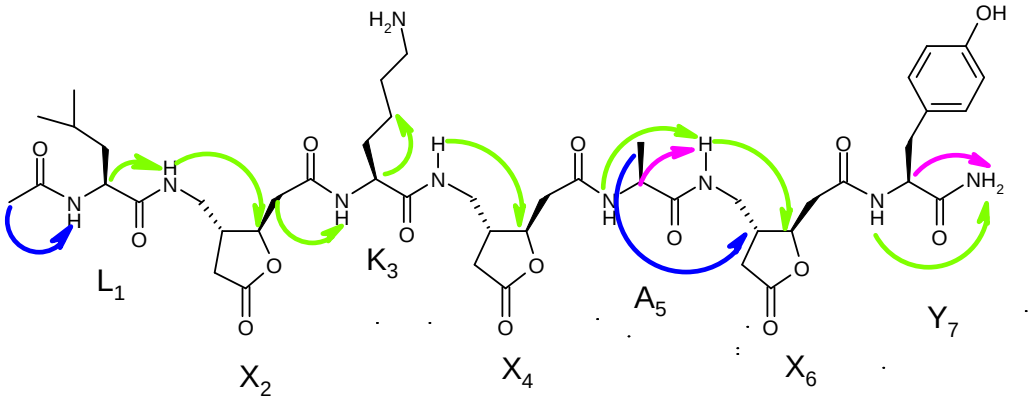

118 δ-amino acid: R,R enantiomer

Figure 86. Summary of the interresidue NOE constraints observed for the peptide **118** in methanol-d_3 at 303 K (pink arrows: strong NOEs; green arrows: medium NOEs; blue arrows: weak NOEs).

The temperature coefficients and coupling constants of **118** are reported in Figure 87. It can be noted that the amide protons of the alanine-δ-lactone motif in **117** and **118** show comparable temperature coefficients.

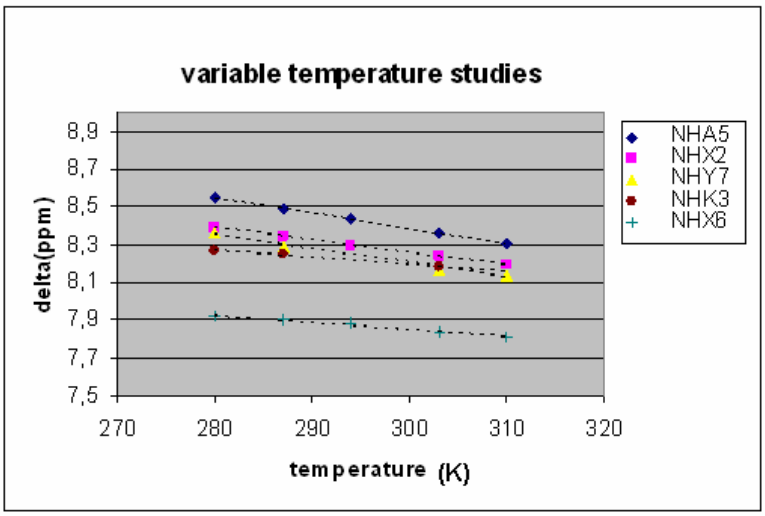

	-Δδ(ppm)/ ΔT(K)	$^3J_{HN\text{-}H\alpha}$ (Hz)
NHL_1		
NHX_2	6.6	
NHK_3	4.0	
NHX_4		
NHA_5	8.0	6.6
NHX_6	3.7	
NHY_7	7.4	8.4

Figure 87. Temperature coefficient for the NHs and vicinal coupling constants for HN-Hα in methanol-d_3 for **118**.

The CD spectrum of **118** at 2 mM in methanol was characterized by a weak positive band at 200 nm, followed by a broad positive band at 230 nm (Figure 88).

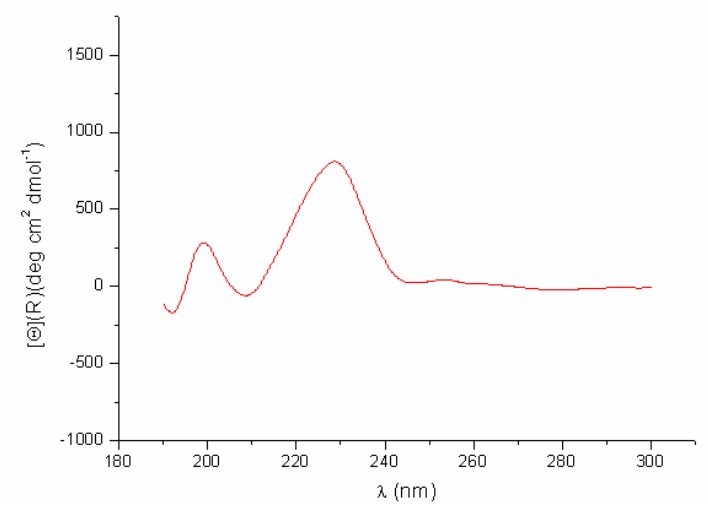

Figure 88. CD spectra of compound **118** (2 mM in methanol). The data are normalized for peptide concentration and number of residues.

III.6. Monomer studies

III.6.1. Previous work on the δ-butyrolactone amino acid

In a previous work carried out by M. Haque[12] in our laboratory in Regensburg, the tetramer **123** consisting of four (S,S)-δ-amino acid units was synthesized (Figure 89). The NMR investigation was not possible due to signal overlapping especially in the NH region.

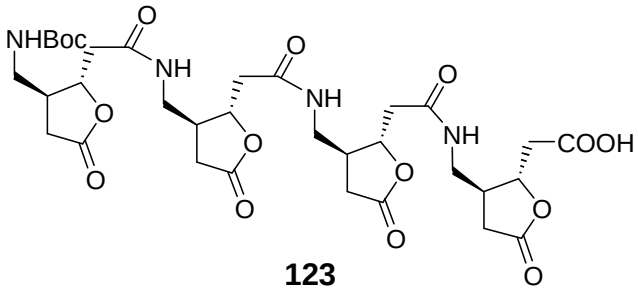

123

Figure 89. Tetramer **123**.

Therefore CD analyses in different solvents were performed (Figure 90). The CD spectra were recorded in the far UV region, at the concentration of 5 mM in TFE, methanol and methanol/water 60:40. In TFE the CD spectrum was characterised by a positive band at 191 nm, and by a broad negative band centred at 214 nm, with a crossover at 204 nm. Changing TFE with methanol doubled the intensity of the negative band, while the shape and the bands position remained the same. The intensity of the negative band further increased in the mixture methanol/water, becoming more than two times higher than in methanol and more than four times higher than in TFE. Again, the shape of the band remained more or less constant, but a better-defined minimum was present at 214 nm. The fact that the CD spectra were solvent dependent indicates that the conformational properties of the peptide are influenced by the environment. An increase in the intensity of CD bands suggests an improved structural stability. For the δ-oligopeptide a stabilisation effect was observed in methanol rather than in TFE, and in the presence also of water rather than in 100% methanol. This behaviour is quite unusual, as the conformation of peptide mimics is normally destabilized by addition of water that is a strong

donor and acceptor of H-bonds. In contrast, TFE is a well-known secondary structure stabilizer, being a strong H-bond donor but a weak H-bond acceptor.

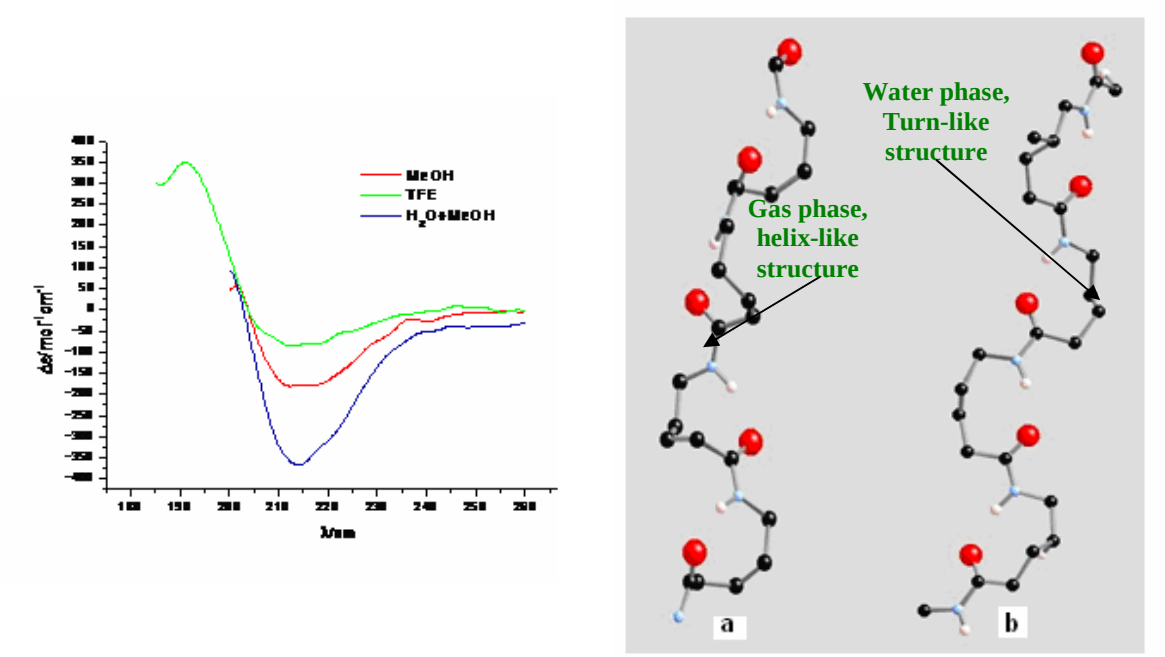

Figure 90. Left: CD spectra in TFE (green), methanol (red) and water/methanol mixture (blue). Right: Hofmann's calculations: a) in gas-phase, helix-like structure; b) in water, turn-like structure.

To reinforce and illustrate these results, molecular modelling experiments were performed at the University of Leipzig by the Hofmann's group and the results showed two families of structures. The first family in gas-phase had a helical tendency (Figure 90 a), whereas the second one in water showed a succession of turn-like structures (Figure 90 b)**.** In both cases, the secondary structures seemed to be stabilized by H-bonds formed between the carbonyl and the NH of the same lactone residue (8-membered hydrogen-bonded ring). Another feature distinguishing both Hofmann's structures is the conformation of the lactone. In the case of the calculations in gas-phase both substituents on the cycle are occupying an axial position, whereas the calculations in water show the two "arms" of the lactone in an equatorial position. It was not possible to confirm by NMR and X-ray any of the information obtained from the computational and CD data.

III.6.2. New analyses on the monomer

In order to gain further information about such structures in solutions, we decided to perform conformational studies on the monomer. First we wanted to control its ability to form an internal H-bond (8-membered H-bonded ring) that would confirm the possible stabilization of the structures described by Hofmann's calculations and, secondly, we wanted to study the lactone ring conformation as it could play a crucial role in the structural behaviour of further lactone-containing peptidomimetics.

Design and synthesis

This kind of conformational studies based on monomeric structures have been previously reported by Gellman and co-workers[31] in their attempt to evaluate folding properties of β- and γ-aminoacids. To study the particular H-bond preferred conformation of our lactone we needed two types of compounds. In the first one, only one hydrogen bond would be possible, and in the second one the monomer could adopt two hydrogen bond patterns. Thus, we synthesised compounds **125** and **126** as described in Scheme 12. In the first step the Boc-protected lactone derivative **106** was coupled to a mono or dialkylated amine. The resulting compound **124** was Boc deprotected by treating it with TFA in dry CH_2Cl_2, and finally the amino group was acetylated to afford our model compounds **125** and **126**.

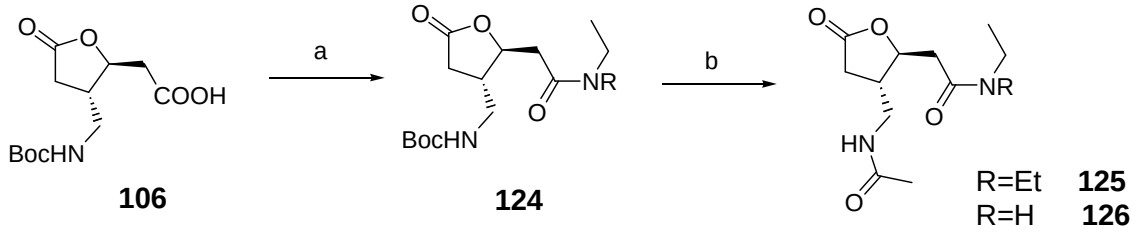

106 **124**

Scheme 12. Synthesis of compounds **125** and **126**. Reagents:

a) NHEtR, EDC, HOBt, DMF, 42% when R=H and 65% when R=Et; b) (i) TFA, dry CH_2Cl_2 ; (ii) Ac_2O, THF, 65% when R=H and 60% when R=Et.

Conformational analyses

We studied both compounds first by NMR and, secondly, by IR in CH_2Cl_2 at low concentration (3 mM) and room temperature (Figure 91).

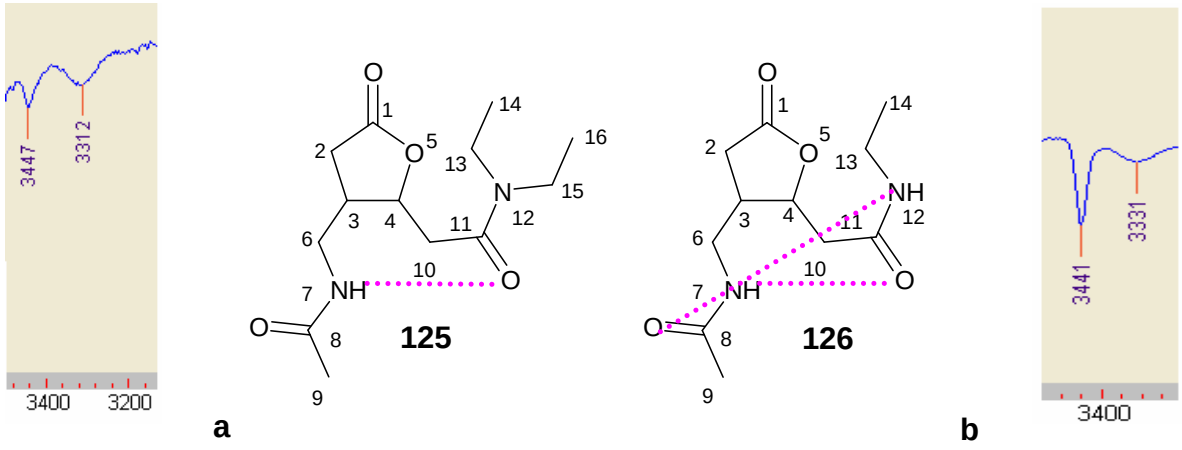

Figure 91. a) IR studies of **125**; b) IR studies of **126**. The possible hydrogen bonds are shown in magenta.

In the IR spectra it is possible to observe two N–H stretch bands for amide protons: the highest one about 3400 cm^{-1} indicates an amide in a non-hydrogen-bonded state, whereas the lowest one appearing near 3300 cm^{-1} corresponds to an amide in hydrogen-bonded state.

The disubstituted amide in **125** presented two IR bands at 3347 and 3312 cm^{-1} with similar intensity (Figure 91 a), whereas the monosubstituted compound **126** showed an intense band in the non-hydrogen-bonded NH region at 3441 cm^{-1} and a weaker band in the region of H-bonded amides at 3331 cm^{-1} (Figure 91 b). These data suggest that the intraresidue H-bond is favoured in the monomer **125** comporting only one H-bond possibility, whereas in the monosubstituted derivative **126** with more possible combinations, the non-H-bonded state is preferred. These analyses confirm that an intraresidue H-bond is possible in our structure, supporting indeed the H-bond pattern described in Hofmann's structures.

In NMR investigations two parameters were considered. On the one hand, variable temperature studies gave the temperature coefficients that in some cases can be correlated with the H-bonding state of amide protons. On the other hand, NOESY experiments gave insight about the distance between two protons in the space.

In variable temperature studies the NH(7) of the disubstituted lactone **125** showed a high temperature coefficient (-9.2 ppb/K), typical value for non-hydrogen-bonded state, and NOESY spectra performed at room temperature did not show any intra-strand NOE contacts. In contrast, the monosubstituted lactone **126** appeared to adopt two distinct behaviours depending on the temperature in which it was studied, at room temperature and at 225 K. The temperature coefficient for the NH(7) (-8.9 ppb/K) was similar to the one in the disubstituted lactone, whereas the NH(12) showed a lower value of $\Delta\delta/\Delta T$ = -6 ppb/K. For this compound NOESY experiments were performed at room temperature and at 225 K, and an intra-strand NOE cross peak was found at low temperature between CH_3(9) and NH(12). These two parameters, NOE contacts and temperature coefficient, found for NH(12) suggest a preferred H-bonding pattern involving NH(12) and CO(8) of **126** at low temperature.

Investigations on the ring conformation

The γ-butyrolactone system possesses great importance in the chemistry of natural products.[32, 33] Therefore, considerable interest is given at the synthesis and structural characterization of substituted γ-butyrolactones.

One advantage of using γ-butyrolactone as synthetic intermediate is the low conformational flexibility: indeed, one needs to consider only the interconversion between two envelope forms A and B, in which $\alpha = \beta = H$[34] (Figure 92). In this case the interconversion barrier is quite low and the lactone adopts both shapes in solution. However, when substituents are introduced on such a small ring, both the ring structure and the equilibrium between the A and B forms are greatly affected, and the analysis in NMR spectra of ring protons turns into a complicated task.

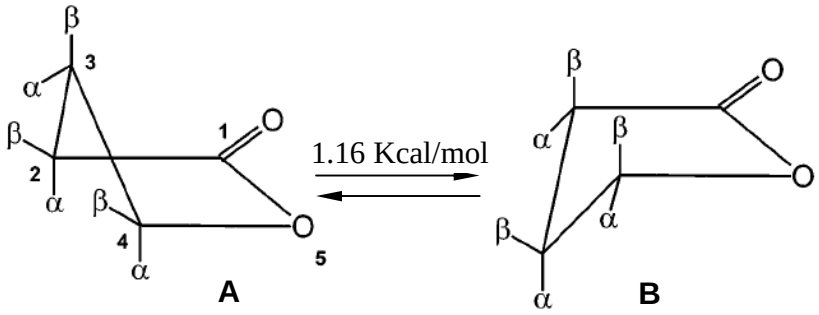

Figure 92. Interconversion of γ-lactone A in B.

To evaluate the substituted γ-lactone conformer distribution in solution several methods have been developed based on experimental vicinal and geminal coupling constants combined with conformational studies by molecular mechanics.[34-36] In our case, experimental data gave a really large value of $J_{3\text{-}4}$ for both disubstituted **125** and monosubstituted **126** monomers, which was 12.3 and 13.1 Hz, respectively. Such large coupling constants are in agreement with *trans* protons 3 and 4 occupying both a diaxial position on the lactone ring. We then compared these values with the one of the coupling constant from the dimethylated lactone **127** (Figure 93), which was previously synthesized by Delatouche in our group. In this case the coupling constant value between H_3 and H_4 was 9.8 Hz. It has been earlier demonstrated on 2,4 disubstituted lactones that 1-3 diaxial strains are quite disfavouring in term of energy in γ-butyrolactones.[34] Thus, in our dimethylated compound **127** the conformer A that shows a 1-3 diaxial strain between the methyl group in position 2 and the lactone arm in position 4 should be unstable, while the predominant conformation in solution should be the conformation B, in which H_4 and one methyl group in position 2 are diaxial (Figure 93).

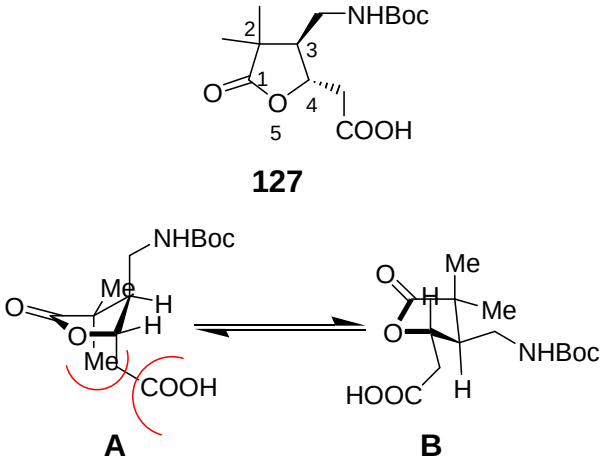

Figure 93. Interconversion between the two envelope conformations A and B of **127**.

The results suggested by the coupling constants were then supported by molecular mechanics calculations using MMFF force field in the program Spartan,[37] which gave the conformation with the two arms in an equatorial position as energetic minimum for both lactones **125** and **126** (Figure 94).

E=-57,62Kcal/mol

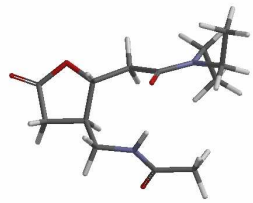

125

H_3CCH_{2A} 157.77°
H_3CCH_{2B} 32.96°
H_3CCH_4 -162.71

E=-67,84Kcal/mol

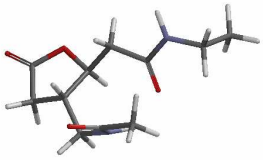

126

H_3CCH_{2A} -158.05°
H_3CCH_{2B} -33.21°
H_3CCH_4 163.23°

Figure 94. Energy minimum of 125 and 127 based on a molecular mechanics study with the force field MMFF of the Spartan program.

Finally, analysis of the crystal structure data[12] obtained by Haque gave further evidence of the equatorial distribution of the two lactone arms (Figure 95).

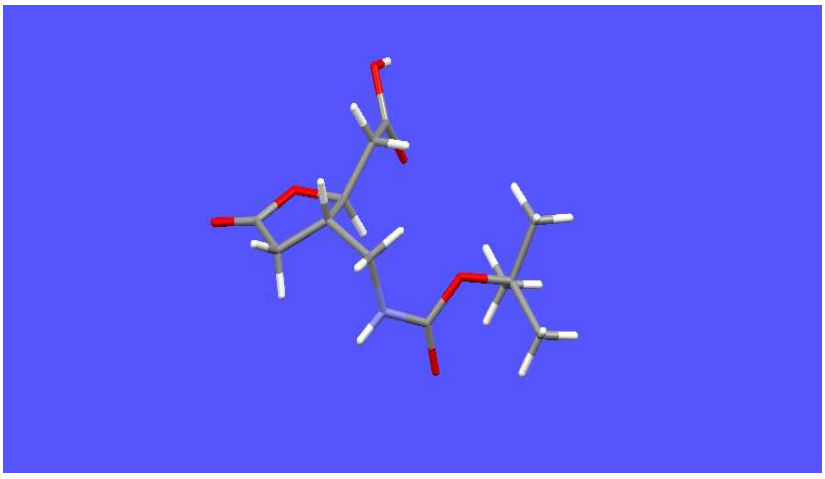

Figure 95. X-ray structure of compound **106**.

III.7. Influence of the (R,R)-δ-lactone amino acid on the α-helix stability

III.7.1. Aim of the study

As it as been described before, on the one hand, this cyclic scaffold **107** can be described as δ-amino acid bearing a lactone ring at β- and γ-positions (Figure 96). On the other hand, it mimics a glycyl-glycyl dipeptide unit **128**, in which the amide bond is replaced by a lactone ring. We have investigated the folding properties of these building blocks in homo-δ-oligomers[12] as well as in hetero-α,δ-oligomers. We have previously shown that the δ-lactone amino acid unit possesses a tendency to build loop- or turn-like elements.

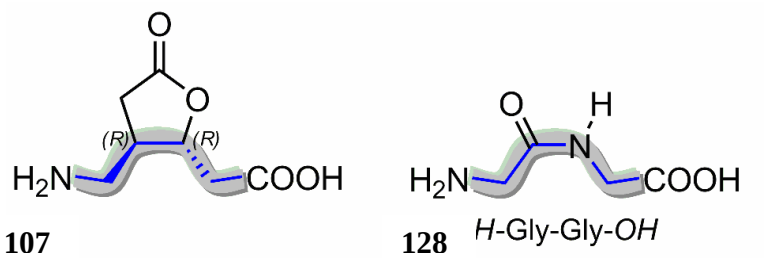

107 **128**

Figure 96. Structure of pentalactone-compound **107** and of glycyl-glycine **128**.

The aim of the experiment described in the following paragraphs was to evaluate the influence of this δ-amino acid on the helical structure of α-amino acid sequences. To carry out this study we used as peptide reference the peptide **129**, that was designed by Serrano's group[38] in 1995 and adopts an α-helical structure (Figure 97). This peptide is composed of eighteen amino acids and shows in the *N*-terminal part two crucial motifs for the helix initiation: the hydrophobic staple and the capping box. The hydrophobic staple consists of residues Phe-2 and Leu-7. A second helix inducer effect comes from the presence of the capping box consisting of Ser-3 and Glu-6.[39] NMR analysis of this peptide in aqueous solutions have shown that the helical part of the peptide starts at Lys-4 and stops around Arg-15.

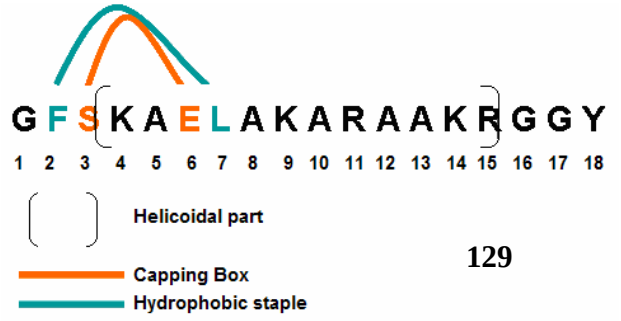

Figure 97. Peptide reference **129** used in our studies.

This peptide **129** was analysed using CD spectroscopy and led to a CD spectrum with a maximum at 195 nm and two minima at 208 and 222 nm (Figure 98 b). Replacement of Phe-2 by Ala (peptide **130**, Figure 98 a) led to a destabilization of the helix, as indicated by the reduced intensity of the CD spectrum of **130** (Figure 98 b).

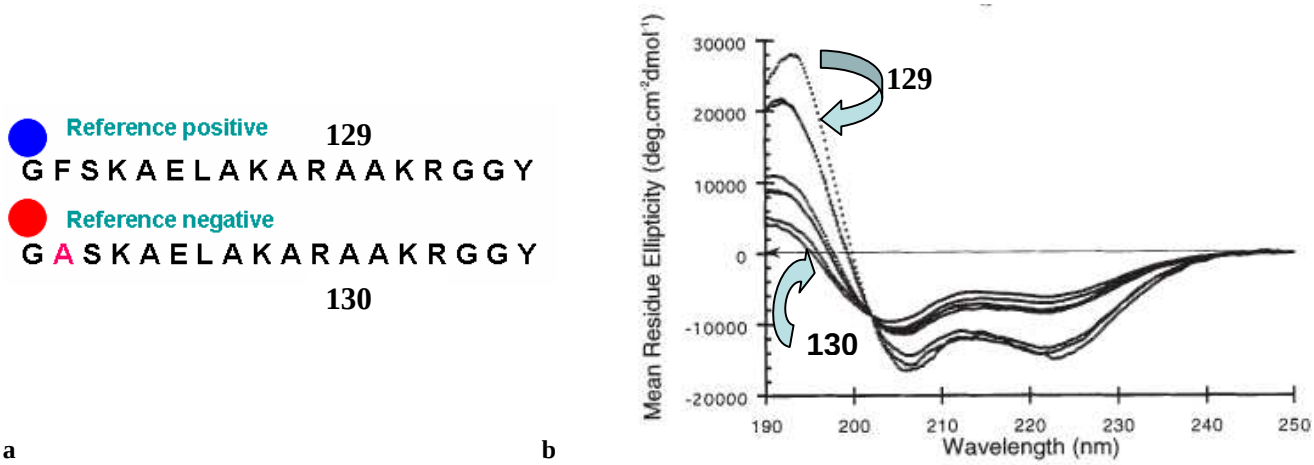

Figure 98. a) Peptide references used in our studies; b) CD spectra of **129** and **130** and other analogs, as reported by Serrano and co-workers.[38] (Reproduction by courtesy of Dr. Serrano).

Thus, we chosed these two peptides as references to carry out our studies. The reference called "positive" **129** included Phe-2, whereas the reference called "negative" included Ala-2 (Figure 98 a).

III.7.2. Design of the modified peptides

In order to check the compatibility of our amino acid with the helical structure of an α-peptide, we decided to introduce the lactone unit in the C-terminal part of the helix of the reference peptide **130** (from Lys-9 to Arg-14), by substituting either the two residues Arg-11 and Ala-12 (peptide **131**) or Ala-10 and Arg-11 (peptide **132**, Figure 99).

Figure 99. Peptide mimics **131** and **132** containing the lactone unit in the helical part.

Moreover, we introduced one lactone unit in the N-terminal part of the peptide: indeed, we substituted Ser3 and Lys-4, thus introducing the lactone between the two residues that should build the hydrophobic staple (peptide **133**, Figure 100). As a final test, we designed an analog of the latter peptide **133** that contains the substitution Phe-2/Ala, thus replacing one of the two partners of the hydrophobic staple (peptide **134**, Figure 100). The goal of this last test was to see if our lactone would be able to restore the hydrophobic staple properties and to induce the helix.

Figure 100. Peptide mimics **133** and **134** containing the lactone unit in the N-terminal part of the helix.

III.8. Synthesis of peptides 129-134

The synthesis of peptides **129-134** was performed on solid phase using Fmoc-chemistry on Rink amide MBHA resin (loading 0.6 mmol g^{-1}) (Scheme 13). The seven first amino acids were introduced using a single coupling procedure (75 min), whereas the following amino acids were introduced by a double coupling procedure (2 x 45 min). We used Fmoc-amino acid/HOBt/HBTU/DIPEA (5:5:5:10 equiv.) in DMF/NMP (80:20, v/v), followed by Fmoc removal with 25% piperidine in DMF/NMP (80:20, v/v) (2 x 15 min). To monitor the progress of the synthesis, test cleavages using small amounts of resin were conducted and the resulting samples were analyzed by MALDI-ToF-MS and analytical HPLC. The last step was the N-terminal acetylation using acetic anhydride (8 equiv.) and DIPEA (7 equiv.). Final cleavage of the peptide from the resin and simultaneous side-chain deprotection was achieved by treatment with a TFA/water/TIS mixture (90:5:5) for 2.5 hours. The peptide was then precipitated from ice-cold diethyl ether, centrifuged and subjected to three ether-washing/centrifugation cycles to remove the scavengers.

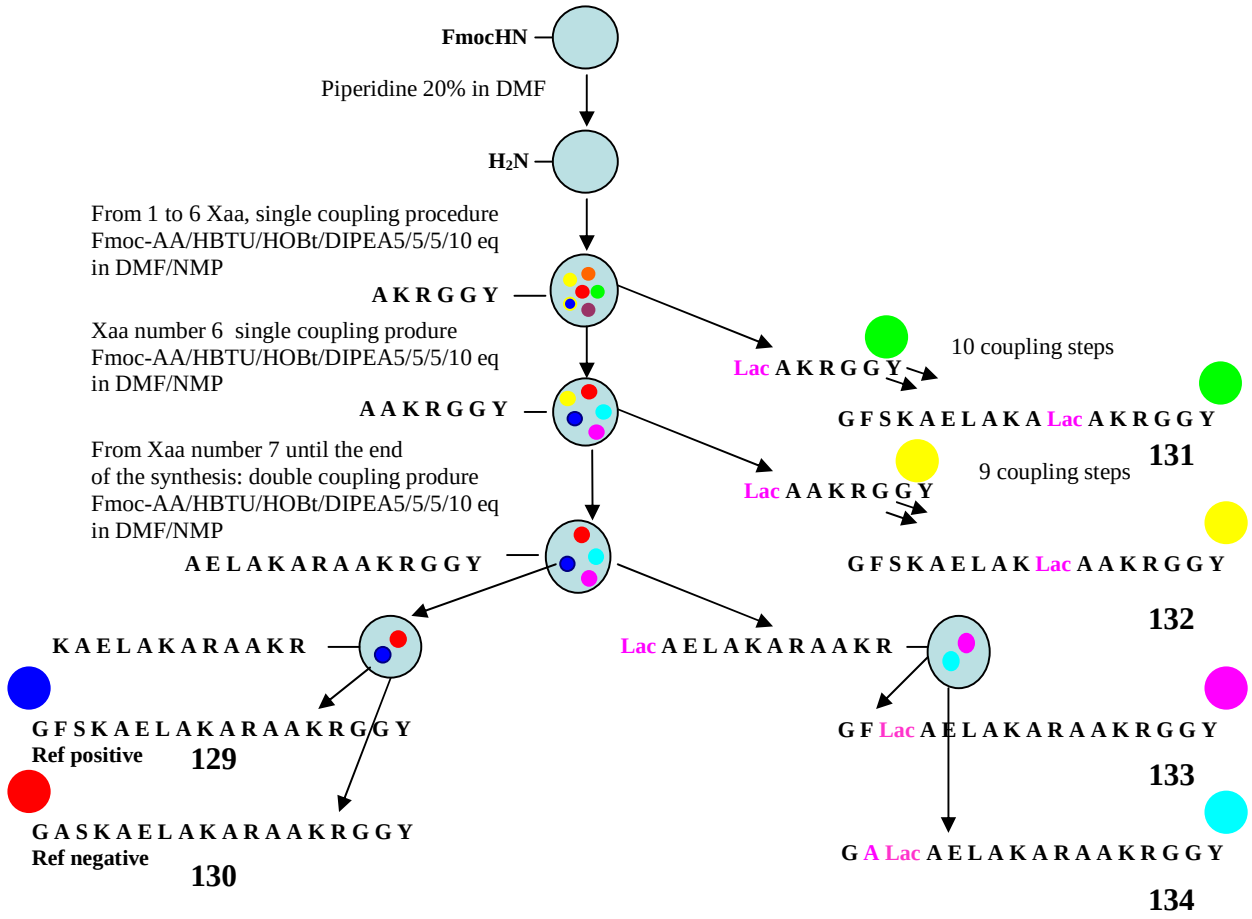

Scheme 13. Synthetic procedure for the six peptides **129**-**134**.

Each peptide was then purified by preparative HPLC. Each pure peptide was obtained in mg scale and submitted to circular dichroism analyses. The circular dichroism was recorded at 5 °C in phosphate buffer at pH 7.0 as it was described by Serrano and co-workers.[38]

III.9. Results and discussion

The CD spectra of the synthesized peptides are shown in Figure 101. It can be noted, that introduction of the lactone led to the loss of the α-helical structure in any case. Indeed, the minimum at 222 nm characteristic for α-helices was replaced by a weak shoulder, while the

minimum near 208 nm decreased intensity and was slightly blue-shifted to 205 nm. Such CD curves are similar to the one reported in the literature for the 3_{10} helix.[40]

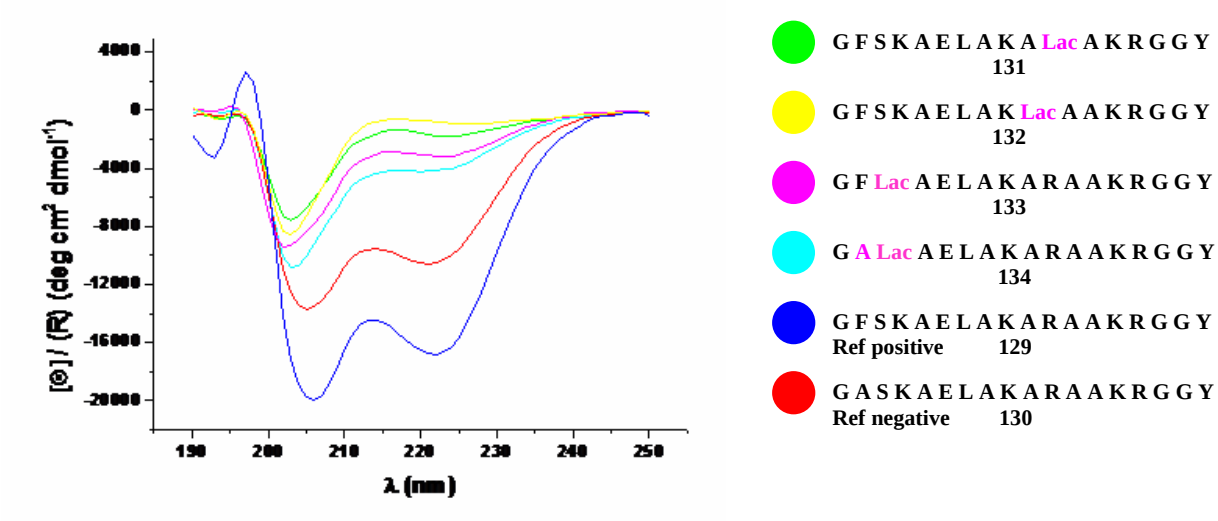

Figure 101. CD spectra recorded at 5 °C in phosphate buffer pH=7 and at 0.5 mM. The concentration of the peptides was controlled previously by UV measurement.

As described before, the α-helix is the most common regular secondary structure of peptides and proteins. However, 3_{10} helices are also observed in nature. The latter are more tightly bond and more elongated than the α-helix. The set of ϕ and ψ torsion angles of the α- and 3_{10}-helices does not differ much, falling within the same region of the Ramachandran map (Table 5).

Parameter	α-Helix	3_{10}-Helix
Φ (°)	-63	-57
Ψ (°)	-42	-30

Table 5. Average torsion angles for α- and 3_{10}-helices based on α-amino acids.

However, their intramolecular C=O$^{\cdots}$ H-N H-bonding schemes are remarkably distinct, being of the 1←4 type (sub-type III or helical β-turn[41]) in the 3_{10}-helix, and of the 1←5 type (helical α-bend[42]) in the α-helix[43] (Figure 102).

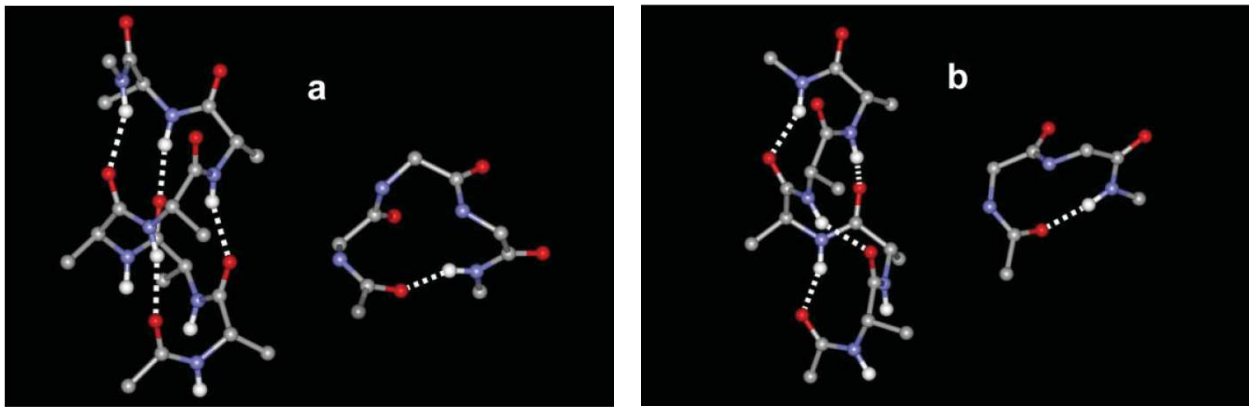

Figure 102. a) The α-helix and its building block, the helical α-turn (or C_{13}-conformation); b) The 3_{10}-helix and its building block, the helical (type III) β-turn (or C_{10}-conformation). From Toniolo *et al*.[43]
(Reproduction by courtesy of Prof. Toniolo).

Theoretical calculations have predicted a very low conformational energy barrier separating these two secondary structures.[44] It has been shown that factors influencing the folding through one or the other conformation are: the solvent properties, the length of the peptide, the temperature, and, of course, changes in the amino acid composition.

Recently, Toniolo and co-workers[45] reported an example of homooligomer made of α,α-amino acids able to fold either in α-helix or in 3_{10}-helix depending on the solvent. As an example,[45] the Ac-[L-(αMe)Val]$_7$-NH^{i}Pr showed two different folding properties in MeOH, in which it adopts a 3_{10}-helix structure, and in the acidic alcohol HFIP, where it adopts an α-helical structure (Figure 103).

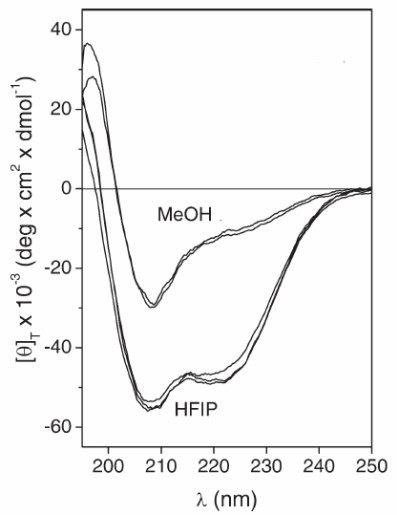

Figure 103. CD spectra of Ac-[L-(αMe)Val]$_7$-NHiPr in methanol and HFIP solutions. Reported from Toniolo and co-workers.[45] (Reproduction by courtesy of Prof. Toniolo).

According to the analysis of Toniolo's group that demonstrated the different peptide folding behaviour depending on the solvent, we performed further CD analyses of peptides **129-134** in TFE that is know to be a secondary structure stabilizer, as it is a strong H-bond donor and a weak H-bond acceptor, and, consequently, it interacts with carbonyl groups of peptides which are able to build bifurcated H-bonds without the necessity of breaking the intramolecular H-bond.

In our CD analyses in TFE, we can see differences in the structural behaviour of our modified peptides. While **131**, **133** and **134** showed α-helix-like CD profiles, **132** seemed to maintain the structure it already adopted in water (Figure 102), showing the typical CD profile for a 3_{10}-helix (Figure 104).

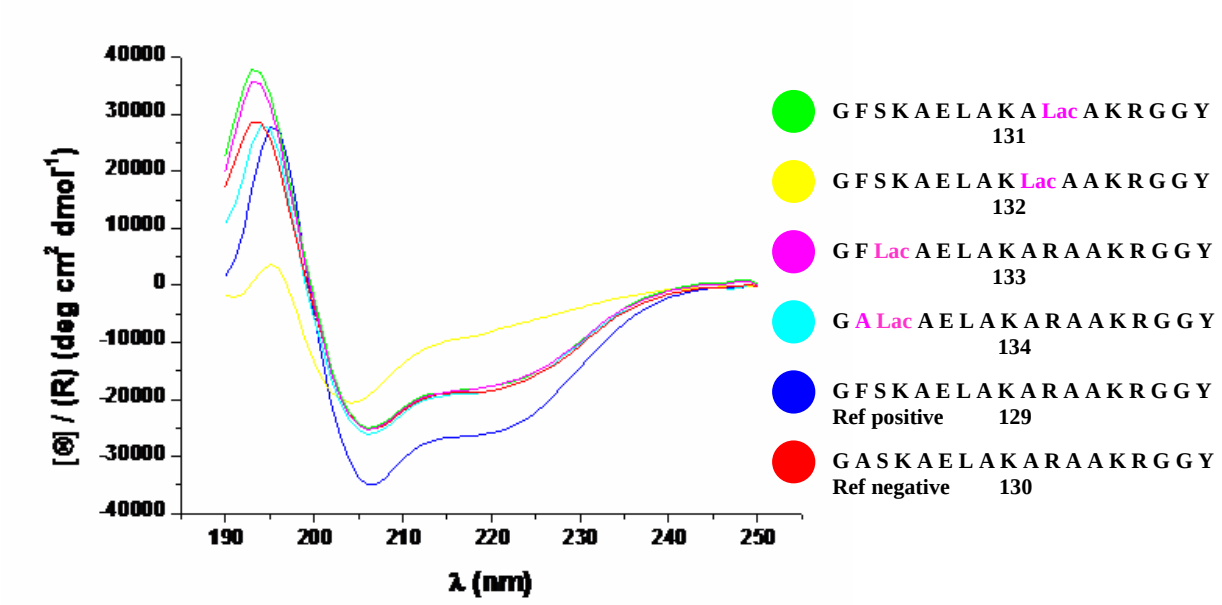

Figure 104. CD spectra recorded at 5 °C in TFE and at 0.3 mM. The concentration of the peptides was controlled previously by UV measurement.

We can conclude from these last experiments, that the introduction of the lactone in already existing α-helical peptides has an influence on their secondary structure preferences. In water, a non-stabilizing solvent, the presence of one lactone unit in the proximity of the N-end or C-end of a α-amino acid sequence with strong α-helix propensity seems to favour the building of the 3_{10}-helix at the expense of the α-helix. In contrast, in the structure-stabilizing solvent TFE, the presence of the lactone unit does not prevent the formation of the α-helix, as indicated by the fact that the CD spectra of the lactone-containing peptides **131**, **133** and **134** are superimposable with the CD spectrum of the "negative" reference peptide **130**. The striking behaviour of peptide **132**, whose structure preference seems to be less solvent-dependent, might be due to the fact that the shift of the lactone position toward the central part of an α-amino acid sequence prevented the formation of a single α-helix segment, while favouring the formation of short 3_{10}-helical structures of α-amino acids.

III.10. Conclusion

The synthetic studies performed on oligomers containing the butyrolactone δ-amino acids have shown that these interesting new scaffolds are compatible with the solid-phase methodology, which allows for a comfortable and efficient preparation of a large number of compounds. Moreover, the structural analyses of the synthesized peptide mimics have given insights in the conformational properties of peptide backbones based on alternated α/δ-units. In fact, the presence of the δ-residue seems to favour the formation of loops or isolated turn-like elements, whereas no periodic structures were observed. However, conformational analyses of δ-homooligomers support the presence of ordered structures, like turn-like repeats stabilized by intra-residue CO-NH H-bonds. Moreover, introduction of a δ-amino acid unit in proximity of the N- or C-end of a α-helical peptide chain seems to destabilize the α-helix in water, but not to prevent its formation in a structure-stabilizing solvent. In contrast, the δ-amino acid unit can act as a helix breaker when introduced into a α-helical segment, thus favouring the 3_{10}-helix over the α-helix.

References of Chapter III

1. Hanessian, S.; Luo, X.; Schaum, R.; Michnick, S., Design of Secondary Structures in Unnatural Peptides: Stable Helical gamma -Tetra-, Hexa-, and Octapeptides and Consequences of alpha -Substitution. *J. Am. Chem. Soc.* **1998,** 120, (33), 8569-8570.
2. Seebach, D.; Brenner, M.; Rueping, M.; Jaun, B., γ^2-, γ^3-, and $\gamma^{2,3,4}$-Amino acids, coupling to γ-hexapeptides: CD spectra, NMR solution and X-ray crystal structures of γ-peptides. *Chem. Eur. J.* **2002,** 8, (3), 573-584.
3. Szabo, L.; Smith, B. L.; McReynolds, K. D.; Parrill, A. L.; Morris, E. R.; Gervay, J., Solid Phase Synthesis and Secondary Structural Studies of (1->5) Amide-Linked Sialooligomers. *J. Org. Chem.* **1998,** 63, (4), 1074-1078.
4. Hann, M. M.; Sammes, P. G.; Kennewell, P. D.; Taylor, J. B., On double bond isosters of the peptide bond: an enkephalin analogue. *J. Chem. Soc., Chem. Commun.* **1980,** 24, 234-235.
5. Rai, R.; Vasudev, P. G.; Ananda, K. R., S.; Shamala, N.; Karle, I. L.; Balaram, P., Hybrid peptides: expanding the β Turn in Peptide Hairpins by the insertion of β-, γ-, and δ-Residues. *Chemistry* **2007,** 13, (20), 5917-5926.
6. Nowick, J. S.; Brower, J. O., A new turn structure for the formation of β-hairpins in peptides. *J. Am. Chem. Soc.* **2003,** 125, (4), 876-877.
7. Smith, M. D.; Long, D. D.; Marquess, D. G.; Claridge, T. D. W.; Fleet, G. W. J., Synthesis of oligomers of tetrahydrofuran amino acids: furanose carbopeptoids. *Chem. Commun.* **1998**, (18), 2039-2040.
8. Gervay, J.; Flaherty, T. M.; Nguyen, C., Solution phase synthesis of (1->5)-amide linked sugar amino acid dimers derived from sialic acids. *Tetrahedron Lett.* **1997,** 38, (9), 1493-1496.
9. Chakraborty, T. K.; Jayaprakash, S.; Srinivasu, P.; Chary, M. G.; Diwan, P. V.; Nagaraj, R.; Sankar, A. R.; Kunwar, A. C., Synthesis and structural studies of oligomers of 6-amino-2,5-anhydro-6-deoxy-D-mannonic acid. *Tetrahedron Lett.* **2000,** 41, (42), 8167-8171.
10. Claridge, T. D. W.; Long, D. D.; Baker, C. M.; Odell, B.; Grant, G. H.; Edwards, A. A.; Tranter, G. E.; Fleet, G. W. J.; Smith, M. D., Helix-Forming Carbohydrate Amino Acids. *J. Org. Chem.* **2005,** 70, (6), 2082-2090, and references therein.
11. Claridge, T. D. W.; Lopez-Ortega, B.; Jenkinson, S. F.; Fleet, G. W. J., Secondary structural investigations into homo-oligomers of δ-2,4-*cis* oxetane amino acids. *Tetrahedron Asymmetry* **2008,** 19, 984-988.
12. Haque, M. M., Enantioselective synthesis of new conformationally constrained sugar-like γ-, δ-, ε-amino acids, δ-peptides and nucleoside amino acids, PhD work. **2005**.
13. Nosse, B.; Chhor, R. B.; Jeong, W. B.; Boehm, C.; Reiser, O., Facile Asymmetric Synthesis of the Core Nuclei of Xanthanolides, Guaianolides, and Eudesmanolides. *Org. Lett.* **2003,** 5, (6), 941-944, and references therein.
14. Meindl, W. R.; von Angerer, E.; Schonenberger, H.; Ruckdeschel, G., Benzylamines: synthesis and evaluation of antimycobacterial properties. *J Med Chem* **1984,** 27, (9), 1111-8.
15. Burk, M. J.; Allen, J. G., A Mild Amide to Carbamate Transformation. *J. Org. Chem.* **1997,** 62, (20), 7054-7057.
16. Williams, R. M.; Armstrong, R. W.; Maruyama, L. K.; Dung, J. S.; P., A. O., Divergent, generalized synthesis of unsymmetrically substituted 2,5-piperazinediones. *J. Am. Chem. Soc.* **1985,** 107 (11), 3246–3253.
17. Chakraborty, T. K.; Ghosh, A., A convenient synthesis of chiral β^3-amino acids. *Synlett* **2002**, (12), 2039-2040.
18. Wüthrich, K., NMR of proteins and nucleic acids. *Wiley, New York.* 1986.

19. Belvisi, L.; Gennari, C.; Mielgo, A.; Potenza, D.; Scolastico, C., Conformational preferences of peptides containing reverse-turn mimetic bicyclic lactams. Inverse γ-turns versus type-II' β-turns. Insights into β-hairpin stability. *Eur. J. Org. Chem.* **1999**, (2), 389-400.
20. Pardi, A.; Billeter, M.; Wuthrich, K., Calibration of the angular dependence of the amide proton-Calpha proton coupling constants, ^{3}JHNα , in a globular protein. Use of ^{3}JHNα for identification of helical secondary structure. *J. Mol. Biol.* **1984,** 180, (3), 741-51.
21. Chakrabartty, A.; Kortemme, T.; Padmanabhan, S.; Baldwin, R. L., Aromatic side-chain contribution to far-ultraviolet circular dichroism of helical peptides and its effect on measurement of helix propensities. *Biochemistry* **1993,** 32, (21), 5560-5.
22. Lisowski, M.; Olczak, J.; Zabrocki, J., Circular dichroic properties of the tyrosine residues in tetrazole analogues of opioid peptides. *J. Pept. Sci.* **2006,** 12, (4), 297-302.
23. Greenfield, N. J., Methods to estimate the conformation of proteins and polypeptides from circular dichroism data. *Anal. Biochem.* **1996,** 235, (1), 1-10.
24. Sewald, N. J.; H.-D., Peptides: Chemistry and Biology. Wiley, New York 2002.
25. Lau, S. Y.; Taneja, A. K.; Hodges, R. S., Synthesis of a model protein of defined secondary and quaternary structure. Effect of chain length on the stabilization and formation of two-stranded alpha-helical coiled-coils. *J Biol Chem* **1984,** 259, (21), 13253-61.
26. http://www.imb-jena.de/ImgLibDoc/ftir/IMAGE_FTIR.html.
27. Dado, G. P.; Gellman, S. H., Structural and thermodynamic characterization of temperature-dependent changes in the folding pattern of a synthetic triamide. *J. Am. Chem. Soc.* **1993,** 115, (10), 4228-45.
28. McKay, F. C.; Albertson, N. F., New Amine-masking Groups for Peptide Synthesis. *J. Am. Chem. Soc.* **1957,** 79, (17), 4686-4690.
29. Carpino, L. A., The 9-fluorenylmethyloxycarbonyl family of base-sensitive amino-protecting groups. *Acc. Chem. Res.* **1987,** 20, 401-407.
30. Carpino, L. A.; Han, G. Y., 9-Fluorenylmethoxycarbonyl function, a new base-sensitive amino-protecting group. *J. Am. Chem. Soc.* **1970,** 92, 5748-5749.
31. Dado, G. P.; Gellman, S. H., Intramolecular hydrogen bonding in derivatives of β–Alanine and γ-amino butyric acid: Model studies for the folding of unnatural polypeptide back bones. *J. Am. Chem. Soc.* **1994,** 116, (3), 1054-1052.
32. Franot, C.; Roberts, D. W.; Smith, R. G.; Basketter, D. A.; Benezra, C.; Lepoittevin, J. P., Structure-Activity-Relationships for Contact Allergenic Potential of γ,γ-Dimethyl-γ-Butyrolactone Derivatives .1. Synthesis and Electrophilic Reactivity Studies of Alpha-(Omega-Substituted-Alkyl)-γ,γ-Dimethyl-γ-Butyrolactone S and Correlation of Skin Sensitization Potential and Cross-Sensitization Patterns with Structure. *Chem. Res. Toxicol.* **1994,** 7, (3), 297-306.
33. Tomioka, K.; Cho, Y. S.; Sato, F.; Koga, K., Stereoselective Reactions .14. Efficient Enantioselective Construction of Quaternary Carbon Centers by the Sequential Dialkylation of (S)-γ-[(Trityloxy)Methyl]-γ-Butyrolactone - Synthesis of Optically-Active β, β-Disubstituted γ-Butyrolactones. *J. Org. Chem.* **1988,** 53, (17), 4094-4098.
34. Jaime, C.; Ortuno, R. M.; Font, J., Disubstituted and Trisubstituted γ-Lactones - Conformational Study by Molecular Mechanics Calculations and Coupling-Constant Analysis. *J. Org. Chem.* **1986,** 51, (21), 3946-3951.
35. Dinares, I.; Entrena, A.; Jaime, C.; Segura, C.; Pont, J., Vicinal ring H/H coupling constants of γ-lactones containing two hydroxyl groups. *Electron. J.Theor. Chem.* **1997,** 2, 160-167.
36. Haasnoot, C. A. G.; Deleeuw, F.; Altona, C., The Relationship between Proton-Proton Nmr Coupling-Constants and Substituent Electronegativities .1. an Empirical Generalization of the Karplus Equation. *Tetrahedron* **1980,** 36, (19), 2783-2792.
37. Wavefunction Inc., 18401 Von Karmann Ave., Suite 370, Irvine, CA 92612; J. J. P. Stewart. *J. Comput. Chem.* **1989,** 10, 209.
38. Munoz, V.; Blanco, F. J.; Serrano, L., The hydrophobic-staple motif and a role for loop-residues in alpha-helix stability and protein folding. *Nat. Struct. Biol.* **1995,** 2, (5), 380-5.

39. Harper, J.; Rose, G. D., "Helix stop signals in protein and peptides: the capping box". *Biochemistry* **1993,** 32, (30), 7605-7609.
40. Toniolo, C.; Polese, A.; Formaggio, F.; Crisma, M.; Kamphuis, I., "Circular Dichroism Spectrum of a Peptide 3_{10}-helix" *J. Am. Chem. Soc.* **1996,** 118, (11), 2744.
41. Rose, G. D.; Gierasch, L. M.; Smith, J. A., "Turns in peptides and proteins". *Adv. Protein. Chem.* **1985,** 37, 1-109.
42. Pavone, V.; Gaeta, G.; Lombardi, A.; Nastri, F.; Maglio, O.; Isernia, C.; Saviano, M., "Discovering protein secondary structures: classification and description of isolated alpha-turns". *Biopolymers.* **1996,** 38, (6), 705-21.
43. Crisma, M.; Formaggio, F.; Moretto, A.; Toniolo, C., "Peptide helices based on alpha-amino acids". *Biopolymers* **2006,** 84, (1), 3-12.
44. Millhauser, G. L., "Views of helical peptides: a proposal for the position of 3(10)-helix along the thermodynamic folding pathway". *Biochemistry* **1995,** 34, (12), 3873-7.
45. Moretto, A.; Formaggio, F.; Kaptein, B.; Broxterman, B. Q.; Wu, L.; Keiderling, T. A.; Toniolo, C., "First Homo-peptides undergoing a reversible 3_{10}-helix/α-helix Transition: Critical Main-chain length". *Biopolymers* **2007,** 90, (4), 567-574.

IV. EXPERIMENTAL PART

IV.1. Experimental part chapter II

General chemical techniques:

Usual solvents were purchased from commercial sources. DMF was distilled on $CaSO_4$, THF was distilled on sodium/benzophenone, ACN was distilled on $CaCl_2$, CH_2Cl_2 was distilled from calcium hydride. Pure products were obtained after liquid chromatography using Merck silica gel 60 (40-63 μm). TLC analyses were performed with 0.25 mm 60 F_{254} silica plates (Merck). The plates were visualized with UV light (254 nm) or with a solution of vanillin in ethanol or with a solution of ninhydrin in ethanol. Element analyses (C, H, N) were performed on a Perkin-Elmer CHN Analyser 2400, by the microanalyses Service of the Faculty of Pharmacy in Châtenay-Malabry (France) or by microanalyses Service at I.C.S.N-C.N.R.S. 91198 Gif sur Yvette Cedex. Mass spectra were obtained using a Bruker Esquire electrospray ionization apparatus. IR spectra were recorded on a Bruker Vector 22 FT-IR spectrometer. Melting points were determined on a Kofler melting point apparatus. NMR spectra were recorded on a Bruker AMX 200, (^{1}H, 200 MHz, ^{19}F: 188 MHz ^{13}C, 50 MHz) or a Ultrafield AVANCE 300 (^{1}H, 300 MHz, ^{13}C, 75 MHz) or a Bruker AVANCE 400 (^{1}H, 400 MHz, ^{13}C, 100 MHz). Chemical shift δ are in ppm and the following abbreviations are used: singlet (s), broad singlet (br s), doublet (d), doublet of doublet (dd), triplet (t), multiplet or more overlapping signals (m).

SYNTHESIS OF NON FLUORINATED MOLECULE 52

2-Methoxy-5-nitrobenzoic acid 61.

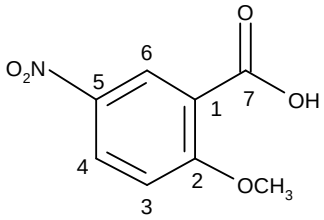

$C_8H_7NO_5$

M = 197.14 g/mol

To an ice-cold suspension of **60** (5.0 g, 32.86 mmol) in concentrated aqueous H_2SO_4 (60 mL) was added dropwise NH_4NO_3 (2.89 g, 36.15 mmol, 1.1 eq). The reaction mixture was stirred at 0°C for 30 min, then at room temperature for 3h and finally was added in water (100 mL). The resulting precipitate was filtered and the pale solid was washed with water (150 mL) and dried (over P_2O_5 in a desiccator) to give **61** as a white solid (5.2 g, 80%).

^{1}H NMR (300 MHz, $CDCl_3$) δ ppm 9.01 (d, *J* = 2.9 Hz, 1H, H_6), 8.46 (dd, *J* = 9.2 and 2.9 Hz, 1H, H_4), 7.18 (d, *J* = 9.2 Hz, 1H, H_3), 4.17 (s, 3H, $OC\underline{H}_3$).

^{13}C NMR (75 MHz, CD_3OD) δ ppm 165.9 (C_7), 163.6 (C_2), 140.3 (C_5), 129.4 (C_4), 126.7 (C_6), 122.8 (C_1), 112.4 (C_3), 55.9 ($O\underline{C}H_3$).

Rf: 0.1 (EtOAc/ cyclohexane: 80/20)

mp: 148-150 °C litt. data:[1] 161-162 °C

IR (cm $^{-1}$): 3258 (NH), 1725 (C=O), 1342 (N–O)

Elemental Anal.	%	Calcul	Found
	C	48.74	48.53
	H	3.58	3.49
	N	7.10	7.05

***N*'-(2-Methoxy-5-nitrobenzoyl)hydrazinecarboxylic acid *tert*-butyl ester 63.**

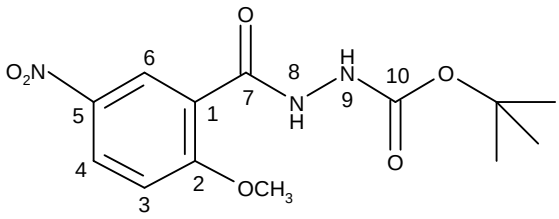

$C_{13}H_{17}N_3O_6$

M = 311.29 g/mol

To a solution of **61** (2.0 g, 10.15 mmol) in dry CH_2Cl_2 (30 mL) was added *tert*-Butyl carbazate (1.48 g, 11.17 mmol, 1.1 eq), DIPEA (5.3 mL, 30.45 mmol, 3 eq), HOBt (1.5 g, 11.17 mmol, 1.1 eq) and EDCI (2.14 g, 11.17 mmol, 1.1 eq). The reaction mixture was stirred under argon for 6 h. The solvent was evaporated under reduced pressure and the residue was dissolved in EtOAc (150 mL). The organic phase was washed with 10% aqueous citric acid (100 mL), water (100 mL), 10% aqueous K_2CO_3 (100 mL), and brine (100 mL). The organic phase was dried over Na_2SO_4, filtered and concentrated under reduced pressure. The resulting crude was purified by chromatography on silica gel and eluted with EtOAc/cyclohexane (30/70). The product was obtained as a white powder (4.1 g, 85%). A purification by chromatography on silica gel, eluting with EtOAc/cyclohexane (5/5), afforded 2.7 g (86%) of **63** as a white powder.

^{1}H NMR (300 MHz, $CDCl_3$) δ ppm 9.40 (br s, 1H, H_8), 9.07 (d, *J* = 2.9 Hz, 1H, H_6), 8.35 (dd, *J* = 9.1 and 2.9 Hz, 1H, H_4), 7.10 (d, *J* = 9.2 Hz, 1H, H_3), 7.00 (br s, 1H, H_9), 4.12 (s, 3H, O$\underline{C}H_3$), 1.51 (s, 9H, $C\underline{H}_3$Boc).

^{13}C NMR (50 MHz, $CDCl_3$) δ ppm 162.0 (C_7), 161.7 (C_2), 155.1 (C_{10}), 141.9 (C_5), 128.7 (C_4), 128.5 (C_6), 120.3 (C_1), 111.9 (C_3), 82.0 ($\underline{C}$Boc), 57.3 (O$\underline{C}H_3$), 28.2 ($\underline{C}H_3$Boc).

Rf: 0.3 (EtOAc/ cyclohexane: 60/40)

mp: 148-150 °C (crude)

IR (cm $^{-1}$): 3410 (NH), 1741(C=O), 1678 (C=O).

***N*'-(5-Amino-2-methoxybenzoyl)hydrazinecarboxylic acid *tert*-butyl ester 64.**

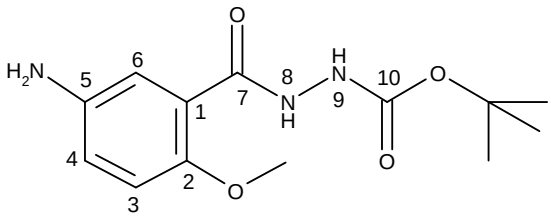

$C_{13}H_{19}N_3O_4$

M = 281.31 g/mol

To a solution of **63** (1.5 g, 4.8 mmol) in MeOH (100 mL) at room temperature was added Pd/C 10 % (150 mg). The mixture was hydrogenated at athmospheric pressure overnight and filtered through a pad of Celite. The filtrate was concentrated to give 1.30 g (96%) of **64** as a beige foam.

^{1}H NMR (300 MHz, CD_3OD) δ ppm 7.31 (br s, 1H, H_6), 6.92-6.84 (m, 2H, H_3, H_4), 3.84 (br s, 3H, $OC\underline{H}_3$), 1.45 (s, 9H, $C\underline{H}_3$Boc).

^{13}C NMR (75 MHz, CD_3OD) δ ppm 168.2 (C_7), 157.8 (C_{10}), 152.2 (C_2), 142.7 (C_5), 122.5 (C_1), 122.2 (C_4), 119.5 (C_6), 114.7 (C_3), 81.9 ($\underline{C}$Boc), 57.1 ($OC\underline{H}_3$), 29.1 ($\underline{C}H_3$Boc).

Rf: 0.3 (EtOAc/ cyclohexane: 80/20)

IR (cm $^{-1}$): 3290 (NH), 1734 (C=O), 1657 (C=O)

***N*'-(5-Acetylamino-2-methoxybenzoyl)hydrazinecarboxylic acid *tert*-butyl ester 65.**

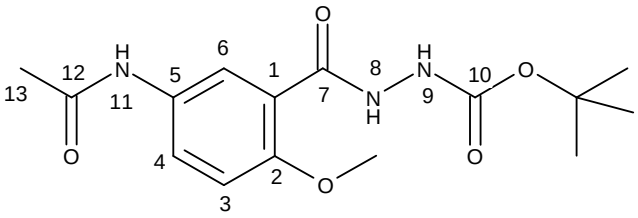

$C_{15}H_{21}N_3O_5$

M = 323.34 g/mol

A solution of **64** (1.22 g, 4.3 mmol) in dry THF (17 mL) was heated at 70 °C and acetic anhydride (2.4 mL, 24.0 mmol, 5 eq) was added dropwise to this solution. The reaction mixture was stirred for 1 hour at 70 °C. The solvent of reaction was evaporated under reduced pressure to yield **65** as a white powder (1.4 g, quantative yield). This crude product was used without any further purification in the course of the synthesis.

^{1}H NMR (300 MHz, DMSO-*d*6) δ ppm 9.92 (s, 1H, H_9), 9.60 (s, 1H, H_8), 8.90 (s, 1H, H_{11}), 7.90 (s, 1H, H_6), 7.80 (m, 1H, H_4), 7.07 (d, *J* = 9.0 Hz, 1H, H_3), 3.83 (s, 3H, $OC\underline{H}_3$), 2.02 (s, 3H, H_{13}), 1.42 (s, 9H, $C\underline{H}_3$Boc).

^{13}C NMR (75 MHz, DMSO-*d*6) δ ppm 167.9 (C_{12}), 164.9 (C_7), 155.1 (C_{10}), 152.6 (C_2), 132.4 (C_5), 123.1 (C_4), 121.2 (C_6), 112.2 (C_3), 79.0 (<u>C</u>Boc), 55.9 (O<u>C</u>H$_3$), 28.0 (<u>C</u>H$_3$Boc), 23.7 (C_{13}).

Rf: 0.2 (EtOAc/cyclohexane: 80/20)

mp: 209-211 °C

IR (cm $^{-1}$): 3275 (NH), 1712 (C=O), 1665 (C=O).

Elemental. Anal.	%	Calcul	Found
	C	55.72	55.53
	H	6.55	6.46
	N	13.00	12.89

***N*-(3-Hydrazinocarbonyl-4-methoxyphenyl)acetamide, trifluoroacetic acid salt 66.**

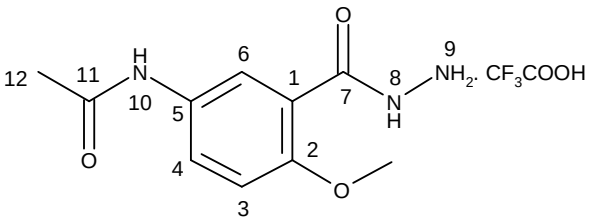

$C_{11}H_{13}N_3O_3.CF_3COOH$

M = 337.25 g/mol

Compound **65** (1.4 g, 4.3 mmol) was suspended in CH_2Cl_2 (72 mL) and trifluoroacetic acid (3.2 mL, 189.5 mmol, 55 eq) was then added dropwise at room temperature. The reaction mixture was stirred at room temperature for 5 h. Solvent was evaporated under reduced pressure to yield a light brown solid **66** (2.6 g, quantitative yield). This crude product was used without any further purification in the course of the synthesis.

^{1}H NMR (300 MHz, DMSO-*d*6) δ ppm 10.84 (br s, 3H, H_9), 10.71 (s, 1H, H_8), 10.01 (s, 1H, H_{10}), 8.06 (d, *J* = 2.7 Hz, 1H, H_6), 7.77 (dd, *J* = 9.0 and 2.8 Hz, 1H, H_4), 7.16 (d, *J* = 9.0 Hz, 1H, H_3), 3.88 (s, 3H, OC<u>H</u>$_3$), 2.03 (s, 3H, H_{13}).

^{13}C NMR (75 MHz, CD$_3$OD) δ ppm 171.7 (C_{11}), 166.0 (C_7), 161.1 (CF_3<u>C</u>OOH), 155.8 (C_2), 133.7 (C_5), 127.1 (C_4), 124.3 (C_6), 119.4 (C1), 115.4 (<u>C</u>F$_3$COOH), 113.5 (C_3), 56.9 (O<u>C</u>H$_3$), 23.6 (C_{12}).

Rf: 0.5 (EtOAc/MeOH/NH_4OH: 79/20/1)

[2-[*N*'-(5-Acetylamino-2-methoxybenzoyl)hydrazino]-1-(3,4-dimethoxy-benzyl)-2-oxoethyl]carbamic acid 9*H*-fluoren-9-ylmethyl ester 68.

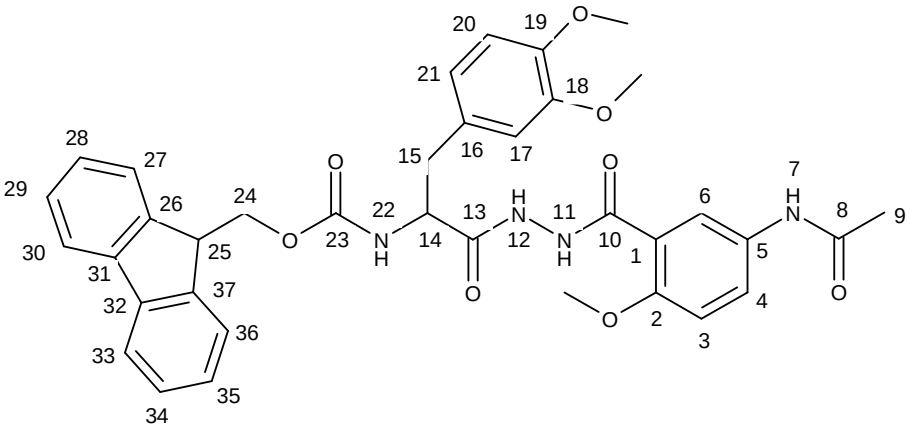

$C_{36}H_{36}N_4O_8$

M = 652.25 g/mol

To a solution of **66** (200 mg, 0.60 mmol) and Fmoc-*L*-3,4-dimethoxyphenylalanine (266 mg, 0.60 mmol, 1.0 eq) in dry DMF (14 mL) was added, after stirring for 5 min at room temperature, 2,4,6-collidine (350 µL, 2.63 mmol, 5.0 eq), HOBt (88.5 mg, 0.70 mmol, 1.1 eq) and HBTU (248 mg, 0.70 mmol, 1.1 eq). The mixture was stirred at room temperature under argon atmosphere for 6 h. After removal of the solvent under reduced pressure, the residue was dissolved in EtOAc (30 mL). The organic phase was washed with 10% aqueous citric acid (20 mL), water (20 mL), 10% aqueous Na_2CO_3 (20 mL) and brine (20 mL). The organic layer was dried over Na_2SO_4, filtered and concentrated. A purification by trituration in EtOAc afforded 194 mg (50%) of **68** as a white solid.

^{1}H NMR (300 MHz, DMSO-*d*6) δ ppm 10.58 (m, 1H, H_{11}), 10.10 (br s, 1H, H_{12}), 10.04 (m, 1H, H_7), 7.98-6.81 (m, 14 H, H_3, H_4, H_6, H_{17}, $H_{20,}$ $H_{21,}$ H_{27}, H_{28}, H_{29}, H_{30}, $H_{33,}$ H_{34}, H_{35}, H_{36}), 4.35 (m, 1H, H_{14}), 4.17-4.10 (m, 3H, $H_{24,}$ H_{25}), 3.87 (s, 3H, OC$\underline{H}_3$), 3.73 (s, 3H, OC$\underline{H}_3$), 3.68 (s, 3H, OC$\underline{H}_3$), 3.03 (m, 1H, H_{15a}), 2.80 (m, 1H, H_{15b}), 2.02 (s, 3H, H_9).

^{13}C NMR (75 MHz, DMSO-*d*6) δ ppm 170.1 (C_{13}), 168.1 (C_8), 163.1 (C_{10}), 155.8 (C_{23}), 152.6 (C_2), 148.3, 147.3 ($C_{18,}$ C_{19}), 143.8, 140.6 ($C_{26,}$ $C_{37,}$ $C_{31,}$ C_{32}), 132.7 (C_5), 130.4 (C_{16}), 127.6, 127.0, 125.3, 123.4, 121.2, 120.1, 113.2, 112.4, 111.5 (C_3, $C_{4,}$ C_6, $C_{17,}$ C_{20}, $C_{21,}$ C_{27}, C_{28}, $C_{29,}$ $C_{30,}$ $C_{31,}$ $C_{33,}$ C_{34}, C_{35}, C_{36}), 120.1 (C_1), 65.7 (C_{24}), 56.2 (OC$\underline{H}_3$), 55.3 (2 OC$\underline{H}_3$), 55.1 (C_{14}), 46.5 (C_{25}), 37.3 (C_{15}), 23.4 (C_9).

Rf: 0.7 (EtOAc/MeOH : 85/15)

mp: 208-210 °C (crude)

IR (cm^{-1}): 3480 (NH), 1742 (C=O), 1644 (C=O)

HRMS (EI) *m/e*: $[M+Na]^+$ calcd 675.2431, found 675.2408

Elemental Anal.	%	Calcul(+1.5H_2O)	Found
	C	54.87	54.87
	H	6.57	5.81
	N	9.70	9.41

***N*-(3-{*N*'-[2-Amino-3-(3,4-dimethoxyphenyl)propionyl]hydrazinocarbonyl}-4-methoxyphenyl)acetamide 69.**

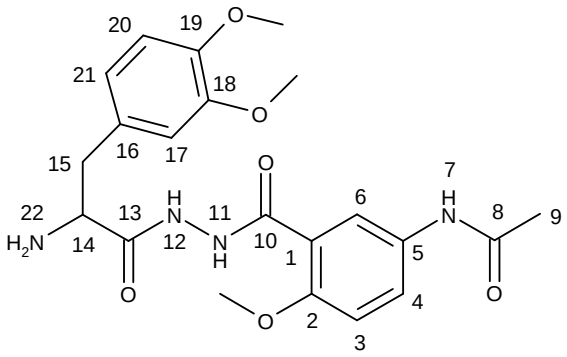

$C_{21}H_{26}N_4O_6$

M = 430.19 g/mol

To compound **68** (159 mg, 0.24 mmol) was added a solution of piperidine in DMF (10% v/v, 2.4 mL). The mixture was stirred at room temperature for 4.0 h. The organic phase was evaporated. The crude product **69**, 115 mg of a light yellow solid (quantitative yield), was used without any further purification in the course of the synthesis.

^{1}H NMR (300 MHz, DMSO-*d*6) δ ppm 10.10 (br s, 1H, H_{12}), 7.95 (d, *J* = 2.6 Hz, 1H, H_6), 7.76 (dd, *J* = 9.0 and 2.7 Hz, 1H, H_4), 7.10 (d, *J* = 9.0 Hz, 1H, H_3), 6.86-6.71 (m, 3H, $H_{17,}$ $H_{20,}$ H_{21}), 3.84 (s, 3H, O$\underline{C}H_3$), 3.70 (s, 3H, O$\underline{C}H_3$), 3.68 (s, 3H, O$\underline{C}H_3$), 3.49 (m, 1H, H_{14}), 2.89 (dd, *J* = 13.3 and 4.8 Hz, 1H, H_{15a}), 2.56 (m, 1H, H_{15b}), 2.00 (s, 3H, H_9).

^{13}C NMR (75 MHz, DMSO-*d*6) δ ppm 172.2 (C_{13}), 168.0 (C_8), 162.0 (C_{10}), 152.0 (C_2), 148.5, 147.3 ($C_{18,}$ C_{19}), 132.8 (C_5), 130.9 (C_{16}), 120.0 (C_1), 123.4, 121.3, 113.2, 112.4, 111.7 ($C_{3,}$ C_4, C_6, $C_{17,}$ $C_{20,}$ C_{21}), 56.2 (O$\underline{C}H_3$), 55.5 (O$\underline{C}H_3$), 55.4 (O$\underline{C}H_3$), 54.9 (C_{14}), 40.9 (C_{15}), 23.8 (C_9).

Rf: 0.2 (EtOAc/MeOH : 85/15)

IR (cm^{-1}): 3230 (NH), 1656 (C=O)

MS (ESI Positive) m/z: 453 $[M+Na]^+$

***N*-[2-[*N*'-(5-Acetylamino-2-methoxybenzoyl)hydrazino]-1-(3,4-dimethoxybenzyl)-2-oxoethyl]-2-(3-phenoxyphenyl)acetamide 52.**

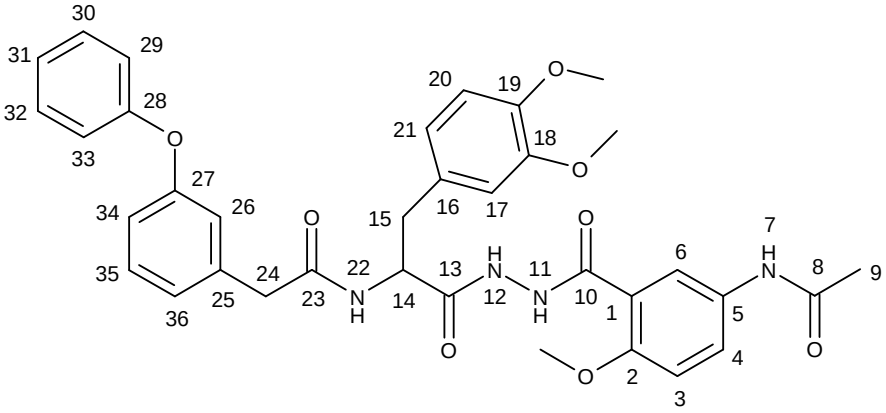

$C_{35}H_{36}N_4O_8$

M = 640.25 g/mol

To a solution of **69** (79 mg, 0.18 mmol) and 3-phenoxyphenylacetic acid (45 mg, 0.20 mmol, 1.1 eq) in dry DMF (7 mL) was added, after stirring for 5 min at room temperature, 2,4,6-collidine (50 µL, 0.36 mmol, 2.0 eq), HOBt (27 mg, 0.20 mmol, 1.1 eq) and HBTU (75 mg, 0.20 mmol, 1.1 eq). The mixture was stirred at room temperature under argon atmosphere for 20 h. After removal of the solvent under reduced pressure, the residue was dissolved in EtOAc (20 mL). The organic phase was successively washed with 10% aqueous citric acid (15 mL), water (15 mL), 10% aqueous K_2CO_3 (15 mL) and brine (15 mL). The organic layer was concentrated. A purification by chromatography on silica gel, eluting with EtOAc/MeOH (8/2), afforded 87 mg (75%) of **52** as a white powder.

^{1}H NMR (300 MHz, DMSO-*d*6) δ ppm 10.50 (br s, 1H, H_{11}), 10.10 (br s, 1H, H_{12}), 10.00 (s, 1H, H_7), 8.32 (d, *J* = 7.5 Hz, 1H, H_{22}), 7.95 (d, *J* = 2.6 Hz, 1H, H_6), 7.76 (dd, *J* = 8.9 and 2.6 Hz, 1H, H_4), 7.10 (d, *J* = 9.0 Hz, 1H, H_3), 7.39-6.72 (m, 13H, H_3, H_{17}, H_{20}, H_{21}, H_{26}, H_{29}, H_{30}, H_{31}, H_{32}, H_{33}, H_{34}, H_{35}, H_{36}), 4.62 (m, 1H, H_{14}), 3.86 (s, 3H, OC$\underline{H}_3$), 3.68 (s, 6H, 2 OC$\underline{H}_3$), 3.40 (d, *J* = 6.9 Hz, 2H, H_{24}), 3.01 (m, 1H, H_{15a}), 2.75 (m, 1H, H_{15b}), 2.01 (s, 3H, H_9).

^{13}C NMR (75 MHz, $CDCl_3$) δ ppm 169.0 (C_{23}), 168.2 (C_8), 164.0 (C_{10}), 157.0, 155.6 (C_{27}, C_{28}), 152.0 (C_2), 147.5, 147.0 (C_{18}, C_{19}), 134.8 (C_{25}), 133.0 (C_5), 129.3, 128.9, 124.0, 122.9, 122.7, 121.4, 120.9, 118.4, 118.2, 116.6, 111.7, 111.0, 109.7 (C_3, C_4, C_6, C_{17}, C_{20}, C_{21}, C_{26}, C_{29}, C_{30}, C_{31}, C_{32}, C_{33}, C_{34}, C_{35}, C_{36}), 127.3 (C_{16}), 116.5 (C_1), 55.6 (O$\underline{C}H_3$), 54.6 (O$\underline{C}H_3$), 54.5 (O$\underline{C}H_3$), 51.5 (C_{14}), 42.51 (C_{24}), 39.6 (C_{15}), 22.8 (C_9).

Rf: 0.5 (EtOAc/MeOH : 90/10)

mp: 108 - 110 °C (crude)

IR (cm^{-1}): 3273 (NH), 1649 (C=O)

MS (ESI Positive) m/z: 663 $[M+Na]^+$

Elemental Anal.

%	Calcul(+3.5H_2O)	Found
C	59.73	59.50
H	6.17	5.32
N	7.96	7.62

SYNTHESIS OF FLUORINATED MOLECULE 54

3-(*N'*-*tert*-Butoxycarbonylhydrazino)-4,4,4-trifluorobutyric acid ethyl ester 72.

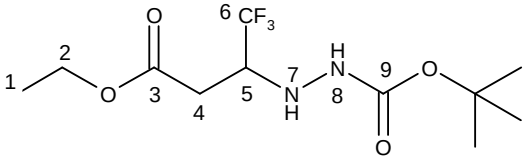

$C_{11}H_{19}F_3N_2O_4$

M = 300.13 g/mol

To a solution of **71** (2.00 g, 11.9 mmol) in MeOH (5 mL) was added *tert*-Butyl carbazate (4.72 g, 23.8 mmol, 3 eq). The mixture was stirred for 3 days at 70 °C in a sealed tube. After concentration in vacuo, the purification by chromatography on silica gel (EtOAc/cycloexane 5/5) gave 3.37 g (94%) of **72** as a colorless oil.

^{1}H NMR (200 MHz, $CDCl_3$) δ ppm 6.48 (br s, 1 H, H_8), 4.80 (br s, 1 H, H_7), 4.46 (q, *J* = 7.2 Hz, 2H, H_2), 4.16 (m, 1H, H_5), 2.90 (m, 2H, H_4), 1.71 (s, 9H, C$\underline{H}_3$Boc), 1.53 (t, *J* = 7.2 Hz, 3H, H_1).

^{13}C NMR (75 MHz, $CDCl_3$) δ ppm 169.8 (C_3), 125.3 (q, *J* = 279.8 Hz, C_6), 81.3 ($\underline{C}$Boc), 61.3 (C_2), 58.5 (q, *J* = 27.8 Hz, C_5), 32.1 (C_4), 28.2 ($\underline{C}H_3$Boc), 14.0 (C_1).

^{19}F (188 MHz, $CDCl_3$) δ ppm -75.3 (d, *J* = 5.6 Hz).

Rf: 0.3 (EtOAc/cyclohexane : 20/80)

IR (cm^{-1}): 3193 (NH), 1715 (C=O), 1157 (C-O), 1121 (C-O), 774 (CF_3)

MS (ESI Positive) m/z: 323 $[M+Na]^+$

Elemental Anal.	%	Calcul	Found
	C	44.00	43.72
	H	6.38	6.16
	N	9.33	9.69

3-(*N'*-*tert*-Butoxycarbonylhydrazino)-4,4,4-trifluorobutyric acid 73.

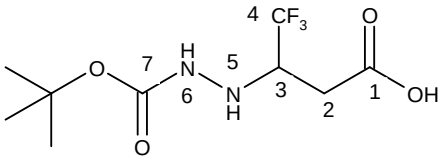

$C_9H_{15}F_3N_2O_4$

M = 272.10 g/mol

To a solution of **72** (500 mg, 1.67 mmol) in THF/MeOH (2,5 mL / 2,5 mL) was added a 2N aqueous NaOH (917 µl, 1.84 mmol, 1.1 eq). The mixture was stirred for 2 h at room temperature. After concentration in vacuo, the residue was diluted with water (5 mL). Then EtOAc (6 mL) and 1N aqueous HCl (2 mL) were added. The separated organic phase was dried (Na_2SO_4), filtered and concentrated to yield 444 mg (98%) of **73** as a white solid.

^{1}H NMR (300 MHz, DMSO-*d*6) δ ppm 12.54 (br s, 1H, COO<u>H</u>), 8.39 (br s, 1H, H_6), 3.82 (m, 1H, H_3), 2.61 (dd, *J* = 16.6 and 5.4 Hz, 1H, H_{2a}), 2.44 (dd, *J* = 16.6 and 6.8Hz, 1H, H_{2b}), 1.38 (s, 9H, C<u>H</u>$_3$Boc).

^{13}C NMR (75 MHz, DMSO-*d*6) δ ppm 170.8 (C_1), 156.4 (C_7), 125.9 (q, *J* = 280.5 Hz, C_4), 78.9 (<u>C</u>Boc), 57.4 (C_3), 32.4 (C_2), 28.0 (<u>C</u>H_3Boc).

^{19}F (188 MHz, DMSO-*d*6) δ ppm -74.1 (d, *J* = 6.8 Hz).

Rf: 0.3 (EtOAc/cyclohexane: 70/30)

mp: 138-140 °C (crude)

IR (cm^{-1}): 3325 (NH), 3100 (OH), 1732 (C=O), 1687 (C=O), 1122 (C-O), 760 (CF_3)

MS (ESI Negative) m/z: 271 $[M-H]^-$

Elemental Anal.	%	Calcul	Found
	C	39.71	39.83
	H	5.55	5.50
	N	10.29	10.29

2-[3-(*N'*-*tert*-Butoxycarbonylhydrazino)-4,4,4-trifluorobutyrylamino]-3-phenyl-propionic acid methyl ester 75.

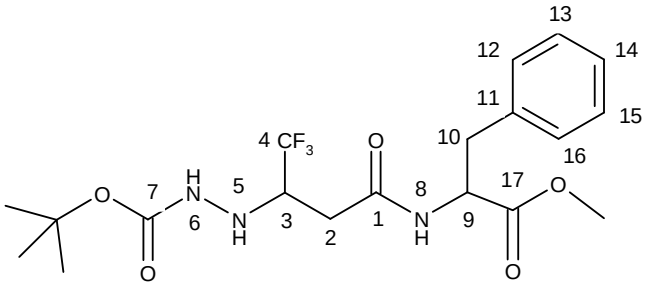

$C_{19}H_{26}F_3N_3O_6$
M = 433.18 g/mol

To a solution of **73** (100 mg, 0.37 mmol) and phenylalanine methyl ester hydrochloride (88 mg, 0.41 mmol, 1.1 eq) in dry CH_2Cl_2 (3 mL) and dry DMF (1 mL) was added DIPEA (135 µL, 0.82 mmol, 2.0 eq), HOBt (55 mg, 0.41 mmol, 1.1 eq) and HBTU (155 mg, 0.41 mmol, 1.1 eq). The mixture was stirred at room temperature under argon atmosphere for 23 h. After removal of the solvent under reduced pressure, the residue was dissolved in EtOAc (10 mL). The organic solution was successively washed with 10% aqueous citric acid (10 mL), water (10 mL), 10% aqueous K_2CO_3 (10 mL), brine (10 mL) and dried over Na_2SO_4. The organic layer was evaporated and the residue was triturated with petroleum ether to yield 146 mg (91%) of **75** as a white solid.

^{1}H NMR (400 MHz, DMSO-*d*6) δ ppm 8.56;8.58 (2 d, *J* = 6.3;6.4 Hz, 1H, $H_{8,}$ 2 dia), 8.36 (m, 1H, H_6), 7.27-7.17 (m, 5H, H_{ar}), 4.98;5.02 (2 br s, 1H, $H_{5,}$ 2 dia), 4.46 (m, 1H, H_9), 3.73 (m, 1H, H_3), 3.56;3.57 (2s, 3H, O$\underline{C}H_{3,}$ 2 dia), 3.00 (dd, *J* = 13.6 and 5.8 Hz, 1H, H_{10a}), 2.89 (m, 1H, H_{10b}), 2.38-2.48 (m, 2H, H_2), 1.36;1.37 (s, 9H, C$\underline{H}_3$Boc, 2 dia).

^{13}C NMR (100 MHz, DMSO-*d*6) δ ppm 172.2;172.1 ($C_{17,}$ 2 dia), 168.7 (C_1), 156.7 (C_7), 137.5;137.4 ($C_{11,}$ 2 dia), 129.4;129.3 (C_{13}, $C_{15,}$ 2 dia), 128.7 ($C_{12,}$ C_{16}), 127.0 (C_{14}), 126.3 (q, *J* = 278.0 Hz, C_4), 79.3 ($\underline{C}$Boc), 58.3;58.0 (2 m, $C_{3,}$ 2 dia), 54.1;54.0 ($C_{9,}$ 2 dia), 52.1;52.2 (O$\underline{C}H_{3,}$ 2 dia), 37.2;37.1 ($C_{10,}$ 2 dia), 33.4 (C_2), 28.5 ($\underline{C}H_3$Boc).

^{19}F (188 MHz, DMSO-*d*6) δ ppm (-73.6) – (-73.8) (m).

Rf: 0.7 (EtOAc/cyclohexane: 70/30)

mp: 94-96 °C (crude)

IR (cm^{-1}): 3351 (NH), 3288 (NH), 1739 (C=O), 1709 (C=O), 1683 (C=O), 1164 (C-O), 1124 (C-O), 698 (CF_3)

MS (ESI Positive) m/z: 456 $[M+Na]^+$

Elemental Anal.

%	Calcul	Found
C	52.65	52.15
H	6.05	6.07
N	9.69	9.37

3-Phenyl-2-(4,4,4-trifluoro-3-hydrazinobutyrylamino)propionic acid methyl ester, trifluoro-acetic acid salt 76.

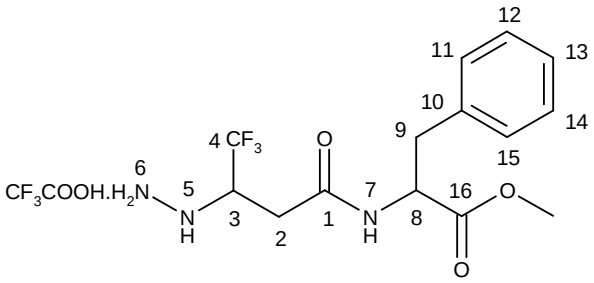

$C_{14}H_{18}F_3N_3O_3.CF_3COOH$

M = 447.15

Compound **75** (134 mg, 0.31 mmol) was dissolved in CH_2Cl_2 (7 mL) and trifluoroacetic acid (1.4 mL, 18.6 mmol, 60.0 eq) was added dropwise at room temperature. The reaction mixture was stirred for 2 h. Solvent was evaporated under reduced pressure to yield an orange solid oil **76** (159 mg, with excess of TFA). Azeotropic removal of excess TFA with toluene gave a crude product used without further purification in the course of the synthesis.

^{1}H NMR (300 MHz, $CDCl_3$) δ ppm 8.11 (bs, 3H, H_6), 7.27-7.13 (m, 5H, H_{ar}), 4.41 (br s, 1H, H_8), 3.78 (m, 1H, H_3), 3.71 (s, 3H, O$C\underline{H}_3$), 3.33 (m, 2H, H_9), 3.11 (m, 1H, H_{2a}), 2.59 (m, 1H, H_{2b}).

^{13}C NMR (100 MHz, $CDCl_3$) δ ppm 169.4 (C_{16}), 158.9 (q, *J* = 31.0 Hz, $CF_3\underline{C}OOH$), 133.2 (C_{10}), 129.4, 129.1 ($C_{11,}$ C_{15}, $C_{12,}$ C_{14}), 128.0 (C_{13}), 114.8 (q, *J* = 284.2 Hz, $\underline{C}F_3COOH$), 54.6 (C_8), 53.3 (O$\underline{C}$H3), 52.8 (C_3), 36.0 (C_9), 30.8;30.4 ($C_{2,}$ 2 dia).

^{19}F (188 MHz, DMSO-*d*6) δ ppm -76.4 ($C\underline{F}_3COOH$), -78.0 (d, *J* = 5.6 Hz).

Rf: 0.7 (EtOAc/MeOH/NH_4OH: 79/20/1)

2-(3-{*N*'-[3-(3,4-Dimethoxyphenyl)-2-(9*H*-fluoren-9-ylmethoxycarbonylamino)propionyl] hydrazino}-4,4,4-trifluorobutyrylamino)-3-phenylpropionic acid methyl ester 77.

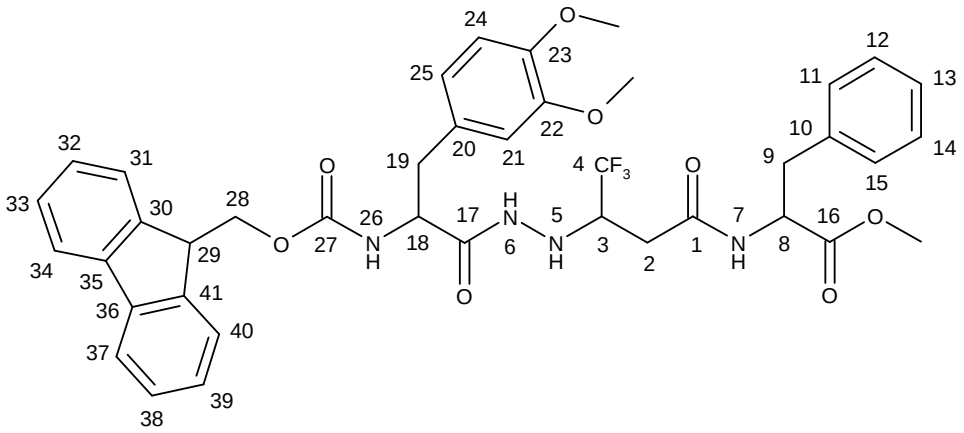

$C_{40}H_{41}F_3N_4O_8$

M = 762.29 g/mol

To a solution of **76** (300 mg, 0.67 mmol) and Fmoc-*L*-3,4-dimethoxyphenylalanine (300 mg, 0.67 mmol, 1.0 eq) in dry DMF (14 mL) was added, after stirring for 5 min at room temperature, 2,4,6-collidine (357 µL, 2.68 mmol, 4.0 eq), HOBt (99 mg, 0.74 mmol, 1.1 eq) and HBTU (279 mg, 0.74 mmol, 1.1 eq). The mixture was stirred at room temperature under argon atmosphere for 21 h. After removal of the solvent under reduced pressure, the residue was dissolved in EtOAc (14 mL). The organic phase was washed with 10% aqueous citric acid (14 mL), water (14 mL), 10% aqueous K_2CO_3 (14 mL) and brine (14 mL). The organic layer was dried over Na_2SO_4, filtered and concentrated. A purification by chromatography on silica gel, eluting with EtOAc/cyclohexane (5/5), afforded 112 mg (22%) of **77** as a white powder.

^{1}H NMR (400 MHz, DMSO-*d*6) δ ppm 9.63 (br s, 1H, H_6), 8.61 (d, *J* = 7.4 Hz, 1H, H_7), 7.87 (d, *J* = 7.5 Hz, 2H, H_{34}, H_{37}), 7.66-7.61 (m, 3H, H_{31}, H_{40}, H_{26}), 7.40 (m, 2H, H_{33}, H_{38}), 7.32-7.20 (m, 7H, H_{11}, H_{12}, H_{13}, H_{14}, H_{15}, H_{32}, H_{39}), 6.94 (d, *J* = 11.8 Hz, 1H, H_{24}), 6.79 (m, 2H, H_{21}, H_{25}), 5.48 (m, 1H, H_5), 4.50 (m, 1H, H_8), 4.16-4.14 (m, 4H, H_{18}, H_{28}, H_{29}), 3.80 (m, 1H, H_3), 3.71 (s, 3H, OC$\underline{H}_3$), 3.67 (s, 3H, OC$\underline{H}_3$), 3.57 (s, 3H, OC$\underline{H}_3$), 3.02 (dd, *J* = 13.8 and 5.9 Hz, 1H, H_{9a}), 2.92 (m, 1H, H_{9b}), 2.84 (m, 1H, H_{19a}), 2.70 (m, 1H, H_{19b}), 2.50 (m, 2H, H_2).

^{13}C NMR (100 MHz, DMSO-*d*6) δ ppm 171.8 (C_{17}), 171.4;171.2 (C_{16}, 2 dia), 168.2 (C_1), 155.7 (C_{27}), 148.4 (C_{23}), 147.4 (C_{22}), 143.9;143.7 (C_{30}, C_{41}), 140.6 (C_{35}, C_{36}), 137.0;136.9 (C_{10}, 2 dia), 130.0 (C_{20}), 129.0 (C_{11}, C_{15}), 128.2 (C_{12}, C_{14}), 127.6 (C_{33}, C_{38}), 127.0 (C_{32}, C_{39}), 126.5 (C_{13}), 125.3 (C_{31}, C_{40}), 121.2 (C_{25}), 120.1 (C_{34}, C_{37}), 113.1 (C_{24}), 111.6 (C_{21}), 65.7 (C_{28}), 55.3 (2 O$\underline{C}$H3), 55.0 (C_{29}), 53.7;53.6 (C_8, 2 dia), 51.8 (O$\underline{C}$H3), 46.5 (C_{18}), 37.1 (C_{19}), 36.7 (C_9), 32.9 (C_2).

^{19}F (188 MHz, DMSO-*d*6) δ ppm (-73.8) – (-73.9) (m).

Rf: 0.6 (EtOAc/cyclohexane: 70/30)

mp: 178-180 °C (crude)

IR (cm^{-1}): 3304 (NH), 1738 (C=O), 1686 (C=O), 1667 (C=O), 1170 (C-O), 1121 (C-O), 698 (CF_3)

MS (ESI Positive) m/z: 785 $[M+Na]^+$

Elemental Anal.	%	Calcul (+ 1 H_2O)	Found
	C	61.57	61.72
	H	5.57	5.17
	N	7.18	7.15

2-(3-{*N*'-[2-Amino-3-(3,4-dimethoxyphenyl)propionyl]hydrazino}-4,4,4-trifluoro-butyrylamino)-3-phenylpropionic acid methyl ester 78.

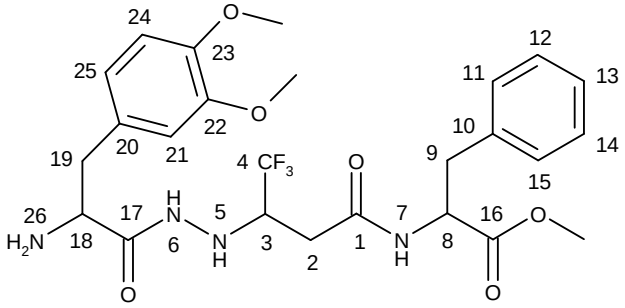

$C_{25}H_{31}F_3N_4O_6$

M = 540.22 g/mol

To compound **77** (115 mg, 0.15 mmol) was added a solution of piperidine in DMF (10% v/v, 4 mL). The mixture was stirred at room temperature for 1.30 h. The organic phase was evaporated. The crude product **78**, 70 mg of a white solid (84%), was used without any further purification in the course of the synthesis.

^{1}H NMR (300 MHz, CD_3OD) δ ppm 7.31-7.21 (m, 5H, $H_{11,}$ $H_{12,}$ $H_{13,}$ $H_{14,}$ H_{15}), 6.86-6.71 (m, 3H, $H_{21,}$ $H_{24,}$ H_{25}), 4.94 (m, 1H, H_8), 4.71 (m, 1H, H_{18}), 3.80 (s, 3H, $OC\underline{H}_3$), 3.78 (s, 3H, $OC\underline{H}_3$), 3.68 (s, 3H, $OC\underline{H}_3$), 3.49 (m, 1H, H_3), 3.12 (m, 2H, H_9), 2.91 (dd, *J* = 13.7 and 7.1 Hz, 1H, $H1_{9a}$), 2.68 (dd, *J* = 13.7 and 7.0 Hz, 1H, H_{19b}), 2.41 (m, 2H, H_2).

^{13}C NMR (75 MHz, CD_3OD) δ ppm 176.0, 173.6, 171.3 ($C_{17,}$ $C_{1,}$ C_{16}), 150.5, 149.5 ($C_{22,}$ C_{23}), 138.2 (C_{10}), 131.3 (C_{20}), 130.3, 129.5 ($C_{11,}$ $C_{12,}$ C_{14}, C_{15}), 127.9 (C_{13}), 122.9 (C_{25}), 114.3, 113.2 ($C_{21,}$ C_{24}), 60.0 (q, *J* = 28.2 Hz, C_3), 56.5 (O$\underline{C}$H3), 56.4 (O$\underline{C}$H3), 55.6 (C_8), 52.8 (O$\underline{C}$H3), 45.9 (C_{18}), 41.8 (C_{19}), 38.3 (C_9), 34.0 (C_2).

Rf: 0.2 (CH_2Cl_2/MeOH: 97/3)

2-[3-(*N'*-{3-(3,4-Dimethoxyphenyl)-2-[2-(3-phenoxyphenyl)acetylamino]propionyl}hydrazino)-4,4,4-trifluorobutyrylamino]-3-phenylpropionic acid methyl ester 54.

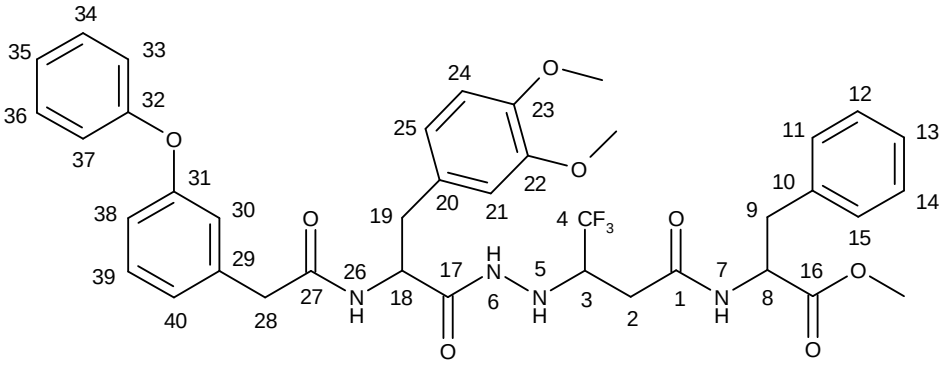

$C_{39}H_{41}F_3N_4O_8$

M = 750.29 g/mol

To a solution of **78** (70 mg, 0.13 mmol) and 3-phenoxyphenylacetic acid (32 mg, 0.14 mmol, 1.1 eq) in dry DMF (4 mL) was added, after stirring for 5 min at room temperature, DIPEA (66 µL, 0.45 mmol, 3.0 eq), HOBt (19 mg, 0.14 mmol, 1.1 eq) and HBTU (53 mg, 0.14 mmol, 1.1 eq). The mixture was stirred at room temperature under argon atmosphere for 24 h. After removal of the solvent under reduced pressure, the residue was dissolved in EtOAc (12 mL). The organic solution was washed with 10% aqueous citric acid (12 mL), water (12 mL), 10% aqueous K_2CO_3 solution (12 mL) and brine (12 mL). The organic layer was dried over Na_2SO_4, filtered and concentrated. A purification by chromatography on silica gel, eluting with EtOAc/cyclohexane (6/4), afforded 40 mg (41%) of **54** as a white powder.

^{1}H NMR (300 MHz, DMSO-*d*6) δ ppm 9.62 (d, *J* = 4.9 Hz, 1H, H_6), 8.60 (d, *J* = 7.6 Hz, 1H, H_7), 8.33, 8.30 (2d, *J* = 8.7 and 9.0 Hz, 1H, H_{26}, 2 dia), 7.40-6.70 (m, 17H, H_{11}, H_{12}, H_{13}, H_{14}, H_{15}, H_{21}, H_{24}, H_{25}, H_{30}, H_{33}, H_{34}, H_{35}, H_{36}, H_{37}, H_{38}, H_{39}, H_{40}), 5.47 (m, 1H, H_5), 5.0 (m, 1H, H_{18}), 4.54-4.39 (m, 1H, H_8), 3.83-3.67 (m, 7H, H_3, 2 O$C\underline{H}_3$), 3.57;3.54 (2s, 3H, O$C\underline{H}_3$, 2 dia), 3.38 (m, 2H, H_{28}), 3.05-2.82 (m, 4H, H_{19}, H_9), 2.68 (m, 1H, H_{2a}), 2.45 (m, 1H, H_{2b}).

^{13}C NMR (100 MHz, DMSO-*d*6) δ ppm 171.7 (C_{16}), 170.9 (C_{17}), 169.5 (C_{27}), 168.2 (C_1), 156.6,156.3 (C_{31}, C_{32}), 148.0, 147.3 (C_{22}, C_{23}), 138.3 (C_{29}), 136.9 (C_{10}), 129.9, 129.4, 129.0, 128.9, 128.2, 126.5, 123.9, 123.3, 121.1, 119.3, 118.5, 116.3 , 112.9, 111.5 (C_{11}, C_{12}, C_{13}, C_{14}, C_{15}, C_{21}, C_{24}, C_{25}, C_{30}, C_{33}, C_{34}, C_{35}, C_{36}, C_{37}, C_{38}, C_{39}, C_{40}), 55.3 (O$\underline{C}$H3), 55.2 (O$\underline{C}$H3), 53.7;53.6 (C_8, 2 dia), 52.7 (C_3), 51.8 (O$\underline{C}$H3), 47.1 (C_{18}), 41.7(C_{28}), 37.4 (C_{19}), 36.7 (C_9), 32.9 (C_2).

^{19}F (188 MHz, $CDCl_3$) δ ppm -74.9 (d, *J* = 7.0 Hz), -75.0 (d, *J* = 6.9 Hz), ratio between the two diastereomers is 40-60% respectively.

Rf: 0.5 (EtOAc/cyclohexane: 70/30)

mp: 138-140 °C (crude)

IR (cm^{-1}): 3277 (NH), 1741 (C=O), 1634 (C=O), 1161 (C-O), 1118 (C-O), 696 (CF_3)

MS (ESI Positive) m/z: 751 $[M+H]^+$

Elemental Anal.	%	Calcul (+ 0.75 H_2O)	Found
	C	61.32	61.37
	H	5.62	5.61
	N	7.34	7.31

SYNTHESIS OF FLUORINATED MOLECULE 55

3-Phenyl-2-(4,4,4-trifluoro-3-{*N*'-[2-(3-phenoxyphenyl)acetyl]hydrazino}butyrylamino)propionic acid methyl ester 55.

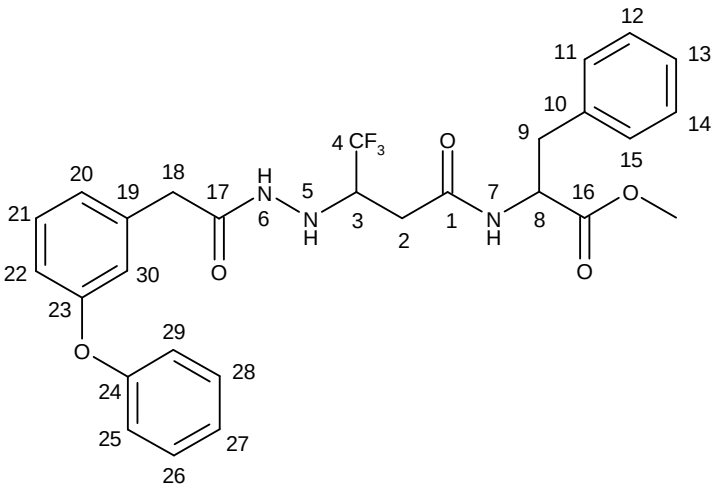

$C_{28}H_{28}F_3N_3O_5$

M = 543.20 g/mol

To a solution of the **76** (309 mg, 0.69 mmol) and 3-phenoxyphenylacetic acid (174 mg, 0.76 mmol, 1.1 eq) in dry DMF (16 mL) was added, after stirring for 5 min at room temperature, 2,4,6-collidine (368 µL, 2.76 mmol, 4.0 eq), HOBt (103 mg, 0.76 mmol, 1.1 eq), and HBTU (288 mg, 0.76 mmol, 1.1 eq). The mixture was stirred at room temperature under argon atmosphere for 24 h. After removal of the solvent under reduced pressure, the residue was dissolved in EtOAc (13 mL). The

organic phase was successively washed with 10% aqueous citric acid (13 mL), water (13 mL), 10% aqueous K_2CO_3 (13 mL) and brine (13 mL). The organic layer was dried over Na_2SO_4, filtered and concentrated. Purification by chromatography on silica gel, using EtOAc/cyclohexane (6/4) as eluent, afforded 159 mg (42%) of **55** as a white powder.

^{1}H NMR (400 MHz, DMSO-*d*6) δ ppm 9.64 (s, 1H, H_6), 8.60;8.59 (2d, *J* = 7.7 and 7.6 Hz, 1H, $H_{7,}$ 2 dia), 7.40-7.11 (m, 9H, $H_{11,}$ $H_{12,}$ $H_{13,}$ $H_{14,}$ $H_{15,}$ $H_{21,}$ $H_{26,}$ $H_{27,}$ H_{28}), 7.02-6.84 (m, 5H, $H_{22,}$ $H_{30,}$ $H_{25,}$ $H_{29,}$ H_{20}), 5.44 (br s, 1H, H_5), 4.48 (m, 1H, H_8), 3.72 (m, 1H, H_3), 3.57 (s, 3H, O$\underline{C}H_3$), 3.38 (m, 2H, H_{18}), 3.01 (dd, *J* = 13.8 and 5.8 Hz, 1H, H_{9a}), 2.90 (m, 1H, H_{9b}), 2.49 (m, 1H, H_{2a}), 2.44 (dd, *J* = 12.8 and 6.1 Hz, 1H, H_{2b}).

^{13}C NMR (100 MHz, DMSO-*d*6) δ ppm 171.8-171.7 ($C_{16,}$ 2 dia), 169.6;169.5 ($C_{17,}$ 2 dia), 168.1 (C_1), 156.5 ($C_{23,}$ C_{24}), 137.9 (C_{19}), 137.0;136.9 ($C_{10,}$ 2 dia), 130.0 (C_{26}, C_{28}), 129.7 (C_{21}), 129.0 (C_{12}, C_{14}), 128.2 (C_{11}, C_{15}), 126.5 (C_{13}), 124.1 (C_{20}), 123.4 (C_{27}), 119.1 (C_{30}), 118.6 ($C_{25,}$ C_{29}), 116.7 (C_{22}), 57.5 (q, *J* = 26.0, C_3), 53.70;53.60 ($C_{8,}$ 2 dia), 51.8 (O$\underline{C}$H3), 40.1 (C_{18}), 36.7 (C_9), 33.0 (C_2).

^{19}F (188 MHz, DMSO-*d*6) δ ppm -74.9 (d, *J* = 7.1 Hz), -75.2 (d, *J* = 6.8 Hz).

Rf: 0.6 (EtOAc/cyclohexane: 60/40)

mp: 82-84 °C (crude)

IR (cm^{-1}): 3285 (NH), 1737 (C=O), 1637 (C=O), 1164 (C-O), 1118 (C-O), 693 (CF_3)

MS (ESI Positive) m/z: 566 $[M+Na]^+$

Elemental Anal.	%	Calcul	Found
	C	61.87	61.61
	H	5.19	5.34
	N	7.73	7.53

SYNTHESIS OF FLUORINATED MOLECULE 56

2-{3-[*N*'-(2-Benzyloxycarbonylamino-6-*tert*-butoxycarbonylaminohexanoyl)hydrazino]-4,4,4-trifluorobutyrylamino} -3-phenylpropionic acid methyl ester 80.

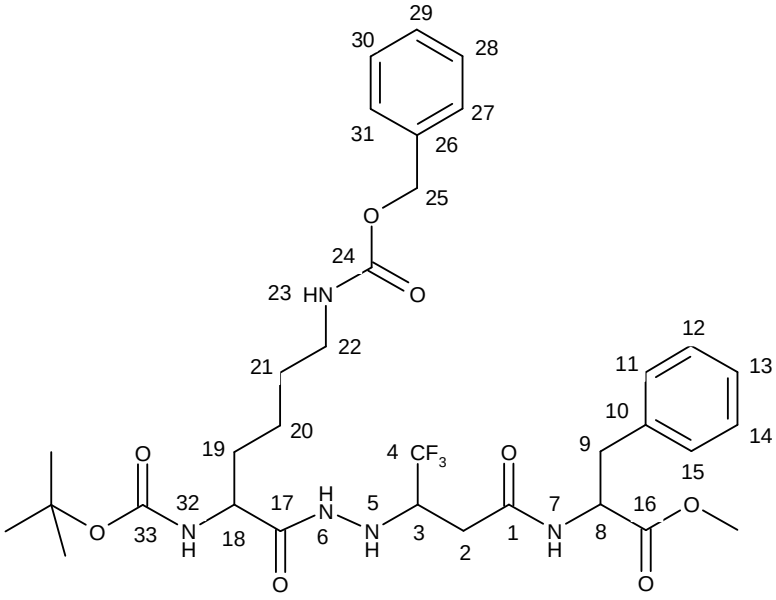

$C_{33}H_{44}F_3N_5O_8$

M = 695.31 g/mol

To a solution of **76** (1.22 g, 2.73 mmol) and N_α-BOC-N_ε-Z-L-lysine (1.52 g, 4.00 mmol, 1.5 eq) in dry DMF (20 mL) was added, after stirring for 5 min at room temperature, DIPEA (2.7 mL, 16.33 mmol, 6.0 eq), HOBt (540 mg, 4.00 mmol, 1.5 eq) and HBTU (1.52 g, 4.00 mmol, 1.5 eq). The mixture was stirred at room temperature under argon atmosphere for 68 h. After removal of the solvent under reduced pressure, the residue was dissolved in EtOAc (15 mL). The organic phase was washed with 10% aqueous citric acid (15 mL), water (15 mL), 10% aqueous K_2CO_3 (15 mL) and brine (15 mL). The organic layer was dried over Na_2SO_4, filtered and concentrated. A purification by chromatography on silica gel, eluting with EtOAc/cyclohexane (4/6) and a trituration in petroleum ether afforded 1.09 g (57%) of **80** as a white solid.

^{1}H NMR (400 MHz, DMSO-*d*6) δ ppm 9.42 (m, 1H, H_6), 8.61 (d, *J* = 7.6 Hz, 1H, H_7), 7.40-7.19 (m, 11 H, H_{11}, H_{12}, H_{13}, H_{14}, $H_{15,}$ $H_{23,}$ H_{27}, H_{28}, H_{29}, H_{30}, H_{31}), 6.81 (m, 1H, H_{32}), 5.40 (bs, 1H, H_5), 5.00 (s, 2H, H_{25}), 4.49 (m, 1H, H_8), 3.83 (m, 1H, H_{18}), 3.74 (m, 1H, H_3), 3.58 (s, 3H, OC$\underline{H}_3$), 3.05-2.89 (m, 4H, $H_{9,}$ H_{22}), 2.46 (m, 2H, H_2), 1.46 (m, 2H, H_{19}), 1.40-1.28 (m, 11H, $H_{21,}$ C$\underline{H}_3$Boc), 1.26 (m, 2H, H_{20}).

^{13}C NMR (100 MHz, DMSO-*d*6) δ ppm 171.8 (C_{16}), 168.1 (C_1), 156.1 (C_{24}), 155.2 (C_{33}), 137.3 (C_{26}), 137.0 (C_{10}), 129.0, 128.9, 128.3, 128.2, 127.7, 126.5 (C_{11}, C_{12}, C_{13}, C_{14}, C_{15}, C_{27}, C_{28}, C_{29}, C_{30}, C_{31}), 78.0 (CBoc), 65.1 (C_{25}), 57.5 (q, *J* = 20.9 Hz, C_3), 53.6 (C_8), 52.8 (C_{18}), 51.8 (O$\underline{C}H_3$), 39.7 (C_{22}), 36.7 (C_9), 32.8 (C_2), 31.3 (C_{19}), 29.0 (C_{21}), 28.1 ($\underline{C}H_3$Boc), 22.7 (C_{20}).

^{19}F (188 MHz, DMSO-*d*6) δ ppm -76.4 (d, *J* = 7.4 Hz), -76.5 (d, *J* = 7.2 Hz).

Rf: 0.6 (EtOAc/cyclohexane: 70/30)

mp: 92-94 °C (crude)

IR (cm^{-1}): 3321 (NH), 1741 (C=O), 1686 (C=O), 1634 (C=O), 1161 (C-O), 1127 (C-O), 698 (CF_3)

HRMS (EI) *m/e*: $[M+Na]^+$ calcd 718.3040, found 718.3019

Elemental Anal.

%	Calcul (+ 1.5 H_2O)	Found
C	54.87	54.87
H	6.57	5.81
N	9.70	9.41

2-{3-[*N*'-(2-Amino-6-benzyloxycarbonylaminohexanoyl)hydrazino]-4,4,4-trifluoro-butyrylamino}-3-phenylpropionic acid methyl ester 81.

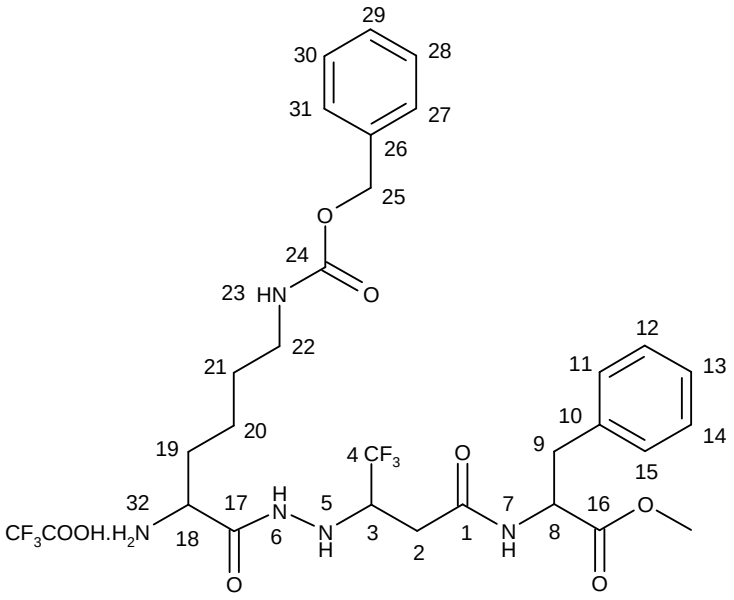

$C_{28}H_{36}F_3N_5O_6.CF_3COOH$

M = 709.28 g/mol

Compound **80** (800 mg, 1.15 mmol) was dissolved in dry CH_2Cl_2 (10 mL) and trifluoroacetic acid (5 mL, 69.00 mmol, 60.0 eq) was added dropwise at room temperature. The reaction mixture was stirred at room temperature for 2 h. Solvent was evaporated under reduced pressure to yield a brown

solid (815 mg). This crude product **81** was used without any further purification in the course of the synthesis.

^{1}H NMR (400 MHz, DMSO-*d*6) δ ppm 9.94 (d, *J* = 4.2 Hz, 1H, H_6), 8.64, 8.61 (2d, *J* = 8.4 and 8.8 Hz, 1H, H_7), 8.17 (m, 3H, H_{32}), 7.38-7.12 (m, 11 H, H_{11}, H_{12}, H_{13}, H_{14}, $H_{15,}$ $H_{23,}$ H_{27}, H_{28}, H_{29}, H_{30}, H_{31}), 5.70 (m, 1H, H_5), 5.00 (s, 2H, H_{25}), 4.50 (m, 1H, H_8), 3.80 (m, 1H, H_3), 3.63 (m, 1H, H_{18}), 3.58 (s, 3H, O$\underline{C}H_3$), 3.02 (m, 1H, H_{9a}), 2.96 (m, 2H, H_{22}), 2.89 (m, 1H, H_{9b}), 2.49 (m, 2H, H_2), 1.66 (m, 2H, H_{19}), 1.39 (m, 2H, H_{21}), 1.26 (m, 2H, H_{20}).

^{13}C NMR (100 MHz, DMSO-*d*6) δ ppm 171.8;171.7 (C_{16}, 2 dia), 168.2, 168.1 (C_1, C_{17}), 156.1 (C_{24}), 137.2;137.0 (C_{26},C_{10}), 129.0, 128.9, 128.3, 128.2, 127.7, 126.6 (C_{11}, $C_{12,}$ C_{13}, $C_{14,}$ C_{15}, $C_{27,}$ C_{28}, $C_{29,}$ $C_{30,}$ C_{31}), 65.1 (C_{25}), 57.5 (q, *J* = 22.4 Hz, C_3), 53.6 (C_8), 51.8 (O$\underline{C}$H3), 50.9 (C_{18}), 40.1 (C_{22}), 36.7 (C_9), 32.8 (C_2), 30.6 (C_{19}), 28.9 (C_{21}), 21.4 (C_{20}).

^{19}F (188 MHz, DMSO-*d*6) δ ppm -76.6 (d, *J* = 7.5 Hz), -76.7 (d, *J* = 5.6 Hz), -76.4 ($C\underline{F}_3$COOH).

Rf: 0.5 (EtOAc/MeOH/NH_4OH: 79/20/1)

mp: 92-94 °C (crude)

IR (cm^{-1}): 3297 (NH), 1666 (C=O), 1172 (C-O), 1130 (C-O), 697 (CF_3)

MS (ESI Negative) m/z: 596 $[M+H]^+$

Elemental Anal.

%	Calcul (+ 2 H_2O)	Found
C	45.12	47.83
H	5.42	5.01
N	9.40	8.93

2-[3-(*N*'-{6-Benzyloxycarbonylamino-2-[2-(3-phenoxy-phenyl)acetylamino]hexanoyl}-hydrazino)-4,4,4-trifluoro-butyrylamino]-3-phenyl-propionic acid methyl ester 82.

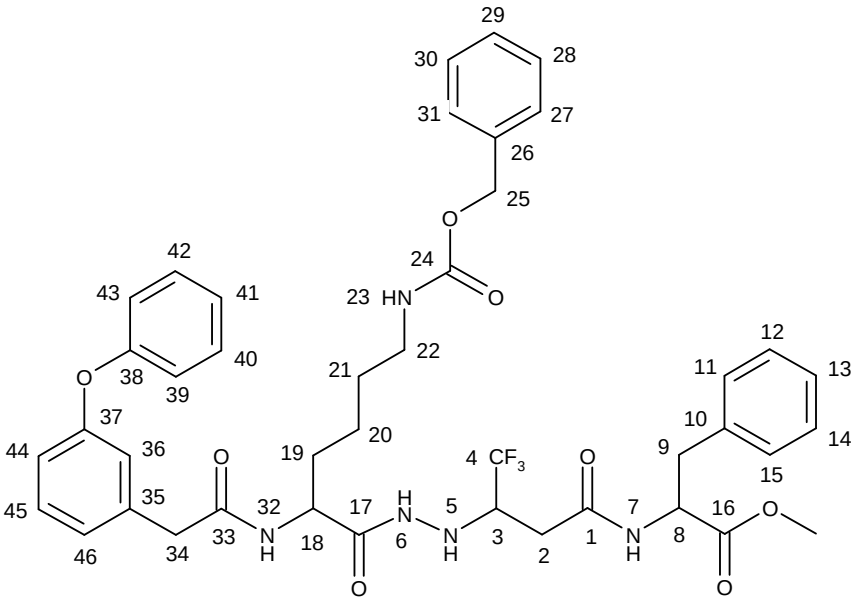

$C_{42}H_{46}F_3N_5O_8$

M = 805.33 g/mol

To a solution of **81** (400 mg, 0.56 mmol) and 3-phenoxyphenylacetic acid (141 mg, 0.62 mmol, 1.1 eq) in dry DMF (12 mL) was added, after stirring for 5 min at room temperature, DIPEA (370 µL, 2.24 mmol, 4.0 eq), HOBt (84 mg, 0.62 mmol, 1.1 eq) and HBTU (235 mg, 0.62 mmol, 1.1 eq). The mixture was stirred at room temperature under argon atmosphere for 24 h. After removal of the solvent under reduced pressure, the residue was dissolved in EtOAc (15 mL). The organic phase was successively washed with 10% aqueous citric acid (15 mL), water (15 mL), 10% aqueous K_2CO_3 (15 mL) and brine (15 mL). The organic layer was dried over Na_2SO_4, filtered and concentrated. A purification by chromatography on silica gel, eluting with EtOAc/cyclohexane (6/4), afforded 322 mg (71%) of **82** as a white powder.

^{1}H NMR (400 MHz, DMSO-*d*6) δ ppm 9.57 (br s, 1H, H_6), 8.61 (m, 1H, H_7), 8.23, 8.21 (2d, *J* = 7.8 Hz, 1H, H_{32}, 2dia), 7.40-7.11 (m, 15 H, H_{11}, H_{12}, H_{13}, H_{14}, H_{15}, H_{23}, H_{27}, H_{28}, H_{29}, H_{30}, H_{31}, H_{40}, H_{41}, H_{42}, H_{45}), 7.02-6.98 (m, 3H, H_{39}, H_{43}, H_{46}), 6.92 (s, 1H, H_{36}), 6.83 (d, *J* = 8.0 Hz, 1H, H_{44}), 5.43 (br s, 1H, H_5), 5.00 (s, 2H, H_{25}), 4.47 (m, 1H, H_8), 4.16 (m, 1H, H_{18}), 3.74 (m, 1H, H_3), 3.57 (s, 3H, O$\underline{C}H_3$), 3.40 (d, *J* = 15 Hz, 1H, H_{34a}), 3.48 (d, *J* = 15 Hz, 1H, H_{34b}), 3.01 (dd, *J* = 13.8 and 5.6 Hz, 1H, H_{9a}), 2.93-2.88 (m, 3H, H_{9b}, H_{22}), 2.46 (m, 2H, H_2), 1.53 (m, 2H, H_{19}), 1.36 (m, 2H, H_{21}), 1.20 (m, 2H, H_{20}).

^{13}C NMR (100 MHz, CD_3OD) δ ppm 173.6 (C_{16}, C_{17}), 171.2;171.1 (C_1), 158.9 (C_{24}), 158.6 (C_{33}), 138.8 (C_{35}), 138.4 (C_{26}), 138.0 (C_{10}), 130.9, 130.8, 130.2, 129.5, 128.9, 128.8, 127.9, 125.1, 124.4, 120.5, 119.9, 118.2 (C_{11}, C_{12}, C_{13}, C_{14}, C_{15}, C_{27}, C_{28}, C_{29}, C_{30}, C_{31}, C_{36}, C_{39}, C_{40}, C_{41}, C_{42}, C_{43}, C_{44}, C_{45}, C_{46}), 67.3 (C_{25}), 59.5 (q, *J* = 27.6 Hz, C_3), 55.5;55.4 (C_8, 2 dia), 53.3;53.2 (O<u>C</u>H3, 2 dia), 52.8;52.7 (C_{18}, 2 dia), 43.3 (C_{34}), 41.4 (C_{22}), 38.4;38.3 (C_9, 2 dia), 34.1 (C_2), 32.7;32.6 (C_{19}, 2 dia), 30.4 (C_{21}), 23.9 (C_{20}).

^{19}F (188 MHz, DMSO-*d*6) δ ppm -76.4 (d, *J* = 7.3 Hz).

Rf: 0.4 (EtOAc/cyclohexane: 70/30)

mp: 130-132 °C (crude)

IR (cm^{-1}): 3386 (NH), 1739 (C=O), 1687 (C=O), 1634 (C=O), 1166 (C-O), 1122 (C-O), 697 (CF_3)

MS (ESI Positive) m/z: 806 $[M+H]^+$

Elemental Anal.

%	Calcul (+ 0.75 H_2O)	Found
C	61.60	61.65
H	5.86	5.67
N	8.55	8.45

2-[3-(*N*'-{6-Amino-2-[2-(3-phenoxyphenyl)acetylamino]hexanoyl}hydrazino)-4,4,4-trifluoro-butyrylamino]-3-phenyl-propionic acid methyl ester, trifluoro-acetic acid salt 56.

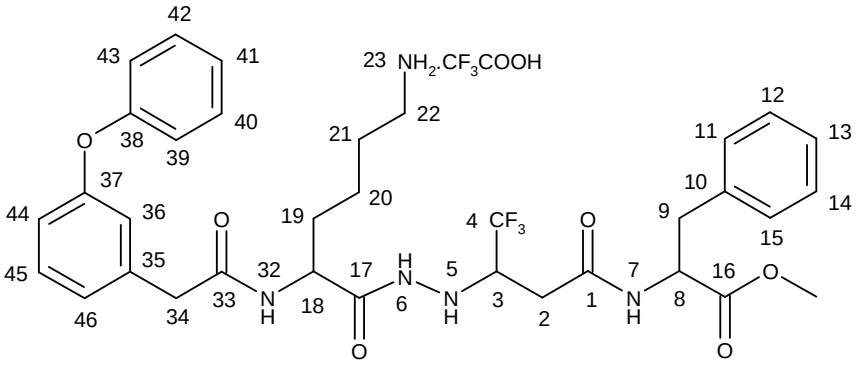

$C_{34}H_{40}F_3N_5O_6.CF_3COOH$

M = 785.31

To a solution of **82** (264 mg, 0.33 mmol) in MeOH (20 mL) at room temperature was added Pd/C 20% (53 mg). The mixture was hydrogenated at athmospheric pressure overnight and filtered through a pad of Celite. Before the total evaporation under reduced pressure, trifluoro acetic acid (245 µL, 3.3, 10 eq) was added to give **56** as a beige hygroscopic solid (259 mg) without any further purification.

^{1}H NMR (400 MHz, DMSO-*d*6) δ ppm 9.60 (br s, 1H, H_6), 8.62, 8.60 (2d, *J* = 5.8 and 6.9 Hz, 1H, $H_{7,}$ 2dia), 8.25, 8.23 (2d, *J* = 8.2 and 8.3 Hz, 1H, H_{32}, 2dia), 7.73 (br s, 3H, H_{23}), 7.41-6.83 (m, 14 H, H_{11}, H_{12}, H_{13}, H_{14}, $H_{15,}$ $H_{36,}$ $H_{39,}$ H_{40}, H_{41}, H_{42}, H_{43}, $H_{44,}$ H_{45}, H_{46}), 5.43 (br s, 1H, H_5), 4.47 (m, 1H, H_8), 4.18 (br s, 1H, H_{18}), 3.75 (br s, 1H, H_3), 3.58 (1s, 3H, O$\underline{C}H_3$), 3.46 (m, 2H, H_{34}), 3.01 (m, 1H, H_{9a}), 2.92 (m, 1H, H_{9b}), 2.70 (br s, 2H, H_{22}), 2.43 (m, 2H, H_2), 1.58-1.48 (m, 4H, H_{19}, H_{21}), 1.24 (m, 2H, H_{20}).

^{13}C NMR (100 MHz, DMSO-*d*6) δ ppm 171.8;171.7 (C_{16}, 2dia), 171.0 (C_{17}), 169.7 (C_{33}), 168.2;168.1 (C_1, 2dia), 157.9 (q, *J* = 31.0 Hz, $CF_3\underline{C}OOH$) 156.6,156.5 (C_{37}, C_{38}), 138.5 (C_{35}), 137.0;136.9 (C_{10}, 2dia), 130.0, 129.6, 129.0, 128.6, 128.2, 126.6, 124.2, 123.4, 119.2, 118.6, 116.5 (C_{11}, $C_{12,}$ C_{13}, $C_{14,}$ C_{15}, C_{36}, $C_{39,}$ $C_{40,}$ C_{41}, C_{42}, C_{43}, C_{44}, C_{45},C_{46}), 117.3 (q, *J* = 299.0 Hz, $\underline{C}F_3COOH$), 57.5 (q, *J* = 23.5 Hz, C_3), 53.7;53.6 ($C_{8,}$ 2 dia), 51.8 (O$\underline{C}$H3), 50.8;50.7 ($C_{18,}$ 2 dia), 41.8 (C_{34}), 38.6 (C_{22}), 36.7 (C_9), 33.0 (C_2), 31.5 (C_{19}), 26.5 (C_{21}), 22.1(C_{20}).

^{19}F (188 MHz, CD_3OD) δ ppm (-78.0) – (-78.1) (m), -78.8 ($C\underline{F}_3COOH$).

mp: 90-92 °C (crude)

IR (cm^{-1}): 3266 (NH), 1730 (C=O), 1655 (C=O), 1177 (C-O), 1128 (C-O), 695 (CF_3)

MS (ESI Positive) m/z: 672 $[M+H]^+$

Elemental Anal.

%	Calcul (+ 3 H_2O)	Found
C	51.51	51.37
H	5.66	5.11
N	8.35	7.91

2-{3-[*N'*-(6-Amino-2-*tert*-butoxycarbonylaminohexanoyl)hydrazino]-4,4,4-trifluorobutyrylamino}-3-phenylpropionic acid methyl ester, citric acid salt 83.

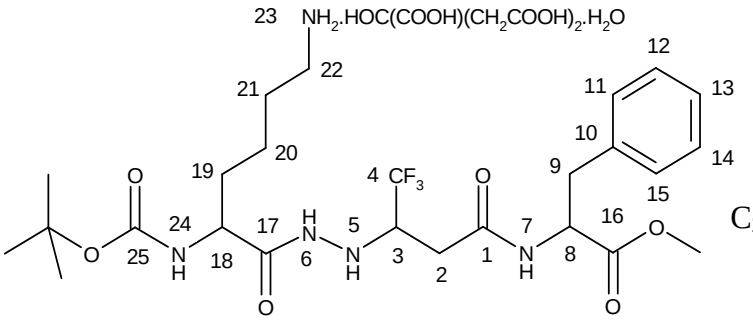

$C_{25}H_{38}F_3N_5O_6.HOC(COOH)(CH_2COOH)_2.H_2O$

M = 771,43 g/mol

To a solution of **80** (100 mg, 0.14 mmol) in MeOH (10 mL) at room temperature was added Pd/C 20% (20 mg). The mixture was hydrogenated at atmospheric pressure overnight and filtered through a pad of Celite. Before the total evaporation under reduced pressure, citric acid monohydrate (10 mg, 0.05 mmol, 0.35 eq) was added. After washing with several organic solvents we obtained 55 mg of **83** (51%) as a white powder.

^{1}H NMR (300 MHz, CD_3OD) δ ppm 7.30-7.20 (m, 5 H, $H_{11,}$ H_{12}, H_{13}, H_{14}, H_{15}), 4.70 (m, 1H, H_8), 4.0 (m, 1H, H_{18}), 3.78 (m, 1H, H_3), 3.69,3.68 (2s, 3H, O$\underline{C}H_3$, 2dia), 3.20-2.70 (m, 8H, H_9, H_{22}, 2 $C\underline{H}_2$ citric acid), 2.53 (m, 2H, H_2), 1.78-1.52 (m, 4H, H_{19}, H_{21}), 1.48-1.41 (m, 11H, $C\underline{H}_3$Boc, H_{20}).

^{13}C NMR (75 MHz, CD_3OD) δ ppm 176.8, 175.0 (C=O citric acid), 173.5, 171.2 (C_{16}, C_{17}), 157.0 (C_{25}), 138.1 (C_{10}), 130.3, 129,5 ($C_{12,}$ $C_{14,}$ $C_{11,}$ C_{15}), 127.9 (C_{13}), 80.7 ($\underline{C}$Boc), 60.0 ($\underline{C}$–OH citric acid), 55.6;55.5 ($C_{8,}$ 2 dia), 54.6 (O$\underline{C}$H3), 52.8;52.7 ($C_{18,}$ 2 dia), 41.0 (C_{22}), 38.4 (C_9), 34.1 (C_2), 32.8 (C_{19}), 29.8 (C_{21}), 28.7 ($\underline{C}H_3$Boc), 23.9 (C_{20}).

^{19}F (188 MHz, CD_3OD) δ ppm -78.0 (d, *J* = 5.8 Hz), -78.1 (d, *J* = 6.3 Hz).

mp: 260-262 °C (crude)

MS (ESI Positive) m/z: 562 $[M+H]^+$

Elemental Anal.	%	Calcul (+7 H_2O and +3 citric acid)	Found
	C	39.17	38.81
	H	6.22	4.78
	N	5.32	5.81

SYNTHESIS OF FLUORINATED MOLECULE 57

_N_'-(2,2,2-Trifluoro-1-hydrazinocarbonylmethylethyl)hydrazinecarboxylic acid _tert_-butyl ester 85.

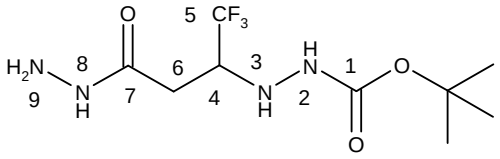

To a solution of **72** (2.0 g, 6.7 mmol) in ethanol (50 mL) was added hydrazine monohydrate (3.34 g, 66.7 mmol, 10.0 eq) and the mixture was stirred at room temperature overnight. After removal of the solvent under reduced pressure, the product **85** was obtained as 2.11 g of a white solid (quantitative yield).

^{1}H NMR (300 MHz, $CDCl_3$) δ ppm 3.60 (m, 1H, H_4), 2.32 (m, 2H, H_6), 1.32 (s, 9H, C$\underline{H}_3$Boc).
^{13}C NMR (75 MHz, $CDCl_3$) δ ppm 173.6 (C_7), 129.4 (q, J = 286.3 Hz, C_5), 85.0 ($\underline{C}$Boc), 62.5 (q, J = 27.7 Hz, C_4), 35.4 (C_6), 32.0 ($\underline{C}H_3$Boc).
^{19}F (188 MHz, CD_3OD) δ ppm -75.1 (d, J = 7.1 Hz).

_N_'-(1-{_N_'-[3-(3,4-Dimethoxyphenyl)-2-(9H-fluoren-9-ylmethoxycarbonylamino)propionyl] hydrazinocarbonylmethyl}-2,2,2-trifluoroethyl)hydrazinecarboxylic acid _tert_-butyl ester 86.

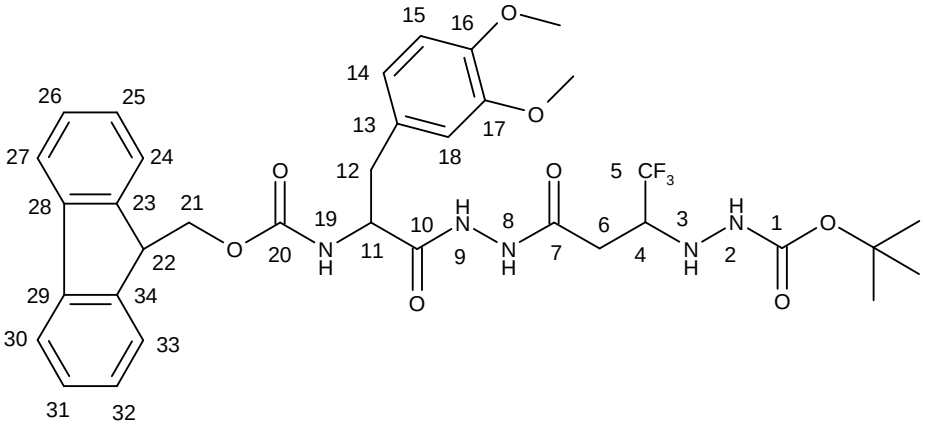

$C_{35}H_{40}F_3N_5O_8$
M = 715.28 g/mol

To a solution of the **85** (100 mg, 0.35 mmol) and Fmoc-_L_-3,4-dimethoxyphenylalanine (157 mg, 0.35 mmol, 1.0 eq) in dry DMF (3 mL) was added, after stirring for 5 min at room temperature,

2,4,6-collidine (140 µL, 1.05 mmol, 3.0 eq), HOBt (53 mg, 0.39 mmol, 1.1 eq) and HBTU (148 mg, 0.39 mmol, 1.1 eq). The mixture was stirred at room temperature under argon atmosphere for 21 h. After removal of the solvent under reduced pressure, the residue was triturated with EtOAc to obtain 171 mg (68%) of **86** as a white solid.

^{1}H NMR (400 MHz, DMSO-*d*6) δ ppm 10.18 (br s, 2H, H_8, H_9), 8.41 (br s, 1H, H_2), 7.81-7.86 (m, 2H, H_{ar}), 7.60 (d, *J* = 7.2 Hz, 2H, H_{ar}), 7.23-7.40 (m, 5H, H_{ar}, H_{19}), 6.98 (d, *J* = 2.8 Hz, 1H, H_{15}), 6.80 (br s, 2H, H_{14}, H_{18}), 5.13 (br s, 1H, H_3), 4.28 (m,1H, H_{11}), 4.10-4.14 (m, 3H, H_{22}, H_{21}), 3.84 (br s, 1H, H_4), 3.70 (s, 3H, OC$\underline{H}_3$), 3.66 (s, 3H, OC$\underline{H}_3$), 2.94 (m, 1H, H_{12a}), 2.72 (m, 1H, H_{12b}), 2.50 (m, 2H, H_6), 1.37 (s, 9H, C$\underline{H}_3$Boc).

^{13}C NMR (100 MHz, DMSO-*d*6) δ ppm 170.8;170.7 ($C_{7,}$ 2 dia), 167.4 (C_{10}), 155.7 (C_{20}), 148.9 (C_{17}), 147.9 (C_{16}), 144.1-144.3 (C_{23}, C_{34}), 141.1 (C_{28}, C_{29}), 130.8 (C_{13}), 128.0, 127.5, 125.7 (C_{24}, C_{25}, C_{26}, C_{31}, C_{32}, C_{33}), 121.8 (C_{14}), 120.5 (C_{27}, C_{30}), 113.9 (C_{18}), 112.3 (C_{15}), 79.3 ($\underline{C}$Boc), 66.2 (C_{21}), 55.9-56.0 (2 O$\underline{C}$H3), 55.3 (C_{11}), 47.0 (C_{22}), 31.9 (C_6), 28.6 ($\underline{C}H_3$Boc).

^{19}F (188 MHz, DMSO-*d*6) δ ppm -73.7.

Rf: 0.4 (EtOAc/cyclohexane: 70/30)

mp: 208-210 °C (crude)

IR (cm^{-1}): 3284 (NH), 1696 (C=O), 1159 (C-O), 1124 (C-O), 738 (CF_3)

MS (ESI Positive) m/z: 738 $[M+Na]^+$

Elemental Anal.	%	Calcul	Found
	C	58.73	58.35
	H	5.63	5.55
	N	9.79	9.76

***N*'-(1-{*N*'-[2-Amino-3-(3,4-dimethoxyphenyl)propionyl]hydrazinocarbonylmethyl}-2,2,2-trifluoroethyl)-hydrazinecarboxylic acid *tert*-butyl ester 87.**

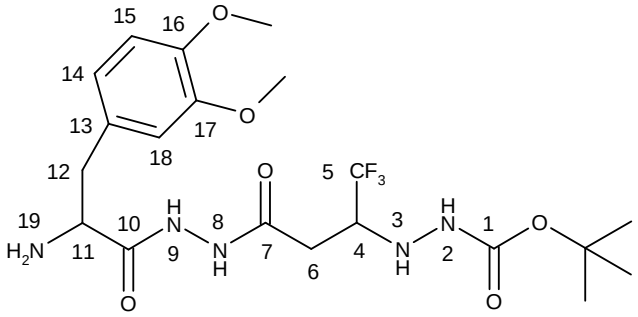

$C_{20}H_{30}F_3N_5O_6$

M = 493.21 g/mol

To compound **86** (382 mg, 0.53 mmol) was added a solution of piperidine in DMF (10% v/v, 5 mL). The mixture was stirred at room temperature for 1.30 h. The organic phase was evaporated. The residue was triturated in Et_2O to yield 231 mg (88%) of **87** as a white solid.

^{1}H NMR (300 MHz, DMSO-*d*6) δ ppm 8.42 (br s, 1H, H_2), 6.83 (br s, 1H, H_{15}), 6.81 (br s, 1H, H_{18}), 6.72 (m, 1H, H_{14}), 5.14 (bs, 1H, H_3), 3.84 (m, 1H, H_{11}), 3.72 (s, 3H, OC$\underline{H}_3$), 3.70 (s, 3H, OC$\underline{H}_3$), 3.44 (m, 1H, H_4), 2.89 (m, 1H, H_{12a}), 2.84 (m, 1H, H_{12b}), 2.54 (dd, *J* = 16.8 and 8.2 Hz, 1H, H_{6a}), 2.49 (m, 1H, H_{6b}), 1.38 (s, 9H, C$\underline{H}_3$Boc).

^{13}C NMR (75 MHz, DMSO-*d*6) δ ppm 172.7 (C_7), 166.7 (C_1), 148.4 (C_{17}), 147.2 (C_{16}), 130.7 (C_{14}), 121.3 (C_{14}), 113.1 (C_{15}), 111.6 (C_{18}), 78.8 ($\underline{C}$Boc), 55.4 (O$\underline{C}$H3), 55.3 (O$\underline{C}$H3), 54.9 (C_{11}), 40.8 (C_{12}), 31.4 (C_6), 28.1 ($\underline{C}H_3$Boc).

^{19}F (188 MHz, DMSO-*d*6) δ ppm (-73.6) – (- 73.8) (m).

Rf: 0.1 (CH_2Cl_2/MeOH: 90/10)

mp: 146-148 °C (crude)

IR (cm^{-1}): 3270 (NH), 3261 (NH), 1726 (C=O), 1678 (C=O), 1159 (C-O), 1130 (C-O), 688 (CF_3)

MS (ESI Positive) m/z: 516 $[M+Na]^+$

Elemental Anal.	%	Calcul(+ 0.5 H_2O)	Found
	C	47.83	47.86
	H	6.23	6.42
	N	13.95	13.50

***N*-[1-(*N*-{3-(3,4-Dimethoxyphenyl)-2-[2-(3-phenoxyphenyl)acetylamino]propionyl}-hydrazinocarbonylmethyl)-2,2,2-trifluoroethyl]hydrazinecarboxylic acid *tert*-butyl ester 57.**

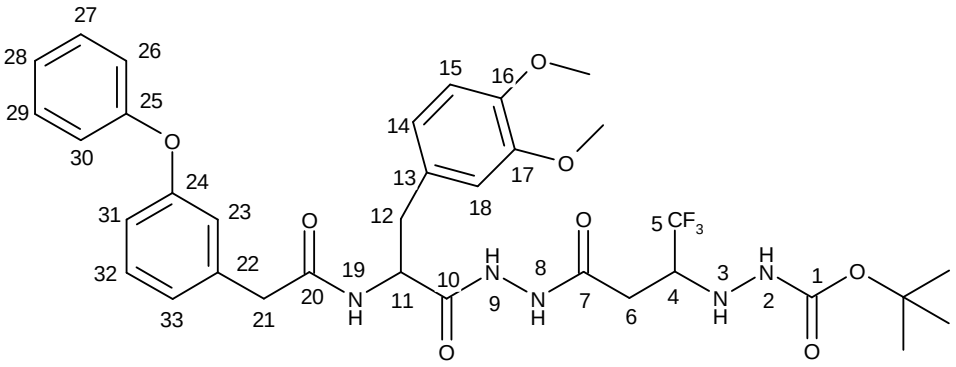

$C_{34}H_{40}F_3N_5O_8$

M = 703.28 g/mol

To a solution of **87** (76 mg, 0.15 mmol) and 3-phenoxyphenylacetic acid (38 mg, 0.17 mmol, 1.1 eq) in dry DMF (4 mL) was added, after stirring for 5 min at room temperature, 2,4,6-collidine (60 µL, 0.45 mmol, 3.0 eq), HOBt (23 mg, 0.17 mmol, 1.1 eq) and HBTU (64 mg, 0.17 mmol, 1.1 eq). The mixture was stirred at room temperature under argon atmosphere for 24 h. After removal of the solvent under reduced pressure, the residue was triturated in EtOAc (15 mL) to obtain 88 mg (84%) of **57** as a white solid.

^{1}H NMR (400 MHz, DMSO-*d*6) δ ppm 10.20, 10.10 (2s, 2H, H_8, H_9), 8.41 (s, 1H, H_2), 8.30 (m, 1H, H_{19}), 7.35 (t, *J* = 7.8 Hz, 2H, H_{27},H_{29}), 7.20 (t, *J* = 8.3 Hz, 1H, H_{32}), 7.12 (t, *J* = 7.8 Hz, 1H, H_{28}), 7.00 (d, *J* = 7.8 Hz, 2H, H_{26}, H_{30}), 6.87-6.69 (m, 6H, H_{18}, H_{14}, H_{15} H_{23}, H_{31}, H_{33}), 5.13 (s, 1H, H_3), 4.55 (m, 1H, H_{11}), 3.85 (br s, 1H, H_4), 3.67 (s, 6H, 2 OC$\underline{H}_3$), 3.40 (m, 2H, H_{21}), 2.93 (m, 1H, H_{12a}), 2.70 (m, 1H, H_{12b}), 2.49 (m, 2H, H_6), 1.38 (s, 9H, C$\underline{H}_3$Boc).

^{13}C NMR (100 MHz, DMSO-*d*6) δ ppm 170.0 (C_{20}), 170.1, 167.4 (C_7, C_{10}), 157.1 (C_{25}), 156.8 (C_{24}), 148.9, 147.9 (C_{16}, C_{17}), 138.8 (C_{22}), 130.4 (C_{27}, C_{29}), 129.9 (C_{32}), 123.8 (C_{28}), 119.0 (C_{26}, C_{30}), 124.5, 121.7, 119.8, 116.8, 113.7, 112.1 (C_{18}, C_{14}, C_{15}, C_{23}, C_{31}, C_{33}), 79.3 (C$\underline{\text{C}}$Boc), 55.9 (O$\underline{\text{C}}$H3), 55.8 (O$\underline{\text{C}}$H3), 52.9 (C_{11}), 42.2 (C_{21}), 38.0 (C_{12}), 31.9 (C_6), 28.6 ($\underline{\text{C}}H_3$Boc).

^{19}F (188 MHz, DMSO-*d*6) δ ppm (-73.6) – (- 73.8) (m).

Rf: 0.4 (EtOAc/cyclohexane: 70/30)

mp: 184-186 °C (crude)

IR (cm^{-1}): 3216 (NH), 1699 (C=O), 1653 (C=O), 1159 (C-O), 1121 (C-O), 691 (CF_3)

MS (ESI Positive) m/z: 726 $[M+Na]^+$

Elemental Anal.	%	Calcul	Found
	C	58.03	57.01
	H	5.73	5.68
	N	9.95	9.86

SYNTHESIS OF FLUORINATED MOLECULE 58

4,4,4-Trifluoro-3-hydrazinobutyric acid ethyl ester, trifluoroacetic acid salt 90.

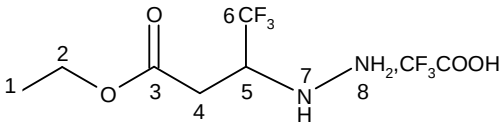

$C_6H_{11}F_3N_2O_2.CF_3COOH$

M = 314.18 g/mol

Compound **72** (200 mg, 0.66 mmol) was dissolved in dry CH_2Cl_2 (2,5 mL) and trifluoroacetic acid (2.5 mL, 33.0 mmol, 50.0 eq) was added dropwise at room temperature. The reaction mixture was stirred at room temperature for 2 h. Solvent was evaporated under reduced pressure to yield light brown solid oil (228 mg, with excess of TFA). Azeotropic removal of excess TFA with toluene. This crude product **90** was used without any further purification in the course of the synthesis.

^{1}H NMR (300 MHz, $CDCl_3$) δ ppm 6.76 (br s, 3 H, H_8), 4.30-4.19 (m, 3H, H_5, H_2), 2.70 (m, 2H, H_4), 1.27 (t, *J* = 6.6 Hz, 3H, H_1).

^{13}C NMR (75 MHz, $CDCl_3$) δ ppm 171.2 (C_3), 159.4 (q, *J* =42.0 Hz, $CF_3\underline{C}OOH$), 114.8 (q, *J* = 284.0 Hz, $\underline{C}F_3COOH$), 62.4 (C_2), 32.7 (C_4), 13.7 (C_1).

^{19}F (188 MHz, $CDCl_3$) δ ppm -75.3 (d, *J* = 6.5 Hz), -75.5 (d, *J* = 6.5 Hz), -76.3 ($C\underline{F}_3COOH$).

Rf: 0.4 (EtOAc/MeOH/NH_4OH: 79/20/1)

3-(*N*'-Benzyloxycarbonylhydrazino)-4,4,4-trifluorobutyric acid ethyl ester 91.

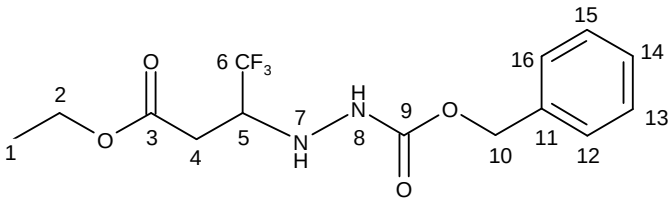

$C_{14}H_{17}F_3N_2O_4$

M = 334.11 g/mol

Compound **90** (207 mg, 0.66 mmol) was dissolved in CH_2Cl_2 (6 mL) and Benzylchloroformiate (104 µL, 0.73 mmol, 1.1 eq) was added dropwise at 0 °C. After was added DIPEA (287 µL, 1.65 mmol, 2.5 eq) and the reaction mixture was stirred at room temperature for 21 h. After removal of the solvent under reduced pressure, the residue was dissolved in EtOAc (9 mL). The organic phase was successively washed with 10% aqueous citric acid (9 mL), water (9 mL), 10% aqueous K_2CO_3 (9 mL) and brine (9 mL). The organic layer was dried over Na_2SO_4, filtered and concentrated. A purification by chromatography on silica gel, eluting with EtOAc/cyclohexane (5/5), afforded 168 mg (76%) of **91** as a colorless oil.

^{1}H NMR (200 MHz, $CDCl_3$) δ ppm 7.42-7.28 (m, 5 H, H_{ar}), 6.29 (br s, 1 H, H_8), 5.11 (s, 2H, H_{10}), 4.20 (q, *J* = 7.2 Hz, 2H, H_2), 3.89 (m, 1H, H_5), 2.58 (m, 2H, H_4), 1.22 (t, *J* = 7.1 Hz, 3H, H_1).

^{13}C NMR (75 MHz, $CDCl_3$) δ ppm 169.7 (C_3), 157.2 (C_9), 135.7 (C_{11}), 128.6 (C_{13}, C_{15}), 128.4 (C_{14}), 128.2 (C_{12}, C_{16}), 125.2 (q, *J* = 279.8 Hz, C_6), 67.5 (C_{10}), 61.5 (C_2), 58.2 (q, *J* = 27.8 Hz, C_5), 32.1 (C_4), 14.0 (C_1).

^{19}F (188 MHz, $CDCl_3$) δ ppm -75.5 (d, *J* = 7.2 Hz).

Rf: 0.6 (EtOAc/cyclohexane: 40/60)

IR (cm^{-1}): 3336 (NH), 1722 (C=O), 1159 (C-O), 1128 (C-O), 699 (CF_3)

MS (ESI Positive) m/z: 357 $[M+Na]^+$

Elemental Anal.	%	Calcul (+ 0.5 H_2O)	Found
	C	49.00	49.05
	H	5.30	4.91
	N	8.17	8.49

***N'*-(2,2,2-Trifluoro-1-hydrazinocarbonylmethylethyl)hydrazinecarboxylic acid benzyl ester 92.**

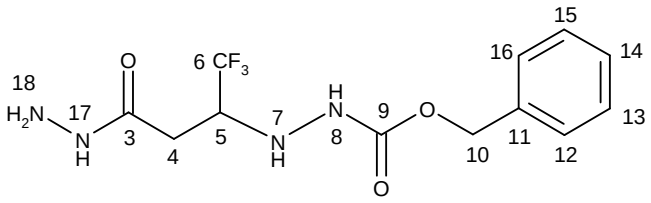

$C_{12}H_{15}F_3N_4O_3$

M = 320.11 g/mol

To a solution of **91** (148 mg, 0.44 mmol) in EtOH (3 mL) was added hydrazine monohydrate (214 µL, 4.4 mmol, 10.0 eq) and the reaction mixture was stirred at room temperature for 23 h. After removal of the solvent under reduced pressure, the final product **92** was obtained as a white solid (140 mg, quantitative yield).

^{1}H NMR (200 MHz, CD_3OD) δ ppm 7.33-7.23 (m, 5 H, H_{12}, H_{13}, H_{14}, $H_{15,}$ H_{16}), 5.09 (s, 2H, H_{10}), 3.80 (m, 1H, H_5), 2.48 (dd, *J* = 4.8 and 15.0 Hz, 1H, H_{4a}), 2.39 (m, 1H, H_{4b}).

^{13}C NMR (75 MHz, CD_3OD) δ ppm 170.9 (C_3), 159.6 (C_9), 138.0 (C_{11}), 129.5 (C_{13}, C_{15}), 129.1 (C_{12}, C_{16}), 129.0 (C_{14}), 123.3 (q, *J* = 279.8 Hz, C_6), 67.9 (C_{10}), 59.5 (q, *J* = 27.8 Hz, C_5), 32.6 (C_4).

^{19}F (188 MHz, CD_3OD) δ ppm -76.9 (d, *J* = 7.3 Hz).

Rf: 0.2 (EtOAc/cyclohexane: 70/30)

mp: 146-148 °C (crude)

IR (cm^{-1}): 3307 (NH), 1705 (C=O), 1654 (C=O), 1174 (C-O), 1120 (C-O), 696 (CF_3)

MS (ESI Positive) m/z: 343 $[M+Na]^+$

Elemental Anal.	%	Calcul (+ 0.4 H_2O)	Found
	C	44.03	43.93
	H	4.88	4.54
	N	17.12	17.57

***N'*-(3-{*N'*-[3-(3,4-Dimethoxyphenyl)-2-(9*H*-fluoren-9-ylmethoxycarbonylamino)propionyl]hydrazino}-3-oxo-1-trifluoromethylpropyl)hydrazinecarboxylic acid benzyl ester 93.**

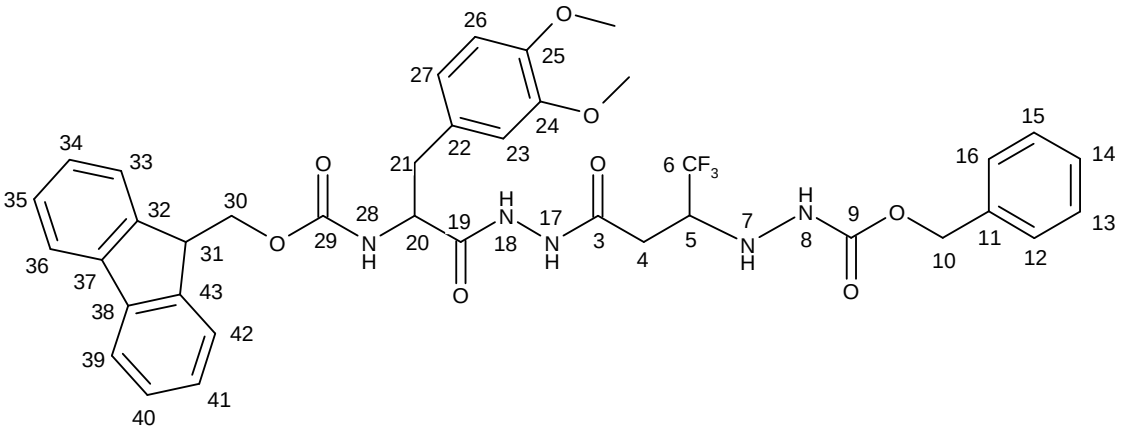

$C_{38}H_{38}F_3N_5O_8$

M = 749.27 g/mol

To a solution of the **92** (359 mg, 1.12 mmol) and Fmoc-*L*-3,4-dimethoxyphenylalanine (501 mg, 1.12 mmol, 1.0 eq) in dry DMF (13 mL) was added, after stirring for 5 min at room temperature, 2,4,6-collidine (447 µL, 3.36 mmol, 3.0 eq), HOBt (166 mg, 1.23 mmol, 1.1 eq) and HBTU (467 mg, 1.23 mmol, 1.1 eq). The mixture was stirred at room temperature under argon atmosphere for 40 h. After removal of the solvent under reduced pressure, the residue was triturated in EtOAc (15 mL) to obtain 560 mg (67%) of **93** as a white solid.

^{1}H NMR (400 MHz, DMSO-*d*6) δ ppm 10.23 (br s, 1H, H_{18}), 10.15 (br s, 1H, H_{17}), 8.90 (br s, 1H, H_8), 7.90 (d, *J* = 7.4 Hz, 2H, $H_{36,}$ H_{39}), 7.70 (d, *J* = 7.6 Hz, 1H, H_{28}), 7.43-7.26 (m, 11 H, $H_{12,}$ H_{13}, H_{14}, H_{15}, $H_{16,}$ $H_{33,}$ H_{34}, H_{35}, H_{40}, $H_{41,}$ H_{42}), 7.01 (br s, 1H, H_{26}), 6.89-6.80 (m, 2 H, H_{23}, H_{27}), 5.36 (br s, 1H, H_7), 5.08 (s, 2H, H_{10}), 4.32 (m, 1H, H_{20}), 4.19-4.10 (m, 3H, $H_{30,}$ H_{31}), 3.93 (m, 1H, H_5), 3.72 (s, 3H, OC$\underline{H}_3$), 3.68 (s, 3H, OC$\underline{H}_3$), 2.99 (m, 1H, H_{21a}), 2.76 (m, 1H, H_{21b}), 2.52 (m, 2H, H_4).

^{13}C NMR (100 MHz, DMSO-*d*6) δ ppm 170.6;170.4 ($C_{19,}$ 2 dia), 166.9 (C_3), 157.0 (C_9), 155.8 (C_{29}), 148.4, 147.4 ($C_{24,}$ C_{25}), 143.8;143.7 (C_{32}, $C_{43,}$ 2 dia), 140.6 ($C_{37,}$ C_{38}), 136.8 (C_{11}), 130.3 (C_{22}), 128.4, 127.9, 127.7, 127.6, 127.0, 125.3 ($C_{12,}$ C_{13}, $C_{14,}$ C_{15}, $C_{16,}$ C_{33}, $C_{34,}$ $C_{35,}$ $C_{40,}$ $C_{41,}$ C_{42}), 120.1 (C_{36}, C_{39}), 113.2 (C_{26}), 121.2, 111.6 (C_{23}, C_{27}), 65.7;65.6 ($C_{30,}$ 2 dia), 59.7 (C_{10}), 55.4 (O$\underline{C}$H3), 55.3 (O$\underline{C}$H3), 54.9 (C_{20}), 46.5 (C_{31}), 37.3 (C_{21}), 31.5 (C_4).

^{19}F (188 MHz, DMSO-*d*6) δ ppm (-73.6)–(-73.8) (m).

Rf: 0.3 (CH_2Cl_2/MeOH: 90/10)

mp: 202-204 °C (crude)

IR (cm^{-1}): 3284 (NH), 1696 (C=O), 1605 (C=O), 1171 (C-O), 1124 (C-O), 692 (CF_3)

MS (ESI Positive) m/z: 772 $[M+Na]^+$

Elemental Anal.	%	Calcul (+ 0.4 H_2O)	Found
	C	60.33	60.57
	H	5.18	4.97
	N	9.26	9.01

***N'*-(3-{*N'*-[2-Amino-3-(3,4-dimethoxyphenyl)propionyl]hydrazino}-3-oxo-1-trifluoromethyl-propyl)hydrazinecarboxylic acid benzyl ester 94.**

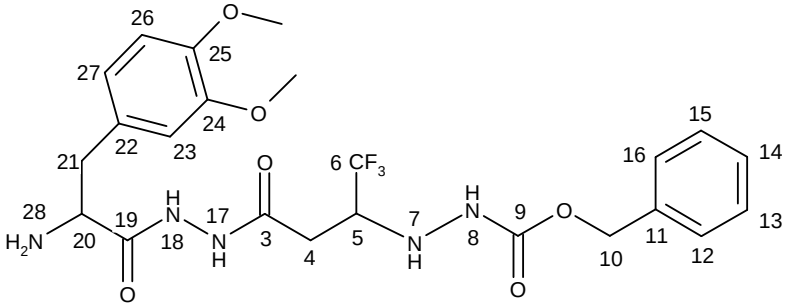

$C_{23}H_{28}F_3N_5O_6$

M = 527.20 g/mol

To compound **93** (70 mg, 0.10 mmol) was added a solution of piperidine in DMF (10% v/v, 2 mL). The mixture was stirred at room temperature for 1.30 h. The organic phase was evaporated. The residue was triturated in Et_2O to yield 37 mg (78%) of **94** as a white powder.

^{1}H NMR (300 MHz, DMSO-*d*6) δ ppm 8.87 (br s, 1H, H_8), 7.40-7.31 (m, 5 H, $H_{12,}$ H_{13}, H_{14}, H_{15}, H_{16}), 6.85-6.70 (m, 3 H, H_{23}, $H_{26,}$ H_{27}), 5.36 (br s, 1H, H_7), 5.06 (s, 2H, H_{10}), 3.90 (m, 1H, H_{20}), 3.73 (s, 3H, OC$\underline{H}_3$), 3.71 (s, 3H, OC$\underline{H}_3$), 3.45 (m, 1H, H_5), 2.90 (m, 1H, H_{21a}), 2.85 (m, 1H, H_{21b}), 2.50 (m, 2H, H_4).

^{13}C NMR (75 MHz, DMSO-*d*6) δ ppm 172.8 (C_{19}), 166.6 (C_3), 156.9 (C_9), 148.4, 147.2 ($C_{24,}$ C_{25}), 136.7 (C_{11}), 130.7 (C_{22}), 128.3, 127.8, 127.7 ($C_{12,}$ C_{13}, $C_{14,}$ C_{15}, C_{16}), 113.1 (C_{26}), 121.3, 111.6 (C_{23}, C_{27}), 65.6 (C_{10}), 55.0 (O$\underline{C}$H3), 54.9 (O$\underline{C}$H3), 54.3 (C_{20}), 40.8 (C_{21}), 31.4 (C_4).

^{19}F (188 MHz, DMSO-*d*6) δ ppm -73.7 (d, *J* = 7.3 Hz).

Rf: 0.8 (EtOAc/MeOH/NH_4OH: 79/20/1)

mp: 102-104 °C (crude)

IR (cm^{-1}): 3229 (NH), 1709 (C=O), 1602 (C=O), 1158 (C-O), 1118 (C-O), 696 (CF_3)

MS (ESI Positive) m/z: 550 $[M+Na]^+$

***N'*-[3-(*N'*-{3-(3,4-Dimethoxyphenyl)-2-[2-(3-phenoxyphenyl)acetylamino]propionyl}hydrazino)-3-oxo-1-trifluoromethyl-propyl]hydrazinecarboxylic acid benzyl ester 58.**

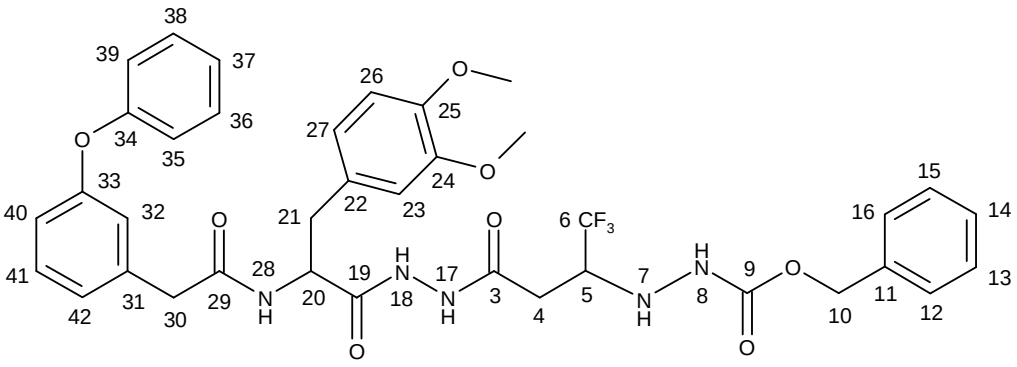

$C_{37}H_{38}F_3N_5O_8$

M = 737.27 g/mol

To a solution of **94** (178 mg, 0.34 mmol) and 3-phenoxyphenylacetic acid (84 mg, 0.37 mmol, 1.1 eq) in dry DMF (11 mL) was added, after stirring for 5 min at room temperature, DIPEA (112 µL, 0.68 mmol, 2.0 eq), HOBt (50 mg, 0.37 mmol, 1.1 eq) and HBTU (140 mg, 0.37 mmol, 1.1 eq). The mixture was stirred at room temperature under argon atmosphere for 38 h. After removal of the solvent under reduced pressure, the residue was triturated in EtOAc (20 mL) to obtain 213 mg (85%) of **58** as a white solid.

^{1}H NMR (400 MHz, DMSO-*d*6) δ ppm 10.22 (br s, 1H, H_{18}), 10.11 (br s, 1H, H_{17}), 8.85 (br s, 1H, H_8), 8.33 (m, 1H, H_{28}), 7.40-7.32 (m, 7H, $H_{12,}$ H_{13}, H_{14}, H_{15}, $H_{16,}$ $H_{36,}$ H_{38}), 7.22 (t, *J* = 8.1 Hz, 1H, H_{41}), 7.14 (t, *J* = 7.1 Hz, 1H, H_{37}), 6.98 (d, *J* = 7.9 Hz, 2H, $H_{35,}$ H_{39}), 6.90-6.71 (m, 6 H, $H_{23,}$ H_{26}, H_{27}, H_{32}, $H_{40,}$ H_{42}), 5.35 (br s, 1H, H_7), 5.07 (s, 2H, H_{10}), 4.58 (m, 1H, H_{20}), 3.91 (m, 1H, H_5), 3.70 (s, 6H, 2OC$\underline{H}_3$), 3.40 (m, 2H, H_{30}), 2.96 (m, 1H, H_{21a}), 2.71 (m, 1H, H_{21b}), 2.55 (m, 2H, H_4).

^{13}C NMR (100 MHz, DMSO-*d*6) δ ppm 170.2 ;170.0 ($C_{19,}$ 2 dia), 169.5 (C_{29}), 166.9 (C_3), 156.9 (C_9), 156.6 (C_{33}), 156.3 (C_{34}), 148.3, 147.4 ($C_{24,}C_{25}$), 138.4 (C_{31}), 136.8 (C_{11}), 130.0 ($C_{36,}$ C_{38}), 129.5 (C_{41}), 128.3, 127.9, 127.7 ($C_{12,}$ C_{13}, $C_{14,}$ C_{15}, C_{16}), 124.0 (C_{42}), 123.3 (C_{37}), 121.2 (C_{27}), 119.4 (C_{32}), 118.5 ($C_{35,}C_{39}$), 116.4 (C_{40}), 113.1 (C_{26}), 111.5 (C_{23}), 65.6 (C_{10}), 55.4 (O$\underline{C}$H3), 55.3 (O$\underline{C}$H3), 52.5 (C_{20}), 41.7 (C_{30}), 37.6 (C_{21}), 31.49 (C_4).

^{19}F (188 MHz, DMSO-*d*6) δ ppm -73.7 (d, *J* = 4.9 Hz).

Rf : 0.6 (CH_2Cl_2/MeOH: 90/10)

mp: 178-180 °C (crude)

IR (cm^{-1}): 3271 (NH), 1704 (C=O), 1601 (C=O), 1161 (C-O), 1121 (C-O), 690 (CF_3)

MS (ESI Positive) m/z: 760 $[M+Na]^+$

Elemental Anal.	%	Calcul (+0.25 H_2O)	Found
	C	59.91	59.93
	H	5.24	5.32
	N	9.44	9.57

Reference of Chapter IV

1. Nowick, J. S.; Pairish, M.; Lee, I. Q.; Holmes, D. L.; Ziller, J. W., An Extended β-Strand Mimic for a Larger Artificial beta -Sheet. *J. Am. Chem. Soc.* **1997,** 119, (23), 5413-5424.

IV.2. Experimental part chapter III

General chemical techniques:

The N^{α}-Fmoc protected amino acids and HBTU were purchased from MultiSynTech (Witten, Germany). Peptide-synthesis grade DMF, NMP, piperidine and diethylether, ACN and TFA for spectroscopy were purchased from Biosolve (Valkenswaard, The Netherlands).
HOBt, DIPEA, TFA, DCM, DMSO, and α-cyano-4-hydroxy-cinnamic acid for mass spectrometry were bought from Fluka (Taufkirchen, Germany). Methanol was obtained from J.T. Baker (Deventer, The Netherlands), TIS from Aldrich (Steinheim, Germany) and TFE from Acros (Geel, Belgium). Acetic anhydride, acetic acid, NaH_2PO_4 and Na_2HPO_4 were purchased from Merck (Darmstadt, Germany). THF was distilled on sodium/benzophenone before use. Pure products were obtained after liquid chromatography using Merck silica gel 60 (40-63 μm mesh). TLC analyses were performed with 0.25 mm 60 F_{254} silica plates (Merck). The plates were visualized with UV light (254 nm) or with a solution of vanillin in ethanol or with a solution of ninhydrin in ethanol. The mass spectra were recorded on Finnigan MAT 95, Varian MAT 311A, Finnigan TSQ 7000 and Future GSG spectrometer (Bruchsal, Germany) for MALDI-ToF-MS analysis. IR spectra were recorded on a Varian 800 FT-IR spectrometer. Optical rotations were measured on a Perkin-Elmer-Polarimeter 241 with sodium lamp at 589 nm in the specified solvent. NMR spectra were recorded on a Bruker AVANCE 300 (300.13 MHz) or a Bruker AVANCE 400 (400.13 MHz) or a Bruker AVANCE 600 (600.13 MHz). The 2D-NMR standard experiments DQF-COSY, 80 ms-TOCSY and 500 ms-ROESY the water resonance was suppressed by using the presaturation method. The concentration of the peptide samples prepared for CD measurements were determined UV spectrophotometrically on a Cary 100 Conc from Varian (Darmstadt, Germany) using 1 cm quartz cuvettes obtained from Hellma (Müllheim, Germany). CD spectra were recorded at room temperature or at 5 °C on a JASCO J710 spectropolarimeter between 300 and 200-180 nm in the specified solvent. The path length of the quartz cuvette was 1.0 mm. For each CD spectrum ten scans were accumulated using a step resolution of 1 nm, a bandwidth of 1 nm, a response time of 2 s, a scan speed of 20 nm min^{-1} and a sensitivity of 10 mdeg, 20 mdeg, depending on the peptide concentration. The background was subtracted to each spectrum. The absorption value is measured as Molar Ellipticity per Residue

(deg cm^2 $dmol^{-1}$). The noise reduction was obtained by a Fourier transform filter using the program Origin 6.0 (OriginLab Corporation, Northampton, USA). Analytical and preparative reverse Phase HPLC was performed on Agilent equipment (Böblingen, Germany) by using the columns: Luna C18(2), 3 μm, 4.60 x 150 mm and the Luna C18(2), 90 μm, 21.2 x 250 mm (Phenomenex, Aschaffenburg, Germany). The flow rate was 1 mL/min for the analytical HPLC runs and 21 mL/min for preparative applications. The binary solvent system (A/B) was: (A) 0.012% TFA in water (B) 0.01% of TFA in ACN. The absorbance was detected at 220 nm.

SYNTHESIS OF MOLECULES 121 AND 120

(3-Aminomethyl-5-oxo-tetrahydro-furan-2-yl)acetic acid, trifluoroacetic acid salt 121.

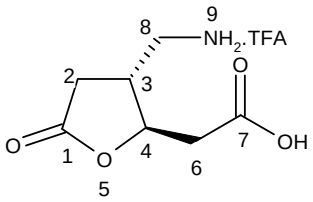

$C_7H_{11}NO_4.CF_3COOH$

M =287.09 g/mol

Compound **107** (100 mg, 0.37 mmol) was dissolved in dry CH_2Cl_2 (5 mL) and trifluoroacetic acid (1.7 mL, 22.0 mmol, 60.0 eq) was added dropwise at room temperature. The reaction mixture was stirred for 2 h. Solvent was evaporated under reduced pressure to yield a brown solid oil **121** (106 mg). This crude product was used without further purification in the course of the synthesis.

^{1}H NMR (300 MHz, CD_3OD) δ ppm 4.69 (m, 1H, H_4), 3.20 (m, 2H, H_8), 2.96-2.71 (m, 4H, H_3, H_6, H_{2a}), 2.51 (dd, J = 17.0 and 6.9 Hz, 1H, H_{2b}).

^{13}C NMR (75 MHz, CD_3OD) δ ppm 177.1 (C_7), 173.4 (C_1), 80.0 (C_4), 42.7 (C_8), 39.9 (C_6), 39.3 (C_2), 33.6 (C_3).

{3-[(9*H*-Fluoren-9-ylmethoxycarbonylamino)-methyl]-5-oxo-tetrahydro-furan-2-yl}acetic acid 120.

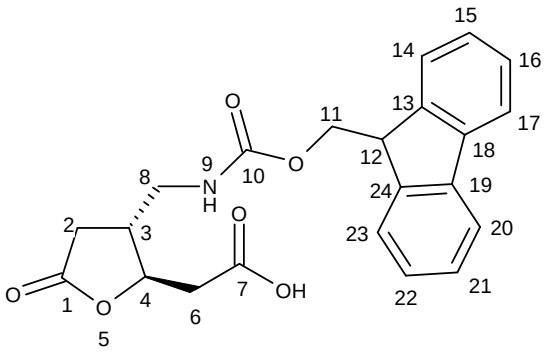

$C_{22}H_{21}NO_6$

M =395.14 g/mol

To a cold (0°C) solution of **121** (106 mg, 0.37 mmol) in dioxane /1M aqueous solution of K_2CO_3 (2 ml /4 ml) was added portionwise FmocOSu (187.2 mg, 0.55 mmol, 1.5 eq.). The reaction was allowed to come at room temperature and stirred overnight. The mixture was poured in water (7 mL) and extracted with EtOAc (3 x 9 mL).

The combined organic layers were dried over Na_2SO_4, filtered and evaporated in vacuo to give a sticky solid wich was purified by column chromatography (PE:EtOAc 2:1) to obtain **120** (86.9 mg, 60%) as a sticky, colorless solid.

^{1}H NMR (300 MHz, CD_3OD) δ ppm 7.80 (d, *J* = 7.4 Hz, 2H, H_{17}, H_{20}), 7.63 (d, *J* = 7.2 Hz, 2H, $H_{14,}$ H_{23}), 7.40-7.27 (m, 4H, $H_{15,}$ $H_{16,}$ H_{21}, H_{22}), 4.64 (m, 1H, H_4), 4.39 (d, *J* = 6.6 Hz, 2H, H_{11}), 4.20 (m, 1H, H_{12}), 3.23 (m, 2H, H_8), 2.73-2.47 (m, 4H, $H_{3,}$ $H_{6,}$ H_{2a}), 2.35 (dd, *J* = 17.2 and 7.0 Hz, 1H, $H_{2b)}$.

^{13}C NMR (75 MHz, CD_3OD) δ ppm 128.8, 128.2, 126.2, 121.0 ($C_{14,}$ C_{15}, $C_{16,}$ C_{17},C_{20}, C_{21}, C_{22}, C_{23}), 81.0 (C_4), 68.2 (C_{11}), 48.6 (C_{12}),43.1 (C_8), 41.9 (C_3), 39.9 (C_2), 33.2 (C_6).

SYNTHESIS OF MOLECULES 125 AND 126

(5-Oxo-tetrahydro-furan-3-ylmethyl)-carbamic acid *tert*-butyl ester; compound with *N*,*N*-diethyl-propionamide 124 a.

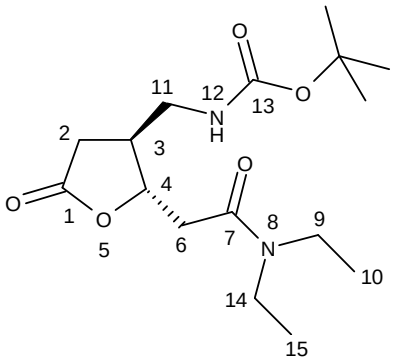

$C_{16}H_{28}N_2O_5$

M =328.20 g/mol

To a solution of **106** (142 mg, 0.52 mmol) and diethylamine (41.8 mg, 0.57 mmol, 1.1 eq) in DMF (8 mL) was added DIPEA (180 µL, 1.04 mmol, 2.0 eq), HOBt (88 mg, 0.57 mmol, 1.1 eq) and HBTU (218 mg, 0.57 mmol, 1.1 eq). The mixture was stirred at room temperature under argon atmosphere for 25 h. After removal of the solvent under reduced pressure, the residue was dissolved in EtOAc (20 mL). The organic solution was successively washed with 10% aqueous citric acid (20 mL), water (20 mL), 10% aqueous K_2CO_3 (20 mL), brine (20 mL). The organic layer was dried over Na_2SO_4, filtered and concentrated. A purification by chromatography on silica gel, eluting with CH_2Cl_2/MeOH (9/1), afforded 110 mg (65%) of **124 a** as a sticky light yellow solid.

^{1}H NMR (300 MHz, $CDCl_3$) δ ppm 5.40 (br s, 1 H, H_{12}), 4.78 (m, 1H, H_4), 3.43-3.15 (m, 6H, H_{11}, H_{14}, H_9), 2.86 (dd, J = 16.3 and 4.3 Hz, 1H, H_{6a}), 2.73-2.58 (m, 2H, H_{6b}, H_{2a}), 2.52 (m, 1H, H_3), 2.38 (dd, J = 18.1 and 5.9 Hz, 1H, H_{2b}), 1.43 (s, 9H, C$\underline{H}_3$Boc), 1.22-1.0 (m, 6H, H_{10}, H_{15}).

^{13}C NMR (75 MHz, $CDCl_3$) δ ppm 175.5 (C_7), 168.1 (C_1), 156.3 (C_{13}), 80.0 ($\underline{C}$Boc), 79.6 (C_4), 42.1, 41.6 (C_9, C_{14}), 40.3 (C_3), 37.9 (C_{11}), 32.4 (C_6), 28.3 ($\underline{C}H_3$Boc), 14.2, 13.0 (C_{10}, C_{15}).

Rf: 0.4 (CH_2Cl_2/MeOH: 90/10)

HRMS (EI) *m/e*: $[M]^+$ calcd 328.1998, found 328.1996

2-[3-(Acetylamino-methyl)-5-oxo-tetrahydro-furan-2-yl]-*N*,*N*-diethyl-acetamide 125.

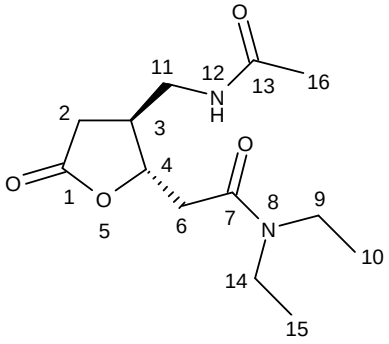

$C_{13}H_{22}N_2O_4$

M =270.16 g/mol

Compound **124 a** (54 mg, 0.18 mmol) was dissolved in dry CH_2Cl_2 (6 mL) and trifluoroacetic acid (3.0 mL, 10.8 mmol, 60.0 eq) was added dropwise at room temperature. The reaction mixture was stirred for 2 h. Solvent was evaporated under reduced pressure to afford the corresponding TFA salt.

A solution of this salt in dry THF (5 mL) was heated at 70 °C and acetic anhydride (32 µL, 0.22 mmol, 1.2 eq) was added dropwise to this solution. The reaction mixture was stirred for 2 hours at 70 °C. The solvent of reaction was evaporated under reduced pressure. A purification by chromatography on silica gel, eluting with CH_2Cl_2/MeOH (9/1), afforded 29 mg (60%) of **126** as a colorless solid oil.

^{1}H NMR (600 MHz, CD_2Cl_2) δ ppm 7.1 (br s, 1H, H_{12}), 4.77 (m, 1 H, H_4), 3.41-3.21 (m, 6H, H_9, H_{14}, H_{11}), 2.88 (dd, *J* = 16.3 and 4.3 Hz, 1H, H_{6a}), 2.72 (dd, *J* = 18.1 and 9.3 Hz, 1H, H_{2a}), 2.66 (dd, *J* = 16.3 and 8.8 Hz, 1H, H_{6b}), 2.49 (m, 1H, H_3), 2.30 (dd, *J* = 18.1 and 5.9 Hz, 1H, H_{2b}), 1.94 (s, 3H, C_{16}), 1.19 (t, *J* = 7.3 Hz, 3H, H_{10}), 1.11 (t, *J* = 7.2 Hz, 3H, H_{15}).

^{13}C NMR (150 MHz, CD_2Cl_2) δ ppm 175.6 (C_7), 170.7 (C_1), 168.8 (C_{13}), 80.3 (C_4), 42.4, 42.3 (C_9, C_{14}), 40.7 (C_{11}), 40.6 (C_3), 38.3 (C_6), 32.4 (C_2), 23.1 (C_{16}), 14.2, 13.1 (C_{10}, C_{15}).

IR in CH_2Cl_2 (cm^{-1}): 3447 (NH), 3312 (NH), 1781 (C=O), 1671 (C=O), 1629 (C=O).

(2S, 3S)-(2-Ethylcarbamoylmethyl-5-oxo-tetrahydro-furan-3-ylmethyl)-carbamic acid *tert*-butyl ester 124 b.

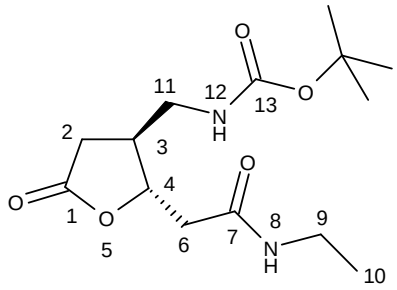

$C_{14}H_{24}N_2O_5$

M = 300.17 g/mol

To a solution of **106** (71 mg, 0.26 mmol) and ethylamine hydrochloride (23.6 mg, 0.29 mmol, 1.1 eq) in DMF (4 mL) was added DIPEA (90 µL, 0.52 mmol, 2.0 eq), HOBt (44 mg, 0.29 mmol, 1.1 eq) and HBTU (109 mg, 0.29 mmol, 1.1 eq). The mixture was stirred at room temperature under argon atmosphere for 23 h. After removal of the solvent under reduced pressure, the residue was dissolved in EtOAc (10 mL). The organic solution was successively washed with 10% aqueous citric acid (10 mL), water (10 mL), 10% aqueous K_2CO_3 (10 mL), brine (10 mL). The organic layer was dried over Na_2SO_4, filtered and concentrated. A purification by chromatography on silica gel, eluting with CH_2Cl_2/MeOH (9/1), afforded 33 mg (42%) of **124 b** as a sticky, light yellow solid.

^{1}H NMR (300 MHz, $CDCl_3$) δ ppm 6.10 (br s, 1 H, H_8), 5.22 (m, 1 H, H_{12}), 4.64 (dd, *J* = 12.6 and 6.3 Hz, 1H, H_4), 3.31-3.22 (m, 4H, H_9, H_{11}), 2.65 (dd, *J* = 16.6 and 8.3 Hz, 1H, H_{2a}), 2.57 (d, *J* = 6.0 Hz, 2H, H_6), 2.52 (m, 1H, H_3), 2.39 (dd, *J* = 16.6 and 7.7 Hz, 1H, H_{2b}), 1.42 (s, 9H, C$\underline{H}_3$Boc), 1.12 (t, *J* = 7.2 Hz, 3H, H_{10}).

^{13}C NMR (75 MHz, $CDCl_3$) δ ppm 175.8 (C_7), 168.8 (C_1), 156.4 (C_{13}), 80.0 ($\underline{C}$Boc), 79.8 (C_4), 41.6 (C_3), 41.2 (C_6, C_{11}), 34.5 (C_9), 32.4 (C_2), 28.3 ($\underline{C}H_3$Boc), 14.63 (C_{10}).

Rf: 0.3 (CH_2Cl_2/MeOH: 90/10)

IR in CH_2Cl_2 (cm^{-1}): 3443 (NH), 1782 (C=O), 1714 (C=O), 1673 (C=O).

HRMS (EI) *m/e*: $[M]^+$ calcd 300.1685, found 300.1685

$[\alpha]^{25}_D$: -19.3 (c 1.0, $CHCl_3$)

2-[3-(Acetylamino-methyl)-5-oxo-tetrahydro-furan-2-yl]-N-ethyl-acetamide 126.

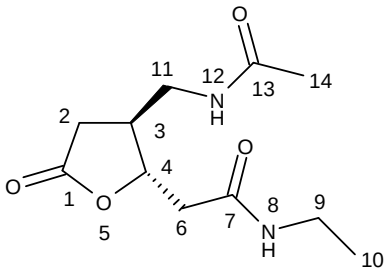

$C_{11}H_{18}N_2O_4$

M = 242.13 g/mol

Compound **124 b** (27 mg, 0.09 mmol) was dissolved in dry CH_2Cl_2 (3 mL) and trifluoroacetic acid (1.5 mL, 5.4 mmol, 60.0 eq) was added dropwise at room temperature. The reaction mixture was stirred for 2 h. Solvent was evaporated under reduced pressure to afford the corresponding TFA salt.

A solution of this salt in dry THF (3 mL) was heated at 70 °C and acetic anhydride (16 µL, 0.11 mmol, 1.2 eq) was added dropwise to this solution. The reaction mixture was stirred for 2 hours at 70 °C. The solvent of reaction was evaporated under reduced pressure. A purification by chromatography on silica gel, eluting with CH_2Cl_2/MeOH (9/1), afforded 14 mg (65%) of **126** as a colorless solid oil.

^{1}H NMR (600 MHz, CD_2Cl_2) δ ppm 6.67 (br s, 1 H, H_{12}), 6.07 (br s, 1 H, H_8), 4.63 (m, 1H, H_4), 3.33 (m, 2H, H_{11}), 3.25 (m, 2H, H_9), 2.66 (dd, *J* = 17.5 and 8.9 Hz, 1H, H_{2a}), 2.58 (d, *J* = 6.2 Hz 2H, H_6), 2.53 (m, 1H, H_3), 2.34 (dd, *J* = 17.5 and 7.5 Hz, 1H, H_{2b}), 1.95 (s, 3H, H_{14}), 1.12 (t, *J* = 7.3 Hz, 3H, H_{10}).

^{13}C NMR (150 MHz, CD_2Cl_2) δ ppm 175.7 (C_1), 171.0 (C_{13}), 169.2(C_7), 80.3 (C_4), 41.3 (C_6), 41.2 (C_{11}), 41.0 (C_3), 34.8 (C_9), 32.7 (C_2), 23.2 (C_{14}), 14.8 (C_{10}).

Rf: 0.3 (CH_2Cl_2/MeOH: 90/10)

IR in CH_2Cl_2 (cm^{-1}): 3441 (NH), 3331 (NH), 1781 (C=O), 1673 (C=O), 1629 (C=O).

HRMS (EI) *m/e*: $[M]^+$ calcd 242.1267, found 242.1269

$[\alpha]^{25}_D$: -17.3 (c 1.0, $CHCl_3$)

METHODS FOR PEPTIDE CHARACTERIZATION

Analytical HPLC

For the analytical HPLC measurements a small amount of the peptide was dissolved in methanol or in millipore water containing 0.1% TFA The binary elution system consisted of 0.012% (v/v) TFA in water (eluent A) and 0.01% (v/v) TFA in ACN (eluent B). The following gradients were applied: 15% B for 3 min, 15-70% B over 40 min, 70-95% B over 50 min and 95% B over 55% (peptides **113** and **114**); 5% B for 5 min, 5-55% B over 45 min, 55-65% B over 50 min and 65-95% B over 60 min (peptides **117**, **118**, **129**-**134**).

MALDI-ToF-MS

For the mass spectrometry MALDI-ToF measurements a small sample of the peptide was dissolved in methanol or in millipore water containing 0.1% TFA and mixed with a solution of α-cyano-4-hydroxycinnamic acid in MeOH/ACN (1:1, v/v).

UV spectroscopy

The concentration of the peptide samples prepared for CD measurements were determined UV spectrophotometrically. By measuring the tyrosine absorption at 280 nm the concentration was calculated according to the Lambert-Beer law using an extinction coefficient of 1480 M^{-1} cm^{-1} per tyrosine residue. The ratio between the peptide concentration values obtained by UV and by weight gave the peptide content. In case of peptides lacking tyrosine or tryptophan residues the peptide contents of similar peptides containing these residues were applied to calculate the concentration.

Boc-F-(S,S)-Lac-F-(S,S)-Lac-F-Bn 113.

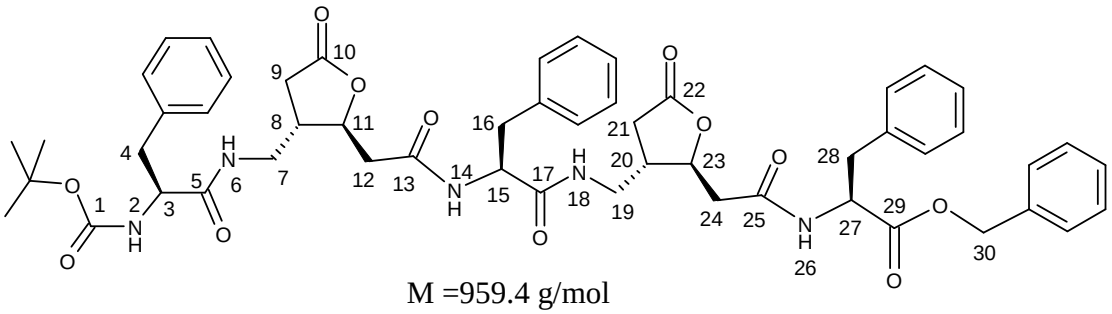

M =959.4 g/mol

^{1}H NMR (600 MHz, CD_3OH, 283 K) δ ppm 8.51 (d, *J* = 8.4 Hz, 1H, H_{26}), 8.39 (d, *J* = 7.2 Hz, 1H, H_{14}), 8.23 (m, 2H, $H_{18,}$ H_6), 7.31-7.11 (m, 20H, H_{ar}), 6.89 (d, *J* = 7.8 Hz, 1H, H_2), 5.46 (s, 2H, H_{30}), 4.70 (m, 1H, H_{26}), 4.48 (m, 1H, H_{14}), 4.37 (m, 2H, H_6, H_{18}), 4.18 (m, 1H, H_2), 3.10-3.30 (m, 6H, H_9, H_{7a}, H_{19a}, H_{21}), 3.10-2.97 (m, 6H, H_{4a} H_{16a}, H_{28}, H_{7b}, H_{19b}), 2.95-2.79 (m, 2H, $H_{4b,}$ H_{16b}), 2.65-2.59 (m, 2H, H_{12a}, H_{24a}), 2.47-2.34 (m, 2H, H_{12b}, H_{24b}), 2.31-2.17 (m, 2H, H_8, H_{20}), 1.43 (s, 9H, C$\underline{H}_3$Boc).

IR in CH_2Cl_2 (cm^{-1}): 3420 (NH), 3314 (NH), 1783(C=O), 1731(C=O), 1672(C=O).

MALDI-ToF-MS: 983 $[M+Na]^+$, 999 $[M+K]^+$

$t_{R:}$ 36.0 min

Boc-F-(R,R)-Lac-F-(R,R)-Lac-F-Bn 114.

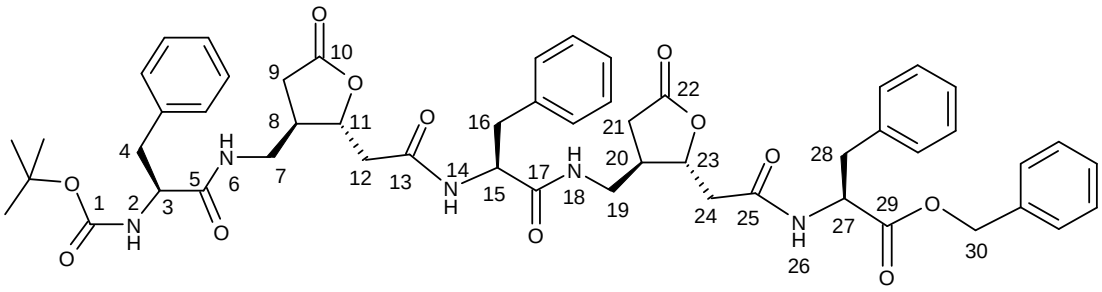

M =959.4 g/mol

^{1}H NMR (600 MHz, $CDCl_3$, 288K) δ ppm 8.56 (d, *J* = 7.8 Hz, 1H, H_{26}), 8.42 (d, *J* = 7.6 Hz, 1H, H_{14}), 8.22 (m, 1H, H_6), 8.04 (m, 1H, H_{18}), 8.38-7.10 (m, 20H, H_{ar}), 6.90 (d, *J* = 7.8 Hz, 1H,

H_2), 5.04 (s, 2H, H_{30}), 4.70 (m, 1H, H_{27}), 4.54 (m, 1H, H_{15}), 4.52-4.42 (m, 2H, H_{11}, H_{23}), 4.26-4.17 (m, 2H, H_3, H_{11}), 3.22-3.16 (m, 3H, H_7, H_{19a}), 3.16-3.10 (m, 3H, H_{19b}, H_{28a}, H_{16a}), 3.0-2.90 (m, 2H, H_{4a}, H_{28b}), 2.93-2.81 (m, 2H, H_{4b}, H_{16b}), 2.56-2.44 (m, 6H, H_{12}, $H_{24,}$ H_{9a}, H_{21a}), 2.35-2.25 (m, 2H, H_{20}, H_8), 2.23-2.14 (m, 2H, H_{9b}, H_{21b}), 1.36 (s, 9H, C$\underline{H}_3$Boc).

IR in CH_2Cl_2 (cm^{-1}): 3421 (NH), 3314 (NH), 1783(C=O), 1733(C=O), 1669(C=O).

HRMS (EI) *m/e*: $[M+H]^+$ calcd 960.4395, found 960.4417

t_R: 37.0 min

Boc-F-(R,R)-Lac-F-(R,R)-Lac-F-(R,R)-Lac-F-Bn 115.

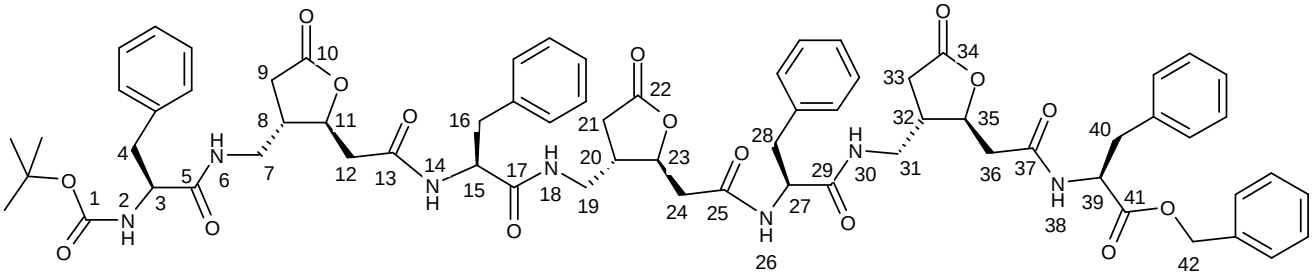

M =1261.6 g/mol

^{1}H NMR (600 MHz, $CDCl_3$, 292K) δ ppm 8.54 (d, *J* = 5.8 Hz, 1H, H_{14}), 8.49 (br s, 1H, H_{26}), 8.34 (d, *J* = 9.5 Hz, 1H, H_{18}), 8.0 (d, *J* = 9.5 Hz, 1H, H_6), 7.74 (d, *J* = 6.8 Hz, 1H, H_{38}), 7.52 (d, *J* = 9.1 Hz, 1H, H_{30}), 7.46-7.0 (m, 25H, H_{ar}), 5.22 (d, *J* = 8.5 Hz, 1H, H_2), 5.17 (d, J_{AB} = 12.1 Hz, 1H, H_{42a}), 5.12 (d, J_{AB} = 12.3 Hz, 1H, H_{42b}), 4.81 (m, 1H, H_{39}), 4.73-4.65 (m, 2H, H_{23}, H_{15}), 4.63 (m, 1H, H_{35}), 4.57 (m, 1H, H_{11}), 4.47 (m, 1H, H_3), 4.22 (m, 1H, H_{27}), 3.90-3.80 (m, 2H, H_{19a}, H_{7a}), 3.72 (m, 1H, H_{31a}), 3.17-2.80 (m, 15H, H_4, H_{16}, H_{24}, H_{36}, H_{28}, H_{40}, H_{31b}, H_{19b}, H_{7b}), 2.80-2.60 (m, 3H, H_{9a}, H_{21a}, H_{33a}), 2.50 (m, 1H, H_8), 2.43-2.10 (m, 5H, H_{33b}, H_{21b} H_{9b}, H_{20}, H_{32}), 1.40 (s, 9H, C$\underline{H}_3$Boc).

IR in CH_2Cl_2 (cm^{-1}): 3420 (NH), 3302 (NH), 1783 (C=O), 1732 (C=O), 1652 (C=O).

MALDI-ToF-MS: 1284 $[M+Na]^+$, 1300 $[M+K]^+$

Ac-K-(S,S)-Lac-Q-(S,S)-Lac-K-CONH$_2$ 116.

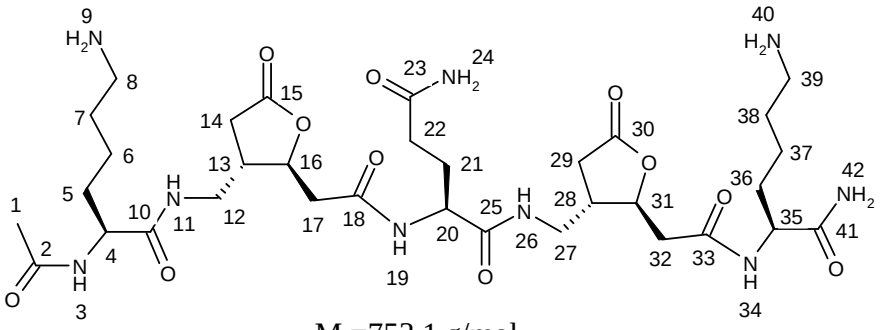

M =753.1 g/mol

^{1}H NMR (600 MHz, CD$_3$OH, 303 K) δ ppm 8.36 (d, *J* = 6.3 Hz, 1H, H$_{19}$), 8.32 (m, 1H, H$_{26}$), 8.27 (m, NH, 1H, H$_{11}$), 8.22 (d, *J* = 7.4 Hz, 1H, H$_{34}$), 8.19 (d, *J* = 6.3 Hz, 1H, H$_3$), 7.74 (br s, 4H, H$_{9,}$ H$_{40}$), 7.65-7.45 (m, 2H, H$_{24}$ or H$_{42}$), 7. 10-7.0 (m, 1H, H$_{24}$ or H$_{42}$), 6.82 (br s, 1H, H$_{24}$ or H$_{42}$), 4.71-4.63 (m, 2H, H$_{16}$, H$_{31}$), 4.39 (m, 1H, H$_{35}$), 4.26-4.22 (m, 2H, H$_{20,}$ H$_4$), 3.38-3.32 (m, 2H, H$_{12,}$ H$_{27}$), 2.99-2.90 (m, 4H, H$_8$, H$_{39}$), 2.79-2.67 (m, 4H, H$_{14a}$, H$_{17a}$, H$_{29a}$, H$_{32a}$), 2.64-2.50 (m, 4H, H$_{13}$, H$_{17b}$, H$_{28,}$ H$_{32b}$), 2.47-2.39 (m, 2H, H$_{14b}$, H$_{29b}$), 2.34 (m, 2H, H$_{22}$), 2.11 (m, 1H, H$_{21a}$), 2.0; 1.96 (s, 3H, H$_{1,}$ 2 conf.), 1.95-1.87 (m, 2H, H$_{21b}$, H$_{36a}$), 1.82 (m, 1H, H$_{5a}$), 1.73-1.61 (m, 6H, H$_7$, H$_{38}$, H$_{5b}$, H$_{36b}$), 1.57-1.36 (m, 4H, H$_{37,}$ H$_6$).

MALDI-ToF-MS: 753 $[M]^+$, 776 $[M+Na]^+$, 792 $[M+K]^+$

Ac-(R,R)-Lac-K-(R,R)-Lac-A-(R,R)-Lac-Y-CONH$_2$ 117.

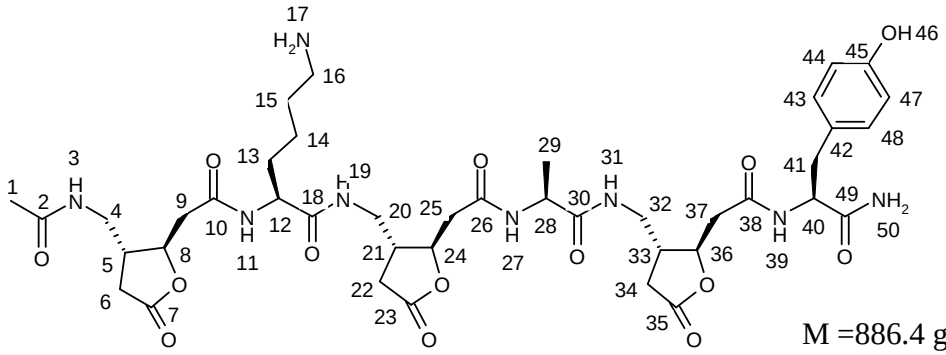

M =886.4 g/mol

^{1}H NMR (600 MHz, CD$_3$OH, 280 K) δ ppm 9.20 (br s, 1H, H$_{46}$), 8.51 (d, *J* = 6.4 Hz, 1H, H$_{27}$), 8.34-8.30 (m, 3H, H$_3$, H$_{19,}$ H$_{39}$), 8.25 (d, *J* = 7.9 Hz, 1H, H$_{11}$), 7.90 (m, 1H, H$_{31}$), 7.71 (br s, 2H, H$_{17}$), 7.65 (br s, 1H, H$_{50a}$), 7.22 (br s, 1H, H$_{50b}$), 7.10 (d, *J* = 8.6 Hz, 2H, H$_{45}$, H$_{47}$), 6.70 (d, *J* = 8.4 Hz, 2H, H$_{44}$, H$_{48}$), 4.70 (m, 1H, H$_{36}$), 4.66-4.58 (m, 2H, H$_{8,}$ H$_{24}$), 4.51 (m, 1H, H$_{40}$), 4.29 (m, 1H, H$_{12}$), 4.22 (m, 1H, H$_{28}$), 3.45 (m, 2H, H$_{20a}$), 3.39-3.27 (m, 2H, H$_{4a}$, H$_{32a}$), 3.26-3.17 (m, 3H, H$_{32b}$, H$_{20b}$, H$_{4b}$), 3.04 (dd, *J* = 5.3 and *J* = 14.0 Hz, 1H, H$_{41a}$), 2.90 (br s, 2H, H$_{16}$), 2.78 (dd, *J* = 9.3 and *J* = 13.9 Hz, 1H, H$_{41b}$), 2.75-2.65 (m, 4H, H$_{6a,}$ H$_{9a,}$ H$_{22a,}$ H$_{34a}$), 2.64-2.51 (m, 7H, H$_5$, H$_{9b}$, H$_{21}$,H$_{25}$, H$_{37}$), 2.47-2.37 (m, 3H, H$_{6b,}$ H$_{22b}$, H$_{33}$), 1.94 (s, 3H, H$_1$), 1.78 (m, 1H, H$_{13a}$), 1.70-1.61 (m, 2H, H$_{15a,}$ H$_{13b}$), 1,58 (m, 1H, H$_{15b}$), 1.41 (m, 2H, H$_{14}$), 1.33 (d, 3H, *J* = 7.3 Hz, H$_{29}$).

HRMS (EI) *m/e*: [M+H]$^+$ calcd 887.4151, found 887.4143

t$_{R:}$ 11.5 min

Ac-L-(R,R)-Lac-K-(R,R)-Lac-A-(R,R)-Lac-Y-CONH$_2$ 118.

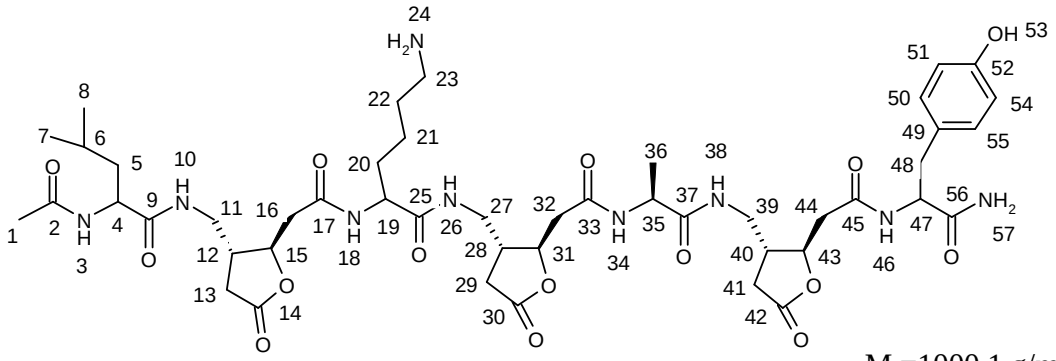

M =1000.1 g/mol

^{1}H NMR (600 MHz, CD$_3$OH, 303 K) δ ppm 9.10 (br s, 1H, H_{53}), 8.37 (d, *J* = 6.5 Hz, 1H, H_{34}), 8.25 (m, 1H, H_{10}), 8.19-8.12 (m, 4H, H_3, H_{18}, H_{26}, H_{46}), 7.84 (m, 1H, H_{38}), 7.70 (br s, 2H, H_{24}), 7.52 (br s, 1H, H_{57a}), 7.10-7.05 (m, 3H, H_{57b}, $H_{54,}$ H_{51}), 6.7 (d, *J* = 8.6 Hz, 2H, H_{55}, H_{50}), 4.80-4.59 (m, 3H, H_{15}, H_{31}, H_{43}), 4.54 (m, 1H, H_{47}), 4.32 (m, 1H, H_{19}), 4.30-4.22 (m, 2H, H_{35}, H_4), 3.48- 3.37 (m, 3H, H_{11a}, H_{27a}, H_{39a}), 3.36-3.22 (m, 3H, H_{11b}, H_{27b}, H_{39b}), 3.05 (dd, *J* = 5.5 and *J* = 14.0 Hz, 1H, H_{48a}), 2.93 (m, 2H, H_{23}), 2.80 (dd, *J* = 9.1 and *J* = 13.9 Hz, 1H, H_{48b}), 2.76-2.63 (m, 6H, $H_{13a,}$ $H_{16a,}$ $H_{29a,}$ H_{32a}, H_{41a}, H_{44}), 2.63-2.54 (m, 6H, H_{12}, H_{16b}, H_{28},H_{32b}, H_{40}, H_{44b}), 2.49-2.35 (m, 3H, $H_{13b,}$ H_{29b}, H_{41b}), 1.98 (s, 3H, H_1), 1.82 (m, 1H, H_{20a}), 1.72-1.58 (m, H, $H_{20b,}$ $H_{22,}$ H_6), 1,58 (m, 2H, H_5), 1.43 (m, 2H, H_{21}), 1.34 (d, *J* = 7.3 Hz, 3H, H_{36}), 0.96 (d, *J* = 6.7 Hz, 3H, H_7 or H_8), 0.92 (d, *J* = 6.7 Hz, 3H, H_7 or H_8).

MALDI-ToF-MS: 1000 $[M]^+$, 1023 $[M+Na]^+$, 1039 $[M+K]^+$

$t_{R:}$ 16.3 min

Ac-G-F-S-K-A-E-L-A-K-A-R-A-A-K-R-G-G-Y-CONH$_2$ 129.

M = 1922.1

MALDI-ToF-MS: 1923 $[M+H]^+$

t$_R$: 20.18 min

Ac-G-A-S-K-A-E-L-A-K-A-R-A-A-K-R-G-G-Y-CONH$_2$ 130.

M = 1845.1

MALDI-ToF-MS: 1846 $[M+H]^+$

t$_R$: 17.51 min

Ac-G-F-S-K-A-E-L-A-K-A-Lac-A-K-R-G-G-Y-CONH$_2$ 131.

M = 1849.0

MALDI-ToF-MS: 1849 $[M]^+$

t$_R$: 21.0 min

Ac-G-F-S-K-A-E-L-A-K-Lac-A-A-K-R-G-G-Y-CONH$_2$ 132.

M = 1848.2

MALDI-ToF-MS: 1849 $[M+H]^+$

t$_R$: 20.51 min

Ac-G-F-Lac-A-E-L-A-K-A-R-A-A-K-R-G-G-Y-CONH$_2$ 133.

M = 1785.0

MALDI-ToF-MS: 1785 $[M]^+$

t$_R$: 18.82 min

Ac-G-A-Lac-A-E-L-A-K-A-R-A-A-K-R-G-G-Y-CONH$_2$ 134.

M = 1861.1

MALDI-ToF-MS: 1862 $[M+H]^+$

t$_R$: 21.89 min

GENERAL CONCLUSIONS

A first objective of my PhD was the synthesis of molecules able to inhibit the 26S proteasome, a multicatalytic protease complex which is responsible for intracellular protein turnover in prokaryotes and eukaryotes. The proteins degraded by the 26S proteasome are various regulators of crucial processes, like the cell-cycle progression, apoptosis, inflammatory responses, NF-kB activation, antigen presentation, and others. Therefore, the proteasome constitutes an interesting target for drug discovery.

In the presented work, we designed, synthesized, and defined the biological profile of a new original series of proteasome inhibitors: four lead compounds with micromolar IC_{50} values. We designed our compounds, by the help of molecular modelling, introducing fluorinated peptidomimetics to exploit the properties of this atom.

In the second part of this project, our attention was turned to the peptidomimetics containing δ-amino acids with the aim to obtain new oligomers of non-natural amino acids. These oligomers form a variety of controlled secondary structures and fall in the domain of "foldamers".

We used the solid-phase methodology to synthesized several α-δ peptides and analytical HPLC and MALDI-TOF-MS to characterize the products. The following step was the evaluation of the properties of these new peptides by using 2D-NMR, FT-IR, circular dicroism, molecular modelling. The structural analyses have given insights in the conformational properties of peptide backbones based on alternated α-δ-units.